Virtual Photon Interactions in High Energy QCD

Dissertation
zur Erlangung des Doktorgrades
des Fachbereiches Physik
der Universität Hamburg

vorgelegt von
Stefan Gieseke
aus Bremen

Hamburg
2001

Gutachter der Dissertation:	Prof. Dr. J. Bartels
	Prof. Dr. B. A. Kniehl
Gutachter der Disputation:	Prof. Dr. J. Bartels
	Prof. Dr. G. Kramer
Datum der Disputation:	10. 7. 2001
Dekan des Fachbereichs Physik und Vorsitzender des Promotionsausschusses:	Prof. Dr. F.-W. Büßer

Abstract

We study the interactions of virtual photons in the high energy limit of Quantum Chromodynamics (QCD). The subject is discussed in terms of two closely linked applications: the calculation of the total cross section for $\gamma^*\gamma^*$-scattering and the description of DIS in the colour dipole model. We calculate virtual corrections in α_s to the process $\gamma^* q \to (q\bar{q})q$ and the tree level process $\gamma^* q \to (q\bar{q}g)q$ in the high energy limit. From this calculation we obtain one-loop corrections to the effective γ^*-reggeon-$q\bar{q}$-vertex in the helicity basis of the virtual photon and the $q\bar{q}$-pair. The loop integrals for the virtual corrections have been performed and expressed in dimensional regularization in terms of logarithms and dilogarithms. We have convoluted the virtual one-loop matrix elements with tree level matrix elements and expressed the integrals over the phase space of the $q\bar{q}$-pair explicitly in terms of a set of standard integrals. The real corrections have been calculated and, in case of the longitudinal polarization, expressed in factorized form. From these calculations, the impact factor of virtual photons will be determined, allowing for a first prediction of the total cross section for $\gamma^*\gamma^*$-scattering in the next-to-leading-log s approximation. The calculations in this thesis extend the photon wave function picture in the colour dipole model to next-to-leading order. For this purpose, the real corrections with a $q\bar{q}g$ final state are analyzed in transverse configuration space and interpreted as a first higher Fock component of the photon wave function. In addition, the matrix elements that have been calculated in this thesis are needed for the calculation of jet cross sections.

Zusammenfassung

Wir untersuchen die Wechselwirkungen von virtuellen Photonen im Hochenergielimes der Quantenchromodynamik. Das Thema wird im Zusammenhang zweier Anwendungen diskutiert: die Berechnung des totalen Wirkungsquerschnittes der $\gamma^*\gamma^*$- Streuung und die Beschreibung tiefinelastischer Streuung im Farbdipolmodell. Wir berechnen virtuelle Korrekturen in α_s zum Prozess $\gamma^* q \to (q\bar{q})q$ sowie den Prozess $\gamma^* q \to (q\bar{q}g)q$ in führender Ordnung; beide im Hochenergielimes. Aus dieser Rechnung erhalten wir Ein-Schleifen-Korrekturen zum effektiven γ^*-Reggeon-$q\bar{q}$-Vertex in der Helizitätsbasis des virtuellen Photons und des $q\bar{q}$-Paares. Die Schleifenintegrale für die virtuellen Korrekturen wurden ausgeführt und in dimensioneller Regularisierung durch Logarithmen und Dilogarithmen ausgedrückt. Wir haben die Interferenzterme der Matrixelemente für die virtuellen Korrekturen mit jenen der führenden Ordnung berechnet und die Integrale über den Phasenraum des $q\bar{q}$-Paares explizit durch einen Satz Standardintegrale ausgedrückt. Wir haben die reellen Korrekturen berechnet und im Falle der longitudinalen Polarisation des virtuellen Photons in faktorisierter Form dargestellt. Auf Grundlage dieser Berechnungen kann der Impact Factor virtueller Photonen berechnet werden und eine erste Vorhersage für den totalen Wirkungsquerschnitt der $\gamma^*\gamma^*$-Streuung in der nächstführenden-log s-Näherung gemacht werden. Die Rechnungen in dieser Arbeit erweitern das Bild der Photonwellenfunktion im Farbdipolmodell zur nächstführenden Ordnung. Zu diesem Zweck haben wir die reellen Korrekturen mit einem $q\bar{q}g$-Endzustand im transversalen Konfigurationsraum analysiert und als erste höhere Fock-Komponente der Photonwellenfunktion interpretiert. Die in dieser Arbeit berechneten Matrixelemente werden des weiteren für die Berechnung von Jet-Wirkungsquerschnitten benötigt.

Contents

Introduction **1**

1 Virtual photon scattering **9**
- 1.1 The colour dipole picture . . . 9
  - The photon wave function at leading order . . . 10
  - The inclusive DIS structure function . . . 13
  - What to expect at NLO? . . . 16
- 1.2 Virtual photon scattering at high energies . . . 17
  - Review of LO BFKL . . . 18
  - NLO BFKL . . . 23
  - General results on impact factors for NLO BFKL . . . 25
  - The limit $Q_1^2 \ll Q_2^2$ . . . 27
  - Calculation of the impact factor for virtual photons . . . 28

2 The vertex $\Gamma^{(1)}_{\gamma^* \to q\bar{q}}$ at NLO **29**
- 2.1 Technical preliminaries . . . 29
- 2.2 Analytic Results . . . 33
  - Calculational methods . . . 33
  - Quark-quark Scattering . . . 34
  - Vertex correction and quark self-energy . . . 37
  - The Box diagram Fig. 2.2.12 . . . 37
  - The Box diagram Fig. 2.2.14 . . . 39
  - The Pentagon diagram Fig. 2.2.13 . . . 43
- 2.3 Renormalization . . . 45
- 2.4 Summary of chapter 2 . . . 46

3 Phase space integrals **47**
- 3.1 Polarizations and kinematical variables . . . 47
- 3.2 Standard integrals . . . 49
- 3.3 Analytic expressions . . . 51
  - Factorized diagrams . . . 52
- 3.4 Summary and outlook for chapter 3 . . . 54

4 Real gluon emission **55**
- 4.1 Kinematics and calculational techniques . . . 55
- 4.2 Results . . . 59
- 4.3 The $q\bar{q}g$ component of the photon wave function . . . 62

4.4 The limit of central emission 64
4.5 Subtraction of the LLA result 66
4.6 Summary and outlook for chapter 4 68

Summary and outlook **69**

A Functions for loop integrals **71**
A.1 Basic functions 71
A.2 More Functions 72
Functions for the two-mass triangle 72
Three-mass triangle functions 72
Adjacent Box 73
One-mass box 74

B Explicit phase space integrals **76**
B.1 Short diagrams 76
Diagram 1 76
Diagram 2+3 78
Diagram 4 79
Diagram 10 81
B.2 Adjacent box 83
B.3 Pentagon 100
B.4 Opposite box 103

Bibliography **119**

Introduction

Quantum Chromodynamics (QCD) is anticipated as the microscopic theory for the description of strong hadronic interactions. From its introduction in the early 1970's until today it has been proven to describe a variety of phenomena (e.g. [1]) from the total rate for the process ($e^+e^- \to$ hadrons) and jet production up to the description of scaling violations in the proton structure function $F_2(x, Q^2)$ via the DGLAP [2] evolution equation. The common basis for these predictions is the application of perturbation theory, which in turn is applicable when the coupling constant is sufficiently small. As a non-Abelian field theory, QCD embodies the phenomenon of asymptotic freedom. After renormalization, the coupling constant α_s depends on a typical scale Q^2 of the problem in such a way, that the coupling vanishes asymptotically for large scales Q^2. Therefore, the applicability of perturbation theory relies upon the presence of a large momentum scale. Being faced with hadronic initial and final states in the calculation of actual cross sections, the application of perturbative methods on the level of the partonic degrees of freedom relies upon a factorization of the process into a hard and a soft part. The soft part includes long-distance effects like the confinement of the partons inside the measured hadrons and is not accessible within perturbation theory. It is possible to perform non-perturbative calculations in the framework of lattice gauge theory. In this thesis we will be concerned only with perturbative dynamics. Nevertheless, we will touch the subject of non-perturbative or soft physics.

As a theory of strong interactions, QCD is meant to describe also small angle hadronic scattering at high energies, including elastic and diffractive scattering or the description of total cross sections. Before the advent of QCD these phenomena were studied in the general framework of Regge theory [3]. It is possible to associate a specific scattering process with the exchange of reggeons, like the $\rho, \omega, \ldots$–mesons. These reggeons appear as poles of the respective scattering amplitude in the complex angular momentum plane and lie on straight Regge trajectories, passing though the physical spin of a particle where the momentum transfer equals the particle's mass.

In the limit of asymptotically large centre of mass energy s and fixed momentum transfer t, called the high energy limit or Regge limit, elastic scattering processes are expected to be dominated by pomeron exchange. The pomeron is associated with the exchange of vacuum quantum numbers between the scattering objects. The property of total hadronic cross sections, not to fall with increasing s, even to rise slowly like

$$\sigma_{\text{tot}} \sim s^{\alpha_{\mathbb{P}}(0)-1}, \qquad \alpha_{\mathbb{P}}(0) - 1 \approx 0.08 \tag{1}$$

is commonly associated with pomeron exchange. This behaviour is found to hold over a wide range of energies, e.g. for $p\bar{p}$-scattering up to the TeV scale at the Tevatron [4]. Since the pomeron is associated with the vacuum structure of field theory and deeply linked to unitarity, a very fundamental property of scattering theory, deeper understanding of the pomeron from a field theory point of view will give deeper insight into strong interaction physics. However, we cannot expect perturbation theory to apply in the description of these phenomena. The physics at small scattering angles implies small momentum transfers, too small to result in a small coupling constant or at least to have a clean factorization of long- and short-distance dynamics.

From the point of view of perturbative QCD (pQCD) the Baliskii-Fadin-Kuraev-Lipatov–equation (BFKL-equation) [5] is a first major step in the description of high energy scattering processes in pQCD. In the Regge limit, the largest contribution to scattering amplitudes comes from leading logarithms in the cms energy, i.e. in pQCD one has to calculate all Feynman diagrams in the kinematic region, where

$$\alpha_s \ll 1, \qquad \alpha_s \log s \sim 1, \tag{2}$$

known as the leading logarithmic approximation (LLA). These diagrams have a ladder structure. For the applicability of pQCD it is strictly inevitable to consider the scattering of small size objects. If we characterize the transverse extension of external particles by mass scales Q_1^2, Q_2^2, we require the Q_i^2 to be in the order of a few GeV in order to apply perturbation theory and they should be of similar size. In such a region, we expect α_s to be small for the whole process and we expect perturbation theory to apply, since the scales Q_1^2, Q_2^2 define the argument of the strong coupling. The rungs of the exchanged ladder, made up by gluon emissions, or certain virtual corrections result in large logarithms in the energy, that can compensate for the smallness of the coupling. Therefore, terms $(\alpha_s \log s)^n$ are of the order of magnitude of one and may contribute at arbitrary powers of α_s. We should note, that the coupling constant is really a constant in LLA, since those diagrams that lead to ultraviolet divergences are formally sub-leading in the above sense.

The BFKL equation is an integral equation for the Green's function of such a ladder exchange, where any number of gluons is taken into account; we may say that the BFKL equation resums the leading logarithms in s. Taking the ladder exchange in the colour singlet state, we have a first perturbative approximation for the pomeron, often called hard pomeron. As the main result, the leading order (LO) BFKL equation leads to cross sections, that rise as fast as

$$\sigma_{\text{tot}} \sim s^{\omega_{\text{BFKL}}}, \qquad \omega_{\text{BFKL}} \approx 0.5 \tag{3}$$

at moderate values for the strong coupling, of about $\alpha_s \approx 0.2$. $1 + \omega_{\text{BFKL}}$ is the intercept of the hard pomeron trajectory. The growth in s is obviously much stronger than it is measured in hadron-hadron scattering. However, there are several reasons that such a strong rise might be a first approximation for the pomeron.

As we have discussed above, we cannot really compare these results from the BFKL approach with the data on hadronic cross sections, since we expect these to be dominated by non-perturbative dynamics. Furthermore, within the BFKL pomeron, non perturbative effects enter via so-called diffusion in transverse momentum space. The transverse momenta of the gluons in the ladder are not restricted in their smallness and therefore they might reach rather small values, even an initially large transverse momentum of several GeV may 'diffuse' down to non-perturbative momenta along the ladder [6, 7], and in fact, the contributions from such small momenta will dominate the process and are even unavoidable for very high energies. Furthermore, we may also question, whether the leading logarithmic approximation is sufficient or not. There might be large NLO corrections. Last but not least it is even possible, that at high energy, the question of the unitarisation of cross sections is already touched, or in other words, if so-called unitarity corrections already play a role [8, 9]. For these reasons, the applicability of the BFKL equation is restricted to the scattering of projectiles of a similar and small transverse size at high but not too high energies.

If we move from hadron-hadron scattering towards deep inelastic e^-p scattering (DIS), we may address the question of the interplay between perturbative and non-perturbative effects in a novel way. At least in part, since we replace one of the two projectiles by a small size object, the highly virtual photon of virtuality Q^2. This virtual photon has a typical transverse extension of the order $1/Q$ and therefore is not affected by long distance or confinement dynamics. The domain of the Regge limit is the region of small values of x, where $x \approx Q^2/s$ is the Bjorken scaling variable. The $\gamma^* p$–cross section under study is closely related to the proton structure function $F_2(x, Q^2)$,

$$\sigma_{T,L}(\gamma^* p) = \frac{4\pi^2 \alpha_{\rm em}}{Q^2} F_{T,L}(x, Q^2). \tag{4}$$

Here, the index (T, L) denotes the transverse and longitudinal polarization of the virtual photon and the usual structure function is simply the sum $F_2 = F_T + F_L$. The rise of the total cross section is reflected by the rise of $F_2(x, Q^2)$ when moving to smaller and smaller values of x and keeping Q^2 fixed. As it is measured in the H1 and ZEUS experiments at HERA there is a power-like increase of $F_2(x, Q^2)$ or, equivalently, $\sigma(\gamma^* p)$, as

$$\sigma(\gamma^* p) \sim (1/x)^\lambda \sim s^\lambda \tag{5}$$

In this case, the value of λ depends very strongly on the virtuality Q^2 of the photon, i.e. on the size, or 'smallness' of the projectile. For large values of $Q^2 \sim 10\,\mathrm{GeV}^2$ we have a large $\lambda \sim 0.3$ while for $Q^2 < 1\,\mathrm{GeV}^2$ we smoothly approach $\lambda \sim 0.08$. This transition between large and small values of λ is sometimes referred to as the transition between the hard and the soft component of the pomeron. Obviously the hard pomeron is associated with small distance physics while for the soft pomeron long distance physics or non-perturbative effects start to play a more and more important role [10]. However, the observation, that λ approaches rather large values for the scattering of projectiles with a small transverse extension, indicates that we are coming close to the domain of the hard BFKL pomeron. Still, we cannot expect the BFKL formalism to be applicable for the description of $F_2(x, Q^2)$, since the proton is involved as a large, non-perturbative object. Instead of the inclusive cross section, we might look at the inclusive production of a forward jet, being initiated by a parton of high transverse momentum [11, 12, 13]. Here, we expect BFKL to be applicable, since the jet transverse momentum serves as a large scale and the BFKL evolution is not affected by any non-perturbative effect. In hadron-hadron collisions this possible application of BFKL to forward jets has been discussed before by Mueller and Navelet [14].

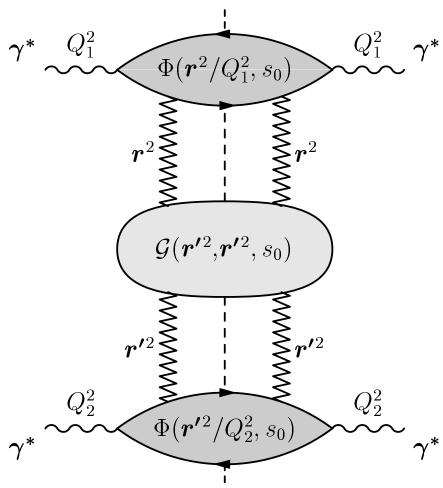

Figure 1: The description of $\gamma^*\gamma^*$-scattering in the high energy limit.

If we move on from DIS towards $\gamma^*\gamma^*$-scattering in the Regge limit (cf. Fig. 1) we are in the very convenient position to completely handle the smallness of our projectiles in terms of their virtualities Q_1^2 and Q_2^2. On the one hand this allows for a careful study of the transition region between small and large virtualities and on the other hand we can 'tune' our virtualities as large as needed for the application of perturbation theory. In particular, we should, in principle, be able to predict the result within perturbative QCD or, in other words, 'test' BFKL dynamics, as it was first proposed in [15, 16] and studied in detail also in [17, 18]. For these reasons the process $\gamma^*\gamma^* \to$ hadrons is often called the 'gold plated process'. Recently, in e^+e^--scattering at LEP, we can study the scattering of two highly virtual photons and especially the total cross section $\sigma_{\mathrm{tot}}^{\gamma^*\gamma^*}$ in so called double-tagged events experimentally. The first results from LEP [19] indicate strongly that fixed order QCD calculations are not sufficient to describe the data: a rise of the cross section is observed, in contrast to a flat fixed-order cross section. On the other hand, the LO BFKL

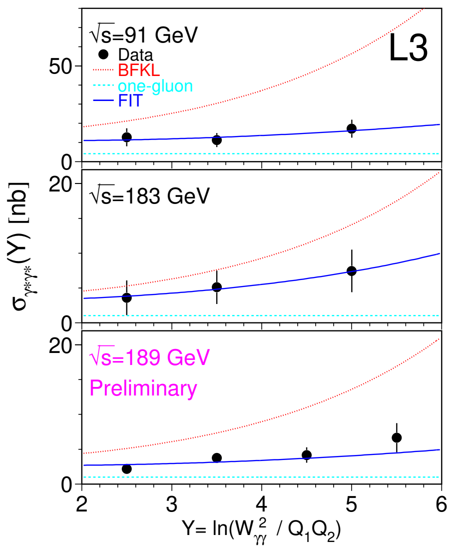

Figure 2: The total cross section $\sigma_{\rm tot}^{\gamma^*\gamma^*}$, measured by L3 at LEP [20].

prediction clearly rises much stronger with s than the data, that prefer a power $\lambda \sim 0.3$, (cf. Fig. 2).

The NLO corrections to the BFKL Kernel, and therefore NLO corrections to the pomeron intercept, have been calculated by Fadin, Lipatov, Camici and Ciafaloni within about ten years [22, 23]. The corrections are quite large and, in fact, they lower the strong rise down to values of about 0.3. However, as a first result these corrections were seen to be unexpectedly large, giving even a negative intercept for realistic values of α_s. This gave rise to numerous studies. The main conclusion is, that one has to take into account properly the implications from the renormalization group behaviour of these corrections. In the collinear limit of gluon emission extra large logarithms of transverse momenta have to be resummed. Doing so, one is able to tame the corrections, resulting in lower values for the pomeron intercept of about 0.3 for realistic values of α_s [25, 26, 24]. This value seems to be compatible with the data.

However, so far the prediction for $\sigma_{\rm tot}^{\gamma^*\gamma^*}$ has not been completely calculated within NLO, yet. In high energy scattering, a basic factorization, known as Regge factorization, holds and is sketched schematically in Fig. 1. The NLO corrections to the BFKL Kernel give rise only to NLO corrections to the Green's function $\mathcal{G}$ of the exchanged reggeized gluons. The coupling of the virtual photons to the reggeized gluons via the so-called photon impact factor Φ is not known to NLO. The impact factor is expected to remove some substantial uncertainties from the NLO BFKL prediction: the overall normalization of the cross section will be fixed and a clear definition of the inherent energy scale will be possible. The calculation of the virtual photon impact factor in NLO is the goal of this thesis.

To conclude, one may say that from studying the scattering of small size objects one may shed some light into the hard component of the pomeron.

Combining the improved knowledge from the description of $\gamma^*\gamma^*$ scattering at NLO with an extension of the photon wave function picture of DIS at small x to NLO, we will improve our present understanding about the transition region between perturbative and non-perturbative QCD. Finally, pinning down the knowledge from the perturbative side we have an excellent starting point to study the transition to the pomeron in hadron hadron scattering.

In this thesis we initiate the program of the calculation of NLO corrections to the virtual photon impact factor. This program is characterized in terms of three major steps:

i) The calculation of virtual corrections to the γ^*-reggeon-$q\bar{q}$ -vertex,

ii) the calculation of real corrections and

iii) the integration over the phase space of intermediate state particles.

The calculation of virtual corrections *(i)* is completed. We have carried out all loop integrations of the occuring diagrams with up to five external legs. We give explicit formulae in terms of an ϵ-expansion in order to regulate ultraviolet and infrared divergences. The finite terms are expressed in terms of special functions, which in turn are combinations of logarithms and dilogarithms. The ultraviolet divergences are renormalized in the $\overline{\mathrm{MS}}$-scheme. The calculation of real corrections *(ii)* is completed as well. We calculate explicit formulae for squared matrix elements, summed over all helicities of final state particles. For longitudinal photons, the results are presented in a compact, factorized form. We transform these results into the transverse configuration space and find first hints for a novel higher Fock component of the virtual photon wave function. The phase space integration *(iii)* is performed in terms of a set of standard integrals. Apart from two more steps, namely the phase space integration of the real corrections and the cancellation of the infrared divergences with those from the virtual corrections, the calculation of the impact factor is completed.

In connection with the corrections from real gluon emission we can conclude about the important extension of the colour dipole model to NLO. We see the beginning of an expansion of the virtual photon in terms of its higher Fock components. The first higher order term, a $q\bar{q}g$ Fock-component of the longitudinally polarized virtual photon, is one of the results from our calculation of the real corrections.

Having performed the calculation of NLO corrections to the photon impact factor, we have calculated the matrix elements for the process $\gamma^* g \to q\bar{q}$ in NLO. The results of this calculation, not integrated over phase space include the differential cross sections for jet production in the $k_\perp$-factorization scheme. Our results allow the extension of recent calculations, where photon and gluon are taken on-shell. The matrix elements can immediately be implemented into NLO Monte-Carlo models.

The outline of this thesis is as follows: we are concerned with the perturbative interaction of virtual photons as external particles in high energy scattering processes. In chapter 1 we give an introduction to high energy interactions of virtual photons in DIS and in $\gamma^*\gamma^*$-scattering, starting with an outline of the photon wave function picture, successfully applied in the description of DIS in the proton rest-frame, followed by a brief introduction to the BFKL formalism in leading and next-to-leading order. This will lead us to the formulation of the program that has been performed in this thesis in order to obtain NLO corrections to the photon wave function picture as well as to the virtual photon impact factors. As the central point of this program, the calculation of virtual corrections is presented in chapter 2. In chapter 3 we outline the phase space integration, whose actual results will be listed in appendix B. In chapter 4 we present the calculation of NLO corrections from an extra real gluon in the final state, including a factorized analytic representation of the results that leads us to new conclusions about the structure of the photon wave function at NLO. Finally we give a brief summary and an outlook to future research work that has become possible on the basis of the results of this thesis.

Chapter 1

Virtual photon scattering

Following this rather broad view on high energy scattering we will take a closer look into what we can learn from studying the scattering of virtual photons: the photon wavefunction picture and the perturbative calculation of the total cross section $\sigma(\gamma^*\gamma^* \to \text{hadrons})$.

1.1 The colour dipole picture

The photon wavefunction picture is a rather intuitive description of $\gamma^* p$ scattering, in the rest frame of the proton. We first want discuss the features of the model at leading order and continue with possible implications of this work at NLO.

The general picture is as follows. In the proton rest frame the life time of the fluctuation of a virtual photon into a $q\bar{q}$-pair is much larger than the actual duration of the interaction between the $q\bar{q}$-pair and the proton. One may therefore consider the virtual photon as an expansion into its strongly interacting Fock components

$$|\,\gamma^*\,\rangle = |\,q\bar{q}\,\rangle + |\,q\bar{q}g\,\rangle + |\,q\bar{q}gg\,\rangle + \cdots \tag{1.1}$$

It is then most convenient to consider the transverse degrees of freedom in configuration space and the longitudinal ones still in longitudinal momentum space.

The $q\bar{q}$-pair in turn can be viewed as a colour dipole, that is then interacting with the proton, independent of its formation by the photon. One could expect that at higher order also higher Fock components, including one additional gluon can be interpreted in the same way, just that there are higher multipoles present.

In this model one may write the total $\gamma^* p$ cross section as a convolution

$$\sigma_{\gamma^* p} = \int d^2\boldsymbol{\rho} \int d\alpha\, \psi^*(\boldsymbol{\rho}, \alpha)\sigma_{q\bar{q}}(\boldsymbol{\rho})\psi(\boldsymbol{\rho}, \alpha), \tag{1.2}$$

like it is sketched in Fig. 1.1.

In the proton rest frame, the photon first fluctuates into a $q\bar{q}$ pair or colour dipole of transverse size $\boldsymbol{\rho}$, the quarks carry light cone momentum fractions α

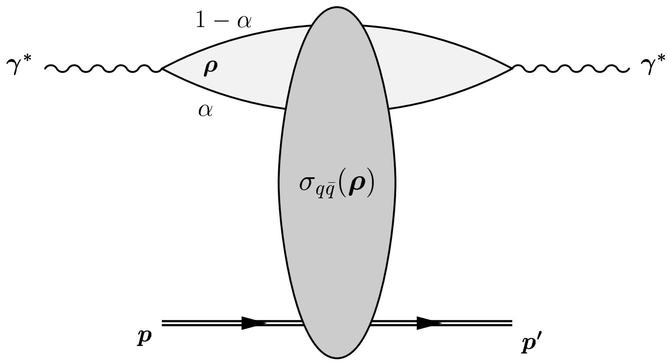

Figure 1.1: The $\gamma^* p$ cross section in the colour dipole model

and $(1-\alpha)$ of the incoming virtual photon. The fluctuation is described by the photon wave function $\psi(\boldsymbol{\rho}, \alpha)$. This dipole interacts with the proton with a cross section $\sigma_{q\bar{q}}(\boldsymbol{\rho})$, and finally the dipole annihilates into a photon again. In fact, we think of this cross section as being the s-channel imaginary part of an elastic amplitude. The important point is, that the lifetime of the dipole is much larger than the interaction itself. In this leading order configuration, the properties of the dipole do not even change as a result of the interaction. In the small size regime, where we are able to describe the dipole perturbatively, the cross section $\sigma_{q\bar{q}}(\boldsymbol{\rho})$ should even vanish as $\rho \to 0$ like ρ^2. This is known as colour transparency. The strength of the dipole interaction is actually proportional to its size. If the dipole appears to be smaller and smaller, the proton will not be able to take notice of its colour charges, since the pair appears to be neutral.

The photon wave function at leading order

We want to take a closer look into how the wave function can be derived perturbatively and how we arrive at the factorized formula (1.2). The concept of the photon wave function is rather well known. In [28] expressions for massless quarks and transverse photons are given explicitly in terms of helicity amplitudes. [29, 30] give explicit expressions for the squared wave functions, including longitudinal photons and also massive quarks. A derivation of the amplitudes in terms of an explicit spinor representation limited to massless quarks is given in [31]. We will therefore reconsider a perturbative derivation of the wave function, including massive fermions. The formulation of the photon wave function in the helicity basis for massive fermions is a new result of our work and has been published in [32].

Let us first suppose, we scatter the virtual photon off a single quark instead of a proton and consider the two Feynman diagrams in Fig. 1.2. To obtain an explicit expression for the photon wave function at leading order we calculate the diagrams in Fig. 1.2 in the helicity basis of the outgoing $q\bar{q}$-pair and for explicit photon polarizations. Finally we will take the Fourier transform and have a closer look at the amplitudes in configuration space, where the conjugate

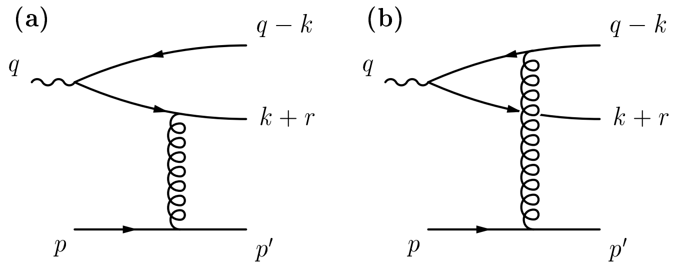

Figure 1.2: Born level diagrams for the photon wave function

variable to the transverse momentum separation of the $q\bar{q}$ pair is its transverse size.

For calculations in the high energy limit it is very convenient to use a Sudakov representation. All momenta are decomposed with respect to the light cone vectors $q' = q + xp$ and p, $q'^2 = p^2 = 0$. Up to corrections of order t/s, the invariant $s = 2p' \cdot q'$ is equal to the cms energy of the incoming virtual photon and the lower quark, $x = Q^2/s$ is the the Bjorken scaling variable and $Q^2 = -q^2$ the virtuality of the photon. We choose the upper quark and antiquark to have a mass m and the lower quark to be massless. As additional momentum variables we choose the the internal quark line in diagram (a) to have the momentum k and the exchanged momentum to be r, as it is labelled in Fig. 1.2. They have the Sudakov decomposition:

$$k = \alpha q' + \beta p + k_\perp, \tag{1.3}$$

$$r = \frac{t}{s} q' + x_{\mathbb{P}} p + r_\perp. \tag{1.4}$$

In this way the quark and antiquark carry momentum fractions α and $(1 - \alpha)$ in the q'-direction. In the following we often use the Euclidean part of the transverse momenta explicitly, e.g. $k_\perp^2 = -\boldsymbol{k}^2$. The transverse momenta $-\boldsymbol{k}$ and $\boldsymbol{k} + \boldsymbol{r}$ are carried by the antiquark and quark, respectively, against the proton that recoils with $-\boldsymbol{r}$. From the on-shell conditions for the outgoing quarks, together with the assumptions that $Q^2 \sim -\boldsymbol{r}^2 = t \ll s$, we find $x_{\mathbb{P}}$ and β to be of the order t/s. To obtain the leading contribution in the high energy limit, we decompose the metric tensor in the gluon propagator as

$$g_{\mu\nu} = \frac{2}{s}(p_\mu q'_\nu + p_\nu q'_\mu) + g^\perp_{\mu\nu} \tag{1.5}$$

and retain only the first term, such that p is contracted with the upper system and q' with the lower system. The other terms will give contributions that are suppressed by powers of t/s. Furthermore, we express the denominators of the quark lines in diagrams (a) and (b), introducing $t_a = k^2$ and $t_b = (q - k - r)^2$ respectively as

$$\begin{aligned} t_a - m^2 &= -\frac{1}{1-\alpha}[\alpha(1-\alpha)Q^2 + \boldsymbol{k}^2 + m^2] \equiv -\frac{1}{1-\alpha} D(\boldsymbol{k}), \\ t_b - m^2 &= -\frac{1}{\alpha}[\alpha(1-\alpha)Q^2 + (\boldsymbol{k}+\boldsymbol{r})^2 + m^2] \equiv -\frac{1}{\alpha} D(\boldsymbol{k}+\boldsymbol{r}). \end{aligned} \tag{1.6}$$

Before writing down the amplitude from the Feynman rules we first simplify the contribution from the lower quark line, which is well known to give

$$\bar{u}(p')\gamma^\mu u(p) \approx 2p^\mu \delta_{\lambda_q \lambda'_q}, \tag{1.7}$$

where λ_q and λ'_q are the helicities of the lower quark line. Contracting with q'_μ from the gluon propagator, we get $s\delta_{\lambda_q,\lambda'_q}$.

After this we may write down the amplitude for one gluon exchange as

$$\mathcal{A} = g t^a_{ij} \delta_{\lambda_q,\lambda'_q} \frac{2s}{t}(-igee_f)\left(\frac{H^a_T}{st_a} - \frac{\bar{H}^a_T}{st_b}\right) \tag{1.8}$$

where e is the (positive) elementary charge and ee_f gives the quark charge, g is the strong coupling constant and t^a_{ij} is a generator of the colour group in the fundamental representation. We define the helicity amplitudes

$$H^a_T = t^a_{ij}\bar{u}_{\lambda'}(k+r)\not{p}(\not{k}+m)\not{\varepsilon}^\gamma v_\lambda(q-k), \tag{1.9}$$

$$\bar{H}^a_T = t^a_{ij}\bar{u}_{\lambda'}(k+r)\not{\varepsilon}^\gamma(\not{q}-\not{k}-\not{r}-m)\not{p} v_\lambda(q-k)\ , \tag{1.10}$$

arising from the upper fermion lines and $\lambda'(\lambda) = \pm$ denotes the helicity of the (anti-)quark. Within these we choose the polarization vector of the virtual photon explicitly as

$$\varepsilon^0 = \frac{1}{Q}(q' + x_B p'), \qquad \varepsilon^\gamma_\perp = \frac{1}{\sqrt{2}}(0,1,\gamma i, 0). \tag{1.11}$$

Here and in the following $\gamma = 0, \pm$ denotes the photon polarization.

We proceed by evaluating the spinor products H^a_T and $\bar{H}^a_T$ in the helicity basis (λ, λ') of the $q\bar{q}$-pair. Therefore, we have to evaluate helicity amplitudes of the general form $\bar{u}_{\lambda'}(k+r)\chi v_\lambda(q-k)$. Since we want to allow for quarks of non-vanishing mass m here, the use of an explicit spinor representation might be much more complicated than in the case of massless fermions. We make use of the helicity method given in [33]. The basic idea of this method is to express spinors for massive particles in terms of massless spinors and to observe, that the above helicity amplitude can be written as a trace:

$$\bar{u}_{\lambda'}(k+r)\chi v_\lambda(q-k) = \mathrm{tr}\, \chi v_\lambda(q-k)\bar{u}_{\lambda'}(k+r). \tag{1.12}$$

With the help of massless spinors it is then possible to express the matrix $v_\lambda(q-k)\bar{u}_{\lambda'}(k+r)$ explicitly in terms of the fermions' helicities and momenta and two reference vectors k_0, k_1, of which the final result will not depend. First of all, we slightly rewrite the expressions for longitudinal and transverse polarizations of the photon for diagram (a),

$$\not{p}(\not{k}+m)\not{\varepsilon}^\gamma = \alpha s \not{\varepsilon}^0 + \frac{s}{2Q}\not{r}_\perp - i\epsilon(\mu, \varepsilon^0, p_{B'}, p_B)\gamma_\mu\gamma_5 \qquad (\gamma = 0), \tag{1.13}$$

$$\not{p}(\not{k}+m)\not{\varepsilon}^\gamma = \alpha s \not{\varepsilon}_\perp + \boldsymbol{\varepsilon}_\perp \cdot \boldsymbol{r}\not{p}' - i\epsilon(\mu, \varepsilon_\perp, p_{B'}, p_B)\gamma_\mu\gamma_5 \qquad (\gamma = \pm) \tag{1.14}$$

and analogously for diagram (b). Here we only kept terms that will be present in the high energy limit. Applying the helicity method we finally obtain for the amplitude (1.8) a result, which can be written in the compact form

$$\mathcal{A} = g t^a_{kl}\delta_{\lambda_q,\lambda'_q}\frac{2s}{t}(-igee_f\, t^a_{ij})\sqrt{\alpha(1-\alpha)}\Big(\Psi(\boldsymbol{k},\alpha) - \Psi(\boldsymbol{k}+\boldsymbol{r},\alpha)\Big). \tag{1.15}$$

Here, $\Psi(\boldsymbol{k},\alpha)$ is the photon wave function that we were after. It contains all dependence of the amplitude on the properties of the virtual photon and the $q\bar{q}$-pair, including helicities. With the notation $\Psi^{\gamma}_{\lambda'\lambda}(\boldsymbol{k})$ for the explicit helicity dependence of the wave function and $\underline{k} = k_x + i\gamma k_y$ for the transverse momenta in the transverse polarization, we get the following explicit results from our calculation:

$$\Psi^{0}_{\pm\mp}(\boldsymbol{k},\alpha) = \frac{2\alpha(1-\alpha)Q}{\alpha(1-\alpha)Q^2+\boldsymbol{k}^2+m^2}, \tag{1.16}$$

$$\Psi^{\pm}_{\pm\mp}(\boldsymbol{k},\alpha) = \frac{\sqrt{2}\alpha\underline{k}}{\alpha(1-\alpha)Q^2+\boldsymbol{k}^2+m^2}, \tag{1.17}$$

$$\Psi^{\pm}_{\mp\pm}(\boldsymbol{k},\alpha) = \frac{-\sqrt{2}(1-\alpha)\underline{k}}{\alpha(1-\alpha)Q^2+\boldsymbol{k}^2+m^2}, \tag{1.18}$$

$$\Psi^{\pm}_{\pm\pm}(\boldsymbol{k},\alpha) = \frac{\sqrt{2}im}{\alpha(1-\alpha)Q^2+\boldsymbol{k}^2+m^2}, \tag{1.19}$$

$$\Psi^{0}_{\pm\pm}(\boldsymbol{k},\alpha) = \Psi^{\pm}_{\mp\mp}(\boldsymbol{k},\alpha) = 0. \tag{1.20}$$

In the term (1.19), that is vanishing for massless quarks, we note a naive helicity conservation like $\gamma = (\lambda+\lambda')/2$. A similar situation was found for (1.16) but here the mass dependence always cancels in the difference of the wave functions. We can understand this as follows: in the massless limit we can only have the configuration $\lambda = -\lambda'$ within the $q\bar{q}$-pair, since the helicity can not flip along the fermion line and has to be opposite between q and $\bar{q}$. On the other hand, in the nonrelativistic limit we have a helicity conservation as we would naively expect it.

In many applications one is, however, interested in the modulus square of the wave functions. Therefore we sum over the helicities of the $q\bar{q}$-pair and also over the two transverse polarizations of the virtual photon. Following eqns. (1.16)–(1.20) we define for the difference of the two wavefunctions in (1.15)[1]:

$$|\Psi_L(\boldsymbol{k},\alpha)|^2 = 8\alpha^2(1-\alpha)^2Q^2\left(\frac{1}{D(\boldsymbol{k})}-\frac{1}{D(\boldsymbol{k}+\boldsymbol{r})}\right)^2 \tag{1.21}$$

$$\begin{aligned}|\Psi_T(\boldsymbol{k},\alpha)|^2 =& 4\left[\alpha^2+(1-\alpha)^2\right]\left(\frac{\boldsymbol{k}}{D(\boldsymbol{k})}-\frac{\boldsymbol{k}+\boldsymbol{r}}{D(\boldsymbol{k}+\boldsymbol{r})}\right)^2\\ &+4m^2\left(\frac{1}{D(\boldsymbol{k})}-\frac{1}{D(\boldsymbol{k}+\boldsymbol{r})}\right)^2.\end{aligned} \tag{1.22}$$

The inclusive DIS structure function

Let us consider the total cross section $\sigma^{\mathrm{tot}}_{\gamma^* p}$ as in (1.2). This is obtained from the imaginary part of the elastic forward scattering amplitude via the optical theorem. Having calculated the amplitude for $\gamma^* q$ scatting we are already very close to the answer. We square eq. (1.15) and replace the contribution from the

[1]Note that we have *summed* over the two photon polarizations, as it is used in a polarization sum. If one is interested in the *average* over the two transverse polarizations of the incoming photon, one has to multiply (1.22) by a factor $\frac{1}{2}$.

lower quark line by a suitable ansatz for the non-perturbative coupling to the proton. Since we are in the high energy limit, we are in the regime of Regge factorization and expect the coupling of the proton to the t-channel gluon not to depend on the $\gamma^* \to q\bar{q}$-splitting above. Instead of the quark coupling we will introduce the unintegrated gluon distribution $\mathcal{F}(x, \boldsymbol{r}^2)$ of the target.

The square of (1.15), divided by s and integrated over the phase space of all final state quarks is the total cross section for $\gamma^* q$-scattering, up to second order in α_s,

$$\sigma_{L,T}(\gamma^* q) = \int d\alpha d^2\boldsymbol{k} \frac{d^2\boldsymbol{r}}{\boldsymbol{r}^4} \left(\frac{\alpha_s C_F}{\pi}\right) \frac{4\pi\alpha_s}{3} \sum_f e_f^2 \frac{3\alpha_{\mathrm{em}}}{4\pi^2} |\Psi_{L,T}(\boldsymbol{k}, \alpha)|^2. \quad (1.23)$$

To gain a simpler expression, we introduce the Fourier transforms $\psi^{\gamma}_{\lambda'\lambda}(\boldsymbol{\varrho}, \alpha)$ of $\Psi^{\gamma}_{\lambda'\lambda}(\boldsymbol{k}, \alpha)$ with respect to $\boldsymbol{k}$,

$$\psi^{\gamma}_{\lambda'\lambda}(\boldsymbol{\varrho}, \alpha) = \int \frac{d^2\boldsymbol{k}}{(2\pi)^2} e^{i\boldsymbol{k}\boldsymbol{\varrho}} \Psi^{\gamma}_{\lambda'\lambda}(\boldsymbol{k}, \alpha) \quad (1.24)$$

Transforming eqns. (1.16)–(1.20) we obtain the following explicit expressions for the conjugated photon wave functions in $\boldsymbol{\varrho}$-space:

$$\psi^{0}_{\pm\mp}(\boldsymbol{\varrho}, \alpha) = \frac{1}{\pi}\alpha(1-\alpha) Q K_0(\delta\varrho), \quad (1.25)$$

$$\psi^{\pm}_{\pm\mp}(\boldsymbol{\varrho}, \alpha) = \frac{i}{\pi}\alpha\delta \frac{\boldsymbol{\varrho}\cdot\boldsymbol{\varepsilon}}{\varrho} K_1(\delta\varrho), \quad (1.26)$$

$$\psi^{\pm}_{\mp\pm}(\boldsymbol{\varrho}, \alpha) = -\frac{i}{\pi}(1-\alpha)\delta \frac{\boldsymbol{\varrho}\cdot\boldsymbol{\varepsilon}}{\varrho} K_1(\delta\varrho), \quad (1.27)$$

$$\psi^{\pm}_{\pm\pm}(\boldsymbol{\varrho}, \alpha) = \frac{im}{2\pi} K_0(\delta\varrho), \quad (1.28)$$

where we used $\delta^2 = \alpha(1-\alpha)Q^2 + m^2$ and $\varrho = |\boldsymbol{\varrho}|$ as a shorthand notation and $K_\nu(z)$ is a modified Bessel function. We average over the quark and antiquark helicities and define the longitudinal and transverse wave functions as

$$|\psi_L(\boldsymbol{\varrho}, \alpha)|^2 = |\psi^0_{+-}|^2 + |\psi^0_{-+}|^2 + |\psi^0_{++}|^2 + |\psi^0_{--}|^2 \quad (1.29)$$

$$= \sum_f e_f^2 \frac{3\alpha_{\mathrm{em}}}{4} 2|\psi^0_{+-}(\boldsymbol{\varrho}, \alpha)|^2 \quad (1.30)$$

$$= \frac{3\alpha_{\mathrm{em}}}{2\pi^2} \sum_f e_f^2\, 4\alpha^2(1-\alpha)^2 Q^2 K_0^2(\delta\varrho), \quad (1.31)$$

$$|\psi_T(\boldsymbol{\varrho}, \alpha)|^2 = \frac{3\alpha_{\mathrm{em}}}{2\pi^2} \sum_f e_f^2 \left\{ \left[\alpha^2 + (1-\alpha)^2\right] K_1^2(\delta\varrho) + m^2 |K_0(\delta\varrho)\right\}. \quad (1.32)$$

Now, we introduce the unintegrated gluon distribution by the replacement

$$\left(\frac{\alpha_s C_F}{\pi}\right) \longrightarrow \mathcal{F}(x, \boldsymbol{r}^2) \quad (1.33)$$

in eq. (1.23). If we had taken a gluon instead of the lower quark, representing the proton, a similar replacement would hold with C_A instead of C_F. If we are at small values of x, we expect the gluon to be dominating. The ordinary gluon distribution $xg(x,Q^2)$ is obtained by integration,

$$xg(x,Q^2) = \int^{Q^2} \frac{d^2\boldsymbol{r}}{\pi \boldsymbol{r}^2} \mathcal{F}(x,\boldsymbol{r}^2) \ . \tag{1.34}$$

Furthermore, we express the wave function by it's Fourier transform. Since in momentum space the wave function always appeared as a difference $\Psi(\boldsymbol{k},\alpha) - \Psi(\boldsymbol{k}+\boldsymbol{r},\alpha)$ we pick up the phase factors in front of the Fourier transformed wave functions:

$$\begin{aligned}
\sigma_{L,T}(\gamma^* q) &= \int d\alpha d^2\boldsymbol{k} \frac{d^2\boldsymbol{r}}{\boldsymbol{r}^4} \frac{4\pi\alpha_s}{3} \mathcal{F}(x,\boldsymbol{r}^2) & (1.35)\\
&\times \int \frac{d^2\boldsymbol{\varrho}}{(2\pi)^2} e^{-i\boldsymbol{k}\cdot\boldsymbol{\varrho}} (1-e^{i\boldsymbol{r}\cdot\boldsymbol{\varrho}}) \psi^*(\boldsymbol{\varrho},\alpha) \\
&\times \int \frac{d^2\boldsymbol{\varrho}'}{(2\pi)^2} e^{-i\boldsymbol{k}\cdot\boldsymbol{\varrho}'} (1-e^{-i\boldsymbol{r}\cdot\boldsymbol{\varrho}'}) \psi(\boldsymbol{\varrho}',\alpha) \\
&= \int d\alpha \frac{d^2\boldsymbol{r}}{\boldsymbol{r}^4} \frac{4\pi\alpha_s}{3} \mathcal{F}(x,\boldsymbol{r}^2) \int \frac{d^2\boldsymbol{\varrho}}{(2\pi)^2} \int \frac{d^2\boldsymbol{\varrho}'}{(2\pi)^2} (1-e^{i\boldsymbol{r}\cdot\boldsymbol{\varrho}})(1-e^{-i\boldsymbol{r}\cdot\boldsymbol{\varrho}'}) \\
&\times \int d^2\boldsymbol{k} e^{-i\boldsymbol{k}\cdot(\boldsymbol{\varrho}'-\boldsymbol{\varrho})} \psi^*(\boldsymbol{\varrho},\alpha)\psi(\boldsymbol{\varrho}',\alpha) & (1.36)
\end{aligned}$$

In the second line we have reshuffled the exponentials in such a way that we have an explicit $\delta(\boldsymbol{\varrho}-\boldsymbol{\varrho}')$-function from the $\boldsymbol{k}$-integral. Using this to integrate the $\boldsymbol{\varrho}'$-integral and defining the dipole cross section as

$$\sigma_{q\bar{q}}(x,\varrho) = \frac{4\pi\alpha_s}{3} \int \frac{d^2\boldsymbol{r}}{\boldsymbol{r}^4} \mathcal{F}(x,\boldsymbol{r}^2)(1-e^{i\boldsymbol{r}\cdot\boldsymbol{\varrho}})(1-e^{-i\boldsymbol{r}\cdot\boldsymbol{\varrho}}) \tag{1.37}$$

we may finally write

$$\sigma_{L,T} = \int d^2\boldsymbol{\varrho} \int d\alpha \, |\psi_{L,T}(\boldsymbol{\varrho},\alpha)|^2 \sigma_{q\bar{q}}(x,\boldsymbol{\varrho}). \tag{1.38}$$

In this calculation we have introduced the photon wave function, describing the splitting of the virtual photon into a $q\bar{q}$-pair. This part of (1.38) is the one, we are able to treat within perturbation theory. The non-perturbative part, that has to be modelled, is represented by the unintegrated gluon distribution (1.33) or directly by the dipole cross section eq. (1.37). In the saturation model by Golec–Biernat and Wüsthoff [27, 34] this cross section is modelled as

$$\sigma_{q\bar{q}} = \sigma_0(1-e^{-\varrho/R}), \tag{1.39}$$

reflecting colour transparency at short distance scales, or small dipole sizes ϱ on the one hand and incorporating unitarity in such a simple way, that the cross section approaches a constant σ_0 for large dipole sizes $\varrho \gg R$. The model has to be seen as in interpolation from perturbative short-distance scales ϱ to the long-range dynamics.

The remarkable result is that with such a simple model one is able to fit HERA-structure function data over a very broad range of x and Q^2. Further, having fixed parameters one may predict diffractive cross sections, since there are no new ingredients involved, but there is an additional square,

$$\sigma_{L,T}^{\text{Diff}} = \int d^2\boldsymbol{\varrho} \int d\alpha\, |\psi_{L,T}(\boldsymbol{\varrho}, \alpha)|^2 \sigma_{q\bar{q}}^2(x_{\mathbb{P}}, \boldsymbol{\varrho}). \tag{1.40}$$

This prediction also holds over a wide range of data.

In addition to the very simple structure of this model, that has a very attractive interpretation in the proton rest frame, it is possible to predict data over a wide range of kinematic variables. Since we may predict the behaviour at small dipole sizes within perturbation theory, the extension of the photon wave function picture to higher orders in α_s would clearly improve the approach.

What to expect at NLO?

At NLO in α_s the structure of the photon wave function picture is not known. As a first naive guess, we may expect extensions for the inclusive cross section in the following way eq. (1.38)

$$\begin{aligned}
\sigma_{NLO} = &\int d^2\boldsymbol{\varrho} \int d\alpha\, \psi_{q\bar{q}}^{(0)}(\boldsymbol{\varrho}, \alpha)^* \sigma_{q\bar{q}}^{(0)}(x, \boldsymbol{\varrho}) \psi_{q\bar{q}}^{(0)}(\boldsymbol{\varrho}, \alpha) \\
&+ \alpha_s \int d^2\boldsymbol{\varrho} \int d\alpha\, \psi_{q\bar{q}}^{(1)}(\boldsymbol{\varrho}, \alpha)^* \sigma_{q\bar{q}}^{(0)}(x, \boldsymbol{\varrho}) \psi_{q\bar{q}}^{(0)}(\boldsymbol{\varrho}, \alpha) \\
&+ \alpha_s \int d^2\boldsymbol{\varrho} \int d\alpha\, \psi_{q\bar{q}}^{(0)}(\boldsymbol{\varrho}, \alpha)^* \sigma_{q\bar{q}}^{(1)}(x, \boldsymbol{\varrho}) \psi_{q\bar{q}}^{(0)}(\boldsymbol{\varrho}, \alpha) \\
&+ \alpha_s \int d^2\boldsymbol{\varrho} \int d^2\boldsymbol{\varrho}' \int d\alpha\, \psi_{q\bar{q}g}^{(0)}(\boldsymbol{\varrho}, \boldsymbol{\varrho}', \alpha, \alpha')^* \sigma_{q\bar{q}g}^{(0)}(x, \boldsymbol{\varrho}, \boldsymbol{\varrho}') \psi_{q\bar{q}g}^{(0)}(\boldsymbol{\varrho}, \boldsymbol{\varrho}', \alpha, \alpha') \\
&+ \cdots \quad .
\end{aligned} \tag{1.41}$$

We might expect to have NLO corrections to the wave function or the dipole cross section as in the second and third line. But also new structures like higher Fock components of the photon wave function may appear. If we go back to our derivation of the leading order formula, we see that the dipole cross section got its contribution from the diagrammatic calculation of the wave function in terms of the Fourier transform. It is not clear if this will still be the case at NLO in the same simple way. At LO we have many nice properties of which it is not clear, whether they persist at NLO. E.g. in eq. (1.37) we have the property of colour transparency just from the factor in the exponentials, that stemmed back from the two different diagrams. A main question of NLO corrections will be their arrangement in terms of corrections to the wave function and to higher order terms in the dipole cross section.

But there are more features of the leading order formula that are not necessarily conserved if we go to higher orders. In deriving (1.38) we have made use of the property that the wave function in momentum space came as a difference with a particular momentum dependence. If this will naively be true at NLO is unclear. This form lead to the possibility to factor out the exponentials from the Fourier transform and to shift them into the definition of the dipole cross section. This will not be the case if it is impossible to write the NLO correction in such a form and this would, due to the loss of factorization, spoil the interpretation in the proton rest frame.

On the basis of a solid calculation of the wave function at NLO, one might think about new structures in terms of this interpretation. New terms in the Fock expansion might well appear. Apart from the question of where to put the corrections it would be most natural that an interpretation in terms of a higher term in the multipole expansion of the colour charges could appear, in this case, this might be a colour octupole.

To summarize, we have seen that the scattering of virtual photons off protons has a very simple interpretation in the proton rest frame, leading to the interpretation of the perturbative part of the description as a wave function for the fluctuation of the virtual photon into a $q\bar{q}$-pair. On this basis the simple and very successful saturation model has been formulated. The calculation of NLO order corrections to this picture might reveal some very interesting insights into the foundations of perturbative interactions between small size virtual photons and large hadrons. This thesis will provide the basic calculations which are needed to answer these questions.

1.2 Virtual photon scattering at high energies

In this section we want to focus on the $\gamma^*\gamma^*$-scattering process. Since we consider the scattering of two very small size objects, we have good reason to be able to describe the total cross section $\sigma_{\text{tot}}^{\gamma^*\gamma^*}$ in terms of a purely perturbative calculation. We consider our process in the kinematical region, where

$$s \gg Q_1^2 \sim Q_2^2 \sim \text{of fixed order.} \tag{1.42}$$

In this region we expect the main contributions to our scattering amplitudes to come from leading logarithms in the energy, while we keep the strong coupling small,

$$\alpha_s \log s \sim 1, \qquad \alpha_s \ll 1. \tag{1.43}$$

The only contribution in this region comes from gluon ladder diagrams of the type sketched in Fig. 1.3. Here, the gluons in the t-channel are reggeized gluons, sketched as zigzag-lines while the emitted gluons are real gluons (curly). The virtualities of the external photons Q_1^2, Q_2^2 serve as the large external scales in the process. In our description we want to keep both virtualities of the same order of magnitude, otherwise additional large logarithms of transverse momenta could be present, i.e. in addition, the gluons were subject to DGLAP evolution.

We obtain the total cross section from the imaginary part of the elastic forward scattering amplitude that in turn is the amplitude for pomeron exchange in the high energy limit. In pQCD this process is associated with the exchange of gluon ladders and the respective amplitude is obtained from the BFKL equation. In this section we briefly outline the principles of this description at LO and NLO. Our focus shall be put onto the calculation of impact factors for NLO processes that are the subject of this thesis.

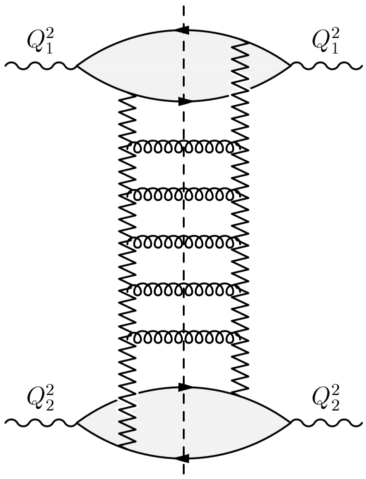

Figure 1.3: The cross section $\sigma_{\mathrm{tot}}^{\gamma^*\gamma^*}$ from LO BFKL ladder exchange.

Review of LO BFKL

The property of the gluon reggeization plays a key role in the derivation of the LO and also NLO BFKL equation. Every amplitude in LLA is expressed in terms of effective vertices between external particles (P) and reggeized gluons (R) and the gluon trajectory function (1.44). The important point is, that any amplitude is indeed found to obey a factorization as it is expected on general grounds from any amplitude in the limit (1.42). This factorization is called Regge-factorization. The reggeization of the gluon means that any amplitude with exchange of gluon quantum numbers reduces to an amplitude with the exchange of a single reggeon, having a trajectory

$$j(t) = 1 + \omega(t) \tag{1.44}$$

For brevity, $\omega(t)$ itself is often called the gluon trajectory function. Up to leading logarithmic accuracy (LLA) it is well-known. The trajectory function (1.44)

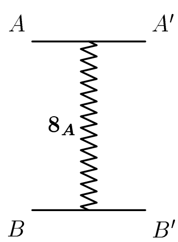

Figure 1.4: Generic diagram for $\mathbf{8}_{\boldsymbol{A}}$-Reggeon exchange.

is obtained in pQCD from a Regge ansatz for the exchange of an antisymmetric octet particle, the reggeized gluon. We make a general ansatz for the general case of the elastic scattering of two particles A and B in the high energy limit for the exchange of a particle with negative signature, as it is sketched in Fig. 1.4,

$$\mathcal{A}_8 = \Gamma_A \frac{s}{t} \left[\left(\frac{s}{-t} \right)^{\omega(t)} + \left(\frac{-s}{-t} \right)^{\omega(t)} \right] \Gamma_B. \tag{1.45}$$

The PPR-vertices Γ_A and Γ_B as well as the trajectory function are supposed to be calculable within perturbation theory. Therefore we make a loop expansion for Γ_A and $\omega(t)$.

$$\Gamma_{A,B} = g\Gamma^{(0)}_{A,B} + g^3\Gamma^{(1)}_{A,B} + \cdots \tag{1.46}$$

$$\omega(t) = g^2\omega^{(1)}(t) + g^4\omega^{(2)}(t) + \cdots . \tag{1.47}$$

Note that the leading term for $\omega(t)$ is already at one loop while $\Gamma_{A,B}$ start with a single strong coupling g. From this ansatz we obtain the following expansion for the Regge ansatz (1.45)

$$\begin{aligned} \mathcal{A}_8 = \; & \alpha_s \frac{s}{t} \Big\{ 2\,\Gamma^{(0)}_A \Gamma^{(0)}_B + \alpha_s \Gamma^{(0)}_A \,\omega^{(1)} \left[\ln \frac{s}{-t} + \ln \frac{-s}{-t} \right] \Gamma^{(0)}_B \\ & + 2\alpha_s \left(\Gamma^{(1)}_A \Gamma^{(0)}_B + \Gamma^{(0)}_A \Gamma^{(1)}_B \right) \Big\}. \end{aligned} \tag{1.48}$$

The very first term is the only term we obtain from a tree level calculation while the additional terms appear in a calculation up to one loop. From a viewpoint of counting α_s together with logarithms, we see that the first line belongs to the leading logarithmic approximation (LLA) while the second line is already beyond LLA, it is in the next-to-leading logarithmic approximation (NLLA), since the additional coupling α_s is not accompanied by a $\log s$. If we want to

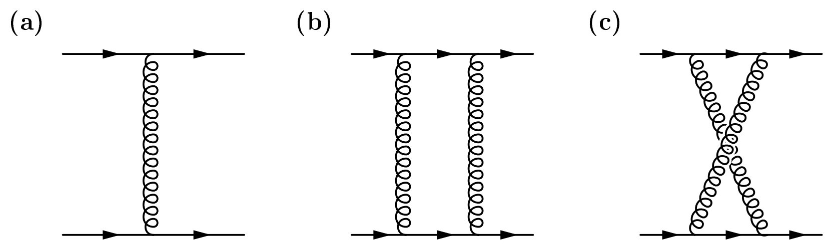

Figure 1.5: Feynman diagrams to calculate high energy scattering amplitudes in the leading logarithmic approximation.

determine the gluon trajectory from the simplest possible process, we might calculate the elastic scattering of two massless quarks in the high energy limit. The leading order calculation in α_s, as sketched in Fig. 1.5 (a), is expected to give the first term in the expansion (1.48). Indeed, we obtain the simple PPR-vertex in the helicity basis of the incoming and outgoing quarks,

$$\Gamma^{(0)}_{QQ} = t^a_{ij}\delta_{hh'}. \tag{1.49}$$

t^a_{ij} denotes the colour group generator we would expect for the coupling of a quark line to an octet particle. Going to one loop order, we may calculate the two gluon exchange amplitudes in Fig. 1.5 (b) and (c). In principle, there are more one-loop diagrams which we should consider, but in LLA these diagrams will not contribute, since they don't give a logarithm in the energy: all ultraviolet divergent diagrams, the vertex and self-energy corrections, do not contribute here. Therefore, α_s is considered to be really a constant. Once, we calculate the contributing diagrams in Fig. 1.5 (b) and (c), they give us the second term in the first line of (1.48) and since we know the PPR vertices from the tree-level calculation, we can identify the trajectory function $\omega^{(1)}(t)$. From the point of view of perturbation theory, $\omega^{(1)}(t)$ represents the virtual corrections to the single gluon exchange and it contains infrared singularities. We can express $\omega^{(1)}(t)$ in space-time dimension $D = 4 - 2\epsilon$ as

$$\omega^{(1)}(t) = \frac{2g^2 N_c}{(4\pi)^{2-\epsilon}} \frac{c_\Gamma (-t)^{-\epsilon}}{\epsilon}. \tag{1.50}$$

For $\epsilon \to 0$ we have $c_\Gamma \approx 1 - \gamma_E \epsilon$ and N_c is the number of colours. It has been proven even to higher orders, that in LLA the Regge ansatz (1.45) for the exchange of an antisymmetric octet is consistent, i.e. given only by the elements $\Gamma^{(0)}_{A,B}$ and $\omega^{(1)}(t)$. Therefore, to LLA the property of the reggeization of the gluon is understood to govern the behaviour of high energy processes in pQCD.

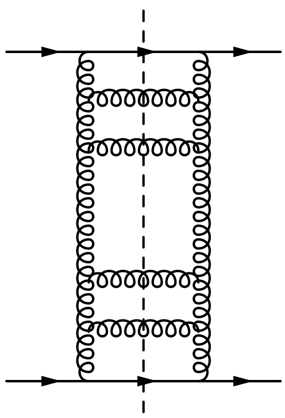

Figure 1.6: Ladder diagram for the calculation of n-gluon emission amplitudes.

Apart from the gluon trajectory (1.50), that represents the virtual part of the LLA corrections, there are also contributions from real gluon emission that lead to large logarithms in the energy. Let us consider the amplitude for elastic quark scattering $A + B \to A' + B'$ in the limit (1.42). Since we expect large logarithms to play an important role, we expect to get contributions from any order in α_s. Therefore, we may determine the s-channel imaginary part of the elastic amplitude $\mathrm{Im}_s \mathcal{A}_{AB}^{A'B'}(s,t)$ from the amplitude for the emission of any number n of gluons $A_{AB}^{A'B'+n}$ as it is sketched in Fig. 1.6,

$$\mathrm{Im}_s\, \mathcal{A}_{AB}^{A'B'}(s,t) = \sum_{n=0}^{\infty} \int d\Phi_{2+n}\, A_{AB}^{A'B'+n} (A_{AB}^{A'B'+n})^*, \tag{1.51}$$

where $d\Phi_{2+n}$ is the phase space measure for the $2+n$-particle intermediate state. The incoming (outgoing) quarks have the light cone momenta $p_A(p'_A)$ and $p_B(p'_B)$. The emitted gluons carry a momentum k_i with a Sudakov decomposition

$$k_i = \alpha_i p_A + \beta_i p_B + k_\perp \tag{1.52}$$

and a colour index d_i. The momenta carried by the t-channel gluons are labelled with q_i and they carry a colour c_i. We expect the contribution to the LLA from the region of phase space, where the Sudakov-components of the emitted gluons are strongly ordered along the ladder,

$$\begin{aligned} &1 \gg \alpha_1 \gg \cdots \gg \alpha_n \gg -t/s \\ &-t/s \ll \beta_1 \ll \cdots \ll \beta_n \ll 1, \end{aligned} \tag{1.53}$$

and the transverse momenta are of fixed order $\boldsymbol{q}_i^2 \sim -t$ and not further constrained. This kinematics, where we have a strong ordering in rapidity is also called Multi-Regge-kinematics (MRK). In this limit, the amplitudes for the emission of n gluons are expected to have the simple Multi-Regge form

$$A_{AB}^{A'B'+n} = 2s\Gamma_{AA'}^{c_1} \left[\frac{1}{t_1} \left(\frac{s}{s_0} \right)^{\omega(t_1)} \right] \gamma_{c_1 c_2}^{d_1} \cdots \gamma_{c_n c_{n+1}}^{d_n} \left[\frac{1}{t_{n+1}} \left(\frac{s}{s_0} \right)^{\omega(t_{n+1})} \right] \Gamma_{BB'}^{c_{n+1}}. \tag{1.54}$$

Herein, $\Gamma_A^{c_1}$ and $\Gamma_B^{c_{n+1}}$ denote the coupling of the external quarks to the reggeized gluons, the PPR-vertex (1.49).

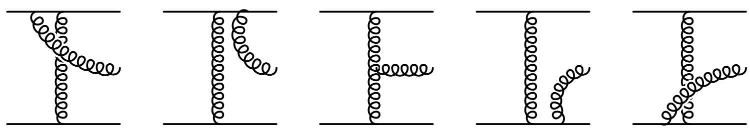

Figure 1.7: Feynman diagrams for the calculation of the effective vertex $\gamma_{cc'}^{d}(q_i, q_{i+1})$.

$\gamma_{c_i c_{i+1}}^{d_i}$ denotes the effective vertex for the emission of a real gluon with colour d_i from a reggeized gluon with colours c_i and c_{i+1} in the initial and final state. In general it is called reggeon-reggeon-particle-vertex or briefly RRP-vertex. In the LLA case it is given by

$$\gamma_{c_i c_{i+1}}^{d_i} = g f_{c_i c_{i+1} d_i} e_\mu^* C^\mu, \tag{1.55}$$

where e_μ^* is the polarization vector of the emitted gluon and C^μ is the nonlocal Lipatov vertex

$$C^\mu(q_{i+1}, q_i) = -(q_i + q_{i+1})_\perp^\mu - \left(\alpha_i + \frac{2\boldsymbol{q}_i^2}{\beta_{i+1} s} \right) p_A^\mu - \left(\beta_{i+1} + \frac{2\boldsymbol{q}_{i+1}^2}{\alpha_i s} \right) p_B^\mu \,. \tag{1.56}$$

The vertex is calculated from the amplitude for the emission of a single gluon in the MRK, $AB \to A'B'g$ with a Regge ansatz like (1.54). The respective Feynman diagrams are shown in Fig. 1.7. The calculation does in fact lead to a Regge type factorization and the vertex is found from the result, since the universal gluon-trajectory function $\omega(t)$ and the PPR vertices $\Gamma_{A,B}$ are already known[2]. The contributions to the LLA, the leading logarithms are finally obtained from the integration over the n gluon phase space. From the effective vertices and the knowledge of the trajectory function one is able to construct a general expression for the sum of all ladder diagrams of the type sketched in Fig. 1.6. The sum over any number of rungs is obtained by the solution of an integral equation.

Let us call $\mathcal{G}_\omega(\boldsymbol{k},\boldsymbol{k}')$ the partial wave of the transition amplitude for two reggeons in the t-channel. Considering the scattering with colour singlet exchange, $\mathcal{G}_\omega$ is the Green's function for the scattering of two reggeized gluons in the forward direction. In the LLA $\mathcal{G}_\omega(\boldsymbol{k},\boldsymbol{k}')$ represents the sum of all ladder diagrams with n gluon rungs and is obtained as a solution of the famous BFKL equation. The amplitude for n gluon emission is constructed from the general amplitude (1.54) for which we have discussed all building blocks, the effective vertices and the gluon trajectory function. Squaring this amplitude, we are left with a sum of amplitudes for any number of rungs. But this sum is identical to the perturbative solution of the integral equation

$$\omega\mathcal{G}_\omega(\boldsymbol{k},\boldsymbol{k}') = \delta^{(D-2)}(\boldsymbol{k}-\boldsymbol{k}') + \int d^{D-2}\tilde{\boldsymbol{k}}\, \mathcal{K}(\boldsymbol{k},\tilde{\boldsymbol{k}})\mathcal{G}(\tilde{\boldsymbol{k}},\boldsymbol{k}'), \tag{1.57}$$

the BFKL equation. The integral kernel $\mathcal{K}(\boldsymbol{k},\boldsymbol{k}')$ reads

$$\mathcal{K}(\boldsymbol{k},\boldsymbol{k}') = 2\omega(-\boldsymbol{k}^2)\delta^{(D-2)}(\boldsymbol{k}-\boldsymbol{k}') + \mathcal{K}_R(\boldsymbol{k},\boldsymbol{k}'). \tag{1.58}$$

Here, $\omega(-\boldsymbol{k}^2)$ is the gluon trajectory function (1.50), the part of the kernel arising form virtual corrections, as we have seen before. The real part of the kernel is basically the square of the effective vertex $\gamma^d_{cc'}(q_i,q_{i+1})$ from (1.55) for the emission of real gluons. In the forward direction it is fairly simple,

$$\begin{aligned} \mathcal{K}_R(\boldsymbol{k},\boldsymbol{k}') =& \frac{1}{(2\pi)^{D-1}\boldsymbol{k}^2\boldsymbol{k}'^2(N^2-1)} \sum_{d,c,c'} |\gamma^d_{cc'}(\boldsymbol{k},\boldsymbol{k}')|^2 & (1.59)\\ =& \frac{g^2N}{(2\pi)^{D-1}}\frac{2}{(\boldsymbol{k}-\boldsymbol{k}')^2}. & (1.60) \end{aligned}$$

One important property of the kernel is its infrared finiteness. We have seen already that the gluon trajectory function had to be regulated e.g. in dimensional regularization, as we did in (1.50). There are also infrared divergences from that part of the phase space where the emitted gluons are soft. However, these two types of divergences cancel out in the kernel, i.e. the BFKL equation is infrared finite to any order in α_s.

[2] In LLA the ansatz (1.54) does not depend on the trajectory function. Therefore, it would be sufficient to know the PPR vertex.

$\mathcal{G}_\omega(\boldsymbol{k},\boldsymbol{k}')$, the partial wave of the gluon ladder, projected into the colour singlet state is a general solution of this equation. If we consider the most relevant case of a Kernel, averaged over azimuthal angles, we can diagonalize the integral equation in terms of the eigenfunctions $(\boldsymbol{k}^2)^{\gamma-1}$ and the corresponding eigenvalue function $\chi(\gamma)$:

$$\int d^{D-2}\boldsymbol{k}'\mathcal{K}(\boldsymbol{k},\boldsymbol{k}')(\boldsymbol{k}'^2)^{\gamma-1} = \frac{N\alpha_s}{\pi}\chi(\gamma)(\boldsymbol{k}^2)^{\gamma-1}. \tag{1.61}$$

The eigenvalue function is expressed in terms of the logarithmic derivative of the Γ-function $\psi(\gamma) = \Gamma'(\gamma)/\Gamma(\gamma)$,

$$\chi(\gamma) = 2\psi(1) - \psi(\gamma) - \psi(1-\gamma). \tag{1.62}$$

With $\gamma = 1/2 + i\nu$ and real and arbitrary ν the eigenfunctions $(\boldsymbol{k}^2)^{i\nu-1/2}$ form a complete set. From this solution we can already estimate the behaviour of cross sections for very high energies: the maximal value of $\chi(1/2+i\nu)$ on the integration contour is $\chi(1/2) = 4\ln 2$, leading to a maximal eigenvalue of the kernel of

$$\omega_{\mathrm{BFKL}} = \frac{4N\alpha_s}{\pi}\ln 2. \tag{1.63}$$

For $N = 3$ colours and $\alpha_s \sim 0.2$ we have $\omega_{\mathrm{BFKL}} \sim 0.5$, leading to the very strong rise of cross sections.

NLO BFKL

As we have seen in the last section, the LO BFKL equation predicts a fairly large rise of total cross sections. Even though, we did not really look at a detailed calculation, but rather took a look into leading terms and even ignored the coupling of external particles, this statement will still hold also for a more detailed calculation. Let us now take a brief look into the long course of the calculation of NLO corrections to the BFKL pomeron.

In the last section we have seen the systematics behind the calculation of high energy amplitudes in pQCD, starting from multi-gluon emission amplitudes and leading to effective vertices for the interaction between reggeized gluons and several external particles. The calculation of NLO corrections to the BFKL equation follows the same strategy. From a general Regge form for different types of amplitudes one is able to extract NLO effective vertices from pQCD amplitudes. During the calculation of higher loop amplitudes, Fadin and Lipatov and collaborators made extensive use of unitarity relations for loop amplitudes. In Fig. 1.8 we have sketched the different types of corrections we have at next-to-leading logarithmic accuracy (NLLA)

$$\alpha_s\left(\alpha_s \log s\right)^n, \qquad n \in \mathbb{N}. \tag{1.64}$$

At NLLA we can have different types of correction, either from additional loops in the amplitude or from the relaxation of the restriction to MRK. The first, purely virtual contribution, sketched in Fig. 1.8a is the correction to the trajectory function of the gluon [35]. The kernel for the real emission of particles, in LLA basically calculated from the square of the RRP-vertex (1.59),

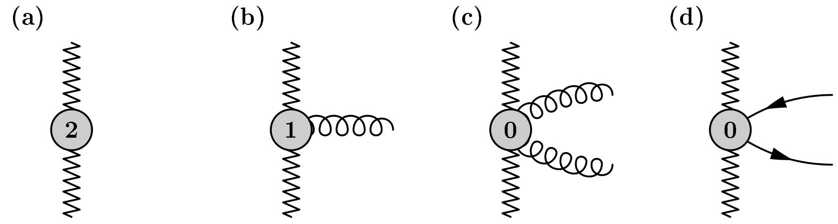

Figure 1.8: Different sources for NLO corrections to the BFKL kernel.

has different sources of NLO corrections. First of all, we can have loop corrections to the emission of a single gluon, Fig. 1.8b [36]. The gluon is, as in LLA (Fig. 1.7), restricted to be emitted in MRK, i.e. with a large rapidity gap to all other particles in the final state.

The other source of corrections arises from the relaxation of the restriction to strongly ordered final states in rapidity or, equivalently, in the Sudakov-variables. Having two particles in the final state emitted close to each other we will not get a large logarithm from the phase space integration and therefore we get a contribution to NLLA. These NLLA contributions to the kernel are calculated at tree level. Besides the emission of two gluons, being close in rapidity (Fig. 1.8c) [37], at NLLA we also have the possibility for the emission of a $q\bar{q}$-pair (Fig. 1.8d) [38], that was suppressed by powers of the energy in LLA.

The NLLA corrections were calculated by Fadin and Lipatov and collaborators during a long course of almost ten years and a first estimate of the size $\omega_{\rm BFKL}^{\rm NLO}$ has has shown that the corrections are fairly large and lower the leading order result. However, even a negative hard pomeron intercept at moderate values of α_s was found. This behaviour triggered a lot of work leading to a good understanding of this behaviour. The pair of gluons being emitted in QMRK may produce large logarithms from the region where the transverse momenta are strongly ordered. These large logarithms spoil the NLLA expansion in α_s and energy logarithms.

A first way out is the restriction of the phase space of the emitted particles in rapidity, called rapidity veto effect and has been studied in [24]. More formal and accurate is a complete DGLAP resummation of these additional logarithms [25]. In both cases, the result is remarkable: the large corrections have turned the extreme behaviour, that leads to a negative pomeron intercept into a rather smooth behaviour of the intercept with α_s leading to values of $\omega \sim 0.3$ to 0.4 for moderate values of $\alpha_s \sim 0.2$.

This is a highly encouraging result, giving hope for a perturbative description of several total cross sections, that are expected to be governed by the hard, perturbative pomeron and rise with a similar power in the energy. Aside of the growth of the structure function $F_2(x, Q^2)$ towards small values of x there is the production of vector mesons at HERA , especially J/ψ and of course there is the total cross section for the scattering of two virtual photons.

General results on impact factors for NLO BFKL

After this very brief discussion of the LO and NLO BFKL kernels we want to return to one of the most interesting applications of this formalism: the scattering of virtual photons. We have already discussed that virtual photons are excellent probes for pQCD due to their small size. Therefore the calculation of the total cross section for $\gamma^*\gamma^* \to$ hadrons was considered as a test of the applicability of the BFKL formalism [15, 16]. Experimental data are recently measured in the reaction $e^+e^- \to e^+e^- + X$ by tagging the outgoing leptons at LEP or at a future Linear Collider and determining the virtualities Q_1^2 and Q_2^2 of the virtual photons. Up to leading order the predictions of the BFKL turned out to be clearly too large [18, 39]. The data lie clearly above the (constant) curve from simple two gluon exchange but much below the LO BFKL prediction.

However, detailed studies show a number of uncertainties. First of all, the results have an intrinsic dependence on the Regge scale. Formally this dependence is of sub-leading order and does not belong to the LLA, though its dependence must not be numerically small in a phenomenological study. Further, in [18] it has been shown that the variation of prediction with the value of α_s is quite substantial. However, the predicted power of the growth in s lies much above the value that is given by the experiments at LEP. All of these caveats clearly point out the need for NLO corrections. First checks, whether the NLO corrections [22, 23] could cure this problem are performed and their hints are very promising [39]. The power of the growths in s seems to be compatible with the expectations from experimental data. But in either case, this comparison cannot be viewed as being serious, since the coupling of the ladder to the virtual photons was still taken in leading order.

The corrections to the impact factors are obtained from the one-loop corrections to the PPR-vertices, with a similar ansatz as in the LLA. The main difference is that at NLO we have two contributions of different type: (a) virtual corrections to the vertex Γ_A, i.e. we extend the expansion (1.46) to NLO and look for the term $\Gamma^{(1)}_{AA'}$, and (b) in addition we can have the emission of one extra gluon in the final state, i.e. another effective vertex of the type[3] $\Gamma^{(0)}_{A(A'+g)}$. The details of the calculations for the impact factor of virtual photons at NLO are the subject of the following chapters. Before turning to the actual calculation, we briefly want to discuss, how the impact factors actually lead to a total cross section and what kinds of subtleties are involved.

We will obtain the total cross section from the imaginary part of the elastic forward scattering amplitude. We will discuss the most general case of a process $A + B \to A' + B'$. In the high energy limit we expect Regge factorization and the answer for the elastic amplitude is expressed most universal in terms of so called impact factors $\Phi_{A,B}(\boldsymbol{k}, s_0)$ and a Green's function $\mathcal{G}_\omega(\boldsymbol{k}, \boldsymbol{k}', s_0)$ for the exchange of the gluon ladder in a definite colour state. The imaginary part of our forward scattering amplitude (1.51) or, equivalently, the total cross section for the scattering of the particles A and B is then written in the following

[3] For two reasons the common term PPR-vertex starts to be confusing, here. First, already at leading order we have a two particle $q\bar{q}$ intermediate state, not a single particle. Second, the additional gluon at NLO will definitely spoil this notation.

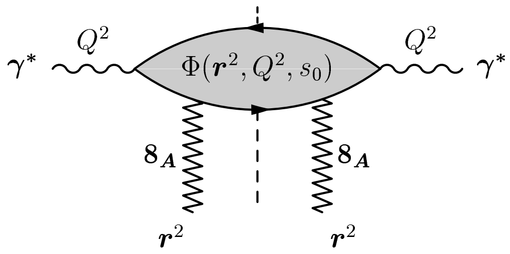

Figure 1.9: The photon impact factor.

factorized form [40, 41], see also Fig. 1,

$$\begin{aligned}\sigma_{AB}(s) =& \frac{1}{(2\pi)^{D-2}} \int \frac{d^{D-2}\boldsymbol{k}}{\boldsymbol{k}^2} \int \frac{d^{D-2}\boldsymbol{k}'}{\boldsymbol{k}'^2} \\ &\times \Phi_A(\boldsymbol{k}, s_0) \left[\int_{\delta-i\infty}^{\delta+i\infty} \frac{d\omega}{2\pi i} \left(\frac{s}{s_0}\right)^{\omega} \mathcal{G}_\omega(\boldsymbol{k}, \boldsymbol{k}', s_0) \right] \Phi_B(\boldsymbol{k}', s_0).\end{aligned} \tag{1.65}$$

We can drop the dependence on the Regge scale parameter s_0 in LLA, since the dependence of the cross section σ_{AB} on this parameter is suppressed logarithmically in the LLA. The impact factors for particle A in (1.65), and analogously the one for B, is defined in terms of the effective vertices in LLA as (we dropped the s_0 dependence here)

$$\Phi_A(\boldsymbol{k}) = \sum_{n=1}^{N} \int \frac{dM^2}{2\pi} d\phi_n |\Gamma_A(\boldsymbol{k})|^2. \tag{1.66}$$

where $d\phi_n$ is the phase space element of a possible n-particle intermediate state and M^2 is the invariant mass of this intermediate state. Further, we have not displayed the sum over the discrete quantum numbers of intermediate particles explicitly. In the impact factor for virtual photons, Fig. 1.9, for example, we have a multi-particle intermediate state. Therein, the effective vertex Γ_{γ^*} is proportional to the photon wave function, that we have discussed in the previous section to leading order. In general, the impact factors $\Phi_{A,B}$ carry all the dependence of the of cross section on the properties of the external particles A and B.

At NLO we cannot drop the dependence on the energy scale in both, impact factor and Green's function, anymore. This may complicate matters, as we will see. Suppose, we choose an energy scale s_1 instead of the scale s_0. Changing the scale in (1.65) leads to

$$\begin{aligned}\sigma_{AB}(s) =& \frac{1}{(2\pi)^{D-2}} \int \frac{d^{D-2}\boldsymbol{k}}{\boldsymbol{k}^2} \int \frac{d^{D-2}\boldsymbol{k}'}{\boldsymbol{k}'^2} \int_{\delta-i\infty}^{\delta+i\infty} \frac{d\omega}{2\pi i} \\ &\times \left(\frac{s}{s_1}\right)^{\omega} \left(\frac{s_1}{s_0}\right)^{\omega} \Phi_A(\boldsymbol{k}, s_0) \mathcal{G}_\omega(\boldsymbol{k}, \boldsymbol{k}', s_0) \Phi_B(\boldsymbol{k}', s_0).\end{aligned} \tag{1.67}$$

While in the LLA the additional factor $(s_1/s_0)^\omega$ is sub-leading, since s_0 and s_1 are arbitrary, but not growing with s, we have to define, how the additional factor has to be absorbed in the scale dependence of the Green's function and the impact factors. In our final result, the left-hand-side of (1.67) will, however, not depend upon the choice of the scale. This clearly shows, that we have to be very careful in defining an impact factor at NLLA, because the definition has to keep track of the choice of s_0 that was used in the determination of the Green's function.

The limit $Q_1^2 \ll Q_2^2$

We want to consider the scattering of two virtual photons with virtualities Q_1^2 and Q_2^2. Let us take the symmetric scale $s_0 = kk'$, $k = |\boldsymbol{k}|$, $k' = |\boldsymbol{k}'|$ as a starting point, which seems to be most natural from the point of view of the Green's function. If we want to consider $\gamma^*\gamma^*$-scattering on the other hand, it would be most natural use the virtualities Q_1^2 and Q_2^2 of the photons as a scale, e.g. as the geometric mean $s_0 = Q_1 Q_2$. Let us share the additional factors from the change of the scale between the two impact factors,

$$\begin{aligned} \sigma_{\gamma^*\gamma^*}(s) =& \frac{1}{(2\pi)^{D-2}} \int_{\delta-i\infty}^{\delta+i\infty} \frac{d\omega}{2\pi i} \int \frac{d^{D-2}\boldsymbol{k}}{\boldsymbol{k}^2} \int \frac{d^{D-2}\boldsymbol{k}'}{\boldsymbol{k}'^2} \\ &\times \left(\frac{s}{Q_1 Q_2}\right)^{\omega} \Phi_{\gamma^*}(\boldsymbol{k}, Q_1) \left(\frac{Q_1}{k}\right)^{\omega} \mathcal{G}_\omega(\boldsymbol{k}, \boldsymbol{k}') \Phi_{\gamma^*}(\boldsymbol{k}', Q_2) \left(\frac{Q_2}{k'}\right)^{\omega} . \end{aligned} \tag{1.68}$$

Note, that we have dropped the s_0 dependence in the Green's function. Furthermore, we introduce the Mellin transforms

$$\Phi_{\gamma^*}(\boldsymbol{k}, Q^2) = \frac{1}{Q^2} \int \frac{d\gamma}{2\pi i} \left(\frac{Q^2}{k^2}\right)^{\gamma} \psi(\gamma) \tag{1.69}$$

$$\mathcal{G}_\omega(\boldsymbol{k}, \boldsymbol{k}') = \int \frac{d\gamma}{2\pi i} \left(\frac{k^2}{k'^2}\right)^{\gamma} \frac{1}{\omega - \chi(\gamma)} , \tag{1.70}$$

where $\chi(\gamma)$ is the eigenvalue function of the BFKL kernel. Substituting with the Mellin transforms in the cross section formula (1.68) and evaluating the integrals over $\boldsymbol{k}$ and $\boldsymbol{k}'$, that are trivially done in terms of δ-function representations, we obtain the following result for the cross section,

$$\begin{aligned} \sigma_{\gamma^*\gamma^*}(s) =& \frac{1}{(2\pi)^{D-2}} \frac{1}{Q_1^2 Q_2^2} \int_{\delta-i\infty}^{\delta+i\infty} \frac{d\omega}{2\pi i} \left(\frac{s}{Q_1 Q_2}\right)^{\omega} \\ &\times \int \frac{d\gamma}{2\pi i} \left(\frac{Q_1^2}{Q_2^2}\right)^{\gamma - \frac{\omega}{2}} \frac{\psi(\gamma - \frac{\omega}{2})\psi(-\gamma - \frac{\omega}{2})}{\omega - \chi(\gamma)} \end{aligned} \tag{1.71}$$

If we consider the limit $Q_1^2 \ll Q_2^2$, the answer for the right hand side is well known in the DGLAP scheme and we may infer a condition on a physical choice for the scale s_0 that is preferred by Green's function and impact factors.

Previously, [25] have considered the impact factors for partons in the anomalous dimension space and have taken a constraint from angular ordering on the impact factor to fix the initial scale.

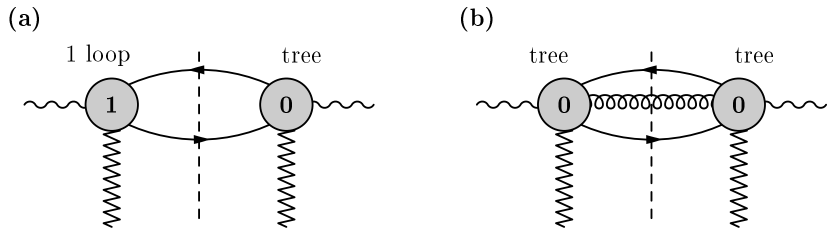

Figure 1.10: Different contributions to the γ^* impact factor at NLO.

Calculation of the impact factor for virtual photons

The photon impact factor is obtained from the energy discontinuity of the amplitude $\gamma^* + reggeon \to \gamma^* + reggeon$ (Fig. 1.9). In leading order α_s this discontinuity is simply the square of the scattering amplitude $\gamma^* + reggeon \to q\bar{q}$ in the tree approximation, and the reggeon, i.e. the reggeized gluon, can be identified with the elementary t-channel gluon (with a particular helicity). In fact, the resulting impact factor at leading order equals the helicity averaged photon wave functions (1.21) and (1.22), integrated over the invariant mass of the $q\bar{q}$-pair or, equivalently, over $d\alpha/\alpha(1-\alpha)$.

In the next-to-leading order new contributions have to be calculated. For the $q\bar{q}$ intermediate state we need the NLO corrections to the $\gamma^* + reggeon \to q\bar{q}$ amplitude either on the left hand side or on the right hand side of the discontinuity line (Fig. 1.10a), and the $q\bar{q}g$ intermediate state requires with leading order amplitudes $\gamma^* + reggeon \to q\bar{q}g$ on both sides of the energy discontinuity line (Fig. 1.10b). The task of calculating the NLO corrections to the photon impact factor therefore can therefore be organized in three steps:

(i) the calculation of the NLO corrections to the $\gamma^* + reggeon \to q\bar{q}$ vertex

(ii) The vertex $\gamma^* \to q\bar{q}g$ in leading order

(iii) the integration over the phase space of the intermediate states.

In chapter 2 we consider the calculation of virtual corrections, step (i) in great detail. The calculation of the real corrections, step (ii) is the subject of chapter 4. The organization of the phase space integration, step (iii), is considered in chapter 3 for the virtual corrections in detail. Explicit results for the phase space integration are given in appendix B.

Chapter 2

The vertex $\Gamma^{(1)}_{\gamma^* \to q\bar{q}}$ at NLO

In this chapter we want to consider the virtual corrections to the γ^* impact factor. As it was outlined in the end of the previous chapter, we obtain the vertex from the one-loop calculation of the process $\gamma^* + q \to q\bar{q} + q$.

2.1 Technical preliminaries

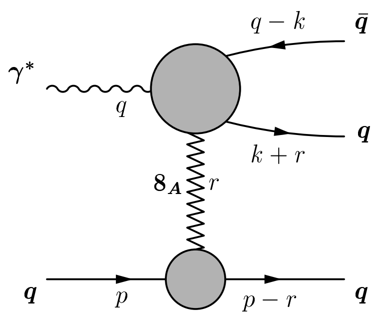

Figure 2.1: Kinematics of the process $\gamma^* + q \to q\bar{q} + q$.

The kinematics is illustrated in Fig. 2.1. As usual, q and p denote the four momenta of the photon and the incoming quark, respectively and $\varepsilon_{L,T}$ the polarization vectors of the photon. We use s to denote the cms energy of the $\gamma^* q$ scattering process, and we introduce the invariants $Q^2 = -q^2$, $t_a = k^2$, $t_b = (q-k-r)^2$, $M^2 = (q+r)^2$, $t = r^2$, and $x = Q^2/2p\cdot q$ for the Bjorken scaling variable. For simplicity, we treat the quarks as massless. We introduce Sudakov variables for all momenta with respect to the light cone vectors $q' = q + xp$ and p, $q'^2 = p^2 = 0$ and $s = 2p \cdot q'$. In this basis, the momenta k and r are written as

$$k = \alpha q' + \beta p + k_\perp \; , \tag{2.1}$$

$$r = \frac{t}{s} q' + \beta_r p + r_\perp \; . \tag{2.2}$$

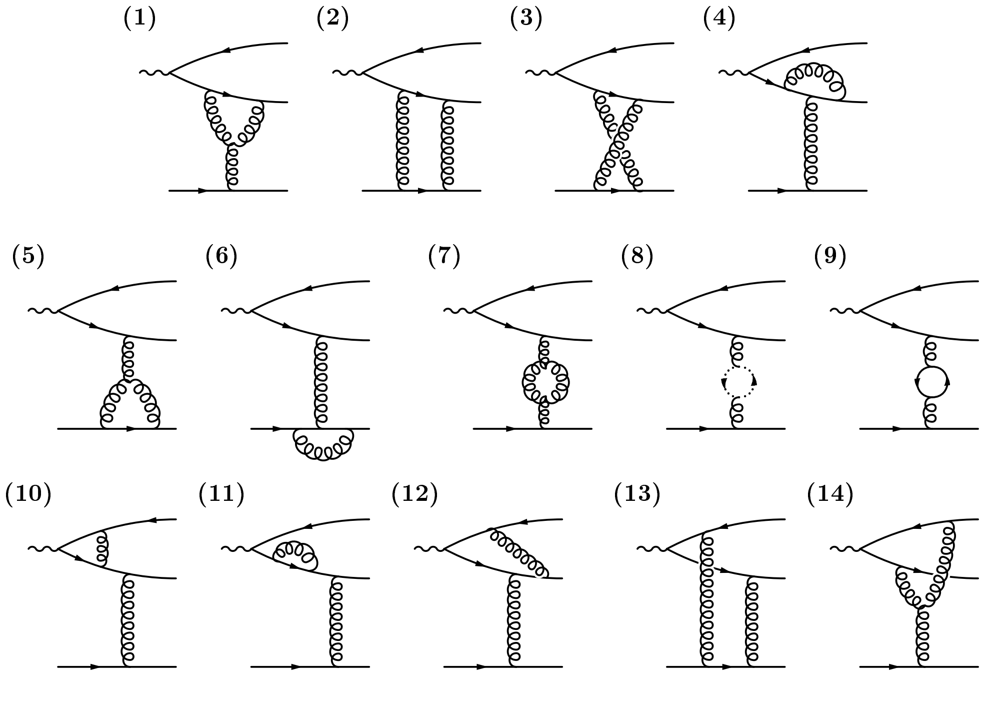

Figure 2.2: Feynman diagrams for the process $\gamma^* + q \to q\bar{q} + q$.

The components β and β_r are given by the on shell conditions for the $q\bar{q}$ pair,

$$\beta s = -\frac{\boldsymbol{k}^2}{1-\alpha} - Q^2, \tag{2.3}$$

$$\beta_r s = \frac{(\boldsymbol{k}+\boldsymbol{r})^2}{\alpha} + \frac{\boldsymbol{k}^2}{1-\alpha} + Q^2. \tag{2.4}$$

The Feynman diagrams which contribute to our NLO-calculation are listed in Fig. 2.2. In addition to the graphs shown, we have to add those diagrams where the t-channel gluon couples to the outgoing antiquark rather than the outgoing quark, except the diagram Fig. 2.2.14. It is easy to see that, for the colour octet t-channel configuration, the sum of all diagrams has to be antisymmetric if we interchange quark and antiquark: $k \to q - k - r$, $\lambda \to \lambda'$. In particular, the 'box' graph shown in Fig. 2.2.14 has to be antisymmetric by itself. We will use the Feynman gauge throughout the calculation, and for the t-channel gluons we decompose the metric tensor according to

$$g_{\mu\nu} = \frac{2}{s}(p_\mu q'_\nu + p_\nu q'_\mu) + g^{\perp}_{\mu\nu}. \tag{2.5}$$

In our calculation we retain only the first term, since the remaining ones are suppressed by powers of the energy. We use the helicity formalism, and our results will be expressed in terms of the following matrix elements:

$$H_T^a = \bar{u}(k+r,\lambda)\not{p}\not{k}\not{\varepsilon}\; \lambda^a v(q-k,\lambda')\;, \tag{2.6}$$
$$\bar{H}_T^a = \bar{u}(k+r,\lambda)\not{\varepsilon}\;(\not{q}-\not{k}-\not{r})\;\not{p}\;\lambda^a v(q-k,\lambda')\;, \tag{2.7}$$
$$H_\varepsilon^a = \bar{u}(k+r,\lambda)\not{\varepsilon}\;\lambda^a v(q-k,\lambda')\;, \tag{2.8}$$
$$H_k^a = \bar{u}(k+r,\lambda)\not{k}\;\lambda^a v(q-k,\lambda')\;, \tag{2.9}$$
$$H_p^a = \bar{u}(k+r,\lambda)\not{p}\;\lambda^a v(q-k,\lambda')\;, \tag{2.10}$$

where $\lambda^a (a = 1,\cdots,8)$ are the colour matrices, and λ and λ' denote the helicities of the outgoing quark pair. Note, that H_T^a and $\bar{H}_T^a$ are identical to the matrix elements (1.9) from the tree level calculation. When interchanging quark and antiquark lines it will be convenient to use the following identity

$$H_T^a + \bar{H}_T^a = sH_\varepsilon^a - 2\varepsilon\cdot pH_k^a - 2\varepsilon\cdot rH_p^a\;. \tag{2.11}$$

We organize our calculations in the following order. We first consider those diagrams (Fig. 2.2.1–9) which can be viewed as "elastic scattering of two quarks", with the upper 'incoming' quark carrying the mass t_a. Correspondingly, the diagrams not shown in Fig. 2.2 define quark-quark scattering with the upper 'incoming' antiquark having the mass t_b. Together with the correction at the photon vertex (Fig. 2.2.10) and the quark self-energy (Fig. 2.2.11), these diagrams are the ones which have to be made ultraviolet finite by renormalization. Following these rather simple diagrams, we turn to the calculation of the box diagrams in Figs. 2.2.12 and 2.2.14, and the pentagon graph shown in Fig. 2.2.13.

We are interested in the high energy limit, where

$$t,\; Q^2,\; t_a,\; t_b,\; M^2\; \ll s\;, \tag{2.12}$$

and we do not impose any restriction on the remaining invariants. The Regge ansatz (1.45) for the scattering amplitude $\gamma^* q \to (q\bar{q})q$ takes the form:

$$T = \Gamma^a_{\gamma^*\to q\bar{q}}\frac{s}{t}\left[\left(\frac{s}{-t}\right)^\omega + \left(\frac{-s}{-t}\right)^\omega\right]\Gamma^a_{qq}\;. \tag{2.13}$$

Here, $1+\omega$ is the gluon trajectory. Expanding all terms in powers on the strong coupling g as in (1.46) and (1.47), we have

$$\omega = g^2\,\omega^{(1)} + g^4\,\omega^{(2)}\;, \tag{2.14}$$
$$\Gamma^a_{\gamma^*\to q\bar{q}} = g\,\Gamma^{(0),a}_{\gamma^*\to q\bar{q}} + g^3\,\Gamma^{(1),a}_{\gamma^*\to q\bar{q}}\;, \tag{2.15}$$
$$\Gamma^a_{qq} = g\,\Gamma^{(0),a}_{qq} + g^3\,\Gamma^{(1),a}_{qq}\;. \tag{2.16}$$

After substituting the corresponding elements in (2.13) with the above expansions, one obtains the following structure of the amplitude

$$T = g^2 T^{(0)} + g^4 T^{(1)} \tag{2.17}$$

with

$$T^{(0)} = \Gamma^{(0),a}_{\gamma^*\to q\bar{q}}\frac{2s}{t}\,\Gamma^{(0),a}_{qq} \tag{2.18}$$

and

$$\begin{aligned} T^{(1)} =& \Gamma^{(1),a}_{\gamma^*\to q\bar{q}}\,\frac{2s}{t}\,\Gamma^{(0),a}_{qq} + \Gamma^{(0),a}_{\gamma^*\to q\bar{q}}\,\frac{2s}{t}\,\Gamma^{(1),a}_{qq} \\ &+ \Gamma^{(0),a}_{\gamma^*\to q\bar{q}}\,\frac{s}{t}\,\omega^{(1)}\left[\ln\frac{s}{-t} + \ln\frac{-s}{-t}\right]\Gamma^{(0),a}_{qq}. \end{aligned} \tag{2.19}$$

Here, e_f represents the charge value of the interacting quark in units of the elementary charge, and the lowest-order expressions on the right hand side of (2.19) are

$$\Gamma^{(0),a}_{qq} = \frac{1}{s}\bar{u}(p-r,\,\lambda_{q'})\not{q}'\lambda^a u(p,\,\lambda_q)\,, \tag{2.20}$$

$$\omega^{(1)}(t) = \frac{2N_c}{(4\pi)^{2-\epsilon}}\,\frac{c_\Gamma}{\epsilon}\,(-t)^{-\epsilon}\,, \tag{2.21}$$

$$\Gamma^{(0),a}_{\gamma^*\to q\bar{q}} = -ie_f e\left(\frac{H^a_T}{st_a} - \frac{\bar{H}^a_T}{st_b}\right)\,, \tag{2.22}$$

here, (2.21) was already discussed in (1.47) and (2.20), as well as (2.22) were obtained in the tree level calculation, cf. (1.8). We expressed the trajectory function in $D = 4 - 2\,\epsilon$ dimensions and used the abbreviation

$$c_\Gamma = \frac{\Gamma(1+\epsilon)\Gamma^2(1-\epsilon)}{\Gamma(1-2\epsilon)} \approx 1 - \gamma_E\epsilon + \frac{1}{2}\left(\gamma_E^2 - \frac{\pi^2}{6}\right)\epsilon^2 + \mathcal{O}(\epsilon^3)\,. \tag{2.23}$$

Here λ_q and $\lambda_{q'}$ are the helicities of the incoming and outgoing quark, respectively, and λ^a are the generators of the colour group. In this chapter, we will present the results of Figs. 2.2.1 – 2.2.14 which can be cast into the form of the right hand side of (2.19). All pieces except for $\Gamma^{(1),a}_{\gamma^*\to q\bar{q}}$ are known from earlier calculations. In particular, the Born result for $\Gamma^{(0),a}_{\gamma^*\to q\bar{q}}$ is well known in the context of the photon wave function formalism, as we have seen in section 1.1. The higher order corrections to the quark-quark-reggeon vertex, $g^3\Gamma^{(1)}_{qq}(t)$, have been calculated in [42]. For vanishing quark masses these corrections are (following the notations of [42]):

$$\Gamma^{(1),a}_{qq}(t) = \lambda^a\left(\Gamma^{(1)}_{qq}(q\bar{q}-\text{state}) + \Gamma^{(1)}_{qq}(gg-\text{state})\right)\delta_{\lambda_q\lambda_{q'}}\,, \tag{2.24}$$

with

$$\begin{aligned} \Gamma^{(1)}_{qq}(q\bar{q}-\text{state}) =& \frac{(-t)^{-\epsilon}}{(4\pi)^{2-\epsilon}}\left[-\frac{n_f}{2}\,\frac{c_\Gamma}{\epsilon(1-2\epsilon)}\left(1 - \frac{1}{3-2\epsilon}\right)\right. \\ &\left. + \frac{c_\Gamma}{2N_c}\left(\frac{2}{\epsilon^2} + \frac{3}{\epsilon} + 8\right)\right] \end{aligned} \tag{2.25}$$

$$\Gamma^{(1)}_{qq}(gg-\text{state}) = \frac{N_c\,(-t)^{-\epsilon}}{(4\pi)^{2-\epsilon}}\left[-\frac{c_\Gamma}{\epsilon^2} + \frac{1}{3}\frac{c_\Gamma}{\epsilon} + \frac{13}{18} + \frac{\pi^2}{2}\right]. \tag{2.26}$$

Inserting these results on the right hand side of (2.19) we can easily obtain $\Gamma^{(1),a}_{\gamma^*\to q\bar{q}}$, which is the goal of this chapter.

For future purposes it will be important to note that the vertex $\Gamma^{(1),a}_{\gamma^*\to q\bar{q}}$ in (2.13) is expected [43] to have a rather complex structure. For example, in the limit of large diffractive masses it will be more convenient to write (2.13) as a sum of two different expressions: the first one depending on M^2 and s, the second one on αs and s (or $(1-\alpha)s$). This decomposition exhibits the reggeization of both the gluon and the quark.

2.2 Analytic Results

We write the NLO amplitude $T^{(1)}$ for the process $\gamma^* + q \to q\bar{q} + q$ as a sum of the different Feynman diagrams:

$$T^{(1)} = \sum_{i=1}^{13} \left(A_i + \bar{A}_i\right) + A_{14}. \tag{2.27}$$

The subscripts i refer to the numbering in Fig. 2.2, and the amplitudes $\bar{A}_i$ correspond to the diagrams which are not shown in Fig. 2.2: they are obtained by interchanging the couplings of t-channel gluons between quark and antiquark lines. Formally, we substitute

$$\begin{aligned} &k \leftrightarrow q-k-r,\ \alpha \leftrightarrow (1-\alpha),\ t_a \leftrightarrow t_b, \\ &H_T^a \leftrightarrow \bar{H}_T^a,\ \varepsilon\cdot k \leftrightarrow -\varepsilon\cdot(k+r),\ \lambda \leftrightarrow \lambda', \end{aligned} \tag{2.28}$$

Under these replacements the matrix elements (2.8)–(2.10) remain unchanged. Finally, A_{14} is antisymmetric with respect to the interchange of quark and antiquark.

Calculational methods

Before presenting explicit analytic expressions for all diagrams we briefly outline the methods we have used to obtain the results.

Starting from the standard Feynman rules of QCD we project the colour in the t-channel into the antisymmetric octet and proceed by introducing Feynman parameters x_i to combine the denominators for the integration of the loop momentum. Only for the simplest diagrams these steps are easily performed by hand. Particularly for the diagrams Fig. 2.2.12–14 this step becomes too tedious. Therefore, we have used the computer algebra system Mathematica with the package FeynCalc [44], in order to reduce the numerators to expressions which contain the helicity matrix elements (2.6) to (2.10), monomials $x_i x_j \cdots$ in the Feynman parameters and, of course, the kinematical invariants. Those diagrams, where the loop integral itself does not depend on the large scale s, the box diagrams Fig. 2.2.12 and Fig. 2.2.14, have to be calculated exactly. The only high energy approximation results from the gluon nonsense helicity (i.e. the first term in (2.5). Diagram Fig. 2.2.13, on the other hand, has first been calculated exactly, and then the high energy limit (2.12) has been taken.

To consider the loop integrations, we had to deal with integrals over the loop momentum itself, which could be easily performed by the usual shift, and with the remaining integrals of the Feynman parameters. Integrals of the latter type are either known, or they could be obtained from known ones with the help of recurrence relations to $\mathcal{O}(\epsilon^0)$ in dimensional regularization. The technical background for these methods is given in [45] and has been applied to almost all cases we are interested in by [46]. We have written a Mathematica package to easily call the results of [46]. In most cases the integrals are recursively expressed in terms of special functions, representing a particular combination of logarithms and dilogarithms for a given n-point function. In the case of diagram Fig. 2.2.14 we have calculated explicit results for integrals with two and three Feynman parameters in the numerator using the derivative method [45]. Also for this task we have used Mathematica.

Finally, after carrying out the integrals, i.e. replacing the monomials of Feynman parameters in our amplitudes with the explicit expressions from our Mathematica package, we have used again FeynCalc to take the high energy limit in the diagrams Figs. 2.2.2, 3, and 13, and to carry out some simplifying algebra. A few final simplifications had to be done by hand. The expressions that we have obtained in this way will be listed in the remainder of this section.

Quark-quark Scattering

It is suggestive to view the diagrams Figs. 2.2.1–9 as a quark-quark scattering processes with one of the incoming quarks being off-shell (with virtuality t_a). We focus on those diagrams in Fig. 2.2, where the t-channel gluon(s) couples to the quark. Those diagrams where the gluon(s) couples to the antiquark are easily obtained by performing the substitutions described after (2.27).

Diagram Fig. 2.2.1 is one of many three point functions with two massive external legs. Loop integrals of this type are well-known, and we have calculated them both by hand and by using computer algebra as outlined above.

$$\begin{aligned} A_1 = \frac{N_c}{2}\frac{1}{(4\pi)^{2-\epsilon}}\Bigg\{ & A^{(0)}\left[\frac{c_\Gamma}{\epsilon}(-t)^{-\epsilon}+2+\frac{2t}{t-t_a}\ln\frac{t}{t_a}\right] \\ & -\frac{(-iee_f)\alpha}{t-t_a}H^a_\varepsilon\frac{2s}{t}\Gamma^{(0),a}_{qq}\left[\frac{c_\Gamma}{\epsilon}(-t)^{-\epsilon}+1-\frac{t}{t-t_a}\ln\frac{t}{t_a}\right]\Bigg\}\ . \end{aligned} \tag{2.29}$$

Here and in the following, we use

$$A^{(0)} = -iee_f\frac{H^a_T}{st_a}\frac{2s}{t}\Gamma^{(0),a}_{qq} \tag{2.30}$$

as a shorthand notation.

In the diagrams Fig. 2.2.2 and Fig. 2.2.3 we have to deal with four-point integrals, where one of the external legs is off-mass shell. Here we make use of the shorthand notations listed in the appendix. The result for the sum of the two diagrams is:

$$\begin{aligned} A_{2+3} = -A^{(0)}N_c\frac{1}{(4\pi)^{2-\epsilon}}\Bigg\{ & \frac{c_\Gamma}{\epsilon^2}\Big[(\alpha s)^{-\epsilon}+(-\alpha s)^{-\epsilon}+(-t)^{-\epsilon}-2(-t_a)^{-\epsilon} \\ & -\frac{t}{t-t_a}\left((-t)^{-\epsilon}-(-t_a)^{-\epsilon}\right)\Big]+\mathrm{Ld}_0^{1\mathrm{m}}(\alpha s,t,t_a)+\mathrm{Ld}_0^{1m}(-\alpha s,t,t_a)\Bigg\} \end{aligned} \tag{2.31}$$

with

$$\mathrm{Ld}_0^{1m}(\alpha s, t, t_a) = \mathrm{Li}_2(1 - \frac{t}{t_a}) + \mathrm{Li}_2(1 - \frac{\alpha s}{t_a}) + \ln\frac{t}{t_a}\ln\frac{\alpha s}{t_a} - \frac{\pi^2}{6} \,.$$

Here, Li_2 is the standard dilogarithm function defined as

$$\mathrm{Li}_2(x) = -\int_0^1 \frac{\ln(1 - xt)}{t} dt \,. \tag{2.33}$$

In order to exhibit the energy dependence we rewrite this expression:

$$\begin{aligned}
A_{2+3} = &- A^{(0)} \frac{N_c}{(4\pi)^{2-\epsilon}} \Big\{ - \frac{c_\Gamma (-t)^{-\epsilon}}{\epsilon} \left[\ln \frac{\alpha s}{-t} + \ln \frac{-\alpha s}{-t} \right] \\
&+ 2 \,\mathrm{Li}_2 \left(1 - \frac{t}{t_a} \right) + \left(\ln \frac{t}{t_a} \right)^2 + \frac{\pi^2}{3} + (-t)^{-\epsilon} \left[\frac{2 c_\Gamma}{\epsilon^2} - \pi^2 \right] \\
&+ \frac{c_\Gamma}{\epsilon^2} \Big[(-t)^{-\epsilon} - 2(-t_a)^{-\epsilon} - \frac{t}{t - t_a} \left((-t)^{-\epsilon} - (-t_a)^{-\epsilon} \right) \Big] \Big\}.
\end{aligned} \tag{2.34}$$

From these two diagrams (and from their respective partners $\bar{A}_{2+3}$) we already get the complete $\ln s$ dependence of our result, in agreement with the rhs of (2.19). In detail, the first line of (2.34) contains, apart from the $\ln \alpha$ dependence, the leading order trajectory function $\omega^{(1)}(t)$ (cf.(2.21), note also, that there is a factor of 2 hidden in the definition of $A^{(0)}$ in comparison with the factors in front of $\omega^{(1)}(t)$ in (2.19)). Furthermore, if we take the limit $t_a \to 0$ in the last two lines, the first three terms in the second line cancel each other, while the last line vanishes and we are left only with the last term of the second line. For symmetry reasons, one half of this term will go to the lower vertex (2.26) (the same result could also have been deduced from [42]). Therefore, the contribution from diagrams 2 and 3 to $\Gamma^{(1),a}_{\gamma^* \to q\bar{q}}$ is just

$$\begin{aligned}
iee_f \frac{H_T^a}{s t_a} \frac{N_c}{(4\pi)^{2-\epsilon}} \Big\{ &- \frac{2 c_\Gamma (-t)^{-\epsilon}}{\epsilon} \ln \alpha + 2 \,\mathrm{Li}_2 \left(1 - \frac{t}{t_a} \right) + \left(\ln \frac{t}{t_a} \right)^2 + \frac{\pi^2}{3} \\
&+ \frac{c_\Gamma}{\epsilon^2} \Big[(-t)^{-\epsilon} - 2(-t_a)^{-\epsilon} - \frac{t}{t - t_a} \left((-t)^{-\epsilon} - (-t_a)^{-\epsilon} \right) \Big] \\
&+ \frac{(-t)^{-\epsilon}}{2} \left[\frac{2 c_\Gamma}{\epsilon^2} - \pi^2 \right] \Big\}.
\end{aligned} \tag{2.35}$$

We emphasize, once more, that the two diagrams $A_{2+3} + \bar{A}_{2+3}$ provide the complete $\ln s$ dependence on the rhs of (2.13). At first sight one might expect that also the pentagon diagrams $A_{13} + \bar{A}_{13}$ might contribute to the energy dependence, since the loop extends over the large scale s. Later we will show that, in fact, this is not the case.

The calculation of Fig. 2.2.4 is very similar to the calculation of Fig. 2.2.1.

We find:

$$A_4 = -\frac{1}{2N_c}\frac{1}{(4\pi)^{2-\epsilon}}\Big\{A^{(0)}\Big[\frac{2c_\Gamma}{\epsilon^2}\left((-t_a)^{-\epsilon}-(-t)^{-\epsilon}\right)-\frac{c_\Gamma}{\epsilon}(-t)^{-\epsilon}$$
$$-4+\frac{2t+t_a}{t-t_a}\ln\frac{t}{t_a}\Big]-iee_f\,\alpha H^a_\varepsilon\frac{2s}{t}\Gamma^{(0),a}_{qq}\left[\frac{2c_\Gamma}{\epsilon^2}\left(\frac{(-t_a)^{-\epsilon}-(-t)^{-\epsilon}}{t-t_a}\right)\right.$$
$$\left.-\frac{2c_\Gamma}{\epsilon}\frac{(-t)^{-\epsilon}}{t-t_a}+\frac{3t+2t_a}{(t-t_a)^2}\ln\frac{t}{t_a}-\frac{5}{t-t_a}\right]\Big\}. \tag{2.36}$$

Diagrams Fig. 2.2.5 and Fig. 2.2.6 are needed to obtain the NLO corrections to the lower vertex $\Gamma^{(1),a}_{qq}$. In agreement with [42] we find:

$$A_5 = -A^{(0)}\,\frac{N_c c_\Gamma}{(4\pi)^{2-\epsilon}}\left(\frac{(-t)^{-\epsilon}}{2\epsilon}+1\right)\,, \tag{2.37}$$

and

$$A_6 = A^{(0)}\,\frac{1}{(4\pi)^{2-\epsilon}}\frac{c_\Gamma}{2N_c}(-t)^{-\epsilon}\left(\frac{2}{\epsilon^2}+\frac{3}{\epsilon}+8\right)\,. \tag{2.38}$$

We note that they can be obtained from Eqs. (2.29) and (2.36) by choosing $\epsilon<0$ and taking the limit $t_a\to 0$.

The calculation of diagrams Figs. 2.2.7–9 is straightforward. They contribute to both the upper and the lower vertex:

$$A_{7+8} = A^{(0)}\,\frac{N_c c_\Gamma}{(4\pi)^{2-\epsilon}}\frac{(-t)^{-\epsilon}}{2\epsilon(1-2\epsilon)}\left(\frac{1}{3-2\epsilon}+3\right)\,, \tag{2.39}$$

Similarly, the $q\bar{q}$-contribution to the gluon-self-energy in Fig. 2.2.9 leads to

$$A_9 = A^{(0)}n_f\,\frac{c_\Gamma}{(4\pi)^{2-\epsilon}}\frac{(-t)^{-\epsilon}}{\epsilon(1-2\epsilon)}\left(\frac{1}{3-2\epsilon}-1\right). \tag{2.40}$$

These diagrams contribute with equal weight to both the upper and to the lower vertex. Therefore, in order to complete the upper reggeon-quark-quark vertex with one off-shell quark, we simply add 1/2 of the sum of (2.39) and (2.40) to the contributions (2.29), (2.36), and (2.37). Similarly, the lower reggeon-quark-quark vertex with all quarks being on-shell is obtained by adding 1/2 of the sum of (2.39) and (2.40) to (2.37), (2.38) and the contribution of the box diagrams Figs. 2.2.2 and 2.2.3:

$$-A^{(0)}\frac{N_c}{(4\pi)^{2-\epsilon}}\frac{(-t)^{-\epsilon}}{2}\left[\frac{2c_\Gamma}{\epsilon^2}-\pi^2\right]. \tag{2.41}$$

To summarize, so far we have analyzed the diagrams Figs. 2.2.1–9. From Figs. 2.2.5, 2.2.6, 1/2 of Figs. 2.2.7–9, and from a piece of Fig. 2.2.2 and 2.2.3. we have reproduced the lower reggeon-quark-quark vertex of [42]. From Figs. 2.2.1, 2.2.4, 1/2 of Figs. 2.2.7–9, and from the major part of Figs. 2.2.2 and 2.2.3 we have computed a new reggeon-quark-quark vertex with one quark having the mass t_a. Moreover, from Figs. 2.2.2 and 2.2.3. we have extracted the $\ln s$ terms of the rhs of (2.19). The remaining diagrams Figs. 2.2.10–14 provide contributions to the upper vertex $\Gamma^{(1),a}_{\gamma^*\to qq}$ only.

Vertex correction and quark self-energy

In this subsection we present the results of the vertex correction Fig. 2.2.10:

$$A_{10} = -\frac{C_{\rm F}}{(4\pi)^{2-\epsilon}}\left\{A^{(0)}\left[\frac{c_\Gamma}{\epsilon}(-t_a)^{-\epsilon} + 4 + \frac{3Q^2}{Q^2+t_a}\ln\frac{-t_a}{Q^2}\right]\right.$$
$$\left. - \Gamma'\frac{2s}{t}\Gamma^{(0),a}_{qq}\left[\frac{4c_\Gamma}{\epsilon}(-t_a)^{-\epsilon} + 10\left(1+\frac{Q^2}{Q^2+t_a}\right)\ln\frac{-t_a}{Q^2}\right]\right\} \tag{2.42}$$

with

$$\Gamma' = -iee_f\,\frac{H^a_p}{s}\frac{\varepsilon\cdot k}{Q^2+t_a}, \tag{2.43}$$

and for the quark self-energy Fig. 2.2.11:

$$A_{11} = -A^{(0)}\frac{C_{\rm F}}{(4\pi)^{2-\epsilon}}(-t_a)^{-\epsilon}\frac{c_\Gamma(1-\epsilon)}{\epsilon(1-2\epsilon)}\,. \tag{2.44}$$

Eqs. (2.42) and (2.44) provide new contributions to the vertex $\Gamma^{(1),a}_{\gamma^*\to qq}$.

The Box diagram Fig. 2.2.12

In this subsection we give the result of the diagram Fig. 2.2.12, which was calculated entirely with the help of the computer algebra (in [46] this diagram has been named ‘adjacent box’). The result will be expressed as follows:

$$A_{12} = \Gamma^{(0),a}_{qq}\frac{2\,s}{t}\left(\frac{-iee_f}{s}\right)\left(-\frac{1}{2N_c}\right)\frac{c_\Gamma}{(4\pi)^{2-\epsilon}}\left[\frac{1}{\epsilon^2}A^{(-2)}_{12} + \frac{1}{\epsilon}A^{(-1)}_{12} + A^{(0)}_{12}\right]. \tag{2.45}$$

Starting with the divergent terms, we have

$$A^{(-2)}_{12} = \frac{2\,\alpha\,H^a_\varepsilon\,s\left((-t)^{-\epsilon} - (-t_a)^{-\epsilon}\right)}{t-t_a} + 2\,H^a_T\left[\frac{(-t)^{-\epsilon} - (-t_a)^{-\epsilon}}{t-t_a} + \right.$$
$$\left.\frac{(-t_a)^{-\epsilon} - Q^{2-\epsilon}}{Q^2+t_a} + \frac{-(-M^2)^{-\epsilon} + Q^{2-\epsilon} + (-t)^{-\epsilon} - 2(-t_a)^{-\epsilon}}{t_a}\right] \tag{2.46}$$

and

$$A^{(-1)}_{12} = 4\,\epsilon\cdot k\,H^a_p\left[\frac{\left((-t)^{-\epsilon} - (-t_a)^{-\epsilon}\right)}{M^2} - \frac{(-t_a)^{-\epsilon}}{Q^2+t_a}\right]$$
$$+ H^a_\varepsilon s\left[\frac{2\,\alpha(-t)^{-\epsilon}}{t-t_a} + \frac{(1-\alpha)\left((-t)^{-\epsilon} - (-t_a)^{-\epsilon}\right)}{M^2}\right]. \tag{2.47}$$

The $\mathcal{O}(\epsilon^0)$ term for the this adjacent box is expressed in terms of many different functions, related to this loop integral. For convenience, the definitions of these functions are listed in the appendix.

$$A^{(0)}_{12} = -2(2H^a_T + s\alpha H^a_\varepsilon){\rm Lc}_0(-Q^2, M^2, t)$$
$$+ \left\{3H^a_T M^2 + H^a_k[6\varepsilon\cdot pM^2 + 2s((8\alpha-3)\varepsilon\cdot k + (5\alpha-3)\varepsilon\cdot r)]\right.$$
$$- s\alpha\,H^a_\varepsilon(3t_a - 2t_b - Q^2) - 2H^a_p(2Q^2\varepsilon\cdot r$$
$$\left. + \varepsilon\cdot k(M^2 - Q^2 - 3t_b))\right\}\frac{{\rm Lc}_1(M^2, -Q^2, t)}{M^2}$$

$$
\begin{aligned}
&+2\big\{H_T^a M^2+2H_k^a(M^2\varepsilon\cdot p-s[\varepsilon\cdot k+(1-\alpha)\varepsilon\cdot r])\\
&\quad+2sH_\varepsilon^a[(1-\alpha)t+\alpha Q^2+t_a]\\
&\quad-4H_p^a[\varepsilon\cdot k(2M^2+Q^2+t)+\varepsilon\cdot r(Q^2+t_a)]\big\}\frac{\mathrm{Lc}_1(-Q^2,M^2,t)}{M^2}\\
&+\big\{2\varepsilon\cdot kH_p^a(2M^2-2Q^2-t_a)-(1-\alpha)sQ^2H_\varepsilon^a-H_T^a(Q^2+t_a)\\
&\quad-2H_k^a[\varepsilon\cdot k(1-2\alpha)s+\varepsilon\cdot p(Q^2+t_a)]\big\}\frac{\mathrm{Lc}_1^{2m}(-Q^2,t_a)}{M^2}\\
&-2\big\{2s\alpha(3\varepsilon\cdot k+\varepsilon\cdot r)H_k^a+sH_\varepsilon^a[\alpha(M^2-Q^2-3t_a)+(t-t_a)]\\
&\quad+H_p^a[3\varepsilon\cdot rt_a+\varepsilon\cdot k\,(4\,t-t_a)]\big\}\frac{\mathrm{Lc}_1^{2m}(t_a,t)}{M^2}\\
&+2\big\{4\varepsilon\cdot pM^2\,H_k^a+3M^2H_T^a-s[\alpha(M^2-2\,Q^2-t)+t]H_\varepsilon^a\\
&\quad-2[\varepsilon\cdot r\,Q^2+\varepsilon\cdot k\,(M^2+Q^2+2\,t)]H_p^a\big\}\frac{\mathrm{Lc}_{1S}(-Q^2,M^2,t)}{M^2t_a}\\
&+4\alpha sH_\varepsilon^a\mathrm{Lc}_2^{2m}(t_a,t)-8\,\varepsilon\cdot k\,H_p^a\mathrm{Lc}_2^{2m}(-Q^2,t_a)\\
&-2\,\big\{H_T^a\,M^2+2H_k^a[\varepsilon\cdot pM^2-s((1-2\alpha)\varepsilon\cdot k+(1-\alpha)\varepsilon\cdot r)]\\
&\quad+2\,H_p^a\varepsilon\cdot k(2M^2+t-t_a)-\alpha sH_\varepsilon^a(Q^2+t_a)\big\}\frac{\mathrm{Lc}_2(-Q^2,M^2,t)}{M^2}\\
&+2\big\{2\varepsilon\cdot k(t_a-M^2)H_p^a+(Q^2+t_a)H_T^a\\
&\quad+2[(1-2\,\alpha)s\varepsilon\cdot k+\varepsilon\cdot p(Q^2+t_a)]H_k^a\big\}\frac{\mathrm{Lc}_3(M^2,-Q^2,t)}{M^2}\\
&-2(2\varepsilon\cdot k\,H_p^a+s\alpha\,H_\varepsilon^a)\mathrm{Lc}_3(-Q^2,M^2,t)-4\,H_T^a\frac{\mathrm{Ld}_0^a(t_a,M^2,-Q^2,t)}{t_a}\\
&+2\big\{t_bM^2H_T^a+st_a[\alpha\,(Q^2+t)-Q^2-2\,\alpha\,M^2-t_b]H_\varepsilon^a\\
&\quad-2t_a[\varepsilon\cdot k\,(2M^2+Q^2+t)+\varepsilon\cdot r\,(t-t_b)]H_p^a\\
&\quad-2[(-(\varepsilon\cdot p\,M^2)+(\varepsilon\cdot k+\varepsilon\cdot r)s)t_a\\
&\quad+s\alpha(2\,\varepsilon\cdot k\,M^2-\varepsilon\cdot r\,t_a)]H_k^a\big\}\frac{\mathrm{Ld}_1(t_a,M^2,-Q^2,t)}{M^2t_a}\\
&-2\{H_T^a+s\,H_\varepsilon^a-2\,\varepsilon\cdot r\,H_p^a\}\mathrm{Ld}_{1S}(t_a,M^2,-Q^2,t)\\
&+\big\{4[\alpha\,s\,(6\,\varepsilon\cdot k\,(t-t_b)+2\,\varepsilon\cdot k\,t_a+2\,\varepsilon\cdot r\,Q^2+3\,\varepsilon\cdot r\,t_a)\\
&\quad-t_a(\varepsilon\cdot p\,M^2+s\,(\varepsilon\cdot k+\varepsilon\cdot r))]H_k^a+4[2\,\varepsilon\cdot r\,t_a\,(t-t_b)\\
&\quad+\varepsilon\cdot k\,(2t(Q^2+t)+(t-t_a)(t_a-2t_b))]H_p^a\\
&\quad-2\,s[\alpha(Q^2+t_a)(2\,Q^2+5t_a)-2(Q^2t+t_at_b)]\,H_\varepsilon^a\\
&\quad-2H_T^aM^2t_a\big\}\frac{\mathrm{Ld}_{21}(t_a,M^2,-Q^2,t)}{2t_aM^2}\\
&+2\big\{-(Q^2+t_a)M^2H_T^a+2[\varepsilon\cdot r\,(Q^2+t_a)\,(t-t_b)\\
&\quad+\varepsilon\cdot k\,((Q^2+t_a)(t-t_a)+(t-t_b)^2)]H_p^a-2[\varepsilon\cdot p\,M^2\,(Q^2+t_a)\\
&\quad-s\,((1-\alpha)\,\varepsilon\cdot r\,(Q^2+t_a)-\varepsilon\cdot k\,(Q^2+t_a-(1-3\,\alpha)\,M^2))]H_k^a\\
&\quad+s\,[(1-\alpha)(Q^2t+t_at_b)-\alpha\,(Q^2+t_a)^2]H_\varepsilon^a\big\}\frac{\mathrm{Ld}_{22}(t_a,M^2,-Q^2,t)}{M^2\,t_a}
\end{aligned}
$$

$$
\begin{aligned}
&+\frac{2\,s\,\alpha\,(Q^2+2\,t_a)\,H_\varepsilon^a\,\mathrm{Ld}_{24}(t_a,M^2,-Q^2,t)}{t_a}\\
&+\big\{24\,\varepsilon\cdot pM^2\,H_k^a+18\,M^2H_T^a-6\,s[t-t_a-\alpha\,(3\,Q^2+2t_a+t_b)]H_\varepsilon^a\\
&\quad-12[\varepsilon\cdot k\,(3\,t-2t_a-t_b)+\varepsilon\cdot r\,(Q^2+t_a)\,)]H_p^a\big\}\frac{\mathrm{Ld}_{2S}(t_a,M^2,-Q^2,t)}{M^2t_a}\\
&+\big\{8\varepsilon\cdot k\,t_a(t_a-t)H_p^a-4(Q^2t+t_at_b)\,H_T^a+8[\varepsilon\cdot k\,s\,(t_a-t)\\
&\quad-\alpha\,\varepsilon\cdot k\,s\,(M^2-2\,t+2\,t_a)-\varepsilon\cdot p\,(Q^2\,t+t_a\,t_b)]H_k^a\big\}\frac{\mathrm{Ld}_{311}(t_a,M^2,-Q^2,t)}{2M^2t_a}\\
&+\big\{4\,\varepsilon\cdot k\,(t-t_a)^2H_p^a-4\,s\,[(\varepsilon\cdot k+\varepsilon\cdot r)\,(t-t_a)\\
&\quad-\alpha\,(2\,\varepsilon\cdot k+\varepsilon\cdot r\;)\,(Q^2+t_b)]H_k^a\\
&\quad-2\,\alpha\,s\,(Q^2\,t+t_at_b)\,H_\varepsilon^a\big\}\frac{\mathrm{Ld}_{314}(t_a,M^2,-Q^2,t)}{M^2t_a}\\
&+4\,(1-\alpha)\,s\,\varepsilon\cdot k\,H_k^a\,\frac{\mathrm{Ld}_{322}(t_a,M^2,-Q^2,t)}{t_a}\\
&-4\,\alpha\,s\,(\varepsilon\cdot k+\varepsilon\cdot r)\,H_k^a\,\frac{\mathrm{Ld}_{344}(t_a,M^2,-Q^2,t)}{t_a}.
\end{aligned}
\tag{2.48}
$$

The Box diagram Fig. 2.2.14

The result of the diagram Fig. 2.2.14 (in [46] named 'opposite box'), can, again, be split into divergent and finite pieces:

$$
A_{14}=\Gamma_{qq}^{(0),a}\,\frac{2s}{t}\left(\frac{-iee_f}{s}\right)\left(\frac{N_c}{2}\right)\frac{1}{(4\pi)^{2-\epsilon}}\left[\frac{c_\Gamma}{\epsilon^2}A_{14}^{(-2)}+\frac{c_\Gamma}{\epsilon}A_{14}^{(-1)}+A_{14}^{(0)}\right].
\tag{2.49}
$$

The term proportional to c_Γ/ϵ^2 reads:

$$
\begin{aligned}
A_{14}^{(-2)}=&\left\{\frac{2\,\varepsilon\cdot p\,H_k^a\;(t_a-t_b)}{Q^2\,t+t_a\,t_b}+\frac{(H_T^a-\bar{H}_T^a)\;(t_a+t_b)}{Q^2\,t+t_a\,t_b}\right.\\
&+\frac{H_\varepsilon^a\,s}{2(t-t_a)^2\,(t-t_b)^2\;(Q^2\,t+t_a\,t_b\;)}\Big[(\alpha\;-(1-\alpha))\,\big(Q^2\,t+t_a\,t_b\big)\\
&\quad\times\big(t^2\;(t_a+t_b)+t_a\,t_b\;(t_a+t_b)-4\,t\,t_a\,t_b\big)\\
&\quad-(t_a-t_b)\;\big(2(t-t_a)^2(t-t_b)^2+\big(Q^2\,t+t_a\,t_b\big)\,\big(t_at_b-t^2\big)\big)\Big]\\
&-\frac{2\;H_p^a}{(t-t_a)\;(t-t_b)\;(Q^2\,t+t_a\,t_b)}\Big[\varepsilon\cdot(k+r)\;(t-t_b)\;\big(t_a\;(t_a-t_b)\\
&\quad\left.+t\;(t_a+t_b)\,\big)+\varepsilon\cdot k\;(t\;-t_a)\,(t_b\,(t_b-t_a)\;+t\;(t_a+t_b))\Big]\right\}(-t)^{-\epsilon}\\
&+\left\{\frac{-2\;\varepsilon\cdot p\,H_k^a\,M^2\,Q^2\;(t_a-t_b)}{(Q^2+t_a)\;(Q^2+t_b)\;(Q^2\,t+t_a\,t_b\;)}+\frac{H_\varepsilon^a\,M^2\,Q^2\,s\;(t_a-t_b\;)}{(Q^2+t_a)\;(Q^2+t_b)\;(Q^2\,t+t_a\,t_b\;)}\right.\\
&+\frac{(H_T^a-\bar{H}_T^a)\,Q^2\;\big({t_a}^2+{t_b}^2-t\;(t_a+t_b)+Q^2\;(t_a+t_b-2\,t)\big)}{(Q^2+t_a)\;(Q^2+t_b)\;(Q^2\,t+t_a\,t_b\;)}
\end{aligned}
$$

$$
\begin{aligned}
&- \frac{2\, H_p^a\, Q^2}{(Q^2+t_a)^2\,(Q^2+t_b)^2\,\left(Q^2\,t+t_a\,t_b\right)}\Big[\varepsilon\cdot k\,\left(Q^2+t_b\right)\,\Big(Q^4\,(t_a-t_b)\\
&+Q^2\,\left(2\,{t_a}^2+t_a\,t_b-{t_b}^2+t\,(t_b-3t_a)\right)+t_a\,\left({t_a}^2+{t_b}^2-t\,(t_a+t_b)\,\right)\Big)\\
&+\varepsilon\cdot(k+r)\,\left(Q^2+t_a\right)\,\Big(Q^4\,(t_b-t_a)+Q^2\,\big(2t_b^2+t_at_b-{t_a}^2+t(t_a-3t_b)\\
&+t_b\,\left({t_a}^2+{t_b}^2-t\,(t_a+t_b)\right)\big)\Big)\Big]\Big\}\left(Q^2\right)^{-\epsilon}\\
+&\Big\{\frac{\left(H_T^a-\bar{H}_T^a\right)\,\left(Q^4+M^2\,Q^2-{t_a}^2\right)}{\left(Q^2+t_a\right)\,\left(Q^2\,t+t_a\,t_b\,\right)}-\frac{2\,\varepsilon\cdot p\,H_k^a\,[{t_a}^2+Q^2\,\left(t+t_a-t_b\,\right)]}{\left(Q^2+t_a\right)\,\left(Q^2\,t+t_a\,t_b\,\right)}\\
&-\frac{H_\varepsilon^a\,s}{(t-t_a)^2\,\left(Q^2+t_a\right)\,\left(Q^2\,t+t_a\,t_b\,\right)}\Big[\alpha\,t_a(Q^4t+t_a^2t_b)\,-t_a^2(t-t_a)^2\\
&+Q^2\,\left(-t^3+t^2\,(t_a\,+t_b)+t\,t_a(t_a-2\,t_b)+t_a^2\,\left(t_b-t_a\right)+\alpha {t_a}^2\,\left(t+t_b\right)\right)\Big]\\
&+\frac{2\,H_p^a}{(t-t_a)\,\left(Q^2+t_a\right)^2\,\left(Q^2\,t+t_a\,t_b\right)}\Big[\varepsilon\cdot k\,\left(t-t_a\right)\,\big(Q^6+M^2\,Q^2\,\left(Q^2-t_a\right)\\
&+Q^4\,t_a+Q^2\,{t_a}^2+{t_a}^3\big)+\varepsilon\cdot(k+r)\,\left(Q^2+t_a\right)\,\big({t_a}^2\,\left(t+t_a\right)\\
&+Q^2\,\left(t_a\,\left(t_a-t_b\right)+t\,\left(2\,t_a+t_b\right)-t^2\right)\,\big)\Big]\Big\}\left(-t_a\right)^{-\epsilon}\\
+&\Big\{\frac{\left(H_T^a-\bar{H}_T^a\right)\,\left(Q^4+M^2\,Q^2-{t_b}^2\right)}{\left(Q^2+t_b\right)\,\left(Q^2\,t+t_a\,t_b\,\right)}+\frac{2\,\varepsilon\cdot p\,H_k^a\,[{t_b}^2+Q^2\,\left(t+t_b-t_a\,\right)]}{\left(Q^2+t_b\right)\,\left(Q^2\,t+t_a\,t_b\,\right)}\\
&-\frac{H_\varepsilon^a\,s}{(t-t_b)^2\,\left(Q^2+t_b\right)\,\left(Q^2\,t+t_a\,t_b\,\right)}\Big[-(1-\alpha)\,t_b(Q^4t+t_b^2t_a)\,+t_b^2(t-t_b)^2\\
&+Q^2\,\big(t^3-t^2\,(t_a\,+t_b)+t\,t_b(2t_a-t_b)+t_b^2\,\left(t_b-t_a\right)\\
&-(1-\alpha){t_b}^2\,\left(t+t_a\right)\big)\Big]\\
&+\frac{2\,H_p^a}{(t-t_b)\,\left(Q^2+t_b\right)^2\,\left(Q^2\,t+t_a\,t_b\right)}\Big[\varepsilon\cdot(k+r)\,\left(t-t_b\right)\,\big(Q^6\\
&+M^2\,Q^2\,\left(Q^2-t_b\right)+Q^4\,t_b+Q^2\,{t_b}^2+{t_b}^3\big)+\varepsilon\cdot k\,\left(Q^2+t_b\right)\,\big({t_b}^2\,\left(t+t_b\right)\\
&+Q^2\,\left(t_b\,\left(t_b-t_a\right)+t\,\left(2\,t_b+t_a\right)-t^2\right)\,\big)\Big]\Big\}\left(-t_b\right)^{-\epsilon}.
\end{aligned}
\tag{2.50}
$$

The c_Γ/ϵ - term is rather simple, since we kept only the first terms in the expansion of powers like $(-t)^{-\epsilon}$ while the logarithms are combined with logarithms from the finite term, leading to significant simplifications:

$$
\begin{aligned}
A_{14}^{(-1)} =&\frac{s\,H_\varepsilon^a[\alpha(t-t_b)-(1-\alpha)(t-t_a)]}{\left(t-t_a\right)\,\left(t-t_b\right)}\\
&-\frac{4\,H_p^a[\varepsilon\cdot k\,\left(Q^2+t_b\,\right)+\varepsilon\cdot(k+r)\,\left(Q^2+t_a\right)]}{\left(Q^2+t_a\right)\,\left(Q^2+t_b\right)}.
\end{aligned}
\tag{2.51}
$$

Finally, the $\mathcal{O}(\epsilon^0)$ term for this opposite box diagram reads:

$$
\begin{aligned}
A_{14}^{(0)} =& \frac{2\,s\,[\alpha(t-t_b)-(1-\alpha)(t-t_a)]\,H_\varepsilon^a}{(t-t_a)\;(t-t_b)} \\
&- \frac{8\,[\varepsilon\cdot(r+k)\left(Q^2+t_a\right)+\varepsilon\cdot k\;\left(Q^2+t_b\right)]H_p^a}{(Q^2+t_a)\;(Q^2+t_b)} \\
&+ \frac{2\,s\,[\alpha\,\varepsilon\cdot(k+r)\;\left(Q^2+t_a\right)\;(t-t_b)+(1-\alpha)\varepsilon\cdot k\,(Q^2+t_b)\,(t-t_a)]H_k^a}{(t-t_a)\,(t-t_b)\,(Q^2+t_a)\,(Q^2+t_b)} \\
&- \frac{\mathrm{Ld}_0^{op}(t_a,t_b,-Q^2,t)}{M^4\;(Q^2\,t+t_a\,t_b)}\Big\{(H_T^a-\bar{H}_T^a)\,M^2\,\Big[3(Q^2t+t_a\,t_b)+M^2(t_a+t_b)\Big] \\
&\quad + 2\,H_k^a\,\Big[\varepsilon\cdot p\,M^4\;(t_a-t_b)-3\,s\;\left(Q^2\,t+t_a\,t_b\right)(\alpha\,\varepsilon\cdot k \\
&\qquad + (1-\alpha)\;\varepsilon\cdot(k+r))\Big]+H_p^a\,\Big[\varepsilon\cdot r\,(t_a-t_b)\big(2Q^4+Q^2(4(t_a+t_b)-5t) \\
&\qquad - 2t(t_a+t_b)+2(t_a+t_b)^2-3t_a\,t_b\big) \\
&\qquad + (\varepsilon\cdot k+\varepsilon\cdot(k+r))\;\left(4tQ^4+Q^2t(9(t_a+t_b)-10t)\right. \\
&\qquad \left. - 2t^2(t_a+t_b)+2t(t_a^2+t_b^2-t_at_b)+3t_at_b(t_a+t_b)\right)\Big] \\
&\quad - \frac{H_\varepsilon^a\,s}{2}\,\Big[(t_a-t_b)(2Q^4-7Q^2t+4Q^2(t_a+t_b)+2(t-t_a-t_b)^2-3t_at_b) \\
&\qquad - 3\,[\alpha-(1-\alpha)](Q^2\,t\;+t_at_b)\,\left(2Q^2+t_a+t_b\right)\Big]\Big\} \\
&- \Big\{\frac{3\,H_\varepsilon^a\,Q^2\,s}{M^2\;(Q^2+t_a)\;(Q^2+t_b)}\Big[\alpha(Q^2+t_a)-(1-\alpha)(Q^2+t_b)\Big] \\
&\quad - \frac{2\,H_p^a\,Q^2}{M^2\,(Q^2+t_a\;)^2\,(Q^2+t_b)^2}\Big[\varepsilon\cdot k\;\left(4M^2+3\,(Q^2+t_a)\right)(Q^2+t_b)^2 \\
&\qquad + \varepsilon\cdot(k+r)\left(4M^2+3(Q^2+t_b)\right)(Q^2+t_a)^2\Big] \\
&\quad - \frac{H_k^a\,Q^2\,s}{M^2\,(Q^2+t_a)^2\,(Q^2+t_b)^2\;(Q^2\,t+t_a\,t_b)}\Big[\varepsilon\cdot k(Q^2+t_b)^2\big(6\alpha(Q^2+t_a) \\
&\qquad \times(t-t_b)+2(1-\alpha)t_aM^2\big)+\varepsilon\cdot(k+r)\,(Q^2+t_a)^2\,\big(6\;(1-\alpha) \\
&\qquad \times\;(Q^2+t_b)(t-t_a)+2\alpha t_bM^2\big)\Big]\Big\}\;\log(Q^2) \\
&+ \Big\{\frac{(H_T^a-\bar{H}_T^a)\,(2\,t-t_a-t_b)}{2\;(t-t_a)\;(t-t_b)}+\frac{H_p^a}{M^2\;(t-t_a)\;(t-t_b)}\Big[\varepsilon\cdot(k+r) \\
&\qquad \times\left(M^2(t_b-t_a)-6t(t-t_b)\right)-\varepsilon\cdot k\;\left(M^2(t_b-t_a)+6t(t-t_a)\right)\Big] \\
&\quad + \frac{H_\varepsilon^a\,s}{2\,M^2\,(t-t_a)^2\,(t-t_b)^2}\Big[t\;(t_a-t_b)\;\big((4t-2\,t_a-2t_b)Q^2-t^2 \\
&\qquad + 3t(t_a+t_b)-2t_a^2-2t_b^2-t_at_b\big) \\
&\qquad + (1-\alpha)\big(-4t^3(t_a+t_b)+t_at_b(t_a+t_b)^2+t^2(7t_a^2+6t_at_b+7t_b^2) \\
&\qquad - t(3t_a^3+5t_a^2t_b+5t_at_b^2+3t_b^3) \\
&\quad + Q^2(-6t^3+7t^2(t_a+t_b)+t_at_b(t_a+t_b)-t(3t_a^2+4t_at_b+3t_b^2))\big)
\end{aligned}
$$

$$
\begin{aligned}
& - \alpha \big(- 4t^3(t_a + t_b) + t_a t_b (t_a + t_b)^2 + t^2 (7t_a^2 + 6t_a t_b + 7t_b^2) \\
& - t(3t_a^3 + 5t_a^2 t_b + 5t_a t_b^2 + 3t_b^3) \\
& + Q^2(-6t^3 + 7t^2(t_a + t_b) + t_a t_b (t_a + t_b) - t(3t_a^2 + 4t_a t_b + 3t_b^2))\big)\Big] \\
- & \frac{H_k^a}{M^2\,(t-t_a)^2\,(t-t_b)^2\,(Q^2\,t + t_a\,t_b)} \Big[\varepsilon\cdot p\,M^2\,(t-t_a)\,(t-t_b)\,(t_a - t_b) \\
& \times \big(Q^2\,t + t_a\,t_b\big) + \varepsilon\cdot k\,s\,t\,(t-t_a)\,\big(2\,M^2\,t_b\,(1-\alpha)\,(t-t_a) \\
& + 6\alpha(Q^2 + t_b)(t-t_b)^2\big) + \varepsilon\cdot(k+r)\,s\,t\,(t-t_b)\,\big(2\,M^2\,t_a\,\alpha\,(t-t_b) \\
& + 6(1-\alpha)(Q^2 + t_a)(t-t_a)^2\big)\Big\}\log(-t) \\
+ & \left\{\frac{H_T^a - \bar{H}_T^a}{2(t_a - t)} + \frac{H_\varepsilon^a\,s}{2\,M^2\,(t-t_a)^2\,(Q^2 + t_a)}\Big[M^2\,\big(Q^2 + t_a\big)\,(t_a - t + 4\alpha t)\right. \\
& - 6t_a(t - ta)(t_a + \alpha Q^2 - (1-\alpha)t)\Big] + \frac{H_p^a}{M^2\,(t-t_a)\,(Q^2 + t_a)^2}\Big[\\
& \quad \varepsilon\cdot r\,M^2\,\big(Q^2 + t_a\big)^2 + 6\,t_a\,\varepsilon\cdot r\,\big(Q^2 + t_a\big)^2 \\
& + 6\,t_a\,\varepsilon\cdot k\,\big(Q^2 + t_a\big)\,\big(Q^2 + t\big) + 4\varepsilon\cdot k\,M^2(Q^2 - t_a)(t_a - t)\Big] \\
+ & \frac{H_k^a}{M^2\,(t-t_a)^2\,(Q^2 + t_a)^2\,(Q^2\,t + t_a\,t_b)}\Big[\varepsilon\cdot p\,M^2\,(t-t_a)\,\big(Q^2 + t_a\big)^2 \\
& \times \big(Q^2\,t + t_a\,t_b\big) + s\,\varepsilon\cdot r\,\Big(2\,\alpha M^2 t + 6\,(1-\alpha)(t-t_a)^2\Big)\,t_a\,\big(Q^2 + t_a\ \big)^2 \\
& + s\,\varepsilon\cdot k\,\big(2\,M^2 t_a[\alpha t(Q^2 + t_a)^2 - Q^2(t-t_a)^2 - 2\alpha Q^2(t-t_a)(t + 2t_a)] \\
& \left. + 6(t-t_a)[t_a(t-t_a)(Q^2 + t_a)^2 - \alpha M^2(Q^4 t + t_a^3)]]\big)\Big]\right\}\log(-t_a) \\
+ & \left\{\frac{H_T^a - \bar{H}_T^a}{2(t_b - t)} + \frac{H_\varepsilon^a\,s}{2\,M^2\,(t-t_b)^2\,(Q^2 + t_b)}\Big[M^2\,\big(Q^2 + t_b\big)\,(t - t_b - 4(1-\alpha)t)\right. \\
& - 6t_b(t-t_b)(\alpha t - t_b - (1-\alpha)Q^2)\Big] + \frac{H_p^a}{M^2\,(t-t_b)\,(Q^2 + t_b)^2}\Big[\\
& - \varepsilon\cdot r\,M^2\,\big(Q^2 + t_b\big)^2 - 6\,t_b\,\varepsilon\cdot r\,\big(Q^2 + t_b\big)^2 \\
& + 6\,t_b\,\varepsilon\cdot(k+r)\,\big(Q^2 + t_b\big)\,\big(Q^2 + t\big) + 4\varepsilon\cdot(k+r)\,M^2(Q^2 - t_b)(t_b - t)\Big] \\
+ & \frac{H_k^a}{M^2\,(t-t_b)^2\,(Q^2 + t_b)^2\,(Q^2\,t + t_a\,t_b)}\Big[-\varepsilon\cdot p\,M^2\,(t-t_b)\,\big(Q^2 + t_b\big)^2 \\
& \big(Q^2\,t + t_a\,t_b\big) + s\,\varepsilon\cdot r\,\Big(-2\,(1-\alpha)M^2 t - 6\,\alpha(t-t_b)^2\Big)\,t_b\,\big(Q^2 + t_b\ \big)^2 \\
& + s\,\varepsilon\cdot(k+r)\,\big(2\,M^2 t_b[(1-\alpha)t(Q^2 + t_b)^2 - Q^2(t-t_b)^2 \\
& - 2(1-\alpha)Q^2(t-t_b)(t + 2t_b)] + 6(t-t_b)[t_b(t-t_b)(Q^2 + t_b)^2 \\
& \left. - (1-\alpha)M^2(Q^4 t + t_b^3)]]\big)\Big]\right\}\log(-t_b). \qquad (2.52)
\end{aligned}
$$

We have cast all our results for A_{14} into a form which manifestly exhibits the antisymmetry under the exchange of q and $\bar{q}$.

The Pentagon diagram Fig. 2.2.13

The result for the pentagon diagram Fig. 2.2.13, is much simpler than one might expect. The reason for this is the fact that, in contrast to the box diagrams Fig. 2.2.12 and 2.2.14, the integrals depend upon the large scale s, and in the high energy limit they can enormously be simplified. As before, we separate divergent and finite pieces:

$$A_{13} = \Gamma_{qq}^{(0),a} \frac{2s}{t} \left(\frac{-iee_f\, t}{s}\right) \left(\frac{N_c}{2}\right) \frac{c_\Gamma}{(4\pi)^{2-\epsilon}} \left[\frac{1}{\epsilon^2} A_{13}^{(-2)} + A_{13}^{(0)}\right]. \tag{2.53}$$

The divergent contribution has the form:

$$\begin{aligned}
A_{13}^{(-2)} &= \frac{1}{t}\left[\frac{H_T^a}{t_a} + \frac{\bar{H}_T^a}{t_b}\right] \left((\alpha\, s)^{-\epsilon} - (-(1-\alpha)\, s)^{-\epsilon}\right) \\
&+ \left\{ \frac{t_a\, t_b}{t(Q^2\, t + t_a\, t_b)} \left[\frac{H_T^a}{t_a} - \frac{\bar{H}_T^a}{t_b}\right] - \frac{2H_T^a}{t\, t_a} \right. \\
&\quad \left. + \frac{2\, H_p^a}{Q^2\, t + t_a\, t_b} \left[\frac{\varepsilon \cdot k\, Q^2}{Q^2 + t_a} - \frac{\varepsilon \cdot (k+r)\, t_a}{t - t_a}\right] \right\} (-t_a)^{-\epsilon} \\
&+ \left\{ \frac{t_a\, t_b}{t(Q^2\, t + t_a\, t_b)} \left[\frac{H_T^a}{t_a} - \frac{\bar{H}_T^a}{t_b}\right] + \frac{2\bar{H}_T^a}{t\, t_b} \right. \\
&\quad \left. - \frac{2\, H_p^a}{Q^2\, t + t_a\, t_b} \left[\frac{\varepsilon \cdot k\, t_b}{t - t_b} - \frac{\varepsilon \cdot (k+r)\, Q^2}{Q^2 + t_b}\right] \right\} (-t_b)^{-\epsilon} \\
&+ \left\{ - \frac{t_a\, t_b}{t(Q^2\, t + t_a\, t_b)} \left[\frac{H_T^a}{t_a} - \frac{\bar{H}_T^a}{t_b}\right] \right. \\
&\quad \left. + \frac{2\, H_p^a}{Q^2\, t + t_a\, t_b} \left[\frac{\varepsilon \cdot k\, t_b}{t - t_b} + \frac{\varepsilon \cdot (k+r)\, t_a}{t - t_a}\right] \right\} (-t)^{-\epsilon} \\
&+ \left\{ - \frac{Q^2}{Q^2\, t + t_a\, t_b} \left[\frac{H_T^a}{t_a} - \frac{\bar{H}_T^a}{t_b}\right] \right. \\
&\quad \left. - \frac{2\, Q^2\, H_p^a}{Q^2\, t + t_a\, t_b} \left[\frac{\varepsilon \cdot k}{Q^2 + t_a} + \frac{\varepsilon \cdot (k+r)}{Q^2 + t_b}\right] \right\} Q^{2-\epsilon},
\end{aligned} \tag{2.54}$$

whereas the finite piece reads:

$$\begin{aligned}
A_{13}^{(0)} &= \frac{t_a\, t_b}{t(Q^2\, t + t_a\, t_b)} \left[\frac{H_T^a}{t_a} + \frac{\bar{H}_T^a}{t_b}\right] \Big[\mathrm{Ld}_0^{\mathrm{a}}(t_a, (1-\alpha)\, s, -Q^2, -\alpha\, s) \\
&- \mathrm{Ld}_0^{\mathrm{a}}(t_b, -\alpha\, s, -Q^2, (1-\alpha)\, s) - \mathrm{Ld}_0^{\mathrm{1m}}((1-\alpha)\, s, t, t_b) + \mathrm{Ld}_0^{\mathrm{1m}}(-\alpha\, s, t, t_a)\Big] \\
&- \frac{2H_T^a}{t\, t_a} \mathrm{Ld}_0^{\mathrm{a}}(t_a, (1-\alpha)\, s, -Q^2, -\alpha\, s) + \frac{2\bar{H}_T^a}{t\, t_b} \mathrm{Ld}_0^{\mathrm{a}}(t_b, -\alpha\, s, -Q^2, (1-\alpha)\, s) \\
&+ \left\{ \frac{t_a\, t_b}{t(Q^2\, t + t_a\, t_b)} \left[\frac{H_T^a}{t_a} - \frac{\bar{H}_T^a}{t_b}\right] \right. \\
&- \left. \frac{2\, H_p^a}{M^2\, (Q^2\, t + t_a\, t_b)} \Big[\varepsilon \cdot k\, (Q^2 + t_b) + \varepsilon \cdot (k+r)\, (Q^2 + t_a)\Big] \right\} \\
&\times\ \mathrm{Ld}_0^{\mathrm{op}}(t_a, t_b, t, -Q^2).
\end{aligned} \tag{2.55}$$

The counterpart $\bar{A}_{13}$ of the pentagon graph Fig. 2.2.13 can be obtained in two different ways. Either we follow the substitution described after (2.27) and simply interchange quark and antiquark $q \leftrightarrow \bar{q}$. Alternatively, we start from Fig. 2.2.13 and perform the crossing $(s \to u \approx -s)$ (an additional minus sign comes from the calor antisymmetry in the t-channel). In the following we present the sum $A_{13} + \bar{A}_{13}$. In order to demonstrate the cancellation of the $\ln s$-dependence we combine the first line of (2.54) with the first three lines of (2.55) (and their counterparts in $\bar{A}_{13}$). The results contain a term proportional to c_Γ/ϵ:

$$
\begin{aligned}
\frac{1}{t}\left[\frac{H_T^a}{t_a} + \frac{\bar{H}_T^a}{t_b}\right] \big[&\ln((1-\alpha)\,s) + \ln(-(1-\alpha)\,s) \\
&- \ln(\alpha\, s) - \ln(-\alpha\, s)\big]. \qquad (2.56)
\end{aligned}
$$

and a finite piece:

$$
\begin{aligned}
&\frac{t_b\, H_T^a + t_a\, \bar{H}_T^a}{t(Q^2\, t + t_a\, t_b)}\Big[\frac{1}{2}\big(\ln((1-\alpha)\,s) - \ln(-(1-\alpha)\,s)\big)^2 - \frac{1}{2}\big(\ln(\alpha\, s) - \ln(-\alpha\, s)\big)^2 \\
&\quad + \big(\ln(-t_a) + \ln(-t_b) - \ln(-t) - \ln(Q^2)\big) \\
&\qquad \times \big(\ln((1-\alpha)\,s) + \ln(-(1-\alpha)\,s) - \ln(\alpha\, s) - \ln(-\alpha\, s)\big)\Big] \\
&+ \frac{H_T^a}{t\, t_a}\Big[\frac{1}{2}\big(\ln(\alpha\, s) - \ln(-\alpha\, s)\big)^2 - \frac{1}{2}\big(\ln((1-\alpha)\,s) - \ln(-(1-\alpha)\,s)\big)^2 \\
&\quad - \big(\ln((1-\alpha)\,s) - \ln(-\alpha\, s)\big)\big(\ln(-(1-\alpha)\,s) - \ln(\alpha\, s)\big) \\
&\quad + \big(\ln(Q^2) - 2\,\ln(-t_a)\big) \\
&\qquad \times \big(\ln((1-\alpha)\,s) + \ln(-(1-\alpha)\,s) - \ln(\alpha\, s) - \ln(-\alpha\, s)\big)\Big] \\
&- \frac{\bar{H}_T^a}{t\, t_b}\Big[\frac{1}{2}\big(\ln((1-\alpha)\,s) - \ln(-(1-\alpha)\,s)\big)^2 - \frac{1}{2}\big(\ln(\alpha\, s) - \ln(-\alpha\, s)\big)^2 \\
&\quad - \big(\ln((1-\alpha)\,s) - \ln(-\alpha\, s)\big)\big(\ln(-(1-\alpha)\,s) - \ln(\alpha\, s)\big) \\
&\quad + \big(\ln(Q^2) - 2\,\ln(-t_b)\big) \\
&\qquad \times \big(\ln(\alpha\, s) + \ln(-\alpha\, s) - \ln((1-\alpha)\,s) - \ln(-(1-\alpha)\,s)\big)\Big] \\
&+ 2\frac{t_b\, H_T^a + t_a\, \bar{H}_T^a}{t(Q^2\, t + t_a\, t_b)}\Big[\mathrm{Li}_2\left(1 + \frac{Q^2}{t_b}\right) - \mathrm{Li}_2\left(1 + \frac{Q^2}{t_a}\right) - \mathrm{Li}_2\left(1 - \frac{t}{t_b}\right) \\
&+ \mathrm{Li}_2\left(1 - \frac{t}{t_a}\right) + \frac{1}{2}\ln^2(-t_b) - \frac{1}{2}\ln^2(-t_a) + \ln(-t_b)\ln\frac{t}{t_b} + \ln(-t_a)\ln\frac{t}{t_a}\Big] \\
&- 4\frac{H_T^a}{t\, t_a}\Big[\frac{\pi^2}{6} - \mathrm{Li}_2\left(1 + \frac{Q^2}{t_a}\right)\Big] + 4\frac{\bar{H}_T^a}{t\, t_b}\Big[\frac{\pi^2}{6} - \mathrm{Li}_2\left(1 + \frac{Q^2}{t_b}\right)\Big]. \qquad (2.57)
\end{aligned}
$$

We can easily observe that the logarithms in s cancel out. Note, however, the nontrivial phase structure: as we have discussed after (2.26), such a phase structure is expected, and in the double-Regge limit $(t, Q^2 \ll M^2 \ll s)$ it will lead to the anticipated decomposition. Finally we mention that, when adding the two pentagon graphs, the remaining four lines in (2.54) and the last two lines in (2.55) are simply multiplied by a factor of 2.

2.3 Renormalization

In this paper the Feynman gauge is adopted in all calculations. In order to regularize the singularities we have used the dimensional regularization procedure. At this stage our results contain both infrared and ultraviolet singularities: standard renormalization will remove the ultraviolet singularities, whereas the infrared singularities will cancel only in the complete NLO result for the photon impact factor [47]. In this section we will perform the renormalization, and we will use the modified minimal subtraction ($\overline{\mathrm{MS}}$) scheme. In order to demonstrate the cancellation of the ultraviolet ϵ-poles, we first list the ultraviolet divergencies of our diagrams in Figs. 2.2.1 and 2.2.4–11 (the box diagrams in Figs. 2.2.2 and 2.2.3, the pentagon graph Fig. 2.2.13, and and the box diagrams Figs. 2.2.12 and 2.2. 14 are ultraviolet finite). Our analysis leads to the following results (deviating from definitions in Eq. (2.17) we now include the coupling constant g):

$$A_1^{UV} = \frac{A^{(0)}g^4}{(4\pi)^{2-\epsilon}}\frac{(-t)^{-\epsilon}}{\epsilon_{UV}}\frac{3N_c}{2}\,, \tag{2.58}$$

$$A_4^{UV} = -\frac{A^{(0)}g^4}{(4\pi)^{2-\epsilon}}\frac{(-t)^{-\epsilon}}{\epsilon_{UV}}\frac{1}{2N_c}\,, \tag{2.59}$$

$$A_5^{UV} = \frac{A^{(0)}g^4}{(4\pi)^{2-\epsilon}}\frac{(-t)^{-\epsilon}}{\epsilon_{UV}}\frac{3N_c}{2}\,, \tag{2.60}$$

$$A_6^{UV} = -\frac{A^{(0)}g^4}{(4\pi)^{2-\epsilon}}\frac{(-t)^{-\epsilon}}{\epsilon_{UV}}\frac{1}{2N_c}\,, \tag{2.61}$$

$$A_{7+8+9}^{UV} = \frac{A^{(0)}g^4}{(4\pi)^{2-\epsilon}}\frac{(-t)^{-\epsilon}}{\epsilon_{UV}}[\frac{5}{3}N_c - \frac{2}{3}n_f]\,, \tag{2.62}$$

$$A_{10}^{UV} = \frac{A^{(0)}g^4}{(4\pi)^{2-\epsilon}}\frac{(-t_a)^{-\epsilon}}{\epsilon_{UV}}C_{\mathrm{F}}\,, \tag{2.63}$$

$$A_{11}^{UV} = -\frac{A^{(0)}g^4}{(4\pi)^{2-\epsilon}}\frac{(-t_a)^{-\epsilon}}{\epsilon_{UV}}C_{\mathrm{F}}\,. \tag{2.64}$$

The poles in A_5 and A_6, coming from the lower vertex correction, as well as the gluon self-energy A_7 to A_9 can be compared to standard textbook results.

In above formulas g, the strong coupling constant, denotes the unrenormalized one, the bare coupling. In order to perform the usual renormalization, we make the replacement:

$$g \to \frac{Z_1 g_r \mu^\epsilon}{Z_2\sqrt{Z_3}} \to g_r\Big[1 - \frac{\alpha_s}{4\pi}\beta_0\left(\frac{1}{\epsilon_{UV}} - \gamma_{\mathrm{E}} + \log(4\pi)\right) + \cdots\Big]\,, \tag{2.65}$$

where $\beta_0 = (\frac{11}{6}N_c - \frac{1}{3}n_f)$, and γ_{E} is the Euler constant. In the $\overline{\mathrm{MS}}$ scheme we have:

$$Z_1 = 1 - \frac{\alpha_s}{4\pi}(N_c + C_F)\Big[\frac{1}{\epsilon_{UV}} - \gamma_{\rm E} + \log(4\pi)\Big], \tag{2.66}$$

$$Z_2 = 1 - \frac{\alpha_s}{4\pi}C_F\Big[\frac{1}{\epsilon_{UV}} - \gamma_{\rm E} + \log(4\pi)\Big], \tag{2.67}$$

$$Z_3 = 1 + \frac{\alpha_s}{4\pi}(\frac{5}{3}N_c - \frac{2}{3}n_f)\Big[\frac{1}{\epsilon_{UV}} - \gamma_{\rm E} + \log(4\pi)\Big], \tag{2.68}$$

for the vertex renormalization, the quark wave function renormalization, and for the gluon wave function renormalization, respectively. Finally, we add the quark self-energy diagrams for the external legs (not shown in Fig. 2.2):

$$A^{UV}_{\rm quark\,self-energy} = -\frac{A^0\, g^4}{(4\pi)^{2-\epsilon}}\frac{C_{\rm F}}{\epsilon_{\rm UV}}. \tag{2.69}$$

It is easy to see that in this way all ultraviolet divergencies cancel. In particular, the ultraviolet divergences in diagrams Figs.2.2.10 and 2.2.11 exactly cancel against each other as expected, similar to situation in the NLO calculation of $\gamma^* \to q\bar{q}$ in the e^+e^- annihilation process.

2.4 Summary of chapter 2

We have calculated the high energy limit of the process $\gamma^* q \to q\bar{q}\, q$ in next-to-leading order and from the results we have extracted the NLO corrections to the coupling of the reggeized gluon to the vertex $\gamma^* \to q\bar{q}$. This calculation represents the first step in the computation of the NLO corrections to the photon impact factor as we have discussed in section 1.2. In addition, we have found the results for the matrix elements of the process $\gamma^* g^* \to q\bar{q}$ in NLO. These results will serve as input for Monte Carlo event generators and will be used to calculate jet cross sections in the $k_\perp$-factorization scheme.

So far, we have listed the results of all one loop diagrams. Using dimensional regularization we have carried out all loop integrations, and our final results are expressed in terms of logarithms and dilogarithms. We also show the explicit dependence upon the helicities of the photon and the quarks. After renormalization our results are free from ultraviolet divergencies, but they still contain infrared singularities which will cancel once all NLO pieces have been calculated and put together. For the photon impact factor this is out of question, since it has an inclusive final state. For the application in a jet cross section, an appropriate jet definition has to be applied.

We have not yet attempted to combine the contributions from the Feynman diagrams into a single compact expression. The results for the individual diagrams are sufficiently complicated and lengthy, and we found it useful to first list them separately. The results of this chapter have been published in [48].

Chapter 3

Phase space integrals

Having computed the virtual corrections to the $\gamma^* R q\bar{q}$-vertex, as the next step in the calculation of the virtual photon impact factor, we have to perform phase space integrals. We may write the contributions to the NLO impact factor from virtual corrections (cf. Fig. 1.10) as

$$\Phi^{\text{virt}}_{\gamma^*\gamma^*} = \int \frac{dM^2_{q\bar{q}}}{2\pi} d\phi_{q\bar{q}} \left(\Gamma^{(1)}_{\gamma^*\to q\bar{q}} \Gamma^{(0)*}_{\gamma^*\to q\bar{q}} + \Gamma^{(0)}_{\gamma^*\to q\bar{q}} \Gamma^{(1)*}_{\gamma^*\to q\bar{q}} \right) . \tag{3.1}$$

We have calculated the contributions to $\Gamma^{(1)}_{\gamma^*\to q\bar{q}}$ in the previous chapter and the born level vertex $\Gamma^{(0)}_{\gamma^*\to q\bar{q}}$ is well known (2.22). The next step is the computation of the sum over the helicities of the final state $q\bar{q}$-pair and the integration over the phase space element

$$\frac{dM^2_{q\bar{q}}}{2\pi} d\phi_{q\bar{q}} = \frac{d\alpha}{2\alpha(1-\alpha)} \frac{d^{2-2\epsilon}\boldsymbol{k}}{(2\pi)^{3-2\epsilon}}. \tag{3.2}$$

This chapter is devoted to a description of the technical steps leading to expressions that are suitable for further numerical or analytical evaluation and finally the analytic expressions for the different diagrams are presented.

3.1 Polarizations and kinematical variables

For the subsequent integration over the phase space (3.2), we change variables from the invariants t_a, t_b and M^2 to the transverse momenta $\boldsymbol{k}^2$, $\boldsymbol{r}^2$ and $(\boldsymbol{k}+\boldsymbol{r})^2$ with the help of the relations $t = -^2$,

$$t_a = -\frac{1}{1-\alpha} \left[\boldsymbol{k}^2 + \alpha(1-\alpha) Q^2 \right] \ , \tag{3.3}$$

$$t_b = -\frac{1}{\alpha} \left[(\boldsymbol{k}+\boldsymbol{r})^2 + \alpha(1-\alpha) Q^2 \right] \ , \tag{3.4}$$

$$M^2 = \frac{\left[\alpha \boldsymbol{k} + (1-\alpha)(\boldsymbol{k}+\boldsymbol{r}) \right]^2}{\alpha(1-\alpha)} \ . \tag{3.5}$$

Following this change of variables, we are left with a limited number of typical propagator-type denominators in the transverse integration variable $\boldsymbol{k}$, stemming from different combinations of invariants,

$$t_a \to D_1 = \boldsymbol{k}^2 + \alpha(1-\alpha)Q^2 \ , \tag{3.6}$$
$$t_b \to D_2 = (\boldsymbol{k}+\boldsymbol{r})^2 + \alpha(1-\alpha)Q^2 \ , \tag{3.7}$$
$$M^2 \to D_3 = (\boldsymbol{k} + (1-\alpha)\boldsymbol{r})^2 \ , \tag{3.8}$$
$$t_a - t \to D_4 = \boldsymbol{k}^2 + \alpha(1-\alpha)Q^2 - (1-\alpha)\boldsymbol{r}^2 \ , \tag{3.9}$$
$$t_b - t \to D_5 = (\boldsymbol{k}+\boldsymbol{r})^2 + \alpha(1-\alpha)Q^2 - \alpha\boldsymbol{r}^2 \ , \tag{3.10}$$
$$t_a + Q^2 \to D_8 = \boldsymbol{k}^2 - (1-\alpha)^2 Q^2 \ , \tag{3.11}$$
$$t_b + Q^2 \to D_9 = (\boldsymbol{k}+\boldsymbol{r})^2 - \alpha^2 Q^2 \ . \tag{3.12}$$

In addition, we define the combination $(Q^2 t + t_a t_b)$ to be written in terms of propagator-type denominators as follows,

$$Q^2\, t + t_a\, t_b = D_6\, D_7 \ . \tag{3.13}$$

Although it is possible to write D_6 and D_7 explicitly propagator-like, we want to avoid it since this form is very artificial.

We choose the polarization vectors of the virtual photon as in the born calculation (1.11) and restrict ourselves to the forward case, i.e. the convolution with the LO vertex in (3.1) is viewed as the interference term of a squared amplitude at NLO and the polarizations of ingoing and outgoing photon are equal. Thereby we sum over the two transverse helicities of the photon, making use of

$$\varepsilon_\mu^+ \varepsilon_\nu^{+*} + \varepsilon_\mu^- \varepsilon_\nu^{-*} = -\delta_{\mu\nu}. \tag{3.14}$$

We calculate the sum over the helicities of the $q\bar{q}$-pair as usual as a trace. This is most efficiently done in one step before the calculation. Since we already reduced the answer in the NLO calculation to five different helicity matrix elements (2.6) to (2.10) we first calculate a table of traces of all possible combinations of helicity matrix elements out of

$$\left\{H_T, \bar{H}_T, H_p, H_k, H_\varepsilon\right\} \times \left\{H_T, \bar{H}_T\right\}^* \tag{3.15}$$

for the two polarizations L and T of the virtual photon. This calculation of traces is done with the help of Mathematica, using the package FeynCalc.

For the longitudinal polarizations we list the results as follows. The traces for the five helicity amplitudes are calculated for the multiplication with the contribution $H_T/(st_a)$ from the tree level amplitude. The combinations with $\bar{H}_T/(st_b)$ are easily obtained from the transformation

$$\alpha \leftrightarrow 1-\alpha \qquad \boldsymbol{k} \leftrightarrow -(\boldsymbol{k}+\boldsymbol{r}) \ . \tag{3.16}$$

For longitudinal photons we obtain the following result for the traces:

$$\mathrm{tr}\, H_T \otimes \frac{H_T^*}{st_a} = -\frac{2\alpha s}{Q^2 D_1}\left[\boldsymbol{k}^2 - \alpha(1-\alpha)Q^2\right]^2 , \tag{3.17}$$

$$\mathrm{tr}\, \bar{H}_T \otimes \frac{H_T^*}{st_a} = -\frac{2(1-\alpha)s}{Q^2 D_1}\left[\boldsymbol{k}^2 - \alpha(1-\alpha)Q^2\right]\left[(\boldsymbol{k}+\boldsymbol{r})^2 - \alpha(1-\alpha)Q^2\right] , \tag{3.18}$$

$$\mathrm{tr}\, H_p \otimes \frac{H_T^*}{st_a} = \frac{2\alpha(1-\alpha)s}{QD_1}\left[\boldsymbol{k}^2 - \alpha(1-\alpha)Q^2\right] , \tag{3.19}$$

$$\mathrm{tr}\, H_k \otimes \frac{H_T^*}{st_a} = -\frac{2}{QD_1}\left[\boldsymbol{k}^2 - \alpha(1-\alpha)Q^2\right]\left[\boldsymbol{k}\cdot(\boldsymbol{k}+\boldsymbol{r}) + \alpha(1-\alpha)Q^2\right] , \tag{3.20}$$

$$\mathrm{tr}\, H_\varepsilon \otimes \frac{H_T^*}{st_a} = -\frac{2}{Q^2 D_1}\left[\boldsymbol{k}^2 - \alpha(1-\alpha)Q^2\right]\left[\boldsymbol{k}\cdot(\boldsymbol{k}+\boldsymbol{r}) - \alpha(1-\alpha)Q^2\right] . \tag{3.21}$$

Considering the transverse polarizations of the virtual photon, we choose to sum over the two transverse polarizations, only in those combinations, where already two polarizations are available. In the case of H_p and H_k we only have the polarization vector from the tree-level amplitude and therefore no simplification will result from the polarization sum. Here, we keep the explicit dependence on the polarization vector from the tree level $\boldsymbol{\varepsilon}'$ that is present in the results:

$$\mathrm{tr}\, H_T \otimes \frac{H_T^*}{st_a} = -\frac{4\alpha s}{D_1}[\alpha^2 + (1-\alpha)^2]\boldsymbol{k}^2 , \tag{3.22}$$

$$\mathrm{tr}\, \bar{H}_T \otimes \frac{H_T^*}{st_a} = -\frac{4\alpha s}{D_1}[\alpha^2 + (1-\alpha)^2]\boldsymbol{k}\cdot(\boldsymbol{k}+\boldsymbol{r}) , \tag{3.23}$$

$$\mathrm{tr}\, H_p \otimes \frac{H_T^*}{st_a} = \frac{2\alpha(1-\alpha)s}{D_1}(1-2\alpha)\boldsymbol{\varepsilon}'\cdot\boldsymbol{k} , \tag{3.24}$$

$$\begin{aligned}\mathrm{tr}\, H_k \otimes \frac{H_T^*}{st_a} = &\frac{2}{D_1}\Big\{\boldsymbol{\varepsilon}'\cdot\boldsymbol{r}\boldsymbol{k}^2 - \boldsymbol{\varepsilon}'\cdot\boldsymbol{k}\Big[(1-2\alpha)\boldsymbol{k}^2 \\ &+ (1-\alpha)\big(2\boldsymbol{k}\cdot\boldsymbol{r} + \alpha(1-2\alpha)Q^2\big)\Big]\Big\} ,\end{aligned} \tag{3.25}$$

$$\mathrm{tr}\, H_\varepsilon \otimes \frac{H_T^*}{st_a} = -\frac{4}{D_1}\Big[\alpha^2\boldsymbol{k}^2 + (1-\alpha)^2\boldsymbol{k}\cdot(\boldsymbol{k}+\boldsymbol{r})\Big] . \tag{3.26}$$

3.2 Standard integrals

Having calculated the traces and replaced the kinematic variables as outlined above, we are left with a long sum of expressions of the following generic kind:

$$J(\boldsymbol{r}^2, Q^2) = \int d\alpha\, C(\alpha, \boldsymbol{r}^2, Q^2) I(\alpha, \boldsymbol{r}^2, Q^2) , \tag{3.27}$$

where $C(\alpha, \boldsymbol{r}^2, Q^2)$ is a coefficient function that does not depend on the $\boldsymbol{k}$-integration, while the integral $I(\alpha, \boldsymbol{r}^2, Q^2)$ has the general form

$$I(\alpha, \boldsymbol{r}^2, Q^2) = \int d^{2-2\epsilon}\boldsymbol{k}\, \frac{P(\boldsymbol{k})}{\prod_{i=1}^{9} D_i^{p_i}} L(\boldsymbol{k}). \tag{3.28}$$

The denominator of $I(\alpha, \boldsymbol{r}^2, Q^2)$ is a product of the two-dimensional propagator-type denominators introduced in eqns. (3.6) to (3.13), having the general form

$$D_i = (\boldsymbol{k} + a_i \boldsymbol{r})^2 + M_i^2 \tag{3.29}$$

and being raised to integer powers p_i. The numerator $P(\boldsymbol{k})$ is a polynomial in the integration variable $\boldsymbol{k}$, and $L(\boldsymbol{k})$ is some logarithmic function of $\boldsymbol{k}$, either a logarithm, a dilogarithm or, most general, a function as it was introduced to express the adjacent box Diagram Fig. 2.2.12. In the simplest case it is 1. Of course, the highest power of $\boldsymbol{k}$ in the polynomial P should be such that the integral does not diverge for large $\boldsymbol{k}$. It will turn out, that this is not always the case for single terms, that are logarithmically or even quadratically divergent. But we will see, that we can always arrange the integrals pairwise, in such a way, that these divergences cancel out.

At this stage we want to cast the integrals in the simplest possible form for later evaluation. Let us consider the functions $L(\boldsymbol{k})$ in (3.28). Suppose L is a single logarithm of $\boldsymbol{k}^2$, then we may write it as a power

$$\log \boldsymbol{k}^2 = \frac{\partial}{\partial p} (\boldsymbol{k}^2)^p \bigg|_{p=0} . \tag{3.30}$$

Since $\boldsymbol{k}^2$ always appears in terms of one of the D_i we may absorb a single logarithm in (3.28) in a generalized power p_i of the respective denominator D_i. If we are faced with $\log^2 \boldsymbol{k}^2$ we have to take into account higher derivatives. If $L(\boldsymbol{k})$ is a dilogarithm $\mathrm{Li}_2(\boldsymbol{k}^2)$, we may rewrite the dilogarithm according to its definition as a parametric integral over a logarithm and finally rewrite the logarithm with the help of (3.30) as a power. Apart from introducing additional integrals over parameters, this method may serve to eliminate special functions out of our integrals (3.28).

Let us consider the polynomials $P(\boldsymbol{k})$ in the numerator of (3.28). They contain the integration variable in terms of the squares $\boldsymbol{k}^2$ and $(\boldsymbol{k}+\boldsymbol{r})^2$. Therefore, we can rewrite every $\boldsymbol{k}$ in the numerator in terms of appropriate propagator factors D_i. Of course, the purpose of rewriting the numerators in terms of D_i is to cancel as many $\boldsymbol{k}$'s out of the numerator, as possible. Since the different denominators D_i are closely related,

$$D_1 = D_4 + (1-\alpha)\,\boldsymbol{r}^2 = D_8 + (1-\alpha)\,Q^2 \,, \tag{3.31}$$

$$D_2 = D_5 + \alpha\,\boldsymbol{r}^2 \qquad = D_9 + \alpha\, Q^2 \,, \tag{3.32}$$

it is not unique, how to replace $\boldsymbol{k}^2$ and $(\boldsymbol{k}+\boldsymbol{r})^2$ by different D_i. We have a choice of different orderings of replacements in the integrals (3.28) and chosen the alternative that has lead to the simplest result. This has been implemented into an algorithm in Mathematica. In this first step only similar denominators, related by (3.31), have been used for cancellations. As a second step we have rewritten any remaining D_i in the numerator in terms of its partner that is obtained by replacing $\boldsymbol{k}^2$ and $(\boldsymbol{k}+\boldsymbol{r})^2$, like in

$$D_1 = D_2 - 2\boldsymbol{k}\cdot\boldsymbol{r} - \boldsymbol{r}^2 \tag{3.33}$$

and similar for $D_4 \leftrightarrow D_5$ and $D_8 \leftrightarrow D_9$. Giving a remainder proportional to $\boldsymbol{k} \cdot \boldsymbol{r}$ or $(\boldsymbol{k}+\boldsymbol{r}) \cdot \boldsymbol{r}$, respectively. This then lead to a similar cancellation of numerator factors D_i with the appropriate denominators, in the same fashion as it happened already in the first step of our consideration. Finally we repeated the same steps to cancel denominators D_3, in rewriting D_i in terms of D_3. This lead us to a form for (3.28), that has a highly reduced number of denominators and only powers

$$(\boldsymbol{k} \cdot \boldsymbol{r})^n \qquad \text{or} \qquad ((\boldsymbol{k}+\boldsymbol{r}) \cdot \boldsymbol{r})^n \tag{3.34}$$

in the numerator. Suppose, we have reduced the number of integration momenta in the numerator as much as possible, using this technique, we can apply additional steps to simplify our integrals. Whenever we observe two denominators, that are related by (3.31) or (3.32) we can simplify our integrand algebraically using the relation

$$\frac{1}{D_i D_j} = \frac{1}{D_j - D_i}\left(\frac{1}{D_i} - \frac{1}{D_j}\right), \tag{3.35}$$

thereby reducing the number of denominator factors by one, since the difference $(D_j - D_i)$ does not depend on $\boldsymbol{k}$ anymore.

Having performed these simplifying steps we are in the best case left with integrals of the form

$$\mathrm{F}i^{k_1 k_2}_{l_1 l_2 l_3 l_4 l_5 l_6 l_7} = \int d^{2-2\epsilon}\boldsymbol{k}\, \frac{(\boldsymbol{k} \cdot \boldsymbol{r})^{k_1}((\boldsymbol{k}+\boldsymbol{r}) \cdot \boldsymbol{r})^{k_2}}{D_1^{l_1} D_2^{l_2} D_3^{l_3} D_4^{l_4} D_5^{l_5} D_8^{l_6} D_9^{l_7}} L_i(\boldsymbol{k}) \tag{3.36}$$

or, in case they contain the term $Q^2 t + t_a t_b = D_6 D_7$,

$$\mathrm{G}i^{k_1 k_2}_{l_1 l_2 l_3 l_4 l_5 l_6 l_7} = \int d^{2-2\epsilon}\boldsymbol{k}\, \frac{(\boldsymbol{k} \cdot \boldsymbol{r})^{k_1}((\boldsymbol{k}+\boldsymbol{r}) \cdot \boldsymbol{r})^{k_2}}{D_1^{l_1} D_2^{l_2} D_3^{l_3} D_4^{l_4} D_5^{l_5} D_6 D_7 D_8^{l_6} D_9^{l_7}} L_i(\boldsymbol{k}). \tag{3.37}$$

The index i is connected with the type of logarithmic function that appears as a factor in the integrand. In a few cases it was not possible to reduce the numerators completely to a form (3.36) or (3.37) without touching the terms D_6 and D_7. In these cases we use the generic abbreviation

$$\mathrm{S}i^{k_1 k_2 k_3 k_4 k_5 k_6 k_7}_{l_1 l_2 l_3 l_4 l_5 l_6 l_7 l_8 l_9} = \int d^{2-2\epsilon}\boldsymbol{k}\, \frac{D_1^{k_1} D_2^{k_2} D_3^{k_3} D_4^{k_4} D_5^{k_5} D_8^{k_6} D_9^{k_7}}{D_1^{l_1} D_2^{l_2} D_3^{l_3} D_4^{l_4} D_5^{l_5} D_6^{l_6} D_7^{l_7} D_8^{l_8} D_9^{l_9}} L_i(\boldsymbol{k}). \tag{3.38}$$

In the final results, we have rescaled all momentum variables with Q in such a way, that the integrals (3.36) to (3.38) are dimensionless and their coefficients are functions of α and the dimensionless variable $\tau = t/Q^2$.

3.3 Analytic expressions

In this section we list the analytic expressions, resulting from the calculation of the traces over the fermion loop and rewriting the transverse integrals in terms of a set of standard integrals. In general we may write the result for the contributions to the impact factor from the virtual corrections in the following way, close to the representation (2.27) of the virtual corrections,

$$\Phi^{\text{virtual}}_{\gamma^*\gamma^*} = \sum_{k=1}^{13} \left[(\Phi_k + \bar{\Phi}_k) + \Phi_{14}\right] + \left[(\Phi_k + \bar{\Phi}_k) + \Phi_{14}\right]^* . \tag{3.39}$$

where the Φ_k are the contributions from the different Feynman diagrams in Fig 2.2. In following, we list the results for every diagram, i.e. the different Φ_k separately. First we split off some factors and the α integration as follows,

$$\Phi_k = \frac{1}{2}\frac{g^4 e^2 e_f^2}{(4\pi)^{2-\epsilon}} \frac{\mathcal{C}_k \delta^{aa'}}{2} \int \frac{d\alpha}{\alpha(1-\alpha)} \mathcal{F}_k \ . \tag{3.40}$$

The first factor reduces to the coupling constants α_{em} and α_s in the limit $\epsilon \to 0$, multiplied by the electric charge of the quark-pair. The second factor contains the colour information. $\mathcal{C}_k = \{N_c/2, 1/(2N_c)\}$ is the same colour factor as the one on amplitude level while $\delta^{aa'}/2 = \operatorname{tr} t^a t^{a'}$ results from the generators in the quark loop. Of course, the only allowed colour state in the t-channel is the singlet, since the external virtual photons are colourless.

We are left with the functions $\mathcal{F}_k$. These functions will be expressed in terms of a sum

$$\mathcal{F}_k = \sum_i \mathcal{F}_k^{(i)} \ . \tag{3.41}$$

The functions $\mathcal{F}_k^{(i)}$ each correspond to a special function $L_i(\boldsymbol{k})$ under the integrand and therefore they will contain an integral like $\mathrm{F}i^{\cdots}_{\cdots}$ with corresponding index i. Let $\mathrm{I}i_k^{(j)}$ be one of the integrals $\mathrm{F}i^{\cdots}_{\cdots}$, $\mathrm{G}i^{\cdots}_{\cdots}$ or $\mathrm{S}i^{\cdots}_{\cdots}$ as they are defined in (3.36)–(3.38), the $\mathcal{F}_k^{(i)}$ are written in terms of dimensionless functions $C_k^{ij}(\alpha,\tau)$ and integrals $\mathrm{I}i_k^{(j)}$, as follows:

$$\mathcal{F}_k^{(i)} = \sum_j C_k^{ij}(\alpha,\tau)\, \mathrm{I}i_k^{(j)} \ . \tag{3.42}$$

For every diagram k, the terms $\mathcal{F}_k^{(i)}$ for every special function i are listed in the remainder of this chapter and in appendix B. Note, that all functions depend on the dimensionless variables α and $\tau = -\boldsymbol{r}^2/Q^2$.

Factorized diagrams

We will list the results of the decomposition diagram by diagram, as we did it for the calculation of the amplitudes. Let us begin with the simplest contributions $\Phi_5, \ldots, \Phi_9$, cf. (2.37) to (2.40). Apart from $A^{(0)}$ they do not depend on α and $\boldsymbol{k}$. Therefore, if we consider $\Phi_k + \bar{\Phi}_k$, the integrand is equal to the respective integrand from the Born-level calculation. This is well known and we have calculated it for different photon polarizations in section 1.1 and referred to it as photon wave function. For the different polarizations (T, L), we obtain for the helicity sums the same as in (1.21) and (1.21), e.g. for longitudinal photons we may write it explicitly as,

$$\begin{aligned}\Phi_L^{(0)} =& \frac{\delta^{aa'}}{2}\alpha_s\alpha_{\rm em}e_f^2\int d\alpha\int d^2\boldsymbol{k}\,|\Psi_L|^2\\ =& 8\alpha_s\alpha_{\rm em}e_f^2\delta^{aa'}\int_0^1 d\alpha\alpha(1-\alpha)\left(1-\int_0^1\frac{\alpha(1-\alpha)\,dx}{\alpha(1-\alpha)-x(1-x)\tau}\right), \quad (3.43)\end{aligned}$$

and similarly for transverse photons. Therefore we may write the the results for the simpler diagrams in a rather compact form, by just replacing $A^{(0)}$ in (2.37) to (2.40) with $\Phi^{(0)}$.

$$\Phi_5+\bar\Phi_5 = -\,\Phi^{(0)}\frac{g^2N_cc_\Gamma}{(4\pi)^{2-\epsilon}}\left(\frac{(\boldsymbol{r}^2)^{-\epsilon}}{2\epsilon}+1\right)\,, \quad (3.44)$$

$$\Phi_6+\bar\Phi_6 = \Phi^{(0)}\frac{1}{(4\pi)^{2-\epsilon}}\frac{c_\Gamma}{2N_c}(\boldsymbol{r}^2)^{-\epsilon}\left(\frac{2}{\epsilon^2}+\frac{3}{\epsilon}+8\right)\,, \quad (3.45)$$

$$\Phi_{7+8}+\bar\Phi_{7+8} = \Phi^{(0)}\frac{N_cc_\Gamma}{(4\pi)^{2-\epsilon}}\frac{(\boldsymbol{r}^2)^{-\epsilon}}{2\epsilon(1-2\epsilon)}\left(\frac{1}{3-2\epsilon}+3\right)\,, \quad (3.46)$$

$$\Phi_9+\bar\Phi_9 = \Phi^{(0)}n_f\,\frac{c_\Gamma}{(4\pi)^{2-\epsilon}}\frac{(\boldsymbol{r}^2)^{-\epsilon}}{\epsilon(1-2\epsilon)}\left(\frac{1}{3-2\epsilon}-1\right). \quad (3.47)$$

The diagram we consider next is the quark self-energy diagram Fig 2.2.11. The result for the amplitude (cf. (2.44)) is still rather simple except one additional complication: apart from $A^{(0)}$ also the the factor $(-t_a)^{-\epsilon}$ depends on the integration variables. We may write the answer in the form (3.40) and make use of the short hand notation for the integrals with

$$L_1(\boldsymbol{k}) = \frac{c_\Gamma(1-\epsilon)}{1-2\epsilon}(-t_a)^{-\epsilon} \quad (3.48)$$

that we have introduced in (3.36). The colour factor for this diagram is $\mathcal{C}_{11} = C_F$. The function $\mathcal{F}_{11}$ has only one term $\mathcal{F}_{11}^{(1)}$. For transverse photons it reads

$$\begin{aligned}\mathcal{F}_{11}^{(1)}(T) =& 2\,\alpha\,(-1+3\,\alpha-4\,\alpha^2+2\,\alpha^3)\,(\mathrm{F1}^{00}_{0100000}-\mathrm{F1}^{00}_{1000000})\\ &+2\,\alpha\,(-1+3\,\alpha-4\,\alpha^2+2\,\alpha^3)\,(-2\,\alpha+2\,\alpha^2+\tau\,)\,\mathrm{F1}^{00}_{1100000}\\ &-4\,(-1+\alpha)^2\,\alpha^2\,(1-2\,\alpha+2\,\alpha^2)\,\mathrm{F1}^{00}_{2000000}\,, \quad (3.49)\end{aligned}$$

and for longitudinal photons,

$$\begin{aligned}\mathcal{F}_{11}^{(1)}(L) =& 4\,(-1+\alpha)^2\,\alpha^2\,(\mathrm{F1}^{00}_{0100000}-\mathrm{F1}^{00}_{1000000})\\ &+8\,(-1+\alpha)^3\,\alpha^3\,(\mathrm{F1}^{00}_{1100000}-\mathrm{F1}^{00}_{2000000})\,. \quad (3.50)\end{aligned}$$

With this example, the notation should be quite clear.

The Diagrams that do not have such a simple structure, are given in the appendix, following the same general pattern. Overall constant factors are defined as above and in the appendix we simply list the different $\mathcal{F}_k^{(i)}(T,L)$.

3.4 Summary and outlook for chapter 3

We have formulated and organized the phase space integration of the virtual contributions to the NLO impact factor of the photon. For this purpose, the traces from the average over quark helicities have been calculated and organized with the help of the Mathematica package FeynCalc. The expressions resulting from the traces have been rewritten in terms of the integration variables, leading to propagator type integrals in the $(2-2\epsilon)$-dimensional transverse momentum space. An algorithm for the reduction of these integrals to a set of simpler integrals has been developed and applied. The final results are expressed explicitly in parts of this section and appendix B and will be a suitable basis for further analytical or numerical studies of the impact factor.

For future numerical studies of the impact factor, we will evaluate the integrals numerically. This will give us the virtual contribution to the impact factor as a function of τ. For an evaluation of the $\gamma^*\gamma^*$ cross section we have to convolute two impact factors with the Green's function $\mathcal{G}_\omega$. As it was outlined in section 1.2 we may find important hints on the proper definition of the virtual photon impact factor from the limit of very different photon virtualities, where we have an overlap with the kinematic regime of DGLAP evolution. In this limit, we have to calculate the Mellin transform of our impact factor, as in (1.69) analytically. Finally, the $\gamma^*\gamma^*$ cross section is obtained from (1.68) in momentum space or from (1.71) in Mellin space.

Chapter 4

Real gluon emission

After the completion of the virtual corrections, the next step in our program to compute the virtual photon impact factor at NLO are the contributions from the emission of real photons, as they were sketched in Fig. 1.10. We will compute these corrections from the process $\gamma^* + q \to (q\bar{q}g) + q$ at leading order in α_s. The corrections, we are interested in, come from the region of phase space, were the $q\bar{q}$-pair as well as the g are emitted in the fragmentation region of the virtual photon, i.e. with a large rapidity gap to the outgoing quark from the lower line. We impose no further restrictions on the $(q\bar{q}g)$-state. Therefore we have to be aware of the fact, that our calculation will include the result of the LLA calculation of the same process, where the gluon is emitted with a large rapidity gap to the lower quark as well as to the $q\bar{q}$-pair.

4.1 Kinematics and calculational techniques

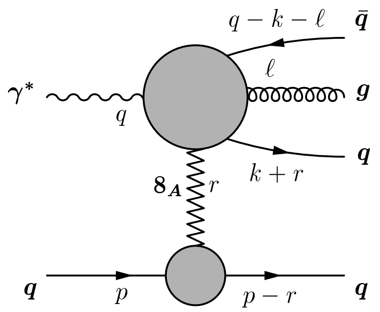

Figure 4.1: Kinematics of the process $\gamma^* + q \to q\bar{q}g + q$.

We label the momenta of the external particles, as depicted in Fig 4.1. The incoming momenta $q = q' - xp$ and p are used to construct the Sudakov basis q', p for the other momenta: q' and p are light cone momenta $q'^2 = p^2 = 0$ and the cm energy of the incoming particles is $s = 2p \cdot q'$. The virtuality of the photon is $q^2 = -Q^2$ and as usual, $x = Q^2/s$. The outgoing momenta are defined by the momentum transfer r, the gluon momentum ℓ and an internal momentum k, such that the quark and antiquark carry a momentum $k+r$ and $q-k-\ell$ respectively. We express these momenta in terms of their Sudakov variables,

$$k = \alpha q' + \beta p + k_\perp \ , \tag{4.1}$$

$$\ell = \alpha_\ell q' + \beta_\ell p + \ell_\perp \ , \tag{4.2}$$

$$r = \alpha_r q' + \beta_r p + r_\perp . \tag{4.3}$$

We introduce the euclidean notation for the twodimensional transverse momenta, e.g. $\boldsymbol{k}^2 = -k_\perp^2$. From the on-shell conditions for the outgoing quarks and the gluon we obtain all β variables and $\alpha_r = t/s$ in terms of transverse momentum invariants, α-variables and the common invariants s and $t = r^2 \approx -\boldsymbol{r}^2$:

$$\beta_\ell s = \frac{\boldsymbol{\ell}^2}{\alpha_\ell} \ , \tag{4.4}$$

$$\beta s = -\frac{(\boldsymbol{k}+\boldsymbol{\ell})^2}{1-\alpha-\alpha_\ell} - \frac{\boldsymbol{\ell}^2}{\alpha_\ell} - Q^2 \ , \tag{4.5}$$

$$\beta_r s = \frac{(\boldsymbol{k}+\boldsymbol{r})^2}{\alpha} + \frac{(\boldsymbol{k}+\boldsymbol{\ell})^2}{1-\alpha-\alpha_\ell} + \frac{\boldsymbol{\ell}^2}{\alpha_\ell} + Q^2 . \tag{4.6}$$

In addition, we define the denominators, that will occur during the calculation,

$$\begin{aligned} D_1 &= (k+\ell+r-q)^2 \\ &= -\bar{\alpha}_1 Q^2 - (\boldsymbol{k}+\boldsymbol{\ell}+\boldsymbol{r})^2 - \frac{\bar{\alpha}_1}{\alpha_1}(\boldsymbol{k}+\boldsymbol{r})^2 - \frac{\bar{\alpha}_1}{\alpha_\ell}\boldsymbol{\ell}^2 \end{aligned} \tag{4.7}$$

$$\begin{aligned} D_2 &= (k+r-q)^2 \\ &= -\alpha_2\, Q^2 - \frac{1}{\alpha_1}(\boldsymbol{k}+\boldsymbol{r})^2] \end{aligned} \tag{4.8}$$

$$\begin{aligned} D_3 &= (k+\ell+r)^2 \\ &= -(\boldsymbol{k}+\boldsymbol{\ell}+\boldsymbol{r})^2 + \frac{\bar{\alpha}_2}{\alpha_1}(\boldsymbol{k}+\boldsymbol{r})^2 + \frac{\bar{\alpha}_2}{\alpha_\ell}\boldsymbol{\ell}^2 \end{aligned} \tag{4.9}$$

$$= \frac{1}{\alpha_\ell\,\alpha_1}\left(-\alpha_\ell\,(\boldsymbol{k}+\boldsymbol{r}) + \alpha_1\,\boldsymbol{\ell}\right)^2 \tag{4.10}$$

$$\begin{aligned} D_4 &= (k-q)^2 \\ &= -\boldsymbol{k}^2 + \frac{\alpha_2}{\bar{\alpha}_1}(\boldsymbol{k}+\boldsymbol{\ell})^2 + \frac{\alpha_2}{\alpha_\ell}\boldsymbol{\ell}^2 \end{aligned} \tag{4.11}$$

$$= \frac{1}{\alpha_\ell\,\bar{\alpha}_1}\left(\alpha_\ell\,(\boldsymbol{k}+\boldsymbol{\ell}) + \bar{\alpha}_1\,\boldsymbol{\ell}\right)^2 \tag{4.12}$$

$$\begin{aligned} D_5 &= (\ell-r)^2 \\ &= -\alpha_\ell\,Q^2 - \frac{\alpha_\ell}{\alpha_1}(\boldsymbol{k}+\boldsymbol{r})^2 - \frac{\alpha_\ell}{\bar{\alpha}_1}(\boldsymbol{k}+\boldsymbol{\ell})^2 - (\boldsymbol{\ell}-\boldsymbol{r})^2 \end{aligned} \tag{4.13}$$

$$\begin{aligned} D_6 &= k^2 \\ &= -\alpha_1\,Q^2 - \boldsymbol{k}^2 - \frac{\alpha_1}{\bar{\alpha}_1}(\boldsymbol{k}+\boldsymbol{\ell})^2 - \frac{\alpha_1}{\alpha_\ell}\boldsymbol{\ell}^2 \end{aligned} \tag{4.14}$$

$$\begin{aligned} D_7 &= (k+\ell)^2 \\ &= -\bar{\alpha}_2\,Q^2 - \frac{1}{\bar{\alpha}_1}(\boldsymbol{k}+\boldsymbol{\ell})^2 \end{aligned} \tag{4.15}$$

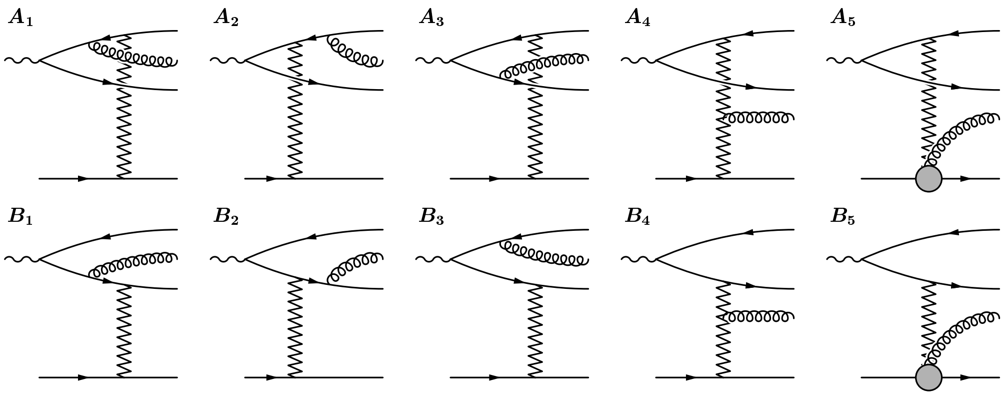

Figure 4.2: Feynman diagrams for the process $\gamma^* + Q \to q\bar{q}g + Q$.

We are interested in the kinematical region, where we have a large rapidity gap between the lower quark and the $(q\bar{q}g)$-system in the final state. This is given by the region, where s is much larger than all transverse momenta $\boldsymbol{k}^2, \boldsymbol{\ell}^2, \boldsymbol{r}^2$. The upper α variables are of order unity, $\alpha, \alpha_\ell \sim 1$ and the upper β variables are of the order t/s. The Feynman diagrams that will contribute in this region are given in Fig. 4.2. Obviously the diagrams in the second line $B_1, \ldots, B_5$ are obtained from the diagrams $A_1, \ldots, A_5$ from the interchange of the quark and antiquark $q \leftrightarrow \bar{q}$ in the upper fermion line. In terms of kinematical variables, the corresponding transformation is

$$\alpha \to 1 - \alpha - \alpha_\ell \tag{4.16}$$
$$\boldsymbol{k} \to -(\boldsymbol{k} + \boldsymbol{r} + \boldsymbol{\ell}). \tag{4.17}$$

To emphasise this symmetry explicitly, we also use the following variables, where we denote variables that are related to each other by the $q \leftrightarrow \bar{q}$ transformation with a bar:

$$\alpha_1 \equiv \alpha \ , \tag{4.18}$$
$$\bar{\alpha}_1 \equiv (1 - \alpha - \alpha_\ell) \ , \tag{4.19}$$
$$\alpha_2 \equiv (1 - \alpha) \ , \tag{4.20}$$
$$\bar{\alpha}_2 \equiv (\alpha + \alpha_\ell). \tag{4.21}$$

Under this transformation, the denominators D_1 to D_7 obey the following relations:

$$D_1 = \bar{D}_6 \ , \tag{4.22}$$
$$D_2 = \bar{D}_7 \ , \tag{4.23}$$
$$D_3 = \bar{D}_4 \ , \tag{4.24}$$
$$D_5 = \bar{D}_5 \ . \tag{4.25}$$

In our calculation we fix the polarisation of the virtual photon either to be

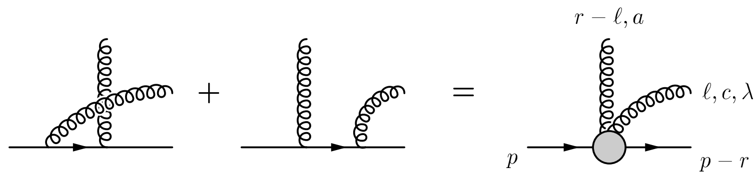

Figure 4.3: Emission of a gluon from the lower quark line.

longitudinal or transverse. The polarisation vectors of the photon are

$$\varepsilon_L = \frac{1}{Q}(q' + xp) \ , \tag{4.26}$$

$$\varepsilon_\pm = \frac{1}{\sqrt{2}}(0, 1, \pm i, 0). \tag{4.27}$$

We may write $\varepsilon_L = q/Q + 2xp/Q$, for the longitudinal polarisation vector. The term that is proportional to the photon momentum q should be zero, due to gauge invariance. Therefore, we simply use the remaining term $\varepsilon_0 = 2xp/Q$ throughout the calculation. In the Born level calculation of the photon wave function, we have used the full longitudinal polarisation vectors. There, it was very instructive to follow the cancellation of different terms due to gauge invariance. In a single diagram these terms even lead to a divergent phase space integral. In the case of transverse photons we calculate the sum over the two possible polarisations denoting it with T, making use of the fact, that in the forward case, this sum is simply

$$\sum_{\lambda=+,-} \varepsilon_\mu^\lambda \varepsilon_\nu^{\lambda *} = -\delta_{\mu\nu}^\perp. \tag{4.28}$$

Concerning the helicities of the outgoing $q\bar{q}$ pair we calculate the sum over all helicity configurations by taking the trace of the arising strings of Dirac matrices.

We perform our calculation in the Feynman gauge. In the high energy limit, we use the decomposition

$$g_{\mu\nu} = \frac{2}{s}\left(p_\mu q'_\nu + p_\nu q'_\mu\right) + g_{\mu\nu}^\perp \tag{4.29}$$

for the metric tensor in the numerator of t-channel gluon propagators and retain only the first term, since the contributions of the other terms will be suppressed by powers of t/s. For the diagrams where the emitted gluon hooks onto the lower fermion line, this is not immediately clear, since the t channel gluon does not carry only small components of the light cone momenta but we checked the calculation against a calculation of these diagrams involving the full metric tensor.

In the Feynman diagrams A_5 and B_5 we have replaced the two diagrams, where the emitted gluon couples to the lower fermion line by one effective diagram, as sketched in Fig. 4.3. Since the gluon is still far from the lower quark in rapidity, we can simplify the part of these diagrams, that is related to the gluon emission in the following simplified way:

$$\bar{u}(p-r,h')\left[\frac{\not{q}'(\not{p}-\not{\ell})\gamma^\lambda}{(p-\ell)^2}t^a t^c + \frac{\gamma^\lambda(\not{p}+\not{\ell}-\not{r})\not{q}'}{(p+\ell-r)^2}t^c t^a\right]u(p,h) \approx \frac{2p^\lambda}{\alpha_\ell}[t^c,t^a]\delta_{hh'} \; . \tag{4.30}$$

Here we used that ℓ has large components only in the q' direction. h and h' denote the helicities of the lower incoming and outgoing quarks, respectively. λ is to be contracted with the polarization vector of the outgoing gluon with colour index c. t^a and t^c are the colour group generators in the fundamental representation and a is the colour index carried by the t-channel gluon.

4.2 Results

As already mentioned above, we summed over the helicities of the outgoing $q\bar{q}$-pair for our process. After writing down the amplitudes $A_1,\ldots,A_5$ we calculated the occuring traces with the help of the Mathematica package FeynCalc [44]. This has been done separately for the longitudinal and the transverse polarization of the virtual photon. However, the results of this calculation are quite lengthy and not very instructive.

Here, we present the results for the longitudinal polarization after performing some simplifying algebra by hand. We have rewritten each squared amplitude in order to reveal its structure in transverse momentum space: we find each contribution to be written in a factorized form, suitable for the wave function interpretation. In this way, one term will belong to the incoming and one term to the outgoing photon. As a first approach, we have performed this step diagram by diagram. The results will be presented in the following form:

$$|\mathcal{M}|^2 = \frac{16\,Q^2\,s^2}{\boldsymbol{r}^4}e^2 e_f^2 g^6(\,t^a\,t^b\,)\,\delta^{ab}\sum_{i,j=1}^{5}\,(\mathcal{A}\mathcal{A}_{ij}\,+\,\mathcal{A}\mathcal{B}_{ij}\,+\,\mathcal{B}\mathcal{A}_{ij}\,+\,\mathcal{B}\mathcal{B}_{ij}) \tag{4.31}$$

The denotation of the pair of $\mathcal{A}_i$ and $\mathcal{B}_j$ follows closely the denotation of the different diagrams in Fig. 4.2, e.g. the result for the interference term of diagram $\boldsymbol{A_1}$ and $\boldsymbol{B_3}$ is labelled $\mathcal{A}\mathcal{B}_{13}$ etc.

From the results of single squared diagrams $|\boldsymbol{A_i}|^2$ we inferred the following vectors in transverse momentum space:

$$\boldsymbol{A}_1 = \alpha_2\,\boldsymbol{\ell} + \alpha_\ell\,(\boldsymbol{k}+\boldsymbol{r}) \tag{4.32}$$
$$\boldsymbol{A}_2 = \bar{\alpha}_1\,\boldsymbol{\ell} + \alpha_\ell\,(\boldsymbol{k}+\boldsymbol{\ell}) \tag{4.33}$$
$$\boldsymbol{A}_3 = \alpha_1\,\boldsymbol{\ell} - \alpha_\ell\,(\boldsymbol{k}+\boldsymbol{r}) \tag{4.34}$$
$$\boldsymbol{A}_4 = \alpha_2\,(\boldsymbol{\ell}-\boldsymbol{r}) + \alpha_\ell\,(\boldsymbol{k}+\boldsymbol{r}) \tag{4.35}$$
$$\boldsymbol{B}_1 = \bar{\alpha}_2\,\boldsymbol{\ell} - \alpha_\ell\,(\boldsymbol{k}+\boldsymbol{\ell}) \tag{4.36}$$
$$\boldsymbol{B}_2 = \alpha_1\,\boldsymbol{\ell} - \alpha_\ell\,(\boldsymbol{k}+\boldsymbol{r}) \tag{4.37}$$
$$\boldsymbol{B}_3 = \bar{\alpha}_1\,\boldsymbol{\ell} + \alpha_\ell\,(\boldsymbol{k}+\boldsymbol{\ell}) \tag{4.38}$$
$$\boldsymbol{B}_4 = \bar{\alpha}_2\,(\boldsymbol{\ell}-\boldsymbol{r}) - \alpha_\ell\,(\boldsymbol{k}+\boldsymbol{\ell})\;. \tag{4.39}$$

Note, that the vectors $\boldsymbol{B}_i$ are obtained from the respective $\boldsymbol{A}_i$ by the transformation (4.16). We found, that also the resulting interference terms revealed a remarkable structure in terms of these vectors. In particular we were able to write the results in a remarkably compact way. We obtained the following results for the diagrams where the t-channel gluons are always attached to the antiquark:

$$\mathcal{A}\mathcal{A}_{11} = -\,C_F\,\frac{2}{D_1^2\,D_2^2}\,\alpha_1\,\bar\alpha_1\,\boldsymbol{A}_1^2 \tag{4.40}$$

$$\mathcal{A}\mathcal{A}_{12} = \frac{1}{N_c}\,\frac{1}{D_1\,D_2^2\,D_4}\,\big(\alpha_1\,\alpha_2\,\boldsymbol{A}_1\,\boldsymbol{A}_2 - \alpha_1\,\alpha_2^2\,\bar\alpha_1\,\boldsymbol{r}^2\big) \tag{4.41}$$

$$\mathcal{A}\mathcal{A}_{13} = -\,C_F\,\frac{2}{D_1^2\,D_2\,D_3}\,\big(\bar\alpha_1^2\,\boldsymbol{A}_1\,\boldsymbol{A}_3 + \bar\alpha_1^2\,(\boldsymbol{k}+\boldsymbol{r})\,(\boldsymbol{k}+\boldsymbol{\ell}+\boldsymbol{r})\big) \tag{4.42}$$

$$\begin{aligned}\mathcal{A}\mathcal{A}_{14} = N_c\,\frac{1}{D_1\,D_2^2\,D_5}\bigg(&\frac{1}{2\,\alpha_\ell}\,\alpha_1\,\big(\alpha_2\,\bar\alpha_1 + 2\,\alpha_\ell^2\big)\,\boldsymbol{A}_1\,\boldsymbol{A}_4\\ &+\frac{1}{2}\alpha_1\,\alpha_2\,\bar\alpha_1^2\,D_2 + \frac{1}{2\,\alpha_\ell}\,\alpha_1\,\alpha_2^2\,\bar\alpha_1\,\boldsymbol{A}_1\boldsymbol{r} - \alpha_1\,\alpha_2^2\,\bar\alpha_1\,\boldsymbol{r}^2\bigg)\end{aligned} \tag{4.43}$$

$$\mathcal{A}\mathcal{A}_{15} = -\,N_c\,\frac{1}{\alpha_\ell\,D_1\,D_2^2\,D_5}\,\alpha_1\,\alpha_2^2\,\bar\alpha_1^2\,\boldsymbol{r}^2 \tag{4.44}$$

$$\mathcal{A}\mathcal{A}_{22} = -\,C_F\,\frac{2}{\bar\alpha_1\,D_2^2\,D_4^2}\,\alpha_1\,\alpha_2^2\,\boldsymbol{A}_2^2 \tag{4.45}$$

$$\begin{aligned}\mathcal{A}\mathcal{A}_{23} = \frac{1}{N_c}\,\frac{1}{D_1\,D_2\,D_3\,D_4}&\big(\alpha_2\,\bar\alpha_1\,\boldsymbol{A}_2\,\boldsymbol{A}_3\\ &+\alpha_2\,\bar\alpha_1\,(\boldsymbol{k}+\boldsymbol{r}-\alpha_1\,\boldsymbol{r})\,(\boldsymbol{k}+\boldsymbol{\ell}+\bar\alpha_1\,\boldsymbol{r})\big)\end{aligned} \tag{4.46}$$

$$\begin{aligned}\mathcal{A}\mathcal{A}_{24} = -\,N_c\,\frac{1}{D_2^2\,D_4\,D_5}\bigg(&\frac{1}{2\,\alpha_\ell\,\bar\alpha_1}\,\alpha_1\,\alpha_2\,\big(\alpha_2\,\bar\alpha_1 + 2\,\alpha_\ell^2\big)\,\boldsymbol{A}_2\,\boldsymbol{A}_4\\ &+\frac{1}{2}\alpha_1\,\alpha_2^2\,\bar\alpha_1\,D_2 + \frac{1}{2\,\alpha_\ell}\,\alpha_1\,\alpha_2^2\,\bar\alpha_1\,\boldsymbol{A}_2\boldsymbol{r} + \alpha_1\,\alpha_2^2\,\bar\alpha_1\,\boldsymbol{r}^2\bigg)\end{aligned} \tag{4.47}$$

$$\mathcal{A}\mathcal{A}_{25} = N_c\,\frac{1}{\alpha_\ell\,D_2^2\,D_4\,D_5}\,\alpha_1\,\alpha_2^3\,\bar\alpha_1\,\boldsymbol{r}^2 \tag{4.48}$$

$$\mathcal{A}\mathcal{A}_{33} = -\,C_F\,\frac{2}{\alpha_1\,D_1^2\,D_3^2}\,\bar\alpha_1^3\,\boldsymbol{A}_3^2 \tag{4.49}$$

$$\begin{aligned}\mathcal{A}\mathcal{A}_{34} = -\,N_c\,\frac{1}{D_1\,D_2\,D_3\,D_5}\bigg(&\frac{1}{2\,\alpha_\ell}\bar\alpha_1\,\big(\alpha_1\,\bar\alpha_1 - \alpha_\ell - 2\,\alpha_\ell^2\big)\,\boldsymbol{A}_3\,\boldsymbol{A}_4\\ &-\frac{1}{2}\,\alpha_1\,\bar\alpha_1^2\,\bar\alpha_2\,D_2 + \alpha_1\,\alpha_2\,\bar\alpha_1^2\,D_7 + \frac{1}{2\,\alpha_\ell}\,\alpha_1\,\alpha_2\,\bar\alpha_1^2\,\boldsymbol{A}_3\boldsymbol{r}\\ &+\alpha_1\,\alpha_2\,\bar\alpha_1^2\,\boldsymbol{r}^2 + \frac{3}{2}\,\alpha_2\,\bar\alpha_1\,\boldsymbol{A}_3\,(\boldsymbol{k}+\boldsymbol{\ell})\bigg)\end{aligned} \tag{4.50}$$

$$\mathcal{A}\mathcal{A}_{35} = N_c\,\frac{1}{\alpha_\ell\,D_1\,D_2\,D_3\,D_5}\,\alpha_1\,\alpha_2\,\bar\alpha_1^2\,\bar\alpha_2\,\boldsymbol{r}^2 \tag{4.51}$$

$$\begin{aligned}\mathcal{A}\mathcal{A}_{44} = -\,N_c\,\frac{1}{D_2^2\,D_5^2}\bigg(&\frac{2}{\bar\alpha_1}\,\boldsymbol{A}_4^2\,\alpha_1\,\big(\alpha_\ell^2 + \alpha_2\,\bar\alpha_1\big) + \alpha_1\,\alpha_2\,\alpha_\ell\,\bar\alpha_1\,D_2\\ &+2\,\alpha_1\,\alpha_2^2\,\bar\alpha_1\,\boldsymbol{r}^2\bigg)\end{aligned} \tag{4.52}$$

$$\mathcal{A}\mathcal{A}_{45} = N_c \,\frac{1}{D_2^2\,D_5^2}\alpha_1\,\alpha_2^2\,\bar{\alpha}_1\,\boldsymbol{r}^2 \tag{4.53}$$

$$\mathcal{A}\mathcal{A}_{55} = 0 \tag{4.54}$$

The results with interchanged indices are related to the above diagrams by complex conjugation and since the diagrams are real, they are equal:

$$\mathcal{A}\mathcal{A}_{ji} = \mathcal{A}\mathcal{A}_{ij}\;. \tag{4.55}$$

The results for the diagrams, where the t-channel gluons are both coupled to the quark are obtained by the transformation (4.16),

$$\mathcal{B}\mathcal{B}_{ij} = \overline{\mathcal{A}\mathcal{A}}_{ij}\;. \tag{4.56}$$

The interference terms between diagrams where one t-channel gluon couples to the quark and the other one to the antiquark are given as follows,

$$\begin{aligned}\mathcal{A}\mathcal{B}_{11} = &-\frac{1}{N_c}\,\frac{1}{D_1\,D_2\,D_6\,D_7}\big(\alpha_1\,\bar{\alpha}_1\,\boldsymbol{A}_1\,\boldsymbol{B}_1\\ &+\alpha_1\,\bar{\alpha}_1\,(\boldsymbol{k}+\alpha_1\,\boldsymbol{r})\,(\boldsymbol{k}+\boldsymbol{\ell}+\bar{\alpha}_2\,\boldsymbol{r})\big)\end{aligned} \tag{4.57}$$

$$\mathcal{A}\mathcal{B}_{12} = C_F\,\frac{2}{D_1\,D_2\,D_3\,D_7}\,\left(\bar{\alpha}_1\,\bar{\alpha}_2\,\boldsymbol{A}_1\,\boldsymbol{B}_2+\bar{\alpha}_1\,\bar{\alpha}_2\,(\boldsymbol{k}+\boldsymbol{r})\,(\boldsymbol{k}+\boldsymbol{\ell}+\boldsymbol{r})\right) \tag{4.58}$$

$$\mathcal{A}\mathcal{B}_{13} = -\frac{1}{N_c}\frac{1}{D_1\,D_2\,D_4\,D_6}\left(\alpha_1^2\,\boldsymbol{A}_1\,\boldsymbol{B}_3-\alpha_1^2\,\alpha_2\,\bar{\alpha}_1\,\boldsymbol{r}^2\right) \tag{4.59}$$

$$\begin{aligned}\mathcal{A}\mathcal{B}_{14} = &-N_c\,\frac{1}{D_1\,D_2\,D_5\,D_7}\bigg(\frac{1}{2\,\alpha_\ell}\,\bar{\alpha}_1\,\left(\alpha_1\,\bar{\alpha}_1-\alpha_\ell-2\,\alpha_\ell^2\right)\boldsymbol{A}_1\,\boldsymbol{B}_4\\ &+\alpha_1\,\bar{\alpha}_1^2\,\bar{\alpha}_2\,D_2-\frac{1}{2}\alpha_1\,\alpha_2\,\bar{\alpha}_1^2\,D_7+\frac{1}{2\,\alpha_\ell}\,\alpha_1\,\alpha_2\,\bar{\alpha}_1\,\bar{\alpha}_2\,\boldsymbol{A}_1\,\boldsymbol{r}\\ &-\alpha_1\,\alpha_2\,\bar{\alpha}_1\,\bar{\alpha}_2\,\boldsymbol{r}^2-\frac{3}{2}\,\bar{\alpha}_1\,\bar{\alpha}_2\,\boldsymbol{A}_1\,(\boldsymbol{k}+\boldsymbol{r})\bigg)\end{aligned} \tag{4.60}$$

$$\mathcal{A}\mathcal{B}_{15} = N_c\,\frac{1}{\alpha_\ell\,D_1\,D_2\,D_5\,D_7}\alpha_1\,\alpha_2\,\bar{\alpha}_1^2\,\bar{\alpha}_2\,\boldsymbol{r}^2 \tag{4.61}$$

$$\begin{aligned}\mathcal{A}\mathcal{B}_{22} = &-\frac{1}{N_c}\,\frac{1}{D_2\,D_3\,D_4\,D_7}\big(\alpha_2\,\bar{\alpha}_2\,\boldsymbol{A}_2\,\boldsymbol{B}_2\\ &+\alpha_2\,\bar{\alpha}_2\,(\boldsymbol{k}+\boldsymbol{r}-\alpha_1\,\boldsymbol{r})\,(\boldsymbol{k}+\boldsymbol{\ell}+\bar{\alpha}_1\,\boldsymbol{r})\big)\end{aligned} \tag{4.62}$$

$$\mathcal{A}\mathcal{B}_{23} = C_F\,\frac{2}{\bar{\alpha}_1\,D_2\,D_4^2\,D_6}\,\alpha_1^2\,\alpha_2\,\boldsymbol{A}_2\boldsymbol{B}_3 \tag{4.63}$$

$$\begin{aligned}\mathcal{A}\mathcal{B}_{24} = &\,N_c\,\frac{1}{D_2\,D_4\,D_5\,D_7}\bigg(\frac{1}{2\,\alpha_\ell}\,\alpha_2\,\left(\alpha_1\,\bar{\alpha}_1-\alpha_\ell-2\,\alpha_\ell^2\right)\boldsymbol{A}_2\,\boldsymbol{B}_4\\ &+\alpha_1\,\alpha_2\,\bar{\alpha}_1\,\bar{\alpha}_2\,D_2-\frac{1}{2}\alpha_1\,\alpha_2^2\,\bar{\alpha}_1\,D_7+\frac{1}{2\,\alpha_\ell}\,\alpha_1\,\alpha_2\,\bar{\alpha}_1\,\bar{\alpha}_2\,\boldsymbol{A}_2\,\boldsymbol{r}\\ &+\alpha_1\,\alpha_2\,\bar{\alpha}_1\,\bar{\alpha}_2\,\boldsymbol{r}^2-\frac{3}{2}\,\alpha_2\,\bar{\alpha}_2\,\boldsymbol{A}_2\,(\boldsymbol{k}+\boldsymbol{r})\bigg)\end{aligned} \tag{4.64}$$

$$\mathcal{A}\mathcal{B}_{25} = -N_c\,\frac{1}{\alpha_\ell\,D_2\,D_4\,D_5\,D_7}\alpha_1\,\alpha_2^2\,\bar{\alpha}_1\,\bar{\alpha}_2\,\boldsymbol{r}^2 \tag{4.65}$$

$$\begin{aligned}\mathcal{A}\mathcal{B}_{33} = &-\frac{1}{N_c}\,\frac{1}{D_1\,D_3\,D_4\,D_6}\big(\alpha_1\,\bar{\alpha}_1\,\boldsymbol{A}_3\,\boldsymbol{B}_3\\ &+\alpha_1\,\bar{\alpha}_1\,(\boldsymbol{k}+\boldsymbol{r}-\alpha_1\,\boldsymbol{r})\,(\boldsymbol{k}+\boldsymbol{\ell}+\bar{\alpha}_1\,\boldsymbol{r})\big)\end{aligned} \tag{4.66}$$

$$\mathcal{AB}_{34} = N_c \frac{1}{D_1\, D_3\, D_5\, D_7} \left(\frac{1}{2\,\alpha_1\,\alpha_\ell} \bar{\alpha}_1^2 \, \left(\alpha_1\,\bar{\alpha}_2 + 2\,\alpha_\ell^2\right) \, \boldsymbol{A}_3\, \boldsymbol{B}_4 \right. \tag{4.67}$$

$$\left. + \frac{1}{2}\alpha_1\,\bar{\alpha}_1^2\,\bar{\alpha}_2\, D_7 + \frac{1}{2\,\alpha_\ell}\alpha_1\,\bar{\alpha}_1^2\,\bar{\alpha}_2\,\boldsymbol{A}_3\,\boldsymbol{r} + \alpha_1\,\bar{\alpha}_1^2\,\bar{\alpha}_2\,\boldsymbol{r}^2 \right) \tag{4.68}$$

$$\mathcal{AB}_{35} = -\, N_c \frac{1}{\alpha_\ell\, D_1\, D_3\, D_5\, D_7} \alpha_1\,\bar{\alpha}_1^2\,\bar{\alpha}_2^2\,\boldsymbol{r}^2 \tag{4.69}$$

$$\begin{aligned} \mathcal{AB}_{44} = N_c \frac{1}{D_2\, D_5^2\, D_7} \Big(& \left(2\,\alpha_1\,\bar{\alpha}_1 + \alpha_\ell - 2\,\alpha_\ell^2\right) \boldsymbol{A}_4\, \boldsymbol{B}_4 \\ & + \frac{1}{2}\alpha_1\,\alpha_\ell\,\bar{\alpha}_1\,\bar{\alpha}_2\, D_2 + \frac{1}{2}\alpha_1\,\alpha_2\,\alpha_\ell\,\bar{\alpha}_1\, D_7 + 2\,\alpha_1\,\alpha_2\,\bar{\alpha}_1\,\bar{\alpha}_2\,\boldsymbol{r}^2 \\ & - \alpha_\ell^2\, (\boldsymbol{k}+\boldsymbol{\ell})\, (\boldsymbol{k}+\boldsymbol{r}) \Big) \end{aligned} \tag{4.70}$$

$$\mathcal{AB}_{45} = -\, N_c \frac{1}{D_2\, D_5^2\, D_7} \alpha_1\,\alpha_2\,\bar{\alpha}_1\,\bar{\alpha}_2\,\boldsymbol{r}^2 \tag{4.71}$$

$$\mathcal{AB}_{55} = 0\,. \tag{4.72}$$

Again, we obtain the remaining terms by complex conjugation, i.e. by the equality

$$\mathcal{AB}_{ij} = \mathcal{BA}_{ji} \tag{4.73}$$

or by using the transformation (4.16)

$$\mathcal{AB}_{ij} = \overline{\mathcal{BA}}_{ij} \tag{4.74}$$

or by the combination of both transformations

$$\mathcal{AB}_{ij} = \overline{\mathcal{BA}}_{ij} = \overline{\mathcal{AB}}_{ji}\,. \tag{4.75}$$

4.3 The $q\bar{q}g$ component of the photon wave function

We will consider the above results in transverse configuration space and reveal their structure in terms of a new $q\bar{q}g$- component of the photon wave function. To this end, we take the Fourier transform of the above results with respect to the transverse momentum variables $\boldsymbol{k}$ and $\boldsymbol{\ell}$, thereby introducing the variables $\boldsymbol{\rho}_1$ and $\boldsymbol{\rho}_2$ denoting two distance vectors in the transverse space of the $q\bar{q}g$-system.

We begin with the terms proportional to $\boldsymbol{A}_i\boldsymbol{A}_j$, which are present in all $\mathcal{AA}_{ij}$ (except for the elements with $j = 5$). For every diagram there is a pair of denominators that we associate with the respective vector $\boldsymbol{A}_i$. As an illustration, we consider the contribution $\mathcal{AA}_{11}$ to (4.31). Obviously we can write it as a product of three terms,

$$\mathcal{AA}_{11} = \frac{(\boldsymbol{A}_1)_m}{D_1 D_2} \left(-2\delta_{mn} C_F \alpha_1 \bar{\alpha}_1\right) \frac{(\boldsymbol{A}_1)_n}{D_1 D_2}\,, \tag{4.76}$$

where the sum over m and n is understood. Defining the Fourier transform of the last factor:

$$\iint \frac{d^2\boldsymbol{k} d^2\boldsymbol{\ell}}{(2\pi)^2} e^{i\boldsymbol{\rho}_1\boldsymbol{k}} e^{i\boldsymbol{\rho}_2\boldsymbol{\ell}} \frac{(\boldsymbol{A}_1)_n}{D_1 D_2} \tag{4.77}$$

and using the definitions (4.7), (4.8) and (4.40), we note that the dependence upon $\boldsymbol{r}$ appears only in combination with the momentum $\boldsymbol{k}$. Changing the integration variable $\boldsymbol{k}$ into $\boldsymbol{k}' = \boldsymbol{k} + \boldsymbol{r}$, the $\boldsymbol{r}$ dependence is shifted into an exponential factor and we can write for (4.77)

$$e^{-i\boldsymbol{\rho}_1 \boldsymbol{r}} \psi^{(1)}_{q\bar{q}g;n}(Q^2; \rho_1, \rho_2, \alpha, \alpha_\ell) \, , \tag{4.78}$$

where we have defined the wave function

$$\psi^{(1)}_{q\bar{q}g;n}(Q^2; \rho_1, \rho_2, \alpha, \alpha_\ell) = \iint \frac{d^2\boldsymbol{k}' d^2\boldsymbol{\ell}}{(2\pi)^2} e^{i\boldsymbol{\rho}_1 \boldsymbol{k}'} e^{i\boldsymbol{\rho}_2 \boldsymbol{\ell}} \frac{(\boldsymbol{A}_1)_n}{D_1 D_2} \, . \tag{4.79}$$

The integrand on the right hand side of this new Fock component of the (longitudinal) photon wave function depends upon $\boldsymbol{k}'$ and $\boldsymbol{\ell}$, but not on $\boldsymbol{r}$. With a similar result for the first term in (4.76), the contribution of $\mathcal{A}\mathcal{A}_{11}$ to the squared matrix element (4.31) takes the form

$$\int d\alpha d\alpha_\ell \int d^2\boldsymbol{\rho}_1 d^2\boldsymbol{\rho}_2 \, \psi^{(1)*}_{q\bar{q}g;m} \sigma^{(11)}_{q\bar{q}g;mn} \psi^{(1)}_{q\bar{q}g;n} \tag{4.80}$$

where

$$\sigma^{(11)}_{q\bar{q}g;mn}(\alpha, \alpha_\ell, \boldsymbol{\rho}_1, \boldsymbol{\rho}_2) = \int d^2\boldsymbol{r} \, e^{i\boldsymbol{\rho}_1 \boldsymbol{r}} \left(-2\delta_{mn} \frac{C_F \alpha_1 \bar{\alpha}_1}{\boldsymbol{r}^4} \right) e^{-i\boldsymbol{\rho}_1 \boldsymbol{r}} . \tag{4.81}$$

In obtaining this last expression we have carried out the integrations in $\boldsymbol{\ell}$ and $\boldsymbol{k}$, which has lead to δ-functions in the $\boldsymbol{\rho}$-vectors: the incoming and the outgoing photons have the same transverse coordinates, i.e. the transverse coordinates of the $q\bar{q}g$ system remain 'frozen' during the interaction with the lower quark.

It is easy to see that a similar analysis applies to the terms proportional to $\boldsymbol{A}_i \boldsymbol{A}_j$ in all other $\mathcal{A}\mathcal{A}_{ij}$. In summary, we transform the transverse momenta in the following way:

$$\frac{\boldsymbol{A}_1}{D_1 D_2} : \qquad \boldsymbol{k}' = \boldsymbol{k} + \boldsymbol{r} \qquad \boldsymbol{\ell}' = \boldsymbol{\ell} \tag{4.82}$$

$$\frac{\boldsymbol{A}_2}{D_2 D_4} : \qquad \boldsymbol{k}' = \boldsymbol{k} + \boldsymbol{r} \qquad \boldsymbol{\ell}' = \boldsymbol{\ell} - \frac{\alpha_\ell}{1-\alpha} \boldsymbol{r} \tag{4.83}$$

$$\frac{\boldsymbol{A}_3}{D_1 D_3} : \qquad \boldsymbol{k}' = \boldsymbol{k} + \boldsymbol{r} \qquad \boldsymbol{\ell}' = \boldsymbol{\ell} \tag{4.84}$$

$$\frac{\boldsymbol{A}_4}{D_2 D_5} : \qquad \boldsymbol{k}' = \boldsymbol{k} + \boldsymbol{r} \qquad \boldsymbol{\ell}' = \boldsymbol{\ell} - \boldsymbol{r} \tag{4.85}$$

In this way we eliminate the dependence upon $\boldsymbol{r}$ from the Fourier transforms and obtain expressions which, after insertion into (4.31), can be interpreted as photon wave function components $\psi^{(i)}_{q\bar{q}g}$. The $\boldsymbol{r}$ dependence is entirely carried by the interaction cross sections $\sigma^{(ij)}_{q\bar{q}g}$, similar as in (4.81). We carry out the transformation of the elements $\boldsymbol{B}_i$ in a similar fashion. The shifts in the $\boldsymbol{k}$ and $\boldsymbol{\ell}$ integrations are just transformed according to (4.16).

As the next class of terms, consider the terms proportional to $\boldsymbol{r}^2$. Starting with $\mathcal{A}\mathcal{A}_{12}$, we proceed as before, but the Fourier transformation is done only for $1/(D_1 D_2)$ and $1/(D_2 D_4)$, respectively: using the same shift of momenta as before, we again find the dependence upon $\boldsymbol{r}$ concentrated in phase factors, and the remaining integrals define new (scalar) contributions to the photon wave functions $\psi^{(1)}_{q\bar{q}g}$ and $\psi^{(2)}_{q\bar{q}g}$ which do not depend upon $\boldsymbol{r}$. The factor $\boldsymbol{r}^2$ goes into the cross section $\sigma^{(12)}_{q\bar{q}g}$.

Next those contributions to $\mathcal{AA}_{ij}$ which contain D_2 or D_7 in the numerator: the first appearance is in $\mathcal{AA}_{14}$, and a quick survey shows that these terms show up only if $i = 4$ or $j = 4$. Therefore, these pieces have to be part of the wave function component $\psi^{(4)}_{q\bar{q}g}$: e.g. $D_2/(D_2 D_5)$ or $D_7/(D_2 D_5)$. Again, the dependence upon $\boldsymbol{r}$ can be factored out and leads to a phase factor which becomes part of the interaction cross section.

Finally, we have contributions proportional to $\boldsymbol{A}_i \boldsymbol{r}$ which appear only for $j = 4$: following again the same steps as before, we take the vector $\boldsymbol{A}_i$ as a part of the wave function $\psi^{(i)}_{q\bar{q}g}$, and we absorb $\boldsymbol{r}$ into the cross section $\sigma^{(i4)}$. The contributions proportional to scalar products such as $(\boldsymbol{k}+\boldsymbol{r})(\boldsymbol{k}+\boldsymbol{l})$ are treated in a similar way: one of the two vectors belongs to the wave function $(\psi^{(i)})^*$, the other belongs to $\psi^{(j)}$. Here we have some freedom in the choice to which wave function a particular term belongs. In any case, the dependence upon $\boldsymbol{r}$ can entirely be absorbed into the interaction cross sections $\sigma_{q\bar{q}g}$.

As result, all terms appearing on the right hand side of $\mathcal{AA}_{ij}$, $\mathcal{AB}_{ij}$ in the results (4.40)–(4.54) and (4.57)–(4.72) can be cast either into the form (4.80) or

$$\int d\alpha d\alpha_\ell \int d^2\boldsymbol{\rho}_1 d^2\boldsymbol{\rho}_2 \psi^{(i)*}_{q\bar{q}g;m} \sigma^{(ij)}_{q\bar{q}g;m} \psi^{(j)}_{q\bar{q}g} \, , \tag{4.86}$$

or into the form

$$\int d\alpha d\alpha_\ell \int d^2\boldsymbol{\rho}_1 d^2\boldsymbol{\rho}_2 \psi^{(i)*}_{q\bar{q}g} \sigma^{(ij)}_{q\bar{q}g} \psi^{(j)}_{q\bar{q}g} \tag{4.87}$$

In other words, we have both scalar and vector-like contributions to the new photon wave function $\psi_{q\bar{q}g}$. In accordance we have a scalar, a vector and a tensor component of the interaction cross section in the basis of transverse configuration space, quite in contrast to the leading order case, cf. (1.36), where the decomposition of the squared matrix element into a dipole cross section and the $q\bar{q}$-component of the photon wave function unambiguously lead to scalar contributions.

At this stage, the matrix of interaction cross sections $\sigma^{(ij)}$ (here the indices i and j have to be extended in order to include $\mathcal{AA}$, $\mathcal{AB}$, $\mathcal{BA}$, and $\mathcal{BB}$, i.e. they run from 1 to 10) is not diagonal: so far our choice of the basis of the wave function components had been dictated by the Feynman diagrams from which we have started our calculations. Since the matrix is symmetric, we can always find a more physical basis in which the interactions are diagonal. In this basis, our cross section can be written as a sum of squares.

4.4 The limit of central emission

As a very stringent test of our results, we have taken the limit where the gluon is not emitted in the fragmentation region of the virtual photon but in the central rapidity region, such that the Sudakov components are strongly ordered:

$$1 \gg \alpha_\ell \gg -t/s \tag{4.88}$$

$$-t/s \ll \beta_\ell \ll 1 \, . \tag{4.89}$$

The Sudakov variables are therefore of the order $\alpha_\ell \sim \beta_\ell \sim \ell/\sqrt{s}$ in the central region, where $\ell = |\boldsymbol{\ell}|$ is of the order of a typical transverse momentum. This region is included in our approach and well known from the leading logarithmic approximation. We may easily observe the result from our calculation in this limit. First of all, the denominators (4.7) to (4.15) are expressed in terms of the two denominators $D(\boldsymbol{k}+\boldsymbol{r})$ and $D(\boldsymbol{k}+\boldsymbol{\ell})$, cf. (1.6) that are well known from Born approximation in the following way,

$$\begin{aligned}
D_1 &\to -\frac{1-\alpha}{\alpha_\ell}\boldsymbol{\ell}^2 \, , \\
D_2 &\to -\frac{1}{\alpha}D(\boldsymbol{k}+\boldsymbol{r}) \, , \\
D_3 &\to \frac{\alpha}{\alpha_\ell}\boldsymbol{\ell}^2 \, , \\
D_4 &\to \frac{1-\alpha}{\alpha_\ell}\boldsymbol{\ell}^2 \, , \\
D_5 &\to -(\boldsymbol{\ell}-\boldsymbol{r})2 \, , \\
D_6 &\to -\frac{\alpha}{\alpha_\ell}\boldsymbol{\ell}^2 \, , \\
D_7 &\to -\frac{1}{1-\alpha}D(\boldsymbol{k}+\boldsymbol{\ell}) \, .
\end{aligned} \tag{4.90}$$

Furthermore, we basically expand the results in powers of α_ℓ and keep only the leading term. It is interesting to follow the contributions of the different diagrams to this limit. For longitudinal polarization we express (4.31) in the simplified form

$$|\mathcal{M}|^2 = \frac{2s^2}{\boldsymbol{r}^4} e^2 e_f^2 g^6 \, N_c \, t^a t^b \, \delta^{ab} \, \frac{\alpha(1-\alpha)|\Psi_L(\boldsymbol{k}+\boldsymbol{\ell},\alpha)|^2}{(\boldsymbol{\ell}-\boldsymbol{r})^2} \sum_{i,j=1}^{5} \mathcal{D}_{ij} \, . \tag{4.91}$$

Here, $|\Psi_L(\boldsymbol{k}+\boldsymbol{\ell},\alpha)|^2$ is defined as in (1.21) but with the t-channel gluon transverse momentum replaced by $\boldsymbol{r} \to \boldsymbol{r}-\boldsymbol{\ell}$. The matrix $\mathcal{D}_{ij}$ is universal for the different couplings of the t-channel to the upper quark or antiquark, i.e. the difference between $\mathcal{A}_i$ and $\mathcal{B}_i$ is represented entirely by the photon wave function. The matrix itself has the rather simple form

$$\begin{pmatrix}
0 & 0 & 0 & \frac{1}{2} & -\frac{\boldsymbol{r}^2}{\boldsymbol{\ell}^2} \\
0 & 0 & 0 & \frac{1}{2} & -\frac{\boldsymbol{r}^2}{\boldsymbol{\ell}^2} \\
0 & 0 & 0 & 0 & 0 \\
\frac{1}{2} & \frac{1}{2} & 0 & -2-2\frac{\boldsymbol{r}^2}{(\boldsymbol{\ell}-\boldsymbol{r})^2} & \frac{\boldsymbol{r}^2}{(\boldsymbol{\ell}-\boldsymbol{r})^2} \\
-\frac{\boldsymbol{r}^2}{\boldsymbol{\ell}^2} & -\frac{\boldsymbol{r}^2}{\boldsymbol{\ell}^2} & 0 & \frac{\boldsymbol{r}^2}{(\boldsymbol{\ell}-\boldsymbol{r})^2} & 0
\end{pmatrix} . \tag{4.92}$$

The contributions from diagrams A_3 and B_3 drop out completely in this limit, since they involve an extra fermion propagator that gives a suppression by a power of α_ℓ. All contributions involving diagrams A_4 and B_4 are non-vanishing but they cancel in the sum, at least in the Feynman gauge, we have worked in. The only contributions being left are those where the emitted gluon couples once to the upper system and once to the lower system, i.e. amplitudes $AA_{i,j}, \ldots$ where $i = 5$ and $j = \{1, 2\}$ and vice versa. The sum of all diagrams in this limit is the given by

$$|\mathcal{M}|^2 = -2s^2 e^2 e_f^2 g^6 \delta^{ab}\, \alpha(1-\alpha)\, |\Psi_L(\boldsymbol{k}+\boldsymbol{\ell}, \alpha)|^2\, \frac{1}{(\boldsymbol{\ell}-\boldsymbol{r})^4}\, \frac{4N_c\, \boldsymbol{r}^2(\boldsymbol{\ell}-\boldsymbol{r})^2}{\boldsymbol{\ell}^2}\, \frac{1}{\boldsymbol{r}^4}\, t^a t^b \tag{4.93}$$

This is exactly what we expect. Apart from phase space factors, we have everything we need: the factor $\alpha(1-\alpha)|\Psi_L|^2$, including the colour factor δ^{ab} gives the impact factor for virtual photons in the LLA, cf. (1.21) and (3.43). The factors $1/(\boldsymbol{r}-\boldsymbol{\ell})^4$ and $1/\boldsymbol{r}^4$ are the propagators of the reggeised gluons in the t-channel and $4N_c\boldsymbol{r}^2(\boldsymbol{r}-\boldsymbol{\ell})^2/\boldsymbol{\ell}^2$ is the square of the Lipatov vertex. Finally, $t^a t^b$ is the LLA quark impact factor.

After integration over phase space, it is exactly this part that has to be subtracted from our result, to obtain the NLLA contribution to the impact factor, to avoid any double counting. The region (4.88) is exactly the region of phase space that contributed to the LO BFKL equation.

4.5 Subtraction of the LLA result

We will briefly outline, how the subtraction of the LLA result works explicitly. Suppose we consider the symmetric situation of $\gamma^*\gamma^*$ scattering with an extra gluon emission instead of $\gamma^* q$-scattering as we have considered so far, i.e. we replace the lower quark with another virtual photon to which the t-channel gluon couples as it does to the photon we have considered so far. I.e. we consider the process $\gamma^*\gamma^* \to (q\bar{q})g(q\bar{q})$.

Due to the symmetry of the problem, we can easily infer the result for the emission of a gluon also in the fragmentation region of the lower photon. Our gluon was only restricted to be far from the quark in rapidity. The limit of being in the central region was included in our calculation. We split the phase space of the gluon in two symmetric regions as follows: using $\ell = |\boldsymbol{\ell}|$, we write the on-shell condition for the gluon as

$$\frac{\alpha_\ell \sqrt{s}}{\ell} \frac{\beta_\ell \sqrt{s}}{\ell} = 1\,, \tag{4.94}$$

showing that the Sudakov variables are restricted to a hyperbola for fixed transverse momentum ℓ. By splitting the phase space in a symmetric way we think about two regions,

$$\text{region 1:} \qquad \alpha_\ell > \ell/\sqrt{s} \qquad \beta_\ell = \frac{\boldsymbol{\ell}^2}{\alpha_\ell s} \tag{4.95}$$

$$\text{region 2:} \qquad \beta_\ell > \ell/\sqrt{s} \qquad \alpha_\ell = \frac{\boldsymbol{\ell}^2}{\beta_\ell s}\,. \tag{4.96}$$

that denote one branch of the hyperbola, each. We just want to consider the cross section of the result in terms of the α_ℓ-dependence. The cross section for our process in the region 1 may be written as

$$\sigma^{(1)}_{\gamma^*\gamma^*} = \int_{\ell/\sqrt{s}}^{1} d\alpha_\ell \, f(\alpha_\ell) \; . \tag{4.97}$$

We have seen, that the limit of central emission is contained in our result. We restrict α_ℓ by an upper limit Λ. The integrand will be expanded in α_ℓ in the central region and starts with a pole[1],

$$f(\alpha_\ell) \approx \frac{\varphi(0)}{\alpha_\ell} + \varphi'(0) + \frac{1}{2}\varphi''(0)\alpha_\ell + \cdots \; . \tag{4.98}$$

Now, we subtract and add the LLA term explicitly,

$$\sigma^{(1)}_{\gamma^*\gamma^*} = \int_{\ell/\sqrt{s}}^{1} d\alpha_\ell \, f(\alpha_\ell) - \int_{\ell/\sqrt{s}}^{\Lambda} d\alpha_\ell \, \frac{\varphi(\alpha_\ell)}{\alpha_\ell} + \int_{\ell/\sqrt{s}}^{\Lambda} d\alpha_\ell \, \frac{\varphi(\alpha_\ell)}{\alpha_\ell} \; . \tag{4.99}$$

If integrate the last term, we get a $\log \sqrt{s}/\ell$. However, the preferred scale choice is $r - \ell$, since this the scale of the reggeon momenta are usually taken as Regge scales. Therefore, we define the LLA result to be

$$\sigma^{\mathrm{LLA}}_{\gamma^*\gamma^*} = \varphi(0) \log \frac{\sqrt{s}}{r-\ell}. \tag{4.100}$$

The integration of the first two terms might be extended down to 0. The correction is of order $\ell/\sqrt{s}$ and therefore negligible. Furthermore, we put the upper limit of the second integral into a step function and compensate for the change of scale in the LLA term. Altogether we obtain

$$\sigma^{(1)}_{\gamma^*\gamma^*} = \int_{\ell/\sqrt{s}}^{1} \left[f(\alpha_\ell) - \frac{\varphi(\alpha_\ell)}{\alpha_\ell}\Theta(\Lambda - \alpha_\ell) \right] d\alpha_\ell + \varphi(0) \log \frac{r-\ell}{\ell}\Lambda + \sigma^{\mathrm{LLA}}_{\gamma^*\gamma^*} \; . \tag{4.101}$$

The dependence on the lower limit ℓ will drop out, when we include region 2. The remaining dependence on the scale Λ and the scale $r - \ell$ chosen in order to fix the desired scale in the LLA term drops out of the final result. However, we can avoid additional problems with the behaviour of the single terms in parts of the phase space. We suggest to consider the limit $Q_1 \ll Q_2^2$ in order to use the constraints we have from the DGLAP approach (cf. section 1.2).

This limit has been considered before [25, 49] to obtain impact factors for the quark and gluon that behave smooth in the collinear limit. In [40, 41] a definition of NLO impact factors was given. This definition was applied to obtain and gluon- and quark impact factors [50, 51]. However, no further physical constraints were taken into account.

[1] There is no pole in (4.93), but the phase space contains one α_ℓ in the denominator.

4.6 Summary and outlook for chapter 4

We have computed the squared matrix elements for the process $\gamma^* + q \to (q\bar{q}g) + q$, summed over the helicities of the $q\bar{q}$-pair and the outgoing gluon in the high energy limit. For a longitudinally polarized virtual photon, the result has been cast into a form, that explicitly exhibits a factorized structure. Transforming the result into the transverse configuration space of the $q\bar{q}$-pair and the emitted gluon, a new $(q\bar{q}g)$-component of the photon emerges. Finally we have tested our result in the limit where the gluon is emitted in the central rapidity region and found agreement with the well known expectation built from the squared Lipatov vertex and the LO photon wave function. We have considered the choice of a proper subtraction method that should use all benefits from the constraints of well-known physical limits.

The results we have obtained may not be quite ready for a final evaluation. The integration over the phase space of the $q\bar{q}g$-system has to be performed. We have to isolate the expected infrared singularities from soft and collinear gluon emission and properly combine the matrix elements with the divergent part of the virtual corrections. We will proceed in the same way as we did with the virtual corrections, i.e. we will formulate the phase space integration in terms of a number of standard integrals, that are already almost given in terms of the denominator structure of our result. Since the problem of infrared singularities is well understood and the formulation in terms of standard integrals has been successfully performed for the virtual corrections we do not expect any problems here.

Summary and outlook

In this thesis we studied the scattering of virtual photons in the high energy limit. The subject was discussed in terms of two closely linked applications: the calculation of the total cross section for $\gamma^*\gamma^*$-scattering and the description of DIS in the colour dipole model.

In the experimental study of $\gamma^*\gamma^*$-scattering as it was by now performed at the CERN e^+e^--collider LEP and as it will be performed at a future linear e^+e^--collider like TESLA, one is able to test the BFKL pomeron. The experiments clearly show a cross section that rises with energy. However, the leading order BFKL-description rises too strong and fixed order calculations do not rise at all with the energy. First studies of NLO BFKL lower the value of the intercept but are not conclusive yet: the impact factor of the virtual photon had not been calculated to NLO.

We have completed the calculation of real and virtual NLO corrections to the effective γ^*-reggeon-$q\bar{q}$-vertex and formulated the integration over the $q\bar{q}$-phase space for the virtual corrections. The loop integrals for the virtual corrections have been performed and expressed in dimensional regularization in terms of logarithms and dilogarithms. We have expressed the phase space integrals explicitly in terms of a set of standard integrals, ready for further studies. The real corrections have been calculated and expressed in a compact way. Still, two more steps have to be done in the future in order to calculate the impact factor: the explicit phase space integration for the real corrections and a final numerical study.

Having completed the last two steps, we will ultimately be able to predict the $\gamma^*\gamma^*$ cross section to NLLA accuracy. This prediction and its comparison with experimental data will be sufficiently accurate to judge about the applicability of the NLO BFKL equation to this process. Important and challenging questions arise immediately: what about the onset of unitarity corrections? Will the perturbation series start to breakdown at TESLA? What about non-perturbative effects from diffusion? It will be interesting to really tune the virtualities of the photons as well in the experiment as in the prediction, to observe the breakdown of the applicability from the perturbative side and the onset of the soft pomeron domain on the experimental side.

The description of DIS with the colour dipole model is very successful and provides us with the clear physical picture of a virtual photon, fluctuating into a colour dipole that interacts with the proton in a non-perturbative way. The natural frame of this description is the proton rest frame in contrast to the usual description of DIS in the infinite momentum frame, where the perturbative DGLAP evolution of non-perturbative input distributions is formulated. The theoretical basis for the separation of the perturbative fluctuation of the virtual photon into a colour dipole on the one hand and the non-perturbative dipole-proton cross-section on the other hand is the $k_\perp$-factorization. Due to its clear physical interpretation and its universality in the successful description of both, inclusive and diffractive data, the dipole picture may be preferable in to the common scheme of collinear factorization in the domain of small x. The calculations of this thesis will allow us to cope up with the precision that is already reached in the DGLAP formalism: we provide NLO corrections to the photon wave function — the perturbative part of the colour dipole model.

We have already seen that we are able to formulate the results from the extra gluon emission in terms of a higher Fock component of the photon wave function and, as expected, an additional correction to the dipole cross section. A future project will be to complete this interpretation also for the virtual corrections. But this is only the first step: the physical content of the colour dipole model is the expansion of the short distance configuration of the colour field that surrounds the virtual photon. Including higher Fock components, we will see new structures and we probably will see them quite naturally as a multipole expansion of the colour field. The first term, the dipole, has properties quite familiar to those, expected from QED, since there are just two opposite colour charges. At higher orders, due to the presence of three different colour charges, the picture might change quite radically. There is the unique opportunity to study these phenomena in detail in the — so far — dipole model.

Apart from inclusive studies, the results of this thesis can and will extend also the calculation of more exclusive quantities in the near future. The inclusion of the virtualities of the photon and the gluon allows for studies of jet cross sections in the $k_\perp$-factorization scheme. The matrix elements that we provide could be included right away in NLO Monte Carlo models, suitable for the study of small x phenomena.

Coming back to the starting point of this thesis, we have seen that there are many challenging questions ranging from soft to hard physics. We have taken the viewpoint of perturbative QCD and worked on the present edge of its applicability close to the non-perturbative domain. The ultimate understanding of the pomeron will be achieved only from a combination of the insights we have gained from perturbative and non-perturbative approaches and remains a challenge for theoretical physics.

Appendix A

Functions for loop integrals

A.1 Basic functions

In this section we define some basic functions, which are closely related to scalar integrals and are built up from Logarithms and Dilogarithms. The functions are defined in [46]. For convenience we list them here.

The triangle functions depend on virtualities p_i^2 of the external legs i, which we denote by p_1^2, p_2^2 and $p_3^2 = s_{12}$. In the case of the two mass triangle, where the second leg is on-shell, $p_2^2 = 0$, we have only one simple logarithm:

$$\mathrm{Lc}_0^{2m}(p_1^2, s_{12}) = \ln \frac{s_{12}}{p_1^2}. \tag{A.1}$$

For the three-mass triangle we have the following function

$$\mathrm{Lc}_0(p_1^2, p_2^2, s_{12}) = \frac{1}{\sqrt{-\Delta_3}} \left[\ln(a^+ a^-) \ln\left(\frac{1-a^+}{1-a^-}\right) + 2\mathrm{Li}_2(a^+) - 2\mathrm{Li}_2(a^-) \right], \tag{A.2}$$

with the definitions

$$\Delta_3 = -p_1^4 - p_2^4 - s_{12}^2 + 2p_1^2 p_2^2 + 2p_1^2 s_{12} + 2p_2^2 s_{12}, \tag{A.3}$$

$$a^{\pm} = \frac{s_{12} + p_2^2 - p_1^2 \pm \sqrt{-\Delta_3}}{2s_{12}}. \tag{A.4}$$

The boxes depend on the virtualities of the external legs (we put $p_4^2 = s_{123}$) and on the invariants $s_{12} = (p_1 + p_2)^2$, $s_{23} = (p_2 + p_3)^2$. In the case of the one-mass box, with only the fourth leg having a virtuality $s_{123} \neq 0$ we have the function

$$\mathrm{Ld}_0^{1m}(s_{12}, s_{23}, s_{123}) = \mathrm{Li}_2\left(1 - \frac{s_{12}}{s_{123}}\right) + \mathrm{Li}_2\left(1 - \frac{s_{23}}{s_{123}}\right) + \ln\frac{s_{12}}{s_{123}} \ln\frac{s_{23}}{s_{123}} - \frac{\pi^2}{6}. \tag{A.5}$$

For the box with the two adjacent legs "‘1"' and "‘4"' being off-shell, ($p_1^2 \neq 0$ and $p_4^2 = s_{123} \neq 0$) we have

$$\mathrm{Ld}_0^{a}(s_{12}, s_{23}, p_1^2, s_{123}) = \mathrm{Li}_2\left(1 - \frac{s_{12}}{s_{123}}\right) - \mathrm{Li}_2\left(1 - \frac{p_1^2}{s_{12}}\right) + \frac{1}{2}\ln\frac{s_{12}^2}{p_1^2 s_{123}} \ln\frac{s_{23}}{s_{123}}. \tag{A.6}$$

Finally, in case of the opposite box, where $p_2^2 \neq 0$ and $p_4^2 = s_{123} \neq 0$ we have

$$\begin{aligned}\mathrm{Ld}_0^{op}(s_{12},s_{23},p_2^2,s_{123}) =\ & \mathrm{Li}_2\left(1-\frac{s_{12}}{s_{123}}\right)+\mathrm{Li}_2\left(1-\frac{s_{23}}{s_{123}}\right)-\mathrm{Li}_2\left(1-\frac{p_2^2}{s_{23}}\right)\\ & -\mathrm{Li}_2\left(1-\frac{p_2^2}{s_{12}}\right)+\mathrm{Li}_2\left(1-\frac{p_2^2 s_{123}}{s_{12}s_{23}}\right)+\ln\frac{s_{12}}{s_{123}}\ln\frac{s_{23}}{s_{123}}. \qquad (A.7)\end{aligned}$$

The pentagon (in our case it always has one virtual external leg, $p_5^2 \neq 0$), will always be expressed in terms of these box functions, since it is basically calculated in terms of boxes, introduced by removing propagators from the pentagon.

A.2 More Functions

In the following we give a list of functions, appearing in our calculations. These functions appear in the tensor decomposition of the loop integrals and will recursively be expressed in terms of the basic functions we introduced in the previous section.

Functions for the two-mass triangle

Here we list the functions which are neede in order to express the tensor integrals of the two-mass triangle. The invariants are explained above.

$$\mathrm{Lc}_1^{2m}(p_1^2,s_{12}) = \frac{\mathrm{Lc}_0^{2m}(p_1^2,s_{12})}{s_{12}-p_1^2} \qquad (A.8)$$

$$\mathrm{Lc}_2^{2m}(p_1^2,s_{12}) = -\frac{p_1^2\mathrm{Lc}_1^{2m}(p_1^2,s_{12})-1}{s_{12}-p_1^2} \qquad (A.9)$$

$$\mathrm{Lc}_3^{2m}(p_1^2,s_{12}) = -\frac{p_1^2\mathrm{Lc}_2^{2m}(p_1^2,s_{12})-1/2}{s_{12}-p_1^2} \qquad (A.10)$$

Three-mass triangle functions

In the tensor decomposition of the three-mass triangle the following functions appear (the Gram-determinant Δ_3 is given in eq. (A.3)):

$$\begin{aligned}\mathrm{Lc}_1(p_1^2,p_2^2,s_{12}) =\ & \frac{1}{\Delta_3}\big[-2p_1^2\ln\frac{s_{12}}{p_1^2}+(p_1^2+p_2^2-s_{12})\ln\frac{s_{12}}{p_2^2}\\ & +p_1^2(s_{12}+p_2^2-p_1^2)\mathrm{Lc}_0(p_1^2,p_2^2,s_{12})\big] \qquad (A.11)\\ \mathrm{Lc}_2(p_1^2,p_2^2,s_{12}) =\ & \frac{1}{2\Delta_3}\big[p_1^2+p_2^2-s_{12}-p_2^2\ln\frac{s_{12}}{p_2^2}\\ & +2p_2^2(p_1^2-p_2^2+s_{12})\mathrm{Lc}_1(p_1^2,p_2^2,s_{12})+p_1^2(-p_1^2+p_2^2+s_{12})\mathrm{Lc}_1(p_2^2,p_1^2,s_{12})\\ & -p_1^2p_2^2\mathrm{Lc}_0(p_1^2,p_2^2,s_{12})\big] \qquad (A.12)\\ \mathrm{Lc}_3(p_1^2,p_2^2,s_{12}) =\ & \frac{1}{2\Delta_3}\big[-2p_1^2+(p_2^2-s_{12})\ln\frac{s_{12}}{p_2^2}+p_1^4\mathrm{Lc}_0(p_1^2,p_2^2,s_{12})\\ & +3p_1^2(-p_1^2+p_2^2+s_{12})\mathrm{Lc}_1(p_1^2,p_2^2,s_{12})\big] \qquad (A.13)\end{aligned}$$

$$\mathrm{Lc}_{1S}(p_1^2,p_2^2,s_{12}) = \frac{1}{2}\left[p_1^2\mathrm{Lc}_1(p_2^2,p_1^2,s_{12}) + p_2^2\mathrm{Lc}_1(p_1^2,p_2^2,s_{12})\right] \tag{A.14}$$

$$\begin{aligned}\mathrm{Lc}_{2S}(p_1^2,p_2^2,s_{12}) &= \frac{1}{4\Delta_3}\left[2p_1^2p_2^2s_{12}\mathrm{Lc}_{1S}(p_1^2,p_2^2,s_{12})\right.\\ &\left. -\frac{1}{6}(p_1^4(s_{12}+p_2^2-p_1^2)\ln\frac{s_{12}}{p_1^2} + p_2^4(s_{12}+p_1^2-p_2^2)\ln\frac{s_{12}}{p_2^2} + 2p_1^2p_2^2s_{12})\right]\end{aligned} \tag{A.15}$$

$$\begin{aligned}\mathrm{Lc}_{3S}(p_1^2,p_2^2,s_{12}) &= \frac{1}{6\Delta_3}\left[2p_1^2p_2^2s_{12}\mathrm{Lc}_{2S}(p_1^2,p_2^2,s_{12})\right.\\ &-\frac{1}{60}(p_1^6(s_{12}+p_2^2-p_1^2)\ln\frac{s_{12}}{p_1^2} + p_2^6(s_{12}+p_1^2-p_2^2)\ln\frac{s_{12}}{p_2^2}\\ &\left.+p_1^2p_2^2s_{12}(p_1^2+p_2^2+s_{12})/2)\right]\end{aligned} \tag{A.16}$$

Adjacent Box

For the box with two adjacent massive external legs we use the abbreviation

$$\Delta_4 = 2s_{23}\left[(s_{123}-s_{12})(s_{12}-p_1^2) - s_{12}s_{23}\right]. \tag{A.17}$$

With this we have the following functions related to higher dimensionial scalar integrals:

$$\begin{aligned}\mathrm{Ld}_{1S}(s_{12},s_{23},p_1^2,s_{123}) &= -\frac{2s_{12}s_{23}}{\Delta_4}\left[\mathrm{Ld}_0^a(s_{12},s_{23},p_1^2,s_{123})\right.\\ &\left.+\frac{1}{2}(s_{123}+p_1^2-s_{23}-2\frac{p_1^2s_{123}}{s_{12}})\mathrm{Lc}_0(p_1^2,s_{23},s_{123})\right]\end{aligned} \tag{A.18}$$

$$\begin{aligned}\mathrm{Ld}_{2S}(s_{12},s_{23},p_1^2,s_{123}) &= -\frac{s_{12}s_{23}}{3\Delta_4}\left[\frac{s_{23}}{2}\ln\frac{s_{123}}{s_{23}} + s_{12}\ln\frac{s_{123}}{s_{12}} - \frac{p_1^2}{2}\ln\frac{s_{123}}{p_1^2}\right.\\ &+s_{12}s_{23}\mathrm{Ld}_{1S}(s_{12},s_{23},p_1^2,s_{123})\\ &\left.+(s_{123}+p_1^2-s_{23}-\frac{2p_1^2s_{123}}{s_{12}})\mathrm{Lc}_{1S}(p_1^2,s_{23},s_{123})\right]\end{aligned} \tag{A.19}$$

$$\begin{aligned}\mathrm{Ld}_{3S}(s_{12},s_{23},p_1^2,s_{123}) &= -\frac{s_{12}s_{23}}{5\Delta_4}\left[\frac{s_{23}^2}{24}\ln\frac{s_{123}}{s_{23}} + \frac{s_{12}^2}{12}\ln\frac{s_{123}}{s_{12}} - \frac{p_1^4}{24}\ln\frac{s_{123}}{p_1^2}\right.\\ &+\frac{s_{12}s_{23}}{12} + s_{12}s_{23}\mathrm{Ld}_{2S}(s_{12},s_{23},p_1^2,s_{123})\\ &\left.+(s_{123}+p_1^2-s_{23}-\frac{2p_1^2s_{123}}{s_{12}})\mathrm{Lc}_{2S}(p_1^2,s_{23},s_{123})\right]\end{aligned} \tag{A.20}$$

In the tensor decomposition of adjacent box integrals the following functions are used:

$$\mathrm{Ld}_1(s_{12},s_{23},p_1^2,s_{123}) = -\left[\mathrm{Ld}_{1S}(s_{12},s_{23},p_1^2,s_{123}) + \mathrm{Lc}_0(p_1^2,s_{23},s_{123})\right] \tag{A.21}$$

$$\begin{aligned}\mathrm{Ld}_{21}(s_{12},s_{23},p_1^2,s_{123}) &= -\frac{2}{s_{12}}\left[3\mathrm{Ld}_{2S}(s_{12},s_{23},p_1^2,s_{123}) + \mathrm{Lc}_{1S}(p_1^2,s_{23},s_{123})\right]\\ &-\mathrm{Lc}_1(s_{23},p_1^2,s_{123})\end{aligned} \tag{A.22}$$

$$\begin{aligned}\mathrm{Ld}_{22}(s_{12},s_{23},p_1^2,s_{123}) &= 2\frac{s_{123}-s_{12}}{s_{12}s_{23}}\left[3\mathrm{Ld}_{2S}(s_{12},s_{23},p_1^2,s_{123})\right.\\ &\left.+\mathrm{Lc}_{1S}(p_1^2,s_{23},s_{123})\right] - \frac{s_{12}}{s_{23}}\mathrm{Lc}_1^{2m}(p_1^2,s_{12}) + \frac{s_{123}}{s_{23}}\mathrm{Lc}_1(s_{23},p_1^2,s_{123})\end{aligned} \tag{A.23}$$

$$\begin{aligned}
\mathrm{Ld}_{24}(s_{12},s_{23},p_1^2,s_{123}) &= 2\frac{p_1^2-s_{12}}{s_{12}s_{23}}\big[3\mathrm{Ld}_{2S}(s_{12},s_{23},p_1^2,s_{123}) \\
&\quad + \mathrm{Lc}_{1S}(p_1^2,s_{23},s_{123})\big] - \frac{s_{12}}{s_{23}}\mathrm{Lc}_1^{2m}(s_{12},s_{123}) + \frac{p_1^2}{s_{23}}\mathrm{Lc}_1(s_{23},p_1^2,s_{123})
\end{aligned} \tag{A.24}$$

$$\begin{aligned}
\mathrm{Ld}_{311}(s_{12},s_{23},p_1^2,s_{123}) &= -\Big(\frac{12}{s_{12}^2}\big[5\mathrm{Ld}_{3S}(s_{12},s_{23},p_1^2,s_{123}) + \mathrm{Lc}_{2S}(p_1^2,s_{23},s_{123})\big] \\
&\quad + \frac{s_{12}+p_1^2}{s_{12}}\mathrm{Lc}_3(s_{23},p_1^2,s_{123}) + \frac{s_{23}}{s_{12}}\mathrm{Lc}_2(p_1^2,s_{23},s_{123})\Big)
\end{aligned} \tag{A.25}$$

$$\begin{aligned}
\mathrm{Ld}_{314}(s_{12},s_{23},p_1^2,s_{123}) &= 12\frac{p_1^2-s_{12}}{s_{12}^2 s_{23}}\big[5\mathrm{Ld}_{3S}(s_{12},s_{23},p_1^2,s_{123}) \\
&\quad + \mathrm{Lc}_{2S}(p_1^2,s_{23},s_{123})\big] + \frac{p_1^4}{s_{12}s_{23}}\mathrm{Lc}_3(s_{23},p_1^2,s_{123}) - \frac{s_{12}+p_1^2}{s_{12}}\mathrm{Lc}_2(p_1^2,s_{23},s_{123}) \\
&\quad - \frac{s_{12}}{2s_{23}}\mathrm{Lc}_1^{2m}(s_{12},s_{123})
\end{aligned} \tag{A.26}$$

$$\begin{aligned}
\mathrm{Ld}_{322}(s_{12},s_{23},p_1^2,s_{123}) &= -\Big(12\frac{(s_{123}-s_{12})^2}{s_{12}^2 s_{23}^2}\big[5\mathrm{Ld}_{3S}(s_{12},s_{23},p_1^2,s_{123}) \\
&\quad + \mathrm{Lc}_{2S}(p_1^2,s_{23},s_{123})\big] + s_{123}\frac{s_{12}s_{123}+p_1^2 s_{123}-2p_1^2 s_{12}}{s_{12}s_{23}^2}\mathrm{Lc}_3(s_{23},p_1^2,s_{123}) \\
&\quad - \frac{s_{12}}{2s_{23}}\mathrm{Lc}_2^{2m}(p_1^2,s_{12}) + s_{12}\frac{s_{12}-s_{123}}{2s_{23}^2}\mathrm{Lc}_1^{2m}(s_{12},s_{123}) \\
&\quad + s_{123}\frac{s_{123}-2s_{12}}{s_{12}s_{23}}\mathrm{Lc}_2(p_1^2,s_{23},s_{123}) + \frac{p_1^2 s_{12}+s_{12}s_{23}-s_{12}s_{123}}{2s_{23}^2}\mathrm{Lc}_1^{2m}(p_1^2,s_{12})\Big)
\end{aligned} \tag{A.27}$$

$$\begin{aligned}
\mathrm{Ld}_{344}(s_{12},s_{23},p_1^2,s_{123}) &= -\Big(12\frac{(s_{12}-p_1^2)^2}{s_{12}^2 s_{23}^2}\big[5\mathrm{Ld}_{3S}(s_{12},s_{23},p_1^2,s_{123}) \\
&\quad + \mathrm{Lc}_{2S}(p_1^2,s_{23},s_{123})\big] + p_1^2\frac{p_1^2-2s_{12}}{s_{12}s_{23}}\mathrm{Lc}_2(p_1^2,s_{23},s_{123}) \\
&\quad + p_1^4\frac{p_1^2-s_{12}}{s_{12}s_{23}^2}\mathrm{Lc}_3(s_{23},p_1^2,s_{123}) + s_{12}\frac{s_{12}-p_1^2}{2s_{23}^2}\mathrm{Lc}_1^{2m}(s_{12},s_{123}) \\
&\quad + \frac{s_{12}}{2s_{23}}\mathrm{Lc}_2^{2m}(s_{12},s_{123})\Big)
\end{aligned} \tag{A.28}$$

One-mass box

For box integrals with one massive external leg we use the abbreviation

$$\Delta_4^{1m} = 2s_{12}s_{23}(s_{123}-s_{12}-s_{23}). \tag{A.29}$$

The functions we are using for tensor integrals are:

$$\mathrm{Ld}_{1S}^{1m}(s_{12},s_{23},s_{123}) = -\frac{2s_{12}s_{23}}{\Delta_4^{1m}}\mathrm{Ld}_0^{1m}(s_{12},s_{23},s_{123}) \tag{A.30}$$

$$\begin{aligned}
\mathrm{Ld}_{2S}^{1m}(s_{12},s_{23},s_{123}) &= -\frac{s_{12}s_{23}}{3\Delta_4^{1m}}\big[s_{12}s_{23}\mathrm{Ld}_{1S}^{1m}(s_{12},s_{23},s_{123}) \\
&\quad + s_{23}\ln\frac{s_{123}}{s_{23}} + s_{12}\ln\frac{s_{123}}{s_{12}}\big]
\end{aligned} \tag{A.31}$$

$$\mathrm{Ld}_1^{1m}(s_{12},s_{23},s_{123}) = -\,\mathrm{Ld}_{1S}^{1m}(s_{12},s_{23},s_{123}) \tag{A.32}$$

$$\mathrm{Ld}_{21}^{1m}(s_{12},s_{23},s_{123}) = -\,\frac{1}{s_{12}}\left[6\mathrm{Ld}_{2S}^{1m}(s_{12},s_{23},s_{123}) + s_{23}\mathrm{Lc}_1^{2m}(s_{23},s_{123})\right] \tag{A.33}$$

$$\mathrm{Ld}_{22}^{1m}(s_{12},s_{23},s_{123}) = \mathrm{Ld}_1^{1m}(s_{12},s_{23},s_{123}) - \mathrm{Ld}_{21}^{1m}(s_{12},s_{23},s_{123}). \tag{A.34}$$

Appendix B

Explicit phase space integrals

In this appendix we list the explicit results for the phase space integrals according to the definitions in chapter 3. We list the results diagram by diagram, following their numbering, as adapted in Fig 2.2. For each diagram we list the results first for longitudinal and then for transverse photons.

B.1 Short diagrams

Diagram 1

The functions L_i in the integrands are defined as

$$\begin{aligned}
&(i=1) \qquad && \frac{c_\Gamma (-t)^{-\epsilon}}{\epsilon} \\
&(i=2) \qquad && \log\frac{t}{t_a} \\
&(i=3) \qquad && \{1\}.
\end{aligned} \tag{B.1}$$

and we have a colour factor $\mathcal{C}_1 = N_c/2$

Longitudinal

$$\begin{aligned}
\mathcal{F}_1^{(1)}(L) &= 6\,(-1+\alpha)^2\,\alpha^2\,(-\mathrm{F1}^{00}_{0001000} + \mathrm{F1}^{00}_{0100000}) \\
&+ 2\,(-1+\alpha)^2\,\alpha^3\,(-4+4\,\alpha+\tau)\,\mathrm{F1}^{00}_{0101000} \\
&+ \frac{4}{\tau}\,(-1+\alpha)\,\alpha^2\,(2\,\alpha^2+2\,\tau-\alpha\,(2+\tau))\,(-\mathrm{F1}^{00}_{0001000} + \mathrm{F1}^{00}_{1000000}) \\
&+ 8\,(-1+\alpha)^3\,\alpha^3\,(\mathrm{F1}^{00}_{1100000} - \mathrm{F1}^{00}_{2000000}) \\
&- \frac{4}{\tau}\,(-1+\alpha)\,\alpha^2\,(\mathrm{F1}^{01}_{0001000} - \mathrm{F1}^{01}_{1000000})
\end{aligned} \tag{B.2}$$

$$
\begin{aligned}
\mathcal{F}_1^{(2)}(L) = &-2\,(-1+\alpha)^2\,\alpha^2\,(4\,\alpha^2+\alpha\,(-4+\tau)+\tau\ )\,\mathrm{F2}^{00}_{0002000} \\
&-2\,(-1+\alpha)^3\,\alpha^2\,(8\,\alpha+3\,\tau)\,\mathrm{F2}^{00}_{0101000} \\
&+2\,(-1+\alpha)^3\,\alpha^3\,\tau\,(-4+4\,\alpha+\tau)\,\mathrm{F2}^{00}_{0102000} \\
&+\frac{4}{\tau}\,(-1+\alpha)\,\alpha^2\,(6\,\alpha^2+2\,\alpha\,(-3+\tau)-\tau)\,(\mathrm{F2}^{00}_{0001000}-\mathrm{F2}^{00}_{1000000}) \\
&+16\,(-1+\alpha)^3\,\alpha^3\,(\mathrm{F2}^{00}_{1100000}-\mathrm{F2}^{00}_{2000000})-4\,(-1+\alpha)^2\,\alpha^2\,\mathrm{F2}^{01}_{0002000} \\
&+\frac{4}{\tau}\,(-1+\alpha)\,\alpha^2\,(\mathrm{F2}^{01}_{0001000}-\mathrm{F2}^{01}_{1000000})
\end{aligned}
\tag{B.3}
$$

$$
\begin{aligned}
\mathcal{F}_1^{(3)}(L) = &\ 10\,(-1+\alpha)^2\,\alpha^2\,(-\mathrm{F3}^{00}_{0001000}+\mathrm{F3}^{00}_{0100000}) \\
&+2\,(-1+\alpha)^2\,\alpha^3\,(-4+4\,\alpha+\tau)\,\mathrm{F3}^{00}_{0101000} \\
&+\frac{4}{\tau}\,(-1+\alpha)\,\alpha^2\,(2\,\alpha^2+3\,\tau-2\,\alpha\,(1+\tau))\,(-\mathrm{F3}^{00}_{0001000}+\mathrm{F3}^{00}_{1000000}) \\
&+16\,(-1+\alpha)^3\,\alpha^3\,(\mathrm{F3}^{00}_{1100000}-\mathrm{F3}^{00}_{2000000}) \\
&-\frac{4}{\tau}\,(-1+\alpha)\,\alpha^2\,(\mathrm{F3}^{01}_{0001000}-\mathrm{F3}^{01}_{1000000})
\end{aligned}
\tag{B.4}
$$

Transverse

$$
\begin{aligned}
\mathcal{F}_1^{(1)}(T) = &\ 2\,\alpha\,(-1+3\,\alpha-5\,\alpha^2+3\,\alpha^3)\,(-\mathrm{F1}^{00}_{0001000}+\mathrm{F1}^{00}_{0100000}) \\
&+2\,(-1+\alpha)\,\alpha^2\,(-2+6\,\alpha+4\,\alpha^3+\alpha^2\,(-8+\tau))\,\mathrm{F1}^{00}_{0101000} \\
&+\frac{2}{\tau}\,(-1+\alpha)\,\alpha\,(4\,\alpha^3-3\,\tau-2\,\alpha^2\,(2+\tau)+\alpha\,(2+4\,\tau)) \\
&\quad\times(-\mathrm{F1}^{00}_{0001000}+\mathrm{F1}^{00}_{1000000}) \\
&+2\,\alpha\,(-1+3\,\alpha-4\,\alpha^2+2\,\alpha^3)\,(-2\,\alpha+2\,\alpha^2+\tau\ )\,\mathrm{F1}^{00}_{1100000} \\
&-4\,(-1+\alpha)^2\,\alpha^2\,(1-2\,\alpha+2\,\alpha^2)\,\mathrm{F1}^{00}_{2000000} \\
&-\frac{4}{\tau}\,(-1+\alpha)^2\,\alpha\,(\mathrm{F1}^{01}_{0001000}-\mathrm{F1}^{01}_{1000000})
\end{aligned}
\tag{B.5}
$$

$$
\begin{aligned}
\mathcal{F}_1^{(2)}(T) = &-2\,(-1+\alpha)^2\,\alpha\,(4\,\alpha^3+\alpha^2\,(-4+\tau)-2\,\tau+2\,\alpha\,(1+\tau))\,\mathrm{F2}^{00}_{0002000} \\
&-2\,(-1+\alpha)\,\alpha^2\,(8\,\alpha^3-3\,\alpha\,(-4+\tau)+2\,(-2+\tau) \\
&\quad+\alpha^2\,(-16+3\,\tau))\,\mathrm{F2}^{00}_{0101000} \\
&+2\,(-1+\alpha)^2\,\alpha^2\,(-2+6\,\alpha+4\,\alpha^3+\alpha^2\,(-8+\tau))\,\tau\,\mathrm{F2}^{00}_{0102000} \\
&+\frac{4}{\tau}\,(-1+\alpha)\,\alpha^2\,(3+6\,\alpha^2+2\,\alpha\,(-3+\tau)-\tau)\,(\mathrm{F2}^{00}_{0001000}-\mathrm{F2}^{00}_{1000000}) \\
&+4\,\alpha\,(-1+3\,\alpha-4\,\alpha^2+2\,\alpha^3)\,(-2\,\alpha+2\,\alpha^2+\tau\ )\,\mathrm{F2}^{00}_{1100000} \\
&-8\,(-1+\alpha)^2\,\alpha^2\,(1-2\,\alpha+2\,\alpha^2)\,\mathrm{F2}^{00}_{2000000}-4\,(-1+\alpha)^3\,\alpha\,\mathrm{F2}^{01}_{0002000} \\
&+\frac{4}{\tau}\,(-1+\alpha)^2\,\alpha\,(\mathrm{F2}^{01}_{0001000}-\mathrm{F2}^{01}_{1000000})
\end{aligned}
\tag{B.6}
$$

$$\begin{aligned}\mathcal{F}_1^{(3)}(T) &= 2\,\alpha\,(-2+6\,\alpha-9\,\alpha^2+5\,\alpha^3)\,(-\mathrm{F3}^{00}_{0001000}+\mathrm{F3}^{00}_{0100000})\\&+2\,(-1+\alpha)\,\alpha^2\,(-2+6\,\alpha+4\,\alpha^3+\alpha^2\,(-8+\tau))\,\mathrm{F3}^{00}_{0101000}\\&+\frac{4}{\tau}\,(-1+\alpha)\,\alpha\,(\alpha+2\,\alpha^3-2\,\tau+3\,\alpha\,\tau-2\,\alpha^2\,(1+\tau))\\&\quad\times(-\mathrm{F3}^{00}_{0001000}+\mathrm{F3}^{00}_{1000000})\\&+4\,\alpha\,(-1+3\,\alpha-4\,\alpha^2+2\,\alpha^3)\,(-2\,\alpha+2\,\alpha^2+\tau\,)\,\mathrm{F3}^{00}_{1100000}\\&-8\,(-1+\alpha)^2\,\alpha^2\,(1-2\,\alpha+2\,\alpha^2)\,\mathrm{F3}^{00}_{2000000}\\&-\frac{4}{\tau}\,(-1+\alpha)^2\,\alpha\,(\mathrm{F3}^{01}_{0001000}-\mathrm{F3}^{01}_{1000000})\end{aligned}\tag{B.7}$$

Diagram 2+3

For the two boxes, the integrals are still quite compact. We define the functions L_i in the integrands as

$$\begin{aligned}&(i=1) &&2\mathrm{Li}_2\left(1-\frac{t_a}{t}\right)\\&(i=2) &&\frac{c_\Gamma}{\epsilon^2}\frac{t_a}{t-t_a}(-t)^{-\epsilon}\end{aligned}\tag{B.8}$$

and in addition

$$\begin{aligned}&(i=3) &&\frac{\pi^2}{6}+\frac{2c_\Gamma}{\epsilon}(-t)^{-\epsilon}\log\alpha+\frac{c_\Gamma}{\epsilon^2}(-t)^{-\epsilon}\\&(i=4) &&-\frac{c_\Gamma}{\epsilon^2}(-t_a)^{-\epsilon}\\&(i=5) &&-\frac{c_\Gamma}{\epsilon^2}\frac{t_a}{t-t_a}(-t_a)^{-\epsilon}\end{aligned}\tag{B.9}$$

The contributions $\mathcal{F}^{(3)}_{2+3}$ and $\mathcal{F}^{(4)}_{2+3}$ have the same structure as $\mathcal{F}^{(1)}_{2+3}$, therefore they are obtained from the latter just by replacing L_i in the integrand, or equivalently $\mathrm{F1}^{::}_{...}\to\mathrm{F3}^{::}_{...}$ and $\mathrm{F1}^{::}_{...}\to\mathrm{F4}^{::}_{...}$. In the same way $\mathcal{F}^{(5)}_{2+3}$ is obtained from $\mathcal{F}^{(2)}_{2+3}$. The colour factor, we have taken out here, is $\mathcal{C}_{2+3}=N_c$.

Longitudinal

$$\begin{aligned}\mathcal{F}^{(1)}_{2+3}(L) &= 4\,(-1+\alpha)^2\,\alpha^2\,(\mathrm{F1}^{00}_{0100000}-\mathrm{F1}^{00}_{1000000})\\&+8\,(-1+\alpha)^3\,\alpha^3\,(\mathrm{F1}^{00}_{1100000}-\mathrm{F1}^{00}_{2000000})\end{aligned}\tag{B.10}$$

$$\begin{aligned}\mathcal{F}^{(2)}_{2+3}(L) &= -4\,(-1+\alpha)^2\,\alpha^2\,(-\mathrm{F2}^{00}_{0001000}+\mathrm{F2}^{00}_{0100000})\\&-4\,(-1+\alpha)^3\,\alpha^2\,(2\,\alpha+\tau)\,\mathrm{F2}^{00}_{0101000}\\&-\frac{8}{\tau}\,(-1+\alpha)^2\,\alpha^3\,(-\mathrm{F2}^{00}_{0001000}+\mathrm{F2}^{00}_{1000000})\end{aligned}\tag{B.11}$$

Transverse

$$
\begin{aligned}
\mathcal{F}^{(1)}_{2+3}(T) &= 2\,\alpha\,(-1+3\,\alpha-4\,\alpha^2+2\,\alpha^3)\,(\mathrm{F1}^{00}_{0100000}-\mathrm{F1}^{00}_{1000000}) \\
&+ 2\,\alpha\,(-1+3\,\alpha-4\,\alpha^2+2\,\alpha^3)\,(-2\,\alpha+2\,\alpha^2+\tau\ )\,\mathrm{F1}^{00}_{1100000} \\
&- 4\,(-1+\alpha)^2\,\alpha^2\,(1-2\,\alpha+2\,\alpha^2)\,\mathrm{F1}^{00}_{2000000}
\end{aligned} \tag{B.12}
$$

$$
\begin{aligned}
\mathcal{F}^{(2)}_{2+3}(T) &= 2\,\alpha\,(1-3\,\alpha+4\,\alpha^2-2\,\alpha^3)\,(-\mathrm{F2}^{00}_{0001000}+\mathrm{F2}^{00}_{0100000}) \\
&- 2\,\alpha^2\,(-1+3\,\alpha-4\,\alpha^2+2\,\alpha^3)\,(-2+2\,\alpha+\tau)\,\mathrm{F2}^{00}_{0101000} \\
&- \frac{4}{\tau}\,\alpha^2\,(-1+3\,\alpha-4\,\alpha^2+2\,\alpha^3)\,(-\mathrm{F2}^{00}_{0001000}+\mathrm{F2}^{00}_{1000000})
\end{aligned} \tag{B.13}
$$

Diagram 4

The functions L_i in the integrands are defined as

$$
\begin{aligned}
&(i=1) && \frac{c_\Gamma(-t)^{-\epsilon}}{\epsilon^2} \\
&(i=2) && \frac{c_\Gamma(-t_a)^{-\epsilon}}{\epsilon^2} \\
&(i=3) && \frac{c_\Gamma(-t)^{-\epsilon}}{\epsilon} \\
&(i=4) && \log\frac{t}{t_a} \\
&(i=5) && \{1\}\,.
\end{aligned} \tag{B.14}
$$

The colour factor is $\mathcal{C}_4 = -1/(2N_c)$

Longitudinal

$$
\begin{aligned}
\mathcal{F}^{(1)}_{4}(L) &= -4\,(-1+\alpha)^2\,\alpha^2\,(-\mathrm{F1}^{00}_{0001000}+\mathrm{F1}^{00}_{0100000}) \\
&+ 4\,(-1+\alpha)^2\,\alpha^3\,(-4+4\,\alpha+\tau)\,\mathrm{F1}^{00}_{0101000} \\
&+ \frac{8}{\tau}\,(-1+\alpha)\,\alpha^3\,(-2+2\,\alpha+\tau)\,(-\mathrm{F1}^{00}_{0001000}+\mathrm{F1}^{00}_{1000000}) \\
&- 16\,(-1+\alpha)^3\,\alpha^3\,(\mathrm{F1}^{00}_{1100000}-\mathrm{F1}^{00}_{2000000}) \\
&- \frac{8}{\tau}\,(-1+\alpha)\,\alpha^2\,(\mathrm{F1}^{01}_{0001000}-\mathrm{F1}^{01}_{1000000})
\end{aligned} \tag{B.15}
$$

$$
\begin{aligned}
\mathcal{F}^{(2)}_{4}(L) &= 4\,(-1+\alpha)^2\,\alpha^2\,(-\mathrm{F2}^{00}_{0001000}+\mathrm{F2}^{00}_{0100000}) \\
&- 4\,(-1+\alpha)^2\,\alpha^3\,(-4+4\,\alpha+\tau)\,\mathrm{F2}^{00}_{0101000} \\
&- \frac{8}{\tau}\,(-1+\alpha)\,\alpha^3\,(-2+2\,\alpha+\tau)\,(-\mathrm{F2}^{00}_{0001000}+\mathrm{F2}^{00}_{1000000}) \\
&+ 16\,(-1+\alpha)^3\,\alpha^3\,(\mathrm{F2}^{00}_{1100000}-\mathrm{F2}^{00}_{2000000}) \\
&+ \frac{8}{\tau}\,(-1+\alpha)\,\alpha^2\,(\mathrm{F2}^{01}_{0001000}-\mathrm{F2}^{01}_{1000000})
\end{aligned} \tag{B.16}
$$

$$
\begin{aligned}
\mathcal{F}_4^{(3)}(L) &= 4\,(-1+\alpha)^2\,\alpha^3\,(-4+4\,\alpha+\tau)\,\mathrm{F3}^{00}_{0101000} \\
&- \frac{4}{\tau}\,(-1+\alpha)\,\alpha^2\,(4\,\alpha^2+\alpha\,(-4+\tau)+\tau)\,(\mathrm{F3}^{00}_{0001000}-\mathrm{F3}^{00}_{1000000}) \\
&- 8\,(-1+\alpha)^3\,\alpha^3\,(\mathrm{F3}^{00}_{1100000}-\mathrm{F3}^{00}_{2000000}) \\
&- \frac{8}{\tau}\,(-1+\alpha)\,\alpha^2\,(\mathrm{F3}^{01}_{0001000}-\mathrm{F3}^{01}_{1000000})
\end{aligned} \tag{B.17}
$$

$$
\begin{aligned}
\mathcal{F}_4^{(4)}(L) &= -10\,(-1+\alpha)^2\,\alpha^2\,(4\,\alpha^2+\alpha\,(-4+\tau)+\tau\ )\,\mathrm{F4}^{00}_{0002000} \\
&- 2\,(-1+\alpha)^2\,\alpha^2\,(4\,\alpha^2-\tau-\alpha\,(4+\tau))\,\mathrm{F4}^{00}_{0101000} \\
&+ 10\,(-1+\alpha)^3\,\alpha^3\,\tau\,(-4+4\,\alpha+\tau)\,\mathrm{F4}^{00}_{0102000} \\
&+ \frac{4}{\tau}\,(-1+\alpha)\,\alpha^2\,(12\,\alpha^2+2\,\alpha\,(-6+\tau)+\tau)\,(\mathrm{F4}^{00}_{0001000}-\mathrm{F4}^{00}_{1000000}) \\
&+ 16\,(-1+\alpha)^3\,\alpha^3\,(\mathrm{F4}^{00}_{1100000}-\mathrm{F4}^{00}_{2000000}) - 20\,(-1+\alpha)^2\,\alpha^2\,\mathrm{F4}^{01}_{0002000} \\
&+ \frac{12}{\tau}\,(-1+\alpha)\,\alpha^2\,(\mathrm{F4}^{01}_{0001000}-\mathrm{F4}^{01}_{1000000})
\end{aligned} \tag{B.18}
$$

$$
\begin{aligned}
\mathcal{F}_4^{(5)}(L) &= -6\,(-1+\alpha)^2\,\alpha^2\,(-\mathrm{F5}^{00}_{0001000}+\mathrm{F5}^{00}_{0100000}) \\
&+ 10\,(-1+\alpha)^2\,\alpha^3\,(-4+4\,\alpha+\tau)\,\mathrm{F5}^{00}_{0101000} \\
&+ \frac{4}{\tau}\,(-1+\alpha)\,\alpha^2\,(10\,\alpha^2+\tau+2\,\alpha\,(-5+2\,\tau))\,(-\mathrm{F5}^{00}_{0001000}+\mathrm{F5}^{00}_{1000000}) \\
&- 32\,(-1+\alpha)^3\,\alpha^3\,(\mathrm{F5}^{00}_{1100000}-\mathrm{F5}^{00}_{2000000}) \\
&- \frac{20}{\tau}\,(-1+\alpha)\,\alpha^2\,(\mathrm{F5}^{01}_{0001000}-\mathrm{F5}^{01}_{1000000})
\end{aligned} \tag{B.19}
$$

Transverse

$$
\begin{aligned}
\mathcal{F}_4^{(1)}(T) &= -4\,(-1+\alpha)^3\,\alpha\,(-\mathrm{F1}^{00}_{0001000}+\mathrm{F1}^{00}_{0100000}) \\
&+ 4\,(-1+\alpha)\,\alpha^2\,(-2+6\,\alpha+4\,\alpha^3+\alpha^2\,(-8+\tau))\,\mathrm{F1}^{00}_{0101000} \\
&+ \frac{4}{\tau}\,(-1+\alpha)\,\alpha\,(2\,\alpha+4\,\alpha^3+2\,\alpha^2\,(-2+\tau)-\tau)\,(-\mathrm{F1}^{00}_{0001000}+\mathrm{F1}^{00}_{1000000}) \\
&- 4\,\alpha\,(-1+3\,\alpha-4\,\alpha^2+2\,\alpha^3)\,(-2\,\alpha+2\,\alpha^2+\tau\ )\,\mathrm{F1}^{00}_{1100000} \\
&+ 8\,(-1+\alpha)^2\,\alpha^2\,(1-2\,\alpha+2\,\alpha^2)\,\mathrm{F1}^{00}_{2000000} \\
&- \frac{8}{\tau}\,(-1+\alpha)^2\,\alpha\,(\mathrm{F1}^{01}_{0001000}-\mathrm{F1}^{01}_{1000000})
\end{aligned} \tag{B.20}
$$

$$
\begin{aligned}
\mathcal{F}_4^{(2)}(T) &= 4\,(-1+\alpha)^3\,\alpha\,(-\mathrm{F2}^{00}_{0001000}+\mathrm{F2}^{00}_{0100000}) \\
&- 4\,(-1+\alpha)\,\alpha^2\,(-2+6\,\alpha+4\,\alpha^3+\alpha^2\,(-8+\tau))\,\mathrm{F2}^{00}_{0101000} \\
&- \frac{4}{\tau}\,(-1+\alpha)\,\alpha\,(2\,\alpha+4\,\alpha^3+2\,\alpha^2\,(-2+\tau)-\tau)\,(-\mathrm{F2}^{00}_{0001000}+\mathrm{F2}^{00}_{1000000}) \\
&+ 4\,\alpha\,(-1+3\,\alpha-4\,\alpha^2+2\,\alpha^3)\,(-2\,\alpha+2\,\alpha^2+\tau\ )\,\mathrm{F2}^{00}_{1100000} \\
&- 8\,(-1+\alpha)^2\,\alpha^2\,(1-2\,\alpha+2\,\alpha^2)\,\mathrm{F2}^{00}_{2000000} \\
&+ \frac{8}{\tau}\,(-1+\alpha)^2\,\alpha\,(\mathrm{F2}^{01}_{0001000}-\mathrm{F2}^{01}_{1000000})
\end{aligned} \tag{B.21}
$$

$$
\begin{aligned}
\mathcal{F}_4^{(3)}(T) &= 2\,\alpha\,(1-3\,\alpha+2\,\alpha^2\,)\,(-\mathrm{F3}^{00}_{0001000}+\mathrm{F3}^{00}_{0100000}) \\
&+4\,(-1+\alpha)\,\alpha^2\,(-2+6\,\alpha+4\,\alpha^3+\alpha^2\,(-8+\tau))\,\mathrm{F3}^{00}_{0101000} \\
&+\frac{2}{\tau}\,(-1+\alpha)\,\alpha\,(8\,\alpha^3+2\,\alpha^2\,(-4+\tau)-3\,\tau+2\,\alpha\,(2+\tau)) \\
&\quad\times(-\mathrm{F3}^{00}_{0001000}+\mathrm{F3}^{00}_{1000000}) \\
&-2\,\alpha\,(-1+3\,\alpha-4\,\alpha^2+2\,\alpha^3)\,(-2\,\alpha+2\,\alpha^2+\tau\,)\,\mathrm{F3}^{00}_{1100000} \\
&+4\,(-1+\alpha)^2\,\alpha^2\,(1-2\,\alpha+2\,\alpha^2)\,\mathrm{F3}^{00}_{2000000} \\
&-\frac{8}{\tau}\,(-1+\alpha)^2\,\alpha\,(\mathrm{F3}^{01}_{0001000}-\mathrm{F3}^{01}_{1000000})
\end{aligned}
\tag{B.22}
$$

$$
\begin{aligned}
\mathcal{F}_4^{(4)}(T) &= -10\,(-1+\alpha)^2\,\alpha\,(4\,\alpha^3+\alpha^2\,(-4+\tau)-2\,\tau+2\,\alpha\,(1+\tau))\,\mathrm{F4}^{00}_{0002000} \\
&+2\,\alpha\,(1-3\,\alpha+2\,\alpha^2)\,(-\mathrm{F4}^{00}_{0001000}+\mathrm{F4}^{00}_{0100000}) \\
&+2\,\alpha^2\,(-2-14\,\alpha^2-4\,\alpha^4-4\,\alpha\,(-2+\tau)+3\,\tau+\alpha^3\,(12+\tau))\,\mathrm{F4}^{00}_{0101000} \\
&+10\,(-1+\alpha)^2\,\alpha^2\,(-2+6\,\alpha+4\,\alpha^3+\alpha^2\,(-8+\tau))\,\tau\,\mathrm{F4}^{00}_{0102000} \\
&-\frac{4}{\tau}\,(-1+\alpha)\,\alpha\,(12\,\alpha^3+2\,\alpha^2\,(-6+\tau)-2\,\tau+\alpha\,(6+\tau)) \\
&\quad\times(-\mathrm{F4}^{00}_{0001000}+\mathrm{F4}^{00}_{1000000}) \\
&+4\,\alpha\,(-1+3\,\alpha-4\,\alpha^2+2\,\alpha^3)\,(-2\,\alpha+2\,\alpha^2+\tau\,)\,\mathrm{F4}^{00}_{1100000} \\
&-8\,(-1+\alpha)^2\,\alpha^2\,(1-2\,\alpha+2\,\alpha^2)\,\mathrm{F4}^{00}_{2000000}-20\,(-1+\alpha)^3\,\alpha\,\mathrm{F4}^{01}_{0002000} \\
&+\frac{12}{\tau}\,(-1+\alpha)^2\,\alpha\,(\mathrm{F4}^{01}_{0001000}-\mathrm{F4}^{01}_{1000000})
\end{aligned}
\tag{B.23}
$$

$$
\begin{aligned}
\mathcal{F}_4^{(5)}(T) &= 2\,\alpha\,(4-12\,\alpha+11\,\alpha^2-3\,\alpha^3)\,(-\mathrm{F5}^{00}_{0001000}+\mathrm{F5}^{00}_{0100000}) \\
&+10\,(-1+\alpha)\,\alpha^2\,(-2+6\,\alpha+4\,\alpha^3+\alpha^2\,(-8+\tau))\,\mathrm{F5}^{00}_{0101000} \\
&+\frac{4}{\tau}\,(-1+\alpha)\,\alpha\,(10\,\alpha^3-3\,\tau+\alpha\,(5+\tau)+2\,\alpha^2\,(-5+2\,\tau)) \\
&\quad\times\,(-\mathrm{F5}^{00}_{0001000}+\mathrm{F5}^{00}_{1000000}) \\
&-8\,\alpha\,(-1+3\,\alpha-4\,\alpha^2+2\,\alpha^3)\,(-2\,\alpha+2\,\alpha^2+\tau\,)\,\mathrm{F5}^{00}_{1100000} \\
&+16\,(-1+\alpha)^2\,\alpha^2\,(1-2\,\alpha+2\,\alpha^2)\,\mathrm{F5}^{00}_{2000000} \\
&-\frac{20}{\tau}\,(-1+\alpha)^2\,\alpha\,(\mathrm{F5}^{01}_{0001000}-\mathrm{F5}^{01}_{1000000})
\end{aligned}
\tag{B.24}
$$

Diagram 10

The functions L_i in the integrands are defined as

$$
\begin{aligned}
&(i=1) && \frac{c_\Gamma\,(-t_a)^{-\epsilon}}{\epsilon} \\
&(i=2) && \log\left(-\frac{t_a}{Q^2}\right) \\
&(i=3) && \{1\}.
\end{aligned}
\tag{B.25}
$$

The colour factor is $\mathcal{C}_{10} = C_F$.

Longitudinal

$$\begin{aligned}\mathcal{F}_{10}^{(1)}(L) &= 4\,(-1+\alpha)^2\,\alpha^2\,(-\mathrm{F1}^{00}_{0000010}+\mathrm{F1}^{00}_{0100000}) + 16\,(-1+\alpha)^4\,\alpha^2\,\mathrm{F1}^{00}_{0100010}\\ &\quad - 4\,(-1+\alpha)^2\,\alpha^2\,(-3+4\,\alpha)\,(-\mathrm{F1}^{00}_{0000010}+\mathrm{F1}^{00}_{1000000})\\ &\quad - 8\,(-1+\alpha)^3\,\alpha^3\,(\mathrm{F1}^{00}_{1100000}-\mathrm{F1}^{00}_{2000000})\end{aligned} \tag{B.26}$$

$$\begin{aligned}\mathcal{F}_{10}^{(2)}(L) &= 40\,(-1+\alpha)^4\,\alpha^2\,\mathrm{F2}^{00}_{0000020} + 8\,(-1+\alpha)^3\,\alpha^2\,(1+3\,\alpha)\,\mathrm{F2}^{00}_{0100010}\\ &\quad + 40\,(-1+\alpha)^5\,\alpha^2\,\mathrm{F2}^{00}_{0100020}\\ &\quad + 32\,(-1+\alpha)^2\,\alpha^2\,(-1+2\,\alpha)\,(\mathrm{F2}^{00}_{0000010}-\mathrm{F2}^{00}_{1000000})\\ &\quad - 24\,(-1+\alpha)^3\,\alpha^3\,(\mathrm{F2}^{00}_{1100000}-\mathrm{F2}^{00}_{2000000})\end{aligned} \tag{B.27}$$

$$\begin{aligned}\mathcal{F}_{10}^{(3)}(L) &= 4\,(-1+\alpha)^2\,\alpha^2\,(-\mathrm{F3}^{00}_{0000010}+\mathrm{F3}^{00}_{0100000}) + 40\,(-1+\alpha)^4\,\alpha^2\,\mathrm{F3}^{00}_{0100010}\\ &\quad - 4\,(-1+\alpha)^2\,\alpha^2\,(-9+10\,\alpha)\,(-\mathrm{F3}^{00}_{0000010}+\mathrm{F3}^{00}_{1000000})\\ &\quad - 32\,(-1+\alpha)^3\,\alpha^3\,(\mathrm{F3}^{00}_{1100000}-\mathrm{F3}^{00}_{2000000})\end{aligned} \tag{B.28}$$

Transverse

$$\begin{aligned}\mathcal{F}_{10}^{(1)}(T) &= 2\,\alpha\,(-1+5\,\alpha-6\,\alpha^2+2\,\alpha^3)\,(-\mathrm{F1}^{00}_{0000010}+\mathrm{F1}^{00}_{0100000})\\ &\quad + 4\,(-1+\alpha)^2\,\alpha\,(-1+2\,\alpha)\,(1-3\,\alpha+2\,\alpha^2+\tau)\,\mathrm{F1}^{00}_{0100010}\\ &\quad - 2\,\alpha\,(1-7\,\alpha+20\,\alpha^2-22\,\alpha^3+8\,\alpha^4)\,(-\mathrm{F1}^{00}_{0000010}+\mathrm{F1}^{00}_{1000000})\\ &\quad - 2\,\alpha\,(-1+3\,\alpha-4\,\alpha^2+2\,\alpha^3)\,(-2\,\alpha+2\,\alpha^2+\tau\ )\,\mathrm{F1}^{00}_{1100000}\\ &\quad + 4\,(-1+\alpha)^2\,\alpha^2\,(1-2\,\alpha+2\,\alpha^2)\,\mathrm{F1}^{00}_{2000000}\end{aligned} \tag{B.29}$$

$$\begin{aligned}\mathcal{F}_{10}^{(2)}(T) &= 10\,(1-2\,\alpha)^2\,(-1+\alpha)^3\,\alpha\,\mathrm{F2}^{00}_{0000020}\\ &\quad + 2\,(-1+\alpha)\,\alpha\,(-2-20\,\alpha^3+12\,\alpha^4+\alpha\,(5-6\,\tau)+3\,\tau\\ &\qquad + \alpha^2\,(5+6\,\tau))\,\mathrm{F2}^{00}_{0100010}\\ &\quad + 10\,(-1+\alpha)^3\,\alpha\,(-1+2\,\alpha)\,(1-3\,\alpha+2\,\alpha^2+\tau)\,\mathrm{F2}^{00}_{0100020}\\ &\quad + 2\,\alpha\,(3-25\,\alpha+70\,\alpha^2-80\,\alpha^3+32\,\alpha^4)\,(\mathrm{F2}^{00}_{0000010}-\mathrm{F2}^{00}_{1000000})\\ &\quad - 6\,\alpha\,(-1+3\,\alpha-4\,\alpha^2+2\,\alpha^3)\,(-2\,\alpha+2\,\alpha^2+\tau\ )\,\mathrm{F2}^{00}_{1100000}\\ &\quad + 12\,(-1+\alpha)^2\,\alpha^2\,(1-2\,\alpha+2\,\alpha^2)\,\mathrm{F2}^{00}_{2000000}\end{aligned} \tag{B.30}$$

$$\begin{aligned}\mathcal{F}_{10}^{(3)}(T) &= 2\,\alpha\,(-1+8\,\alpha-9\,\alpha^2+2\,\alpha^3)\,(-\mathrm{F3}^{00}_{0000010}+\mathrm{F3}^{00}_{0100000})\\ &\quad + 10\,(-1+\alpha)^2\,\alpha\,(-1+2\,\alpha)\,(1-3\,\alpha+2\,\alpha^2+\tau)\,\mathrm{F3}^{00}_{0100010}\\ &\quad - 4\,\alpha\,(2-11\,\alpha+28\,\alpha^2-29\,\alpha^3+10\,\alpha^4)\,(-\mathrm{F3}^{00}_{0000010}+\mathrm{F3}^{00}_{1000000})\\ &\quad - 8\,\alpha\,(-1+3\,\alpha-4\,\alpha^2+2\,\alpha^3)\,(-2\,\alpha+2\,\alpha^2+\tau\ )\,\mathrm{F3}^{00}_{1100000}\\ &\quad + 16\,(-1+\alpha)^2\,\alpha^2\,(1-2\,\alpha+2\,\alpha^2)\,\mathrm{F3}^{00}_{2000000}\end{aligned} \tag{B.31}$$

B.2 Adjacent box

The following table maps the functions L_i under the integrand in the special integrals Fi to the respective logarithmic functions in the adjacent box, or to the respective pole terms.

$$
\begin{array}{ll}
i = 1 & \mathrm{Lc}_0(-Q^2, M^2, t) \\
i = 2 & \mathrm{Lc}_1(M^2, -Q^2, t) \\
i = 3 & \mathrm{Lc}_1(-Q^2, M^2, t) \\
i = 4 & \mathrm{Lc}_1^{2m}(-Q^2, t_a) \\
i = 5 & \mathrm{Lc}_1^{2m}(t_a, t) \\
i = 6 & \mathrm{Lc}_{1S}(-Q^2, M^2, t) \\
i = 7 & \mathrm{Lc}_2^{2m}(t_a, t) \\
i = 8 & \mathrm{Lc}_3(M^2, -Q^2, t) \\
i = 9 & \mathrm{Lc}_3(-Q^2, M^2, t) \\
i = 10 & \mathrm{Ld}_0^a(t_a, M^2, -Q^2, t) \\
i = 11 & \mathrm{Ld}_1(t_a, M^2, -Q^2, t) \\
i = 12 & \mathrm{Ld}_{1S}(t_a, M^2, -Q^2, t) \\
i = 13 & \mathrm{Ld}_{21}(t_a, M^2, -Q^2, t) \\
i = 14 & \mathrm{Ld}_{22}(t_a, M^2, -Q^2, t) \\
i = 15 & \mathrm{Ld}_{24}(t_a, M^2, -Q^2, t) \\
i = 16 & \mathrm{Ld}_{2S}(t_a, M^2, -Q^2, t) \\
i = 17 & \mathrm{Ld}_{311}(t_a, M^2, -Q^2, t) \\
i = 18 & \mathrm{Ld}_{314}(t_a, M^2, -Q^2, t) \\
i = 19 & \mathrm{Ld}_{322}(t_a, M^2, -Q^2, t) \\
i = 20 & \mathrm{Ld}_{344}(t_a, M^2, -Q^2, t) \\
i = 21 & \frac{c_\Gamma}{\epsilon}(-t)^{-\epsilon} \\
i = 22 & \frac{c_\Gamma}{\epsilon}(-t_a)^{-\epsilon} \\
i = 23 & \frac{c_\Gamma}{\epsilon^2}(-t)^{-\epsilon} \\
i = 24 & \frac{c_\Gamma}{\epsilon^2}(-t_a)^{-\epsilon} \\
i = 25 & \frac{c_\Gamma}{\epsilon^2}(-M^2)^{-\epsilon} \\
i = 26 & \frac{c_\Gamma}{\epsilon^2}(Q^2)^{-\epsilon} \\
i = 27 & \mathrm{Lc}_{22m}(-Q^2, t_a) \\
i = 28 & \mathrm{Lc}_2(-Q^2, M^2, t)
\end{array}
\tag{B.32}
$$

Longitudinal

$$\begin{aligned}\mathcal{F}_{12}^{(1)}(L) &= -24\,(-1+\alpha)\,\alpha^2\,(-2\,\alpha+2\,\alpha^2+\tau\,)\,\mathrm{F1}^{00}_{0100000}\\ &+8\,(-1+\alpha)\,\alpha^2\,(-6\,\alpha+6\,\alpha^2+\tau\,)\,\mathrm{F1}^{00}_{1000000}\\ &+8\,(-1+\alpha)\,\alpha^2\,\mathrm{F1}^{01}_{1000000}+40\,(-1+\alpha)\,\alpha^2\,\mathrm{F1}^{10}_{0100000}\end{aligned}\tag{B.33}$$

$$\begin{aligned}\mathcal{F}_{12}^{(2)}(L) &= 2\,\alpha^2\,(2-11\,\alpha+19\,\alpha^2-10\,\alpha^3)\,\tau\,\mathrm{F2}^{00}_{0010000}\\ &+2\,(-1+\alpha)\,\alpha^2\,(12\,\alpha^2+9\,\tau-2\,\alpha\,(6+\tau))\,\mathrm{F2}^{00}_{0100000}\\ &+2\,(-1+\alpha)\,\alpha^2\,(4\,\alpha^4\,(-3+\tau)+12\,\tau^2+\alpha\,(4-19\,\tau-16\,\tau^2)\\ &-2\,\alpha^3\,(-14+16\,\tau+\tau^2)+\alpha^2\,(-20+47\,\tau+9\,\tau^2))\,\mathrm{F2}^{00}_{0110000}\\ &-6\,(-1+\alpha)^2\,\alpha^2\,(4\,\alpha-\tau)\,\mathrm{F2}^{00}_{1000000}\;-2\,(-1+\alpha)^2\,\alpha^2\,(4\,\alpha^3\,(-3+\tau)\\ &+(4-9\,\tau)\,\tau-\alpha\,(4+3\,\tau)+\alpha^2\,(16-11\,\tau-3\,\tau^2))\,\mathrm{F2}^{00}_{1010000}\\ &-4\,\alpha^3\,(2-7\,\alpha+5\,\alpha^2)\,\mathrm{F2}^{01}_{0010000}+12\,(-1+\alpha)^2\,\alpha^2\,\mathrm{F2}^{01}_{1000000}\\ &+4\,(-1+\alpha)^2\,\alpha^2\,(-4+6\,\tau+3\,\alpha\,(6+\tau)+\alpha^2\,(-11+3\,\tau))\,\mathrm{F2}^{01}_{1010000}\\ &+24\,(-1+\alpha)^2\,\alpha^3\,\mathrm{F2}^{02}_{1010000}+4\,(-1+\alpha)^2\,\alpha^2\,(-2+5\,\alpha)\,\mathrm{F2}^{10}_{0010000}\\ &+4\,\alpha^2\,(9-11\,\alpha+2\,\alpha^2)\,\mathrm{F2}^{10}_{0100000}+4\,(-1+\alpha)\,\alpha^2\,(-12\,\tau+2\,\alpha^3\,(3+\tau)\\ &-\alpha^2\,(10+11\,\tau)+\alpha\,(4+18\,\tau))\,\mathrm{F2}^{10}_{0110000}\\ &+8\,(-1+\alpha)^2\,\alpha^2\,(-3+2\,\alpha)\,\mathrm{F2}^{20}_{0110000}\end{aligned}\tag{B.34}$$

$$\begin{aligned}\mathcal{F}_{12}^{(3)}(L) &= 4\,\alpha^2\,(5-21\,\alpha+28\,\alpha^2-12\,\alpha^3)\,\tau\,\mathrm{F3}^{00}_{0010000}\\ &+4\,(-1+\alpha)\,\alpha^2\,(4\,\alpha^2+2\,\tau-\alpha\,(4+5\,\tau))\,\mathrm{F3}^{00}_{0100000}\\ &+4\,(-1+\alpha)\,\alpha^3\,(2+8\,\alpha^3\,(-1+\tau)-8\,\tau^2+\alpha^2\,(18-21\,\tau-5\,\tau^2)\\ &+\alpha\,(-12+13\,\tau+14\,\tau^2))\,\mathrm{F3}^{00}_{0110000}-4\,(-1+\alpha)^2\,\alpha^2\,(4\,\alpha-\tau)\,\mathrm{F3}^{00}_{1000000}\\ &-4\,(-1+\alpha)^2\,\alpha^2\,(8\,\alpha^3\,(-1+\tau)-(-2+\tau)\,\tau-\alpha^2\,(-10+\tau+\tau^2)\\ &-\alpha\,(2+7\,\tau+2\,\tau^2))\,\mathrm{F3}^{00}_{1010000}-8\,\alpha^3\,(5-11\,\alpha+6\,\alpha^2)\,\mathrm{F3}^{01}_{0010000}\\ &+8\,(-1+\alpha)^2\,\alpha^2\,\mathrm{F3}^{01}_{1000000}+8\,(-1+\alpha)^2\,\alpha^2\,(-2+\alpha^2\,(-9+\tau)+\tau\\ &+2\,\alpha\,(5+\tau)\,)\,\mathrm{F3}^{01}_{1010000}+16\,(-1+\alpha)^2\,\alpha^3\,\mathrm{F3}^{02}_{1010000}\\ &+8\,(-1+\alpha)^2\,\alpha^2\,(-5+6\,\alpha)\,\mathrm{F3}^{10}_{0010000}+8\,\alpha^2\,(2-7\,\alpha+5\,\alpha^2)\,\mathrm{F3}^{10}_{0100000}\\ &+8\,(-1+\alpha)\,\alpha^3\,(-3+14\,\tau-20\,\alpha\,\tau+\alpha^2\,(3+5\,\tau))\,\mathrm{F3}^{10}_{0110000}\\ &+80\,(-1+\alpha)^2\,\alpha^3\,\mathrm{F3}^{20}_{0110000}\end{aligned}\tag{B.35}$$

$$\begin{aligned}\mathcal{F}_{12}^{(4)}(L) &= 12\,(-1+\alpha)^2\,\alpha^2\,(-1+2\,\alpha)\,\tau\,\mathrm{F4}^{00}_{0010000}\\ &+4\,\alpha^2\,(-1-2\,\alpha+3\,\alpha^2)\,\tau\,\mathrm{F4}^{00}_{0100000}\\ &-4\,(-1+\alpha)^2\,\alpha^2\,(4\,\alpha^3\,(-2+\tau)+\tau\,(-1+2\,\tau)+\alpha^2\,(10-7\,\tau-3\,\tau^2)\\ &+\alpha\,(-2-2\,\tau+4\,\tau^2))\,\mathrm{F4}^{00}_{0110000}+4\,(-1+\alpha)^3\,\alpha^2\,(4\,\alpha^2\,(-2+\tau)\\ &-\tau+\alpha\,(2+6\,\tau)\,)\,\mathrm{F4}^{00}_{1010000}+24\,(-1+\alpha)^2\,\alpha^3\,\mathrm{F4}^{01}_{0010000}\end{aligned}$$

$$
\begin{aligned}
&+ 12\,(-1+\alpha)^3\,\alpha^2\,(-1+4\,\alpha)\,\mathrm{F4}^{01}_{1010000} - 24\,(-1+\alpha)^3\,\alpha^2\,\mathrm{F4}^{10}_{0010000}\\
&+ 8\,\alpha^2\,(1+2\,\alpha-3\,\alpha^2)\,\mathrm{F4}^{10}_{0100000} - 4\,(-1+\alpha)^2\,\alpha^2\,(1+\alpha\,(5-14\,\tau)\\
&- 6\,\tau + 6\,\alpha^2\,(1+\tau))\,\mathrm{F4}^{10}_{0110000} - 16\,(-1+\alpha)^2\,\alpha^2\,(1+3\,\alpha)\,\mathrm{F4}^{20}_{0110000}
\end{aligned}
\tag{B.36}
$$

$$
\begin{aligned}
\mathcal{F}^{(5)}_{12}(L) &= -12\,\alpha^2\,(-2+7\,\alpha-7\,\alpha^2+2\,\alpha^3)\,\tau\,\mathrm{F5}^{00}_{0010000}\\
&+ 4\,\alpha^2\,(1+5\,\alpha-6\,\alpha^2)\,\tau\,\mathrm{F5}^{00}_{0100000} + 4\,(-1+\alpha)\,\alpha^2\,(-4\,\tau^2+4\,\alpha^4\,(-2+3\,\tau)\\
&- 2\,\alpha\,\tau\,(-6+5\,\tau) + \alpha^3\,(16-24\,\tau-6\,\tau^2) + \alpha^2\,(-8+17\,\tau^2)\ )\,\mathrm{F5}^{00}_{0110000}\\
&- 8\,(-1+\alpha)^2\,\alpha^2\,\tau\,\mathrm{F5}^{00}_{1000000} - 8\,(-1+\alpha)^2\,\alpha^2\,(\alpha\,(-6+\tau)\,\tau + 2\,\tau^2\\
&+ \alpha^3\,(-4+6\,\tau) + \alpha^2\,(4+\tau+\tau^2\ ))\,\mathrm{F5}^{00}_{1010000}\\
&- 24\,\alpha^3\,(2-3\,\alpha+\alpha^2)\,\mathrm{F5}^{01}_{0010000} - 16\,(-1+\alpha)^2\,\alpha^2\,\mathrm{F5}^{01}_{1000000}\\
&- 8\,(-1+\alpha)^2\,\alpha^2\,(3\,\tau+2\,\alpha^2\,(4+\tau)+\alpha\,(-7+3\,\tau))\,\mathrm{F5}^{01}_{1010000}\\
&- 32\,(-1+\alpha)^2\,\alpha^3\,\mathrm{F5}^{02}_{1010000} + 24\,(-2+\alpha)\,(-1+\alpha)^2\,\alpha^2\,\mathrm{F5}^{10}_{0010000}\\
&+ 8\,\alpha^2\,(-1-5\,\alpha+6\,\alpha^2)\,\mathrm{F5}^{10}_{0100000} + 8\,(-1+\alpha)\,\alpha^2\,(\alpha^2\,(1-22\,\tau)+4\,\tau\\
&+ 6\,\alpha^3\,(1+\tau) + \alpha\,(-7+15\,\tau))\,\mathrm{F5}^{10}_{0110000}\\
&+ 16\,(-1+\alpha)^2\,\alpha^2\,(1+6\,\alpha)\,\mathrm{F5}^{20}_{0110000}
\end{aligned}
\tag{B.37}
$$

$$
\begin{aligned}
\mathcal{F}^{(6)}_{12}(L) &= -4\,(-1+\alpha)^2\,\alpha^2\,(8\,\alpha^3+\tau+3\,\alpha\,(-1+3\,\tau)-\alpha^2\,(5+6\,\tau))\,\mathrm{F6}^{00}_{0110000}\\
&+ 8\,(-1+\alpha)^2\,\alpha\,(1+3\,\alpha)\,(\mathrm{F6}^{00}_{0100000} - \mathrm{F6}^{00}_{1000000})\\
&+ 4\,(-1+\alpha)^2\,\alpha^2\,(8\,\alpha^3+3\,\alpha\,(-1+\tau)+5\,\tau-\alpha^2\,(5+6\,\tau))\,\mathrm{F6}^{00}_{1010000}\\
&+ 8\,(-1+\alpha)^2\,\alpha\,(-6\,\alpha^2+6\,\alpha^3+\tau)\,\mathrm{F6}^{00}_{1100000}\\
&+ 4\,(-1+\alpha)^3\,\alpha^2\,(12\,\alpha^3\,(-1+\tau)-\alpha\,\tau+\tau^2-2\,\alpha^2\,(-6+7\,\tau))\,\mathrm{F6}^{00}_{1110000}\\
&- 16\,(-1+\alpha)^2\,\alpha\,(-3\,\alpha^2+3\,\alpha^3+\tau)\,\mathrm{F6}^{00}_{2000000}\\
&- 8\,(-1+\alpha)^3\,\alpha^2\,(-3\,\alpha^2\,(-2+\tau)+6\,\alpha^3\,(-1+\tau)-6\,\alpha\,\tau+2\,\tau^2)\,\mathrm{F6}^{00}_{2010000}\\
&- 8\,(-1+\alpha)^2\,\alpha^2\,(-4+3\,\alpha)\,\mathrm{F6}^{01}_{1010000} - 16\,(-1+\alpha)^2\,\alpha\,\mathrm{F6}^{01}_{2000000}\\
&- 8\,(-1+\alpha)^3\,\alpha^2\,(-11\,\alpha+8\,\alpha^2+4\,\tau)\,\mathrm{F6}^{01}_{2010000} - 16\,(-1+\alpha)^3\,\alpha^2\,\mathrm{F6}^{02}_{2010000}\\
&+ 24\,(-1+\alpha)^2\,\alpha^3\,\mathrm{F6}^{10}_{0110000}
\end{aligned}
\tag{B.38}
$$

$$
\begin{aligned}
\mathcal{F}^{(7)}_{12}(L) &= 16\,(-1+\alpha)\,\alpha^2\,(-2\,\alpha+2\,\alpha^2+\tau\ )\,(\mathrm{F7}^{00}_{0100000} - \mathrm{F7}^{00}_{1000000})\\
&- 16\,(-1+\alpha)\,\alpha^2\,\mathrm{F7}^{01}_{1000000} - 16\,(-1+\alpha)\,\alpha^2\,\mathrm{F7}^{10}_{0100000}
\end{aligned}
\tag{B.39}
$$

$$
\begin{aligned}
\mathcal{F}^{(8)}_{12}(L) &= -16\,(-1+\alpha)^2\,\alpha^2\,(-1+2\,\alpha)\,\tau\,\mathrm{F8}^{00}_{0010000}\\
&+ 8\,\alpha^2\,(1+\alpha-2\,\alpha^2)\,\tau\,\mathrm{F8}^{00}_{0100000} + 8\,(-1+\alpha)^2\,\alpha^2\,(2\,\alpha^3\,(-2+\tau)\\
&+ 2\,\tau^2 + \alpha^2\,(5-3\,\tau-2\,\tau^2) + \alpha\,(-1-2\,\tau+2\,\tau^2))\,\mathrm{F8}^{00}_{0110000}\\
&- 8\,(-1+\alpha)^3\,\alpha^2\,(\alpha+2\,\alpha^2\,(-2+\tau)-\tau+5\,\alpha\,\tau)\,\mathrm{F8}^{00}_{1010000}\\
&- 32\,(-1+\alpha)^2\,\alpha^3\,\mathrm{F8}^{01}_{0010000} - 16\,(-1+\alpha)^3\,\alpha^2\,(-1+4\,\alpha)\,\mathrm{F8}^{01}_{1010000}
\end{aligned}
$$

$$
\begin{aligned}
&+ 32\,(-1+\alpha)^3\,\alpha^2\,\mathrm{F8}^{10}_{0010000} + 16\,\alpha^2\,(-1-\alpha+2\,\alpha^2)\,\mathrm{F8}^{10}_{0100000}\\
&+ 16\,(-1+\alpha)^2\,\alpha^2\,(\alpha-3\,\tau-4\,\alpha\,\tau+2\,\alpha^2\,(1+\tau))\,\mathrm{F8}^{10}_{0110000}\\
&+ 32\,(-1+\alpha)^2\,\alpha^2\,(1+2\,\alpha)\,\mathrm{F8}^{20}_{0110000} \qquad\qquad \text{(B.40)}
\end{aligned}
$$

$$
\begin{aligned}
\mathcal{F}^{(9)}_{12}(L) = &-8\,(-1+\alpha)\,\alpha^2\,(1-5\,\alpha+4\,\alpha^2+2\,\tau)\,\mathrm{F9}^{00}_{0100000}\\
&+ 8\,(-1+\alpha)\,\alpha^2\,(1-5\,\alpha+4\,\alpha^2+\tau)\,\mathrm{F9}^{00}_{1000000} + 8\,(-1+\alpha)\,\alpha^2\,\mathrm{F9}^{01}_{1000000}\\
&+ 24\,(-1+\alpha)\,\alpha^2\,\mathrm{F9}^{10}_{0100000} \qquad\qquad \text{(B.41)}
\end{aligned}
$$

$$
\begin{aligned}
\mathcal{F}^{(10)}_{12}(L) = &-16\,(-1+\alpha)^2\,\alpha^2\,(\mathrm{F10}^{00}_{0100000}-\mathrm{F10}^{00}_{1000000})\\
&- 32\,(-1+\alpha)^3\,\alpha^3\,(\mathrm{F10}^{00}_{1100000}-\mathrm{F10}^{00}_{2000000}) \qquad\qquad \text{(B.42)}
\end{aligned}
$$

$$
\begin{aligned}
\mathcal{F}^{(11)}_{12}(L) = &-4\,\alpha\,(1-8\,\alpha+19\,\alpha^2-16\,\alpha^3+4\,\alpha^4)\,\tau\,\mathrm{F11}^{00}_{0010000}\\
&- 4\,\alpha^2\,(1-8\,\alpha+7\,\alpha^2)\,\tau\,\mathrm{F11}^{00}_{0100000} + 4\,(-1+\alpha)\,\alpha^2\,(20\,\alpha^4\,(-1+\tau)\\
&+ 2\,\tau\,(-1+2\,\tau)+\alpha\,(8-5\,\tau-24\,\tau^2)+\alpha^3\,(48-65\,\tau-7\,\tau^2)\\
&+ \alpha^2\,(-36+52\,\tau+25\,\tau^2))\,\mathrm{F11}^{00}_{0110000} - 20\,(-1+\alpha)^3\,\alpha\,\tau\,\mathrm{F11}^{00}_{1000000}\\
&- 4\,(-1+\alpha)^2\,\alpha\,(20\,\alpha^4\,(-1+\tau)-\alpha\,(-11+\tau)\,\tau-\tau^2\\
&+ \alpha^2\,(-8-22\,\tau+5\,\tau^2)+\alpha^3\,(28-17\,\tau+5\,\tau^2))\,\mathrm{F11}^{00}_{1010000}\\
&+ 8\,(-1+\alpha)^3\,\alpha^3\,(-1+2\,\alpha)\,(-1+\tau)\,\tau\,\mathrm{F11}^{00}_{1110000}\\
&+ 16\,(-1+\alpha)^3\,\alpha^2\,\tau\,\mathrm{F11}^{00}_{2000000}\\
&- 16\,(-1+\alpha)^3\,\alpha^2\,(-1+2\,\alpha)\,\tau\,(\alpha\,(-1+\tau)+\tau)\,\mathrm{F11}^{00}_{2010000}\\
&+ 8\,\alpha^2\,(1-6\,\alpha+7\,\alpha^2-2\,\alpha^3)\,\mathrm{F11}^{01}_{0010000} - 40\,(-1+\alpha)^3\,\alpha\,\mathrm{F11}^{01}_{1000000}\\
&- 8\,(-1+\alpha)^2\,\alpha\,(\alpha\,(10-3\,\tau)-\tau+5\,\alpha^3\,(3+\tau)\\
&+ \alpha^2\,(-29+7\,\tau))\,\mathrm{F11}^{01}_{1010000} + 32\,(-1+\alpha)^3\,\alpha^2\,\mathrm{F11}^{01}_{2000000}\\
&- 16\,(-1+\alpha)^3\,\alpha^2\,(-1+2\,\alpha)\,(\alpha\,(-1+\tau)+3\,\tau)\,\mathrm{F11}^{01}_{2010000}\\
&- 16\,(-1+\alpha)^2\,\alpha^2\,(-3+5\,\alpha)\,\mathrm{F11}^{02}_{1010000} - 32\,(-1+\alpha)^3\,\alpha^2\\
&\quad \times (-1+2\,\alpha)\,\mathrm{F11}^{02}_{2010000} + 8\,(-1+\alpha)^2\,\alpha\,(1-5\,\alpha+2\,\alpha^2)\,\mathrm{F11}^{10}_{0010000}\\
&+ 8\,\alpha^2\,(1-8\,\alpha+7\,\alpha^2)\,\mathrm{F11}^{10}_{0100000} + 8\,(-1+\alpha)\,\alpha^2\,(1-4\,\tau+\alpha^3\,(13+7\,\tau)\\
&+ \alpha\,(-1+28\,\tau)-\alpha^2\,(13+29\,\tau))\,\mathrm{F11}^{10}_{0110000}\\
&+ 16\,(-1+\alpha)^2\,\alpha^2\,(-1+7\,\alpha)\,\mathrm{F11}^{20}_{0110000} \qquad\qquad \text{(B.43)}
\end{aligned}
$$

$$
\begin{aligned}
\mathcal{F}^{(12)}_{12}(L) = &-8\,(-1+\alpha)\,\alpha\,(2\,\alpha^3+2\,\alpha\,(-1+\tau)+\tau)\,\mathrm{F12}^{00}_{0100000}\\
&+ 8\,(-1+\alpha)\,\alpha\,(2\,\alpha^3+2\,\tau-\alpha\,(2+\tau))\,\mathrm{F12}^{00}_{1000000}\\
&- 8\,\alpha\,(3-5\,\alpha+2\,\alpha^2)\,\mathrm{F12}^{01}_{1000000} + 8\,\alpha\,(-1-3\,\alpha+4\,\alpha^2)\,\mathrm{F12}^{10}_{0100000} \qquad \text{(B.44)}
\end{aligned}
$$

$$
\begin{aligned}
\mathcal{F}_{12}^{(13)}(L) &= 2\,\alpha\,(4-16\,\alpha+15\,\alpha^2+7\,\alpha^3-10\,\alpha^4)\,\tau\,\mathrm{F13}^{00}_{0010000}\\
&-2\,(-1+\alpha)\,\alpha^2\,(4\,\alpha^2+3\,\tau-4\,\alpha\,(1+2\,\tau))\,\mathrm{F13}^{00}_{0100000}\\
&-2\,(-1+\alpha)\,\alpha^2\,(2\,\tau\,(-1+2\,\tau)+4\,\alpha^4\,(-7+4\,\tau)+\alpha\,(-2+21\,\tau-24\,\tau^2)\\
&+\alpha^3\,(54-44\,\tau-4\,\tau^2)+\alpha^2\,(-24+9\,\tau+19\,\tau^2))\,\mathrm{F13}^{00}_{0110000}\\
&+2\,(-1+\alpha)^2\,\alpha\,(4\,\alpha^2-8\,\tau+13\,\alpha\,\tau)\,\mathrm{F13}^{00}_{1000000}\\
&+2\,(-1+\alpha)^2\,\alpha\,(-(\alpha\,(-6+\tau)\,\tau)-4\,\tau^2+4\,\alpha^4\,(-7+4\,\tau)\\
&+\alpha^2\,(2-27\,\tau+8\,\tau^2)+\alpha^3\,(26-9\,\tau+17\,\tau^2))\,\mathrm{F13}^{00}_{1010000}\\
&-4\,(-1+\alpha)^3\,\alpha^2\,(-2\,\alpha^2\,(-2+\tau)+\tau^2-\alpha\,\tau\,(3+\tau)\\
&+4\,\alpha^3\,(-1+\tau+\tau^2))\,\mathrm{F13}^{00}_{1110000}+8\,(-1+\alpha)^3\,\alpha^3\,((-2+\tau)\,\tau\\
&+2\,\alpha^2\,(-1+\tau+\tau^2)+\alpha\,(2-\tau+5\,\tau^2\ ))\,\mathrm{F13}^{00}_{2010000}\\
&+4\,\alpha^2\,(-4+8\,\alpha+\alpha^2-5\,\alpha^3)\,\mathrm{F13}^{01}_{0010000}\\
&+4\,(-1+\alpha)^2\,\alpha\,(-8+13\,\alpha)\,\mathrm{F13}^{01}_{1000000}+4\,(-1+\alpha)^2\,\alpha\,(\alpha\,(6-8\,\tau)\\
&-4\,\tau+\alpha^3\,(7+13\,\tau)+\alpha^2\,(-20+19\,\tau))\,\mathrm{F13}^{01}_{1010000}\\
&+8\,(-1+\alpha)^3\,\alpha^2\,(-3\,\tau+10\,\alpha^2\,\tau+\alpha\,(-1+9\,\tau))\,\mathrm{F13}^{01}_{2010000}\\
&+8\,(-1+\alpha)^2\,\alpha^2\,(-8+13\,\alpha)\,\mathrm{F13}^{02}_{1010000}\\
&+32\,(-1+\alpha)^3\,\alpha^2\,(-1+3\,\alpha)\,\mathrm{F13}^{02}_{2010000}\\
&+4\,(-1+\alpha)^2\,\alpha\,(-4+4\,\alpha+5\,\alpha^2)\,\mathrm{F13}^{10}_{0010000}\\
&-4\,\alpha^2\,(3-11\,\alpha+8\,\alpha^2)\,\mathrm{F13}^{10}_{0100000}\\
&-4\,(-1+\alpha)\,\alpha^2\,(2-4\,\tau-29\,\alpha^2\,\tau\\
&+4\,\alpha^3\,(3+2\,\tau)+2\,\alpha\,(-7+15\,\tau))\,\mathrm{F13}^{10}_{0110000}\\
&-8\,(-1+\alpha)^2\,\alpha^2\,(-1+8\,\alpha)\,\mathrm{F13}^{20}_{0110000}
\end{aligned}
\tag{B.45}
$$

$$
\begin{aligned}
\mathcal{F}_{12}^{(14)}(L) &= -4\,\alpha\,(-2+7\,\alpha-5\,\alpha^2-4\,\alpha^3+4\,\alpha^4)\,\tau\,\mathrm{F14}^{00}_{0010000}\\
&-4\,(-1+\alpha)\,\alpha^2\,(-2+4\,\alpha^2+4\,\tau-\alpha\,(2+5\,\tau))\,\mathrm{F14}^{00}_{0100000}\\
&-4\,(-1+\alpha)\,\alpha^2\,(-1-\tau+8\,\tau^2+2\,\alpha^4\,(-9+5\,\tau)+\alpha^3\,(44-43\,\tau-3\,\tau^2)\\
&-2\,\alpha\,(-5+6\,\tau+10\,\tau^2)+\alpha^2\,(-35+46\,\tau+14\,\tau^2))\,\mathrm{F14}^{00}_{0110000}\\
&+4\,(-1+\alpha)^2\,\alpha\,(4\,\alpha^2-6\,\tau+\alpha\,(2+7\,\tau))\,\mathrm{F14}^{00}_{1000000}\\
&+4\,(-1+\alpha)^2\,\alpha\,(-2\,\tau\,(1+\tau)+2\,\alpha^4\,(-9+5\,\tau)+\alpha\,(1+19\,\tau-7\,\tau^2)\\
&+\alpha^2\,(-9-14\,\tau+4\,\tau^2)+\alpha^3\,(26-17\,\tau+9\,\tau^2))\,\mathrm{F14}^{00}_{1010000}\\
&-4\,(-1+\alpha)^3\,\alpha^2\,(-4\,\alpha^2\,(-1+\tau)+(-1+\tau)\,\tau-4\,\alpha\,(-1+\tau)\,\tau\\
&+4\,\alpha^3\,(-1+\tau^2))\,\mathrm{F14}^{00}_{1110000}-16\,(-1+\alpha)^3\,\alpha^3\,(\mathrm{F14}^{00}_{1100000}-\mathrm{F14}^{00}_{2000000})\\
&+8\,(-1+\alpha)^3\,\alpha\,(\alpha^2\,(5-2\,\tau)\,\tau+\tau^2-\alpha\,\tau\,(1+6\,\tau)+2\,\alpha^4\,(-1+\tau^2)\\
&+\alpha^3\,(2-5\,\tau+7\,\tau^2))\,\mathrm{F14}^{00}_{2010000}+8\,\alpha^2\,(-2+3\,\alpha+\alpha^2-2\,\alpha^3)\,\mathrm{F14}^{01}_{0010000}\\
&+8\,(-1+\alpha)^2\,\alpha\,(-6+7\,\alpha)\,\mathrm{F14}^{01}_{1000000}+8\,(-1+\alpha)^2\,\alpha\,(\alpha\,(19-11\,\tau)\\
&-2\,(1+\tau)+7\,\alpha^3\,(1+\tau)+2\,\alpha^2\,(-13+5\,\tau))\ \ \mathrm{F14}^{01}_{1010000}\\
&+8\,(-1+\alpha)^3\,\alpha\,(3\,\tau+2\,\alpha^2\,(3+5\,\tau)+2\,\alpha^3\,(-3+7\,\tau)
\end{aligned}
$$

$$
\begin{aligned}
&- \alpha\,(1 + 23\,\tau))\,\mathrm{F14}^{01}_{2010000} + 16\,(-1+\alpha)^2\,\alpha^2\,(-6+7\,\alpha)\,\mathrm{F14}^{02}_{1010000}\\
&+ 16\,(-1+\alpha)^3\,\alpha\,(1 - 10\,\alpha + 10\,\alpha^2)\,\mathrm{F14}^{02}_{2010000}\\
&+ 8\,(-1+\alpha)^2\,\alpha\,(-2+\alpha+2\,\alpha^2)\,\mathrm{F14}^{10}_{0010000}\\
&- 8\,\alpha^2\,(4 - 9\,\alpha + 5\,\alpha^2)\,\mathrm{F14}^{10}_{0100000} - 8\,(-1+\alpha)\,\alpha^2\,(1 - 8\,\tau + 24\,\alpha\,\tau\\
&- 10\,\alpha^2\,(1+2\,\tau) + \alpha^3\,(9+5\,\tau))\,\mathrm{F14}^{10}_{0110000}\\
&- 16\,(-1+\alpha)^2\,\alpha^2\,(-2+5\,\alpha)\,\mathrm{F14}^{20}_{0110000}
\end{aligned}
\tag{B.46}
$$

$$
\begin{aligned}
\mathcal{F}^{(15)}_{12}(L) &= 4\,(-1+\alpha)\,\alpha^2\,(-1 - 7\,\alpha + 8\,\alpha^2 + 4\,\tau)\,(\mathrm{F15}^{00}_{0100000} - \mathrm{F15}^{00}_{1000000})\\
&+ 4\,(-1+\alpha)^2\,\alpha^2\,(-4\,\alpha + 4\,\alpha^2 + \tau\ )\,\mathrm{F15}^{00}_{1100000}\\
&- 8\,(-1+\alpha)^2\,\alpha^2\,(-2\,\alpha + 2\,\alpha^2 + \tau\ )\,\mathrm{F15}^{00}_{2000000}\\
&- 16\,(-1+\alpha)\,\alpha^2\,\mathrm{F15}^{01}_{1000000} - 8\,(-1+\alpha)^2\,\alpha^2\,\mathrm{F15}^{01}_{2000000}\\
&- 16\,(-1+\alpha)\,\alpha^2\,\mathrm{F15}^{10}_{0100000}
\end{aligned}
\tag{B.47}
$$

$$
\begin{aligned}
\mathcal{F}^{(16)}_{12}(L) &= -12\,(-1+\alpha)^2\,\alpha^2\,(16\,\alpha^3 + 3\,\tau + 5\,\alpha\,(-1+3\,\tau)\\
&- \alpha^2\,(11+6\,\tau))\,\mathrm{F16}^{00}_{0110000} + 24\,(-1+\alpha)^2\,\alpha\,(1+3\,\alpha)\,(\mathrm{F16}^{00}_{0100000} - \mathrm{F16}^{00}_{1000000})\\
&+ 12\,(-1+\alpha)^2\,\alpha^2\,(16\,\alpha^3 + 9\,\tau + \alpha\,(-5+3\,\tau) - \alpha^2\,(11+6\,\tau))\,\mathrm{F16}^{00}_{1010000}\\
&+ 24\,(-1+\alpha)^2\,\alpha\,(-6\,\alpha^2 + 6\,\alpha^3 + \tau)\,\mathrm{F16}^{00}_{1100000}\\
&+ 12\,(-1+\alpha)^3\,\alpha^2\,(12\,\alpha^3\,(-1+\tau) - \alpha\,\tau + \tau^2 - 2\,\alpha^2\,(-6+7\,\tau))\,\mathrm{F16}^{00}_{1110000}\\
&- 48\,(-1+\alpha)^2\,\alpha\,(-3\,\alpha^2 + 3\,\alpha^3 + \tau)\,\mathrm{F16}^{00}_{2000000}\\
&- 24\,(-1+\alpha)^3\,\alpha^2\,(-3\,\alpha^2\,(-2+\tau) + 6\,\alpha^3\,(-1+\tau) - 6\,\alpha\,\tau + 2\,\tau^2)\,\mathrm{F16}^{00}_{2010000}\\
&- 24\,(-1+\alpha)^2\,\alpha^2\,(-7+4\,\alpha)\,\mathrm{F16}^{01}_{1010000} - 48\,(-1+\alpha)^2\,\alpha\,\mathrm{F16}^{01}_{2000000}\\
&- 24\,(-1+\alpha)^3\,\alpha^2\,(-11\,\alpha + 8\,\alpha^2 + 4\,\tau)\,\mathrm{F16}^{01}_{2010000}\\
&- 48\,(-1+\alpha)^3\,\alpha^2\,\mathrm{F16}^{02}_{2010000} + 24\,(-1+\alpha)^2\,\alpha^2\,(1+8\,\alpha)\,\mathrm{F16}^{10}_{0110000}
\end{aligned}
\tag{B.48}
$$

$$
\begin{aligned}
\mathcal{F}^{(17)}_{12}(L) &= 4\,(-1+\alpha)^2\,\alpha\,(-1+2\,\alpha)\,\tau\,\mathrm{F17}^{00}_{0010000} - 4\,\alpha^2\,(-1+\alpha^2)\,\tau\,\mathrm{F17}^{00}_{0100000}\\
&+ 4\,(-1+\alpha)^2\,\alpha^2\,(2\,\alpha^3\,(-1+\tau) + 2\,\tau\,(1+2\,\tau) - \alpha\,(1+8\,\tau)\\
&+ \alpha^2\,(3 + 2\,\tau - \tau^2))\,\mathrm{F17}^{00}_{0110000} - 4\,(-1+\alpha)^3\,\alpha\,\tau\,\mathrm{F17}^{00}_{1000000}\\
&- 4\,(-1+\alpha)^2\,\alpha\,(2\,\alpha^4\,(-1+\tau) - \tau^2 + 3\,\alpha\,\tau\,(1+\tau) + \alpha^3\,(3 + 4\,\tau + \tau^2)\\
&- \alpha^2\,(1 + 11\,\tau + 3\,\tau^2))\,\mathrm{F17}^{00}_{1010000}\\
&+ 4\,(-1+\alpha)^3\,\alpha^3\,\tau\,(1 + 4\,\alpha^2 + 3\,\tau - 2\,\alpha\,(3+\tau))\,\mathrm{F17}^{00}_{1110000}\\
&- 8\,(-1+\alpha)^3\,\alpha^2\,\tau\,(\alpha + 2\,\alpha^3 - \tau + 5\,\alpha\,\tau - 2\,\alpha^2\,(2+\tau))\,\mathrm{F17}^{00}_{2010000}\\
&+ 8\,(-1+\alpha)^2\,\alpha^2\,\mathrm{F17}^{01}_{0010000} - 8\,(-1+\alpha)^3\,\alpha\,\mathrm{F17}^{01}_{1000000}\\
&- 8\,(-1+\alpha)^2\,\alpha\,(-\tau + \alpha^3\,(1+\tau) + \alpha\,(2+\tau) - \alpha^2\,(4+\tau))\,\mathrm{F17}^{01}_{1010000}\\
&+ 8\,(-1+\alpha)^3\,\alpha^2\,(3\,\tau + 2\,\alpha^2\,(1+\tau) - \alpha\,(1+9\,\tau))\,\mathrm{F17}^{01}_{2010000}\\
&- 16\,(-1+\alpha)^3\,\alpha^2\,\mathrm{F17}^{02}_{1010000} - 16\,(-1+\alpha)^3\,\alpha^2\,(-1+2\,\alpha)\,\mathrm{F17}^{02}_{2010000}
\end{aligned}
$$

$$
\begin{aligned}
&- 8\,(-1+\alpha)^3\,\alpha\,\mathrm{F17}^{10}_{0010000} + 8\,\alpha^2\,(-1+\alpha^2)\,\mathrm{F17}^{10}_{0100000}\\
&+ 8\,(-1+\alpha)^2\,\alpha^2\,(-1+\alpha-4\,\tau-2\,\alpha\,\tau+\alpha^2\,(1+\tau))\,\mathrm{F17}^{10}_{0110000}\\
&+ 16\,(-1+\alpha)^2\,\alpha^2\,(1+\alpha)\,\mathrm{F17}^{20}_{0110000}
\end{aligned} \tag{B.49}
$$

$$
\begin{aligned}
\mathcal{F}^{(18)}_{12}(L) = {}& 4\,(-1+\alpha)^2\,\alpha\,(-1+2\,\alpha)\,\tau\,\mathrm{F18}^{00}_{0010000} - 8\,(-1+\alpha)\,\alpha^3\,\tau\,\mathrm{F18}^{00}_{0100000}\\
&+ 4\,(-1+\alpha)^2\,\alpha^2\,(3\,\tau+4\,\alpha^3\,(-1+2\,\tau)+\alpha^2\,(6-11\,\tau-4\,\tau^2)\\
&+ 2\,\alpha\,(-1-2\,\tau+4\,\tau^2))\,\mathrm{F18}^{00}_{0110000} - 4\,(-1+\alpha)^2\,\alpha\,(-3+2\,\alpha)\,\tau\,\mathrm{F18}^{00}_{1000000}\\
&- 4\,(-1+\alpha)^2\,\alpha\,(\alpha^3\,(6-7\,\tau)-4\,\tau^2+3\,\alpha\,\tau\,(2+\tau)+4\,\alpha^4\,(-1+2\,\tau)\\
&- \alpha^2\,(2+11\,\tau+\tau^2))\,\mathrm{F18}^{00}_{1010000} - 4\,(-1+\alpha)^3\,\alpha^2\,\tau\,(\alpha^2\,(8-6\,\tau)\\
&+ 4\,\alpha^3\,(-1+\tau)+\tau-\alpha\,(2+\tau)\,)\,\mathrm{F18}^{00}_{1110000} - 4\,(-1+\alpha)^3\,\alpha\,\tau^2\,\mathrm{F18}^{00}_{2000000}\\
&+ 4\,(-1+\alpha)^3\,\alpha\,\tau\,(-6\,\alpha^3\,(-2+\tau)+4\,\alpha^4\,(-1+\tau)+7\,\alpha\,\tau-3\,\tau^2\\
&- \alpha^2\,(4+11\,\tau+\tau^2))\,\mathrm{F18}^{00}_{2010000} + 8\,(-1+\alpha)^2\,\alpha^2\,\mathrm{F18}^{01}_{0010000}\\
&- 8\,(-1+\alpha)^2\,\alpha\,(-3+2\,\alpha)\,\mathrm{F18}^{01}_{1000000} - 8\,(-1+\alpha)^2\,\alpha\,(4\,\alpha-4\,\tau\\
&+ 2\,\alpha^3\,(1+\tau)-\alpha^2\,(8+\tau))\,\mathrm{F18}^{01}_{1010000} - 16\,(-1+\alpha)^3\,\alpha\,\tau\,\mathrm{F18}^{01}_{2000000}\\
&+ 8\,(-1+\alpha)^3\,\alpha\,(4\,\alpha^3-\alpha\,(-8+\tau)\,\tau-5\,\tau^2\\
&- \alpha^2\,(2+13\,\tau+2\,\tau^2)\,)\,\mathrm{F18}^{01}_{2010000} - 16\,(-1+\alpha)^2\,\alpha^2\,(-3+2\,\alpha)\,\mathrm{F18}^{02}_{1010000}\\
&- 16\,(-1+\alpha)^3\,\alpha\,\mathrm{F18}^{02}_{2000000} - 16\,(-1+\alpha)^3\,\alpha\,(2\,\alpha\,(-1+\tau)+2\,\tau\\
&+ \alpha^2\,(3+\tau))\,\mathrm{F18}^{02}_{2010000} - 32\,(-1+\alpha)^3\,\alpha^2\,\mathrm{F18}^{03}_{2010000}\\
&- 8\,(-1+\alpha)^3\,\alpha\,\mathrm{F18}^{10}_{0010000} + 16\,(-1+\alpha)\,\alpha^3\,\mathrm{F18}^{10}_{0100000}\\
&+ 8\,(-1+\alpha)^2\,\alpha^2\,(-1+\alpha-8\,\alpha\,\tau+2\,\alpha^2\,(1+\tau))\,\mathrm{F18}^{10}_{0110000}\\
&+ 32\,(-1+\alpha)^2\,\alpha^3\,\mathrm{F18}^{20}_{0110000}
\end{aligned} \tag{B.50}
$$

$$
\begin{aligned}
\mathcal{F}^{(19)}_{12}(L) = {}& -4\,(-1+\alpha)^2\,\alpha\,(1-3\,\alpha+2\,\alpha^2+2\,\tau)\,(\mathrm{F19}^{00}_{0100000} - \mathrm{F19}^{00}_{1000000})\\
&- 4\,(-1+\alpha)^3\,\alpha\,(-1+2\,\alpha)\,\tau\,\mathrm{F19}^{00}_{1100000}\\
&+ 8\,(-1+\alpha)^3\,\alpha\,(-1+2\,\alpha)\,\tau\,\mathrm{F19}^{00}_{2000000}\\
&+ 8\,(-1+\alpha)^2\,\alpha\,\mathrm{F19}^{01}_{1000000} + 8\,(-1+\alpha)^3\,\alpha\,(-1+2\,\alpha)\,\mathrm{F19}^{01}_{2000000}\\
&+ 8\,(-1+\alpha)^2\,\alpha\,\mathrm{F19}^{10}_{0100000}
\end{aligned} \tag{B.51}
$$

$$
\begin{aligned}
\mathcal{F}^{(20)}_{12}(L) = {}& -4\,(-1+\alpha)^2\,\alpha^2\,(-1+2\,\alpha)\,\mathrm{F20}^{00}_{0100000}\\
&+ 4\,(-1+\alpha)^2\,\alpha\,(-\alpha+2\,\alpha^2+2\,\tau\,)\,\mathrm{F20}^{00}_{1000000}\\
&- 4\,(-1+\alpha)^2\,\alpha^2\,(-1+2\,\alpha)\,\tau\,\mathrm{F20}^{00}_{1100000}\\
&+ 8\,(-1+\alpha)^2\,\alpha\,\tau\,(-\alpha+2\,\alpha^2+\tau)\,\mathrm{F20}^{00}_{2000000}\\
&+ 16\,(-1+\alpha)^2\,\alpha\,\mathrm{F20}^{01}_{1000000} + 8\,(-1+\alpha)^2\,\alpha\,(-\alpha+2\,\alpha^2+3\,\tau\,)\,\mathrm{F20}^{01}_{2000000}\\
&+ 16\,(-1+\alpha)^2\,\alpha\,\mathrm{F20}^{02}_{2000000}
\end{aligned} \tag{B.52}
$$

$$
\begin{aligned}
\mathcal{F}_{12}^{(21)}(L) = & -4\,(-1+\alpha)^2\,\alpha^2\,(-\mathrm{F21}^{00}_{0001000}+\mathrm{F21}^{00}_{0100000}) \\
& -4\,(-1+\alpha)^2\,\alpha^3\,(-4+4\,\alpha+\tau)\,\mathrm{F21}^{00}_{0101000} \\
& -4\,(-1+\alpha)^2\,\alpha^2\,(-2\,\alpha^2+2\,\alpha^3+\tau+\alpha\,\tau)\,\mathrm{F21}^{00}_{0110000} \\
& -\frac{8}{\tau}\,(-1+\alpha)\,\alpha^2\,(-2\,\alpha+2\,\alpha^2+\tau)\,(-\mathrm{F21}^{00}_{0001000}+\mathrm{F21}^{00}_{1000000}) \\
& +4\,(-1+\alpha)^3\,\alpha^2\,(2\,\alpha^2-\tau)\,\mathrm{F21}^{00}_{1010000} \\
& +\frac{8}{\tau}\,(-1+\alpha)\,\alpha^2\,(\mathrm{F21}^{01}_{0001000}-\mathrm{F21}^{01}_{1000000}) \\
& -4\,(-1+\alpha)^3\,\alpha^2\,\mathrm{F21}^{01}_{1010000}+4\,(-1+\alpha)^2\,\alpha^2\,(1+3\,\alpha)\,\mathrm{F21}^{10}_{0110000}
\end{aligned} \tag{B.53}
$$

$$
\begin{aligned}
\mathcal{F}_{12}^{(22)}(L) = & -8\,(-1+\alpha)^2\,\alpha^2\,(-\mathrm{F22}^{00}_{0000010}+\mathrm{F22}^{00}_{0100000}) \\
& -16\,(-1+\alpha)^4\,\alpha^2\,\mathrm{F22}^{00}_{0100010} \\
& +4\,(-1+\alpha)^2\,\alpha^2\,(-2\,\alpha^2+2\,\alpha^3+\tau+\alpha\,\tau)\,\mathrm{F22}^{00}_{0110000} \\
& +8\,(-1+\alpha)^2\,\alpha^2\,(-1+2\,\alpha)\,(-\mathrm{F22}^{00}_{0000010}+\mathrm{F22}^{00}_{1000000}) \\
& -4\,(-1+\alpha)^3\,\alpha^2\,(2\,\alpha^2-\tau)\,\mathrm{F22}^{00}_{1010000}+4\,(-1+\alpha)^3\,\alpha^2\,\mathrm{F22}^{01}_{1010000} \\
& -4\,(-1+\alpha)^2\,\alpha^2\,(1+3\,\alpha)\,\mathrm{F22}^{10}_{0110000}
\end{aligned} \tag{B.54}
$$

$$
\begin{aligned}
\mathcal{F}_{12}^{(23)}(L) = & -4\,(-1+\alpha)^2\,\alpha^2\,(-\mathrm{F23}^{00}_{0001000}+\mathrm{F23}^{00}_{0100000}) \\
& -4\,(-1+\alpha)^2\,\alpha^2\,(8\,\alpha^2-2\,\tau+\alpha\,(-8+3\,\tau))\,\mathrm{F23}^{00}_{0101000} \\
& -\frac{8}{\tau}\,(-1+\alpha)\,\alpha^3\,(-4+4\,\alpha+\tau)\,(-\mathrm{F23}^{00}_{0001000}+\mathrm{F23}^{00}_{1000000}) \\
& +16\,(-1+\alpha)^3\,\alpha^3\,(\mathrm{F23}^{00}_{1100000}-\mathrm{F23}^{00}_{2000000}) \\
& +\frac{8}{\tau}\,(-1+\alpha)\,\alpha^2\,(\mathrm{F23}^{01}_{0001000}-\mathrm{F23}^{01}_{1000000})
\end{aligned} \tag{B.55}
$$

$$
\begin{aligned}
\mathcal{F}_{12}^{(24)}(L) = & -\frac{1}{\tau}\,4\,(-1+\alpha)\,\alpha^2\,(8\,\alpha^2-\tau+\alpha\,(-8+3\,\tau)) \\
& \quad\times(-\mathrm{F24}^{00}_{0000010}+\mathrm{F24}^{00}_{0001000})+4\,(-1+\alpha)^2\,\alpha^2\,(-\mathrm{F24}^{00}_{0000010}+\mathrm{F24}^{00}_{0100000}) \\
& +8\,(-1+\alpha)^3\,\alpha^2\,(-1+2\,\alpha)\,\mathrm{F24}^{00}_{0100010} \\
& +4\,(-1+\alpha)^2\,\alpha^2\,(8\,\alpha^2-2\,\tau+\alpha\,(-8+3\,\tau))\,\mathrm{F24}^{00}_{0101000} \\
& -\frac{8}{\tau}\,(-1+\alpha)\,\alpha^2\,(2\,\alpha^2\,(-2+\tau)-4\,\alpha\,(-1+\tau)+\tau) \\
& \quad\times(-\mathrm{F24}^{00}_{0000010}+\mathrm{F24}^{00}_{1000000})-32\,(-1+\alpha)^3\,\alpha^3\,(\mathrm{F24}^{00}_{1100000}-\mathrm{F24}^{00}_{2000000}) \\
& -\frac{8}{\tau}\,(-1+\alpha)\,\alpha^2\,(\mathrm{F24}^{01}_{0001000}-\mathrm{F24}^{01}_{1000000})
\end{aligned} \tag{B.56}
$$

$$
\begin{aligned}
\mathcal{F}_{12}^{(25)}(L) = & -8\,(-1+\alpha)^2\,\alpha^2\,(\mathrm{F25}^{00}_{0100000}-\mathrm{F25}^{00}_{1000000}) \\
& -16\,(-1+\alpha)^3\,\alpha^3\,(\mathrm{F25}^{00}_{1100000}-\mathrm{F25}^{00}_{2000000})
\end{aligned} \tag{B.57}
$$

$$\begin{aligned}\mathcal{F}_{12}^{(26)}(L) &= -8\,(-1+\alpha)^3\,\alpha^2\,(-1+2\,\alpha)\,\mathrm{F26}^{00}_{0100010}\\ &\quad - 8\,(-1+\alpha)^2\,\alpha^2\,(-1+2\,\alpha)\,(\mathrm{F26}^{00}_{0000010} - \mathrm{F26}^{00}_{1000000})\\ &\quad + 16\,(-1+\alpha)^3\,\alpha^3\,(\mathrm{F26}^{00}_{1100000} - \mathrm{F26}^{00}_{2000000})\end{aligned} \tag{B.58}$$

$$\begin{aligned}\mathcal{F}_{12}^{(27)}(L) &= -16\,(-1+\alpha)\,\alpha^2\,(1-3\,\alpha+2\,\alpha^2+\tau)\,\mathrm{F27}^{00}_{0100000}\\ &\quad + 16\,(-1+\alpha)^2\,\alpha^2\,(-1+2\,\alpha)\,\mathrm{F27}^{00}_{1000000}\\ &\quad + 32\,(-1+\alpha)\,\alpha^2\,\mathrm{F27}^{10}_{0100000}\end{aligned} \tag{B.59}$$

$$\begin{aligned}\mathcal{F}_{12}^{(28)}(L) &= -4\,\alpha^2\,(-6+23\,\alpha-27\,\alpha^2+10\,\alpha^3)\,\tau\,\mathrm{F28}^{00}_{0010000}\\ &\quad - 4\,(-1+\alpha)\,\alpha^2\,(4\,\alpha^2+3\,\tau+\alpha\,(-4+6\,\tau))\,\mathrm{F28}^{00}_{0100000}\\ &\quad + 4\,(-1+\alpha)\,\alpha^2\,(12\,\alpha^4\,(-1+\tau)-4\,\tau^2+\alpha\,(4+\tau-8\,\tau^2)\\ &\quad + \alpha^3\,(28-32\,\tau-6\,\tau^2)+\alpha^2\,(-20+19\,\tau+17\,\tau^2))\,\mathrm{F28}^{00}_{0110000}\\ &\quad + 4\,(-1+\alpha)^2\,\alpha^2\,(4\,\alpha-\tau)\,\mathrm{F28}^{00}_{1000000} - 4\,(-1+\alpha)^2\,\alpha^2\,(12\,\alpha^3\,(-1+\tau)\\ &\quad + \tau\,(4+3\,\tau)-\alpha\,(4+15\,\tau)+\alpha^2\,(16-3\,\tau+\tau^2))\,\mathrm{F28}^{00}_{1010000}\\ &\quad - 8\,\alpha^3\,(6-11\,\alpha+5\,\alpha^2)\,\mathrm{F28}^{01}_{0010000} - 8\,(-1+\alpha)^2\,\alpha^2\,\mathrm{F28}^{01}_{1000000}\\ &\quad - 8\,(-1+\alpha)^2\,\alpha^2\,(\alpha\,(-16+\tau)+2\,(2+\tau)+\alpha^2\,(11+\tau))\,\mathrm{F28}^{01}_{1010000}\\ &\quad - 16\,(-1+\alpha)^2\,\alpha^3\,\mathrm{F28}^{02}_{1010000} + 8\,(-1+\alpha)^2\,\alpha^2\,(-6+5\,\alpha)\,\mathrm{F28}^{10}_{0010000}\\ &\quad + 24\,(-1+\alpha)\,\alpha^2\,(1+2\,\alpha)\,\mathrm{F28}^{10}_{0100000}\\ &\quad + 8\,(-1+\alpha)\,\alpha^2\,(4\,\tau+6\,\alpha^3\,(1+\tau)+2\,\alpha\,(-1+7\,\tau)\\ &\quad - \alpha^2\,(4+23\,\tau))\,\mathrm{F28}^{10}_{0110000} + 16\,(-1+\alpha)^2\,\alpha^2\,(1+6\,\alpha)\,\mathrm{F28}^{20}_{0110000}\end{aligned} \tag{B.60}$$

Transverse

$$\begin{aligned}\mathcal{F}_{12}^{(1)}(T) &= -8\,\alpha\,(-12\,\alpha^3+6\,\alpha^4+2\,\tau-\alpha\,(3+4\,\tau)+\alpha^2\,(9+5\,\tau))\,\mathrm{F1}^{00}_{0100000}\\ &\quad + 8\,(-1+\alpha)\,\alpha\,(-6\,\alpha^2+6\,\alpha^3-\tau+\alpha\,(3+\tau)\ )\,\mathrm{F1}^{00}_{1000000}\\ &\quad + 8\,(-1+\alpha)^2\,\alpha\,\mathrm{F1}^{01}_{1000000} + 8\,\alpha\,(2-4\,\alpha+5\,\alpha^2)\,\mathrm{F1}^{10}_{0100000}\end{aligned} \tag{B.61}$$

$$\begin{aligned}\mathcal{F}_{12}^{(2)}(T) &= -2\,\alpha\,(15-60\,\alpha+75\,\alpha^2-43\,\alpha^3+10\,\alpha^4)\,\tau\,\mathrm{F2}^{00}_{0010000}\\ &\quad + 2\,\alpha\,(12\,\alpha^4+6\,\tau+18\,\alpha^2\,(1+\tau)-2\,\alpha^3\,(12+\tau)-\alpha\,(6+13\,\tau))\,\mathrm{F2}^{00}_{0100000}\\ &\quad + 2\,\alpha^2\,(4\,\alpha^5\,(-3+\tau)+2\,(1-2\,\tau)\,\tau+\alpha^2\,(28-33\,\tau-33\,\tau^2)\\ &\quad - 2\,\alpha^4\,(-20+18\,\tau+\tau^2)+2\,\alpha^3\,(-25+32\,\tau+7\,\tau^2)\\ &\quad + \alpha\,(-6-\tau+28\,\tau^2))\,\mathrm{F2}^{00}_{0110000} - 2\,(-1+\alpha)\,\alpha\,(12\,\alpha^3-\tau-3\,\alpha^2\,(4+\tau)\\ &\quad + \alpha\,(6+4\,\tau))\,\mathrm{F2}^{00}_{1000000} - 2\,(-1+\alpha)^2\,\alpha\,(4\,\alpha^4\,(-3+\tau)+7\,\tau^2\\ &\quad - \alpha\,\tau\,(1+13\,\tau)+\alpha^3\,(16-11\,\tau-3\,\tau^2)+\alpha^2\,(-6+10\,\tau+\tau^2))\,\mathrm{F2}^{00}_{1010000}\\ &\quad - 4\,(-1+\alpha)^2\,\alpha^2\,(-4+5\,\alpha)\,\mathrm{F2}^{01}_{0010000} + 4\,(-1+\alpha)^2\,\alpha\,(-1+3\,\alpha)\,\mathrm{F2}^{01}_{1000000}\\ &\quad + 4\,(-1+\alpha)^2\,\alpha\,(-4\,\tau+\alpha^2\,(19+2\,\tau)+\alpha^3\,(-11+3\,\tau)\end{aligned}$$

$$+ \alpha\,(-9 + 7\,\tau))\,\mathrm{F2}^{01}_{1010000} + 8\,(-1 + \alpha)^2\,\alpha^2\,(-1 + 3\,\alpha)\,\mathrm{F2}^{02}_{1010000}$$
$$+ 4\,(-1 + \alpha)^3\,\alpha\,(-4 + 5\,\alpha)\,\mathrm{F2}^{10}_{0010000} + 4\,\alpha\,(-3 + 7\,\alpha - 12\,\alpha^2$$
$$+ 2\,\alpha^3)\,\mathrm{F2}^{10}_{0100000} + 4\,\alpha^2\,(-1 + \alpha + 4\,\tau - 28\,\alpha\,\tau + 2\,\alpha^4\,(3 + \tau)$$
$$+ 3\,\alpha^2\,(3 + 11\,\tau) - \alpha^3\,(15 + 14\,\tau))\,\mathrm{F2}^{10}_{0110000}$$
$$+ 8\,\alpha^2\,(-1 + 7\,\alpha - 8\,\alpha^2 + 2\,\alpha^3)\,\mathrm{F2}^{20}_{0110000} \tag{B.62}$$

$$\mathcal{F}^{(3)}_{12}(T) = -4\,\alpha\,(7 - 26\,\alpha + 42\,\alpha^2 - 34\,\alpha^3 + 12\,\alpha^4)\,\tau\,\mathrm{F3}^{00}_{0010000}$$
$$+ 4\,\alpha\,(4\,\alpha^4 + 2\,\tau - \alpha^3\,(8 + 5\,\tau) - \alpha\,(2 + 7\,\tau) + \alpha^2\,(6 + 11\,\tau))\,\mathrm{F3}^{00}_{0100000}$$
$$+ 4\,\alpha^2\,(8\,\alpha^5\,(-1 + \tau) + 6\,(1 - 2\,\tau)\,\tau + \alpha^2\,(18 + 2\,\tau - 51\,\tau^2)$$
$$+ \alpha^4\,(26 - 29\,\tau - 5\,\tau^2) + \alpha^3\,(-32 + 28\,\tau + 27\,\tau^2) + \alpha\,(-4 - 15\,\tau + 40\,\tau^2))$$
$$\times\,\mathrm{F3}^{00}_{0110000} - 4\,(-1 + \alpha)\,\alpha\,(4\,\alpha^3 - \tau + 2\,\alpha\,(1 + \tau) - \alpha^2\,(4 + \tau))\,\mathrm{F3}^{00}_{1000000}$$
$$- 4\,(-1 + \alpha)^2\,\alpha\,(8\,\alpha^4\,(-1 + \tau) + \tau^2 + \alpha\,\tau\,(3 + \tau) - \alpha^3\,(-10 + \tau + \tau^2)$$
$$- \alpha^2\,(4 + 6\,\tau + \tau^2))\,\mathrm{F3}^{00}_{1010000} + 8\,\alpha^2\,(3 - 11\,\alpha + 14\,\alpha^2 - 6\,\alpha^3)\,\mathrm{F3}^{01}_{0010000}$$
$$+ 8\,(-1 + \alpha)^3\,\alpha\,\mathrm{F3}^{01}_{1000000} + 8\,(-1 + \alpha)^2\,\alpha\,(\alpha^3\,(-9 + \tau) - \tau - \alpha\,(4 + \tau)$$
$$+ \alpha^2\,(11 + \tau))\,\mathrm{F3}^{01}_{1010000} + 16\,(-1 + \alpha)^3\,\alpha^2\,\mathrm{F3}^{02}_{1010000}$$
$$+ 8\,(-1 + \alpha)^2\,\alpha\,(3 - 8\,\alpha + 6\,\alpha^2)\,\mathrm{F3}^{10}_{0010000}$$
$$+ 8\,\alpha\,(-1 + 5\,\alpha - 9\,\alpha^2 + 5\,\alpha^3)\,\mathrm{F3}^{10}_{0100000} + 8\,\alpha^2\,(-3 + \alpha\,(9 - 40\,\tau) + 12\,\tau$$
$$+ \alpha^4\,(3 + 5\,\tau) - \alpha^3\,(1 + 27\,\tau) + \alpha^2\,(-8 + 51\,\tau))\,\mathrm{F3}^{10}_{0110000}$$
$$+ 16\,\alpha^2\,(-3 + 10\,\alpha - 12\,\alpha^2 + 5\,\alpha^3)\,\mathrm{F3}^{20}_{0110000} \tag{B.63}$$

$$\mathcal{F}^{(4)}_{12}(T) = 2\,\alpha\,(4 - 21\,\alpha + 42\,\alpha^2 - 36\,\alpha^3 + 12\,\alpha^4)\,\tau\,\mathrm{F4}^{00}_{0010000}$$
$$+ 2\,\alpha^2\,(3 - 8\,\alpha + 6\,\alpha^2)\,\tau\,\mathrm{F4}^{00}_{0100000} - 2\,\alpha^2\,(8\,\alpha^5\,(-2 + \tau) + \alpha\,\tau\,(-31 + 32\,\tau)$$
$$+ \alpha^2\,(26 + 21\,\tau - 47\,\tau^2) + \alpha^4\,(52 - 30\,\tau - 6\,\tau^2) - 2\,(1 - 5\,\tau + 4\,\tau^2)$$
$$+ \alpha^3\,(-60 + 22\,\tau + 28\,\tau^2))\,\mathrm{F4}^{00}_{0110000} + 4\,(-1 + \alpha)^2\,\alpha\,(4\,\alpha^4\,(-2 + \tau)$$
$$+ \alpha\,(-1 + \tau) + \tau + 2\,\alpha^3\,(5 + \tau) - \alpha^2\,(2 + 7\,\tau))\,\mathrm{F4}^{00}_{1010000}$$
$$+ 12\,(-1 + \alpha)^2\,\alpha^2\,(-1 + 2\,\alpha)\,\mathrm{F4}^{01}_{0010000} + 4\,(-1 + \alpha)^2\,\alpha\,(1 + 3\,\alpha$$
$$- 15\,\alpha^2 + 12\,\alpha^3)\,\mathrm{F4}^{01}_{1010000} - 12\,(-1 + \alpha)^3\,\alpha\,(-1 + 2\,\alpha)\,\mathrm{F4}^{10}_{0010000}$$
$$- 4\,\alpha^2\,(3 - 8\,\alpha + 6\,\alpha^2)\,\mathrm{F4}^{10}_{0100000} - 4\,\alpha^2\,(-6 + \alpha\,(19 - 38\,\tau)$$
$$+ 10\,\tau + 6\,\alpha^4\,(1 + \tau) - 3\,\alpha^3\,(1 + 10\,\tau) + \alpha^2\,(-16 + 53\,\tau))\,\mathrm{F4}^{10}_{0110000}$$
$$+ 8\,\alpha^2\,(3 - 11\,\alpha + 14\,\alpha^2 - 6\,\alpha^3)\,\mathrm{F4}^{20}_{0110000} \tag{B.64}$$

$$\mathcal{F}^{(5)}_{12}(T) = 4\,\alpha\,(1 - 6\,\alpha + \alpha^2 + 5\,\alpha^3 - 6\,\alpha^4)\,\tau\,\mathrm{F5}^{00}_{0010000}$$
$$- 4\,\alpha^2\,(2 - 3\,\alpha + 6\,\alpha^2)\,\tau\,\mathrm{F5}^{00}_{0100000} + 4\,\alpha^2\,(4\,(1 - 2\,\tau)\,\tau + 4\,\alpha^5\,(-2 + 3\,\tau)$$
$$+ \alpha^2\,(16 - 9\,\tau - 36\,\tau^2) - 6\,\alpha^4\,(-4 + 6\,\tau + \tau^2) + \alpha\,(-4 - 3\,\tau + 20\,\tau^2)$$
$$+ \alpha^3\,(-28 + 32\,\tau + 25\,\tau^2))\,\mathrm{F5}^{00}_{0110000} - 4\,(-1 + \alpha)^2\,\alpha\,(-1 + 2\,\alpha)\,\tau\,\mathrm{F5}^{00}_{1000000}$$
$$- 4\,(-1 + \alpha)^2\,\alpha\,(-3\,\tau^2 + 4\,\alpha^4\,(-2 + 3\,\tau) + \alpha\,\tau\,(7 + 4\,\tau)$$

$$+ \alpha^2 (-4 - 11\tau + \tau^2) + 2\alpha^3 (4 + \tau + \tau^2)) \mathrm{F5}^{00}_{1010000} - 4\alpha^2 (-2 + 3\alpha$$
$$- 7\alpha^2 + 6\alpha^3) \mathrm{F5}^{01}_{0010000} - 8(-1+\alpha)^2 \alpha (-1 + 2\alpha) \mathrm{F5}^{01}_{1000000}$$
$$- 8(-1+\alpha)^2 \alpha (2\alpha^2 (-3+\tau) - 2\tau + 2\alpha^3 (4+\tau) + \alpha (3 + 2\tau)) \mathrm{F5}^{01}_{1010000}$$
$$- 16(-1+\alpha)^2 \alpha^2 (-1+2\alpha) \mathrm{F5}^{02}_{1010000}$$
$$+ 4(-1+\alpha)^2 \alpha (2 - \alpha + 6\alpha^2\ ) \mathrm{F5}^{10}_{0010000} + 8\alpha^2 (2 - 3\alpha + 6\alpha^2) \mathrm{F5}^{10}_{0100000}$$
$$+ 8\alpha^2 (-2 + \alpha (2 - 20\tau) + 8\tau + 6\alpha^4 (1+\tau) - \alpha^3 (7 + 26\tau)$$
$$+ \alpha^2 (1 + 37\tau)) \mathrm{F5}^{10}_{0110000} + 16\alpha^2 (-2 + 5\alpha - 9\alpha^2 + 6\alpha^3) \mathrm{F5}^{20}_{0110000} \tag{B.65}$$

$$\mathcal{F}^{(6)}_{12}(T) = -4(-1+\alpha)\alpha^2 (-1 + 8\alpha^4 + 5\tau - 17\alpha\tau$$
$$- \alpha^3 (13 + 6\tau) + \alpha^2 (6 + 20\tau)) \mathrm{F6}^{00}_{0110000}$$
$$+ 12\alpha (-1 + 3\alpha - 4\alpha^2 + 2\alpha^3) (\mathrm{F6}^{00}_{0100000} - \mathrm{F6}^{00}_{1000000})$$
$$+ 4(-1+\alpha)^2 \alpha (\alpha + 8\alpha^4 - 2\tau - \alpha\tau - \alpha^3 (5 + 6\tau) + \alpha^2 (1 + 8\tau)) \mathrm{F6}^{00}_{1010000}$$
$$+ 12\alpha (-1 + 3\alpha - 4\alpha^2 + 2\alpha^3) (-2\alpha + 2\alpha^2 + \tau\ ) \mathrm{F6}^{00}_{1100000}$$
$$+ 4(-1+\alpha)^2 \alpha^2 (\alpha^3 (24 - 26\tau) + 12\alpha^4 (-1+\tau) + 3(-1+\tau)\tau$$
$$+ \alpha (6 + 3\tau - 8\tau^2) + \alpha^2 (-18 + 11\tau + 6\tau^2)) \mathrm{F6}^{00}_{1110000}$$
$$- 24(-1+\alpha)^2 \alpha^2 (1 - 2\alpha + 2\alpha^2) \mathrm{F6}^{00}_{2000000} - 8(-1+\alpha)^3 \alpha (-3\alpha^3 (-2+\tau)$$
$$+ 6\alpha^4 (-1+\tau) - 2\tau^2 + \alpha\tau (5 + 2\tau) - \alpha^2 (3 + 5\tau)) \mathrm{F6}^{00}_{2010000}$$
$$- 8(-1+\alpha)^2 \alpha (2 - 4\alpha + 3\alpha^2\ ) \mathrm{F6}^{01}_{1010000}$$
$$- 8(-1+\alpha)^3 \alpha (-11\alpha^2 + 8\alpha^3 - 4\tau + \alpha (6 + 4\tau)) \mathrm{F6}^{01}_{2010000}$$
$$- 16(-1+\alpha)^4 \alpha \mathrm{F6}^{02}_{2010000} + 8\alpha^2 (-1 + 4\alpha - 6\alpha^2 + 3\alpha^3) \mathrm{F6}^{10}_{0110000} \tag{B.66}$$

$$\mathcal{F}^{(7)}_{12}(T) = 16\alpha^2 (-1 - 4\alpha^2 + 2\alpha^3 + \alpha (3+\tau)) \mathrm{F7}^{00}_{0100000}$$
$$- 16(-1+\alpha)\alpha (\alpha - 2\alpha^2 + 2\alpha^3 - \tau + \alpha\tau) \mathrm{F7}^{00}_{1000000}$$
$$- 16(-1+\alpha)^2 \alpha \mathrm{F7}^{01}_{1000000} - 16\alpha^3 \mathrm{F7}^{10}_{0100000} \tag{B.67}$$

$$\mathcal{F}^{(8)}_{12}(T) = -4\alpha (2 - 12\alpha + 27\alpha^2 - 24\alpha^3 + 8\alpha^4) \tau \mathrm{F8}^{00}_{0010000}$$
$$- 4\alpha^2 (2 - 5\alpha + 4\alpha^2) \tau \mathrm{F8}^{00}_{0100000} + 4\alpha^2 (4\alpha^5 (-2+\tau) - 4(-1+\tau)\tau$$
$$+ \alpha^2 (18 + 9\tau - 26\tau^2) - 2\alpha^4 (-13 + 7\tau + 2\tau^2) + 4\alpha (-1 - 3\tau + 4\tau^2)$$
$$+ \alpha^3 (-32 + 9\tau + 17\tau^2)) \mathrm{F8}^{00}_{0110000} - 8(-1+\alpha)^2 \alpha^2 (2\alpha^3 (-2+\tau) + 2\tau$$
$$- 2\alpha (1 + 3\tau) + \alpha^2 (5 + 3\tau)) \mathrm{F8}^{00}_{1010000}$$
$$- 16(-1+\alpha)^2 \alpha^2 (-1 + 2\alpha) \mathrm{F8}^{01}_{0010000}$$
$$- 8(-1+\alpha)^2 \alpha^2 (3 - 10\alpha + 8\alpha^2) \mathrm{F8}^{01}_{1010000}$$
$$+ 16(-1+\alpha)^3 \alpha (-1 + 2\alpha) \mathrm{F8}^{10}_{0010000} + 8\alpha^2 (2 - 5\alpha + 4\alpha^2) \mathrm{F8}^{10}_{0100000}$$
$$+ 8\alpha^2 (-3 + \alpha (9 - 22\tau) + 6\tau + 4\alpha^4 (1+\tau) - \alpha^3 (3 + 19\tau)$$

$$+\,\alpha^2\,(-7+32\,\tau))\,\mathrm{F8}^{10}_{0110000}+16\,\alpha^2\,(-2+7\,\alpha-9\,\alpha^2+4\,\alpha^3)\,\mathrm{F8}^{20}_{0110000} \tag{B.68}$$

$$\begin{aligned}\mathcal{F}^{(9)}_{12}(T) &= -8\,\alpha\,(-9\,\alpha^3+4\,\alpha^4+\tau-\alpha\,(2+3\,\tau)+\alpha^2\,(7+3\,\tau))\,\mathrm{F9}^{00}_{0100000}\\ &+8\,(-1+\alpha)\,\alpha\,(-5\,\alpha^2+4\,\alpha^3-\tau+\alpha\,(2+\tau)\,)\,\mathrm{F9}^{00}_{1000000}\\ &+8\,(-1+\alpha)^2\,\alpha\,\mathrm{F9}^{01}_{1000000}+8\,\alpha\,(1-3\,\alpha+3\,\alpha^2)\,\mathrm{F9}^{10}_{0100000}\end{aligned} \tag{B.69}$$

$$\begin{aligned}\mathcal{F}^{(10)}_{12}(T) &= 8\,\alpha\,(1-3\,\alpha+4\,\alpha^2-2\,\alpha^3)\,(\mathrm{F10}^{00}_{0100000}-\mathrm{F10}^{00}_{1000000})\\ &-8\,\alpha\,(-1+3\,\alpha-4\,\alpha^2+2\,\alpha^3)\,(-2\,\alpha+2\,\alpha^2+\tau\,)\,\mathrm{F10}^{00}_{1100000}\\ &+16\,(-1+\alpha)^2\,\alpha^2\,(1-2\,\alpha+2\,\alpha^2)\,\mathrm{F10}^{00}_{2000000}\end{aligned} \tag{B.70}$$

$$\begin{aligned}\mathcal{F}^{(11)}_{12}(T) &= -4\,(1-3\,\alpha-6\,\alpha^2+16\,\alpha^3-10\,\alpha^4+4\,\alpha^5)\,\tau\,\mathrm{F11}^{00}_{0010000}\\ &-4\,\alpha^2\,(2-7\,\alpha+7\,\alpha^2)\,\tau\,\mathrm{F11}^{00}_{0100000}\;+4\,\alpha^2\,(2+20\,\alpha^5\,(-1+\tau)-8\,\tau^2\\ &+\alpha^2\,(58-59\,\tau-66\,\tau^2)+\alpha^4\,(68-85\,\tau-7\,\tau^2)+2\,\alpha\,(-9+5\,\tau+21\,\tau^2)\\ &+\alpha^3\,(-90+114\,\tau+37\,\tau^2))\,\mathrm{F11}^{00}_{0110000}\\ &-4\,(-1+\alpha)^2\,(1-5\,\alpha+5\,\alpha^2)\,\tau\,\mathrm{F11}^{00}_{1000000}\\ &-4\,(-1+\alpha)^2\,(20\,\alpha^5\,(-1+\tau)+\tau^2-3\,\alpha\,\tau\,(1+\tau)+\alpha^2\,(2+22\,\tau-8\,\tau^2)\\ &+\alpha^3\,(-14-18\,\tau+3\,\tau^2)+\alpha^4\,(28-17\,\tau+5\,\tau^2))\,\mathrm{F11}^{00}_{1010000}\\ &+8\,(-1+\alpha)^2\,\alpha^3\,(-1+\tau)\,\tau\,(-1-\alpha+2\,\alpha^2+\tau\,)\,\mathrm{F11}^{00}_{1110000}\\ &+8\,(-1+\alpha)^2\,\alpha\,(1-2\,\alpha+2\,\alpha^2)\,\tau\,\mathrm{F11}^{00}_{2000000}\\ &-16\,(-1+\alpha)^3\,\alpha^2\,(-1+2\,\alpha)\,\tau\,(\alpha\,(-1+\tau)+\tau)\,\mathrm{F11}^{00}_{2010000}\\ &+8\,\alpha^2\,(1-3\,\alpha+4\,\alpha^2-2\,\alpha^3)\,\mathrm{F11}^{01}_{0010000}\\ &-8\,(2-10\,\alpha+20\,\alpha^2-17\,\alpha^3+5\,\alpha^4)\,\mathrm{F11}^{01}_{1000000}\\ &-8\,(-1+\alpha)^2\,(\alpha^2\,(15-6\,\tau)+\tau+5\,\alpha^4\,(3+\tau)-\alpha\,(2+3\,\tau)\\ &+\alpha^3\,(-27+5\,\tau))\,\mathrm{F11}^{01}_{1010000}+16\,(-1+\alpha)^2\,\alpha\,(1-2\,\alpha+2\,\alpha^2\,)\,\mathrm{F11}^{01}_{2000000}\\ &-16\,(-1+\alpha)^3\,\alpha^2\,(-1+2\,\alpha)\,(\alpha\,(-1+\tau)+3\,\tau)\,\mathrm{F11}^{01}_{2010000}\\ &-16\,(-1+\alpha)^2\,\alpha\,(1-5\,\alpha+5\,\alpha^2)\,\mathrm{F11}^{02}_{1010000}\\ &-32\,(-1+\alpha)^3\,\alpha^2\,(-1+2\,\alpha)\,\mathrm{F11}^{02}_{2010000}\\ &+8\,(-1+\alpha)^2\,\alpha\,(1-2\,\alpha+2\,\alpha^2\,)\,\mathrm{F11}^{10}_{0010000}\\ &+8\,\alpha^2\,(2-7\,\alpha+7\,\alpha^2)\,\mathrm{F11}^{10}_{0100000}+8\,\alpha^2\,(8\,\tau+\alpha^4\,(13+7\,\tau)-\alpha^3\,(27+35\,\tau)\\ &-\alpha\,(5+38\,\tau)+\alpha^2\,(19+60\,\tau))\,\mathrm{F11}^{10}_{0110000}\\ &+16\,\alpha^2\,(-2+9\,\alpha-14\,\alpha^2+7\,\alpha^3)\,\mathrm{F11}^{20}_{0110000}\end{aligned} \tag{B.71}$$

$$\begin{aligned}\mathcal{F}^{(12)}_{12}(T) &= -8\,\alpha\,(1-2\,\alpha+2\,\alpha^2)\,(-1+\alpha^2+2\,\tau)\,\mathrm{F12}^{00}_{0100000}\\ &+8\,(-1+3\,\alpha-4\,\alpha^2+2\,\alpha^3)\,(\alpha+\alpha^2-\tau)\,\mathrm{F12}^{00}_{1000000}\\ &+8\,(1-3\,\alpha+4\,\alpha^2-2\,\alpha^3)\,\mathrm{F12}^{01}_{1000000}+16\,\alpha\,(1-2\,\alpha+2\,\alpha^2)\,\mathrm{F12}^{10}_{0100000}\end{aligned} \tag{B.72}$$

$$\mathcal{F}_{12}^{(13)}(T) = 2\,(2-25\,\alpha+58\,\alpha^2-63\,\alpha^3+43\,\alpha^4-10\,\alpha^5)\,\tau\,\mathrm{F13}^{00}_{0010000}$$
$$+\,2\,\alpha\,(-4\,\alpha^4-2\,\tau+8\,\alpha^3\,(1+\tau)-2\,\alpha^2\,(3+4\,\tau)+\alpha\,(2+5\,\tau))\,\mathrm{F13}^{00}_{0100000}$$
$$-\,2\,\alpha^2\,(2\,\tau\,(2+\tau)+4\,\alpha^5\,(-7+4\,\tau)+\alpha^2\,(54-3\,\tau-35\,\tau^2)$$
$$-\,2\,\alpha^4\,(-41+30\,\tau+2\,\tau^2)+2\,\alpha^3\,(-47+26\,\tau+10\,\tau^2)$$
$$+\,\alpha\,(-14-9\,\tau+12\,\tau^2))\,\mathrm{F13}^{00}_{0110000}+2\,(-1+\alpha)\,(4\,\alpha^4$$
$$+\,\alpha^2\,(2-24\,\tau)-2\,\tau+13\,\alpha\,\tau+\alpha^3\,(-4+13\,\tau))\,\mathrm{F13}^{00}_{1000000}$$
$$+\,2\,(-1+\alpha)^2\,(\alpha^2\,(31-5\,\tau)\,\tau+2\,\tau^2+4\,\alpha^5\,(-7+4\,\tau)-\alpha\,\tau\,(2+13\,\tau)$$
$$-\,\alpha^3\,(14+38\,\tau+3\,\tau^2)+\alpha^4\,(26-9\,\tau+17\,\tau^2))\,\mathrm{F13}^{00}_{1010000}$$
$$-\,4\,(-1+\alpha)^2\,\alpha^2\,(\alpha\,(2+6\,\tau-8\,\tau^2)+\tau\,(-2+\tau+\tau^2\,)$$
$$+\,4\,\alpha^4\,(-1+\tau+\tau^2)-2\,\alpha^3\,(-4+3\,\tau+2\,\tau^2)$$
$$+\,\alpha^2\,(-6-3\,\tau+7\,\tau^2+2\,\tau^3))\,\mathrm{F13}^{00}_{1110000}+8\,(-1+\alpha)^3\,\alpha\,(-\tau^2+\alpha\,\tau\,(2+\tau)$$
$$+\,\alpha^2\,(-1-3\,\tau+\tau^2)+2\,\alpha^4\,(-1+\tau+\tau^2)+\alpha^3\,(2-\tau+5\,\tau^2))\,\mathrm{F13}^{00}_{2010000}$$
$$-\,4\,(-1+\alpha)^2\,\alpha^2\,(-4+5\,\alpha)\,\mathrm{F13}^{01}_{0010000}$$
$$+\,4\,(-1+\alpha)^2\,(2-11\,\alpha+13\,\alpha^2)\,\mathrm{F13}^{01}_{1000000}+4\,(-1+\alpha)^2\,(\alpha^2\,(11-13\,\tau)$$
$$+\,2\,\tau-2\,\alpha\,(1+4\,\tau)+\alpha^4\,(7+13\,\tau)+\alpha^3\,(-17+16\,\tau))\,\mathrm{F13}^{01}_{1010000}$$
$$+\,8\,(-1+\alpha)^3\,\alpha\,(\alpha-\tau-2\,\alpha\,\tau+10\,\alpha^3\,\tau+\alpha^2\,(-1+9\,\tau))\,\mathrm{F13}^{01}_{2010000}$$
$$+\,8\,(-1+\alpha)^2\,\alpha\,(2-11\,\alpha+13\,\alpha^2)\,\mathrm{F13}^{02}_{1010000}$$
$$+\,32\,(-1+\alpha)^3\,\alpha^2\,(-1+3\,\alpha)\,\mathrm{F13}^{02}_{2010000}$$
$$+\,4\,(-1+\alpha)^3\,\alpha\,(-4+5\,\alpha)\,\mathrm{F13}^{10}_{0010000}$$
$$+\,4\,\alpha\,(1-3\,\alpha+6\,\alpha^2-8\,\alpha^3)\,\mathrm{F13}^{10}_{0100000}-4\,\alpha^2\,(-1+2\,\tau+4\,\alpha^4\,(3+2\,\tau)$$
$$+\,9\,\alpha^2\,(1+5\,\tau)-3\,\alpha\,(1+6\,\tau)-\alpha^3\,(17+32\,\tau))\,\mathrm{F13}^{10}_{0110000}$$
$$+\,8\,\alpha^2\,(1-5\,\alpha+12\,\alpha^2-8\,\alpha^3)\,\mathrm{F13}^{20}_{0110000} \tag{B.73}$$

$$\mathcal{F}_{12}^{(14)}(T) = -4\,(-1+\alpha+2\,\alpha^2+5\,\alpha^3-12\,\alpha^4+4\,\alpha^5\,)\,\tau\,\mathrm{F14}^{00}_{0010000}$$
$$-\,4\,\alpha\,(-1+\alpha+4\,\alpha^4+2\,\tau-6\,\alpha\,\tau+2\,\alpha^2\,(1+5\,\tau)-\alpha^3\,(6+5\,\tau))\,\mathrm{F14}^{00}_{0100000}$$
$$-\,4\,\alpha^2\,(2\,\alpha^5\,(-9+5\,\tau)+\alpha^2\,(58-48\,\tau-40\,\tau^2)+2\,(1+\tau-4\,\tau^2)$$
$$+\,\alpha^4\,(62-53\,\tau-3\,\tau^2)+\alpha^3\,(-85+82\,\tau+18\,\tau^2)$$
$$+\,\alpha\,(-19+7\,\tau+32\,\tau^2))\,\mathrm{F14}^{00}_{0110000}$$
$$+\,4\,(-1+\alpha)\,(\alpha+4\,\alpha^4-3\,\tau+12\,\alpha\,\tau-16\,\alpha^2\,\tau+\alpha^3\,(-2+7\,\tau))\,\mathrm{F14}^{00}_{1000000}$$
$$+\,4\,(-1+\alpha)^2\,(3\,\alpha\,(-3+\tau)\,\tau+\tau^2+2\,\alpha^5\,(-9+5\,\tau)+\alpha^2\,(2+26\,\tau-10\,\tau^2)$$
$$-\,\alpha^3\,(15+11\,\tau+5\,\tau^2)+\alpha^4\,(26-17\,\tau+9\,\tau^2))\,\mathrm{F14}^{00}_{1010000}$$
$$-\,4\,\alpha\,(-1+3\,\alpha-4\,\alpha^2+2\,\alpha^3)\,(-2\,\alpha+2\,\alpha^2+\tau\,)\,\mathrm{F14}^{00}_{1100000}$$
$$-\,4\,(-1+\alpha)^2\,\alpha^2\,(2\,(-1+\tau)\,\tau+\alpha\,(2+3\,\tau-5\,\tau^2)+4\,\alpha^4\,(-1+\tau^2)$$
$$-\,4\,\alpha^3\,(-2+\tau+\tau^2)+2\,\alpha^2\,(-3+\tau+\tau^2+\tau^3))\,\mathrm{F14}^{00}_{1110000}$$
$$+\,8\,(-1+\alpha)^2\,\alpha^2\,(1-2\,\alpha+2\,\alpha^2)\,\mathrm{F14}^{00}_{2000000}$$
$$+\,8\,(-1+\alpha)^3\,\alpha\,(2\,\tau^2-\alpha\,\tau\,(1+4\,\tau)+2\,\alpha^4\,(-1+\tau^2)$$

$$
\begin{aligned}
&- \alpha^2 (1 - 5\tau + \tau^2) + \alpha^3 (2 - 5\tau + 7\tau^2))\, \mathrm{F14}^{00}_{2010000} \\
&- 8(-1+\alpha)^2 \alpha^2 (-1 + 2\alpha)\, \mathrm{F14}^{01}_{0010000} \\
&+ 8(-1+\alpha)^2 (3 - 9\alpha + 7\alpha^2)\, \mathrm{F14}^{01}_{1000000} \\
&+ 8(-1+\alpha)^2 (\alpha^2 (20 - 18\tau) + 5\alpha(-1+\tau) + \tau + 7\alpha^4 (1+\tau) \\
&+ \alpha^3 (-23 + 7\tau))\, \mathrm{F14}^{01}_{1010000} + 8(-1+\alpha)^3 \alpha (7\tau \\
&+ 2\alpha^2 (3 + 5\tau) + 2\alpha^3 (-3 + 7\tau) - \alpha(1 + 19\tau))\, \mathrm{F14}^{01}_{2010000} \\
&+ 16(-1+\alpha)^2 \alpha (3 - 9\alpha + 7\alpha^2\ )\, \mathrm{F14}^{02}_{1010000} \\
&+ 16(-1+\alpha)^3 \alpha (3 - 10\alpha + 10\alpha^2)\, \mathrm{F14}^{02}_{2010000} \\
&+ 8(-1+\alpha)^3 \alpha (-1 + 2\alpha)\, \mathrm{F14}^{10}_{0010000} \\
&+ 8\alpha (1 - 4\alpha + 8\alpha^2 - 5\alpha^3)\, \mathrm{F14}^{10}_{0100000} - 8\alpha^2 (8\tau + \alpha^4 (9 + 5\tau) \\
&- 4\alpha^3 (5 + 6\tau) + 4\alpha^2 (4 + 11\tau) - \alpha(5 + 32\tau))\, \mathrm{F14}^{10}_{0110000} \\
&- 16\alpha^2 (-2 + 8\alpha - 11\alpha^2 + 5\alpha^3)\, \mathrm{F14}^{20}_{0110000}
\end{aligned} \tag{B.74}
$$

$$
\begin{aligned}
\mathcal{F}^{(15)}_{12}(T) &= 4\alpha^2 (-4 - 15\alpha^2 + 8\alpha^3 + \alpha(11 + 4\tau))\, \mathrm{F15}^{00}_{0100000} \\
&- 4(-1+\alpha)\alpha(-7\alpha^2 + 8\alpha^3 - 4\tau + 4\alpha(1+\tau))\, \mathrm{F15}^{00}_{1000000} \\
&+ 4(-1+\alpha)\alpha^2 (-2 - 8\alpha^2 + 4\alpha^3 + \alpha(6+\tau))\, \mathrm{F15}^{00}_{1100000} \\
&- 8(-1+\alpha)^2 \alpha (\alpha - 2\alpha^2 + 2\alpha^3 - \tau + \alpha\tau)\, \mathrm{F15}^{00}_{2000000} \\
&- 16(-1+\alpha)^2 \alpha\, \mathrm{F15}^{01}_{1000000} - 8(-1+\alpha)^3 \alpha\, \mathrm{F15}^{01}_{2000000} - 16\alpha^3\, \mathrm{F15}^{10}_{0100000}
\end{aligned} \tag{B.75}
$$

$$
\begin{aligned}
\mathcal{F}^{(16)}_{12}(T) &= -12(-1+\alpha)\alpha^2 (-3 + 16\alpha^4 + \alpha(2 - 27\tau) + 9\tau - 3\alpha^3 (9 + 2\tau) \\
&+ 6\alpha^2 (2 + 5\tau))\, \mathrm{F16}^{00}_{0110000} \\
&+ 36\alpha(-1 + 3\alpha - 4\alpha^2 + 2\alpha^3)(\mathrm{F16}^{00}_{0100000} - \mathrm{F16}^{00}_{1000000}) \\
&+ 12(-1+\alpha)^2 \alpha (16\alpha^4 - 4\tau + \alpha(3+\tau) + \alpha^2 (1 + 6\tau) \\
&- \alpha^3 (11 + 6\tau))\, \mathrm{F16}^{00}_{1010000} + 36\alpha(-1 + 3\alpha - 4\alpha^2 + 2\alpha^3)(-2\alpha + 2\alpha^2 + \tau) \\
&\quad \times \mathrm{F16}^{00}_{1100000} + 12(-1+\alpha)^2 \alpha^2 (\alpha^3 (24 - 26\tau) + 12\alpha^4 (-1+\tau) \\
&+ 3(-1+\tau)\tau + \alpha(6 + 3\tau - 8\tau^2) + \alpha^2 (-18 + 11\tau + 6\tau^2))\, \mathrm{F16}^{00}_{1110000} \\
&- 72(-1+\alpha)^2 \alpha^2 (1 - 2\alpha + 2\alpha^2)\, \mathrm{F16}^{00}_{2000000} - 24(-1+\alpha)^3 \alpha (-3\alpha^3 \\
&\quad \times (-2+\tau) + 6\alpha^4 (-1+\tau) - 2\tau^2 + \alpha\tau(5 + 2\tau) - \alpha^2 (3 + 5\tau))\, \mathrm{F16}^{00}_{2010000} \\
&- 24(-1+\alpha)^2 \alpha (3 - 5\alpha + 4\alpha^2\ )\, \mathrm{F16}^{01}_{1010000} \\
&- 24(-1+\alpha)^3 \alpha (-11\alpha^2 + 8\alpha^3 - 4\tau + \alpha(6 + 4\tau))\, \mathrm{F16}^{01}_{2010000} \\
&- 48(-1+\alpha)^4 \alpha\, \mathrm{F16}^{02}_{2010000} + 24\alpha^2 (-3 + 11\alpha - 16\alpha^2 + 8\alpha^3)\, \mathrm{F16}^{10}_{0110000}
\end{aligned} \tag{B.76}
$$

$$
\begin{aligned}
\mathcal{F}^{(17)}_{12}(T) &= 4\alpha(3 - 3\alpha - 2\alpha^2 + 2\alpha^3)\tau\, \mathrm{F17}^{00}_{0010000} \\
&- 4(-1+\alpha)\alpha^3 \tau\, \mathrm{F17}^{00}_{0100000} + 4(-1+\alpha)\alpha^2 (\alpha + 2\alpha^4 (-1+\tau) + 11\alpha\tau
\end{aligned}
$$

$$
\begin{aligned}
&- \tau\,(2 + 3\,\tau) - \alpha^3\,(-5 + \tau^2) + \alpha^2\,(-4 - 11\,\tau + 3\,\tau^2))\,\mathrm{F17}^{00}_{0110000}\\
&- 4\,(-1 + \alpha)^3\,\alpha\,\tau\,\mathrm{F17}^{00}_{1000000} - 4\,(-1 + \alpha)^2\,\alpha\,(2\,\alpha^4\,(-1 + \tau) - 3\,\tau^2\\
&+ \alpha\,\tau\,(7 + 2\,\tau) + \alpha^3\,(3 + 4\,\tau + \tau^2) - \alpha^2\,(1 + 13\,\tau + 2\,\tau^2))\,\mathrm{F17}^{00}_{1010000}\\
&+ 4\,(-1 + \alpha)^3\,\alpha^2\,\tau\,(\alpha + 4\,\alpha^3 + 3\,\alpha\,\tau - \tau^2 - 2\,\alpha^2\,(3 + \tau))\,\mathrm{F17}^{00}_{1110000}\\
&- 8\,(-1 + \alpha)^3\,\alpha^2\,\tau\,(2\,\alpha^3 - 2\,\tau - 2\,\alpha^2\,(2 + \tau) + \alpha\,(2 + 5\,\tau))\,\mathrm{F17}^{00}_{2010000}\\
&+ 8\,(-1 + \alpha)\,\alpha^3\,\mathrm{F17}^{01}_{0010000} - 8\,(-1 + \alpha)^3\,\alpha\,\mathrm{F17}^{01}_{1000000}\\
&- 8\,(-1 + \alpha)^2\,\alpha\,(-2\,\tau + \alpha\,(1 + \tau) + \alpha^3\,(1 + \tau) - \alpha^2\,(4 + \tau))\,\mathrm{F17}^{01}_{1010000}\\
&+ 8\,(-1 + \alpha)^3\,\alpha^2\,(-1 + 2\,\alpha)\,(\alpha - 4\,\tau + \alpha\,\tau)\,\mathrm{F17}^{01}_{2010000}\\
&- 16\,(-1 + \alpha)^3\,\alpha^2\,\mathrm{F17}^{02}_{1010000} - 16\,(-1 + \alpha)^3\,\alpha^2\,(-1 + 2\,\alpha)\,\mathrm{F17}^{02}_{2010000}\\
&- 8\,(-1 + \alpha)^2\,\alpha^2\,\mathrm{F17}^{10}_{0010000} + 8\,(-1 + \alpha)\,\alpha^3\,\mathrm{F17}^{10}_{0100000}\\
&+ 8\,(-1 + \alpha)\,\alpha^2\,(1 + \alpha^2\,(1 - 4\,\tau) + 3\,\alpha\,(-1 + \tau) + \tau + \alpha^3\,(1 + \tau))\,\mathrm{F17}^{10}_{0110000}\\
&+ 16\,(-1 + \alpha)^2\,\alpha^3\,\mathrm{F17}^{20}_{0110000}
\end{aligned}
\tag{B.77}
$$

$$
\begin{aligned}
\mathcal{F}^{(18)}_{12}(T) &= 4\,\alpha\,(6 - 9\,\alpha + \alpha^2 + 2\,\alpha^3)\,\tau\,\mathrm{F18}^{00}_{0010000}\\
&- 4\,\alpha^2\,(1 - 3\,\alpha + 2\,\alpha^2)\,\tau\,\mathrm{F18}^{00}_{0100000}\\
&+ 4\,(-1 + \alpha)\,\alpha^2\,(4\,\alpha^4\,(-1 + 2\,\tau) + \tau\,(-3 + 7\,\tau) + \alpha\,(2 + 8\,\tau - 22\,\tau^2)\\
&+ \alpha^3\,(10 - 19\,\tau - 4\,\tau^2) + 2\,\alpha^2\,(-4 + 3\,\tau + 9\,\tau^2))\,\mathrm{F18}^{00}_{0110000}\\
&- 8\,(-1 + \alpha)^3\,\alpha\,\tau\,\mathrm{F18}^{00}_{1000000} - 4\,(-1 + \alpha)^2\,\alpha\,(\alpha^3\,(6 - 7\,\tau) - 13\,\tau^2\\
&+ 4\,\alpha^4\,(-1 + 2\,\tau) + 3\,\alpha\,\tau\,(5 + 2\,\tau) + \alpha^2\,(-2 - 16\,\tau + \tau^2))\,\mathrm{F18}^{00}_{1010000}\\
&- 4\,(-1 + \alpha)^3\,\alpha^2\,\tau\,(\alpha^2\,(8 - 6\,\tau) + 4\,\alpha^3\,(-1 + \tau) - (-1 + \tau)\,\tau\\
&+ \alpha\,(-2 - \tau + 2\,\tau^2\ ))\,\mathrm{F18}^{00}_{1110000} - 4\,(-1 + \alpha)^3\,\alpha\,\tau^2\,\mathrm{F18}^{00}_{2000000}\\
&+ 4\,(-1 + \alpha)^3\,\alpha\,\tau\,(-6\,\alpha^3\,(-2 + \tau) + 4\,\alpha^4\,(-1 + \tau) + 15\,\alpha\,\tau - 7\,\tau^2\\
&- \alpha^2\,(8 + 11\,\tau + \tau^2))\,\mathrm{F18}^{00}_{2010000}\\
&+ 16\,(-1 + \alpha)\,\alpha^3\,\mathrm{F18}^{01}_{0010000} - 16\,(-1 + \alpha)^3\,\alpha\,\mathrm{F18}^{01}_{1000000}\\
&- 8\,(-1 + \alpha)^2\,\alpha\,(-9\,\alpha^2 - 8\,\tau + 3\,\alpha\,(1 + \tau) + 2\,\alpha^3\,(1 + \tau))\,\mathrm{F18}^{01}_{1010000}\\
&- 16\,(-1 + \alpha)^3\,\alpha\,\tau\,\mathrm{F18}^{01}_{2000000} + 8\,(-1 + \alpha)^3\,\alpha\,(4\,\alpha^3 - \alpha\,(-12 + \tau)\,\tau - 9\,\tau^2\\
&- \alpha^2\,(2 + 13\,\tau + 2\,\tau^2)\ )\,\mathrm{F18}^{01}_{2010000}\\
&- 32\,(-1 + \alpha)^3\,\alpha^2\,\mathrm{F18}^{02}_{1010000} - 16\,(-1 + \alpha)^3\,\alpha\,\mathrm{F18}^{02}_{2000000}\\
&- 16\,(-1 + \alpha)^3\,\alpha\,(2\,\alpha\,(-1 + \tau) + 3\,\tau + \alpha^2\,(3 + \tau))\,\mathrm{F18}^{02}_{2010000}\\
&- 32\,(-1 + \alpha)^3\,\alpha^2\,\mathrm{F18}^{03}_{2010000} - 16\,(-1 + \alpha)^2\,\alpha^2\,\mathrm{F18}^{10}_{0010000}\\
&+ 8\,\alpha^2\,(1 - 3\,\alpha + 2\,\alpha^2)\,\mathrm{F18}^{10}_{0100000} + 8\,(-1 + \alpha)\,\alpha^2\,(1 - 5\,\tau - 11\,\alpha^2\,\tau\\
&+ 2\,\alpha^3\,(1 + \tau) + 3\,\alpha\,(-1 + 5\,\tau))\,\mathrm{F18}^{10}_{0110000}\\
&+ 16\,(-1 + \alpha)^2\,\alpha^2\,(-1 + 2\,\alpha)\,\mathrm{F18}^{20}_{0110000}
\end{aligned}
\tag{B.78}
$$

$$
\mathcal{F}^{(19)}_{12}(T) = -4\,(-1 + \alpha)^2\,\alpha\,(1 - 3\,\alpha + 2\,\alpha^2 + 3\,\tau)\,\mathrm{F19}^{00}_{0100000}
$$

$$
\begin{aligned}
&+ 4\,(-1+\alpha)^2\,(\alpha - 3\,\alpha^2 + 2\,\alpha^3 - 2\,\tau + \alpha\,\tau)\,\mathrm{F19}^{00}_{1000000} \\
&- 4\,(-1+\alpha)^2\,\alpha\,\tau\,(-1 - \alpha + 2\,\alpha^2 + \tau\ )\,\mathrm{F19}^{00}_{1100000} \\
&+ 8\,(-1+\alpha)^3\,\alpha\,(-1+2\,\alpha)\,\tau\,\mathrm{F19}^{00}_{2000000} + 8\,(-1+\alpha)^3\,\mathrm{F19}^{01}_{1000000} \\
&+ 8\,(-1+\alpha)^3\,\alpha\,(-1+2\,\alpha)\,\mathrm{F19}^{01}_{2000000} + 8\,(-1+\alpha)^2\,\alpha\,\mathrm{F19}^{10}_{0100000}
\end{aligned} \tag{B.79}
$$

$$
\begin{aligned}
\mathcal{F}^{(20)}_{12}(T) = &-4\,(-1+\alpha)^2\,\alpha^2\,(-1+2\,\alpha)\,\mathrm{F20}^{00}_{0100000} \\
&+ 4\,(-1+\alpha)^2\,\alpha\,(-\alpha + 2\,\alpha^2 + 4\,\tau\ )\,\mathrm{F20}^{00}_{1000000} \\
&- 4\,(-1+\alpha)^2\,\alpha^2\,(-1+2\,\alpha)\,\tau\,\mathrm{F20}^{00}_{1100000} \\
&+ 16\,(-1+\alpha)^2\,\alpha\,\tau\,(-\alpha + \alpha^2 + \tau)\mathrm{F20}^{00}_{2000000} + 8\,\alpha\,(1 - 3\,\alpha + 2\,\alpha^2)\,\mathrm{F20}^{01}_{1000000} \\
&+ 8\,(-1+\alpha)^2\,\alpha\,(-\alpha + 2\,\alpha^2 + 4\,\tau)\,\mathrm{F20}^{01}_{2000000} + 16\,(-1+\alpha)^2\,\alpha\,\mathrm{F20}^{02}_{2000000}
\end{aligned} \tag{B.80}
$$

$$
\begin{aligned}
\mathcal{F}^{(21)}_{12}(T) = &-4\,(-1+\alpha)\,\alpha^3\,(-\mathrm{F21}^{00}_{0001000} + \mathrm{F21}^{00}_{0100000}) \\
&- 4\,(-1+\alpha)\,\alpha^2\,(-2 + 6\,\alpha + 4\,\alpha^3 + \alpha^2\,(-8+\tau))\,\mathrm{F21}^{00}_{0101000} \\
&- 4\,(-1+\alpha)^2\,\alpha^2\,(1 - 2\,\alpha^2 + 2\,\alpha^3 - 2\,\tau + \alpha\,(-1+3\,\tau))\,\mathrm{F21}^{00}_{0110000} \\
&- \frac{8}{\tau}\,(-1+\alpha)\,\alpha\,(\alpha - 2\,\alpha^2 + 2\,\alpha^3 - \tau + \alpha\,\tau)\,(-\mathrm{F21}^{00}_{0001000} + \mathrm{F21}^{00}_{1000000}) \\
&+ 4\,(-1+\alpha)^3\,\alpha\,(2\,\alpha^3 + \tau - \alpha\,(1+\tau))\,\mathrm{F21}^{00}_{1010000} \\
&+ \frac{8}{\tau}\,(-1+\alpha)^2\,\alpha\,(\mathrm{F21}^{01}_{0001000} - \mathrm{F21}^{01}_{1000000}) \\
&- 4\,(-1+\alpha)^4\,\alpha\,\mathrm{F21}^{01}_{1010000} + 4\,(-1+\alpha)^2\,\alpha^2\,(-2+3\,\alpha)\,\mathrm{F21}^{10}_{0110000}
\end{aligned} \tag{B.81}
$$

$$
\begin{aligned}
\mathcal{F}^{(22)}_{12}(T) = &-4\,(-1+\alpha)^2\,\alpha\,(-1+2\,\alpha)\,(-\mathrm{F22}^{00}_{0000010} + \mathrm{F22}^{00}_{0100000}) \\
&- 4\,(-1+\alpha)^2\,\alpha\,(-1+2\,\alpha)\,(1 - 3\,\alpha + 2\,\alpha^2 + \tau)\,\mathrm{F22}^{00}_{0100010} \\
&+ 4\,(-1+\alpha)^2\,\alpha^2\,(1 - 2\,\alpha^2 + 2\,\alpha^3 - 2\,\tau + \alpha\,(-1+3\,\tau))\,\mathrm{F22}^{00}_{0110000} \\
&+ 8\,(-1+\alpha)^2\,\alpha^2\,(-1+2\,\alpha)\,(-\mathrm{F22}^{00}_{0000010} + \mathrm{F22}^{00}_{1000000}) \\
&- 4\,(-1+\alpha)^3\,\alpha\,(2\,\alpha^3 + \tau - \alpha\,(1+\tau))\,\mathrm{F22}^{00}_{1010000} \\
&+ 4\,(-1+\alpha)^4\,\alpha\,\mathrm{F22}^{01}_{1010000} - 4\,(-1+\alpha)^2\,\alpha^2\,(-2+3\,\alpha)\,\mathrm{F22}^{10}_{0110000}
\end{aligned} \tag{B.82}
$$

$$
\begin{aligned}
\mathcal{F}^{(23)}_{12}(T) = &-4\,(-1+\alpha)\,\alpha^3\,(-\mathrm{F23}^{00}_{0001000} + \mathrm{F23}^{00}_{0100000}) \\
&- 4\,(-1+\alpha)\,\alpha^2\,(-4 + 8\,\alpha^3 - 2\,\alpha\,(-6+\tau) + \tau + \alpha^2\,(-16+3\,\tau))\,\mathrm{F23}^{00}_{0101000} \\
&- \frac{4}{\tau}\,(-1+\alpha)\,\alpha\,(4\,\alpha + 8\,\alpha^3 + 2\,\alpha^2\,(-4+\tau) - \tau)\,(-\mathrm{F23}^{00}_{0001000} + \mathrm{F23}^{00}_{1000000}) \\
&+ 4\,\alpha\,(-1 + 3\,\alpha - 4\,\alpha^2 + 2\,\alpha^3)\,(-2\,\alpha + 2\,\alpha^2 + \tau\ )\,\mathrm{F23}^{00}_{1100000} \\
&- 8\,(-1+\alpha)^2\,\alpha^2\,(1 - 2\,\alpha + 2\,\alpha^2)\,\mathrm{F23}^{00}_{2000000} \\
&+ \frac{8}{\tau}\,(-1+\alpha)^2\,\alpha\,(\mathrm{F23}^{01}_{0001000} - \mathrm{F23}^{01}_{1000000})
\end{aligned} \tag{B.83}
$$

$$
\begin{aligned}
\mathcal{F}_{12}^{(24)}(T) = &-\frac{1}{\tau}\, 4\,(-1+\alpha)\,\alpha\,(4\,\alpha+8\,\alpha^3-\tau+\alpha^2\,(-8+3\,\tau)) \\
&\times(-\mathrm{F24}^{00}_{0000010}+\mathrm{F24}^{00}_{0001000})+4\,(-1+\alpha)\,\alpha^3\,(-\mathrm{F24}^{00}_{0000010}+\mathrm{F24}^{00}_{0100000}) \\
&+4\,\alpha\,(-1+3\,\alpha-4\,\alpha^2+2\,\alpha^3)\,(1-3\,\alpha+2\,\alpha^2+\tau)\,\mathrm{F24}^{00}_{0100010} \\
&+4\,(-1+\alpha)\,\alpha^2\,(-4+8\,\alpha^3-2\,\alpha\,(-6+\tau)+\tau+\alpha^2\,(-16+3\,\tau))\,\mathrm{F24}^{00}_{0101000} \\
&-\frac{16}{\tau}\,(-1+\alpha)\,\alpha^2\,(-1+\alpha^2\,(-2+\tau)-2\,\alpha\,(-1+\tau)+\tau)\,(-\mathrm{F24}^{00}_{0000010} \\
&+\mathrm{F24}^{00}_{1000000})-8\,\alpha\,(-1+3\,\alpha-4\,\alpha^2+2\,\alpha^3)\,(-2\,\alpha+2\,\alpha^2+\tau\,)\,\mathrm{F24}^{00}_{1100000} \\
&+16\,(-1+\alpha)^2\,\alpha^2\,(1-2\,\alpha+2\,\alpha^2)\,\mathrm{F24}^{00}_{2000000} \\
&-\frac{8}{\tau}\,(-1+\alpha)^2\,\alpha\,(\mathrm{F24}^{01}_{0001000}-\mathrm{F24}^{01}_{1000000})
\end{aligned}
\tag{B.84}
$$

$$
\begin{aligned}
\mathcal{F}_{12}^{(25)}(T) = &\;4\,\alpha\,(1-3\,\alpha+4\,\alpha^2-2\,\alpha^3)\,(\mathrm{F25}^{00}_{0100000}-\mathrm{F25}^{00}_{1000000}) \\
&-4\,\alpha\,(-1+3\,\alpha-4\,\alpha^2+2\,\alpha^3)\,(-2\,\alpha+2\,\alpha^2+\tau\,)\,\mathrm{F25}^{00}_{1100000} \\
&+8\,(-1+\alpha)^2\,\alpha^2\,(1-2\,\alpha+2\,\alpha^2)\,\mathrm{F25}^{00}_{2000000}
\end{aligned}
\tag{B.85}
$$

$$
\begin{aligned}
\mathcal{F}_{12}^{(26)}(T) = &-4\,\alpha\,(-1+3\,\alpha-4\,\alpha^2+2\,\alpha^3)\,(1-3\,\alpha+2\,\alpha^2+\tau)\,\mathrm{F26}^{00}_{0100010} \\
&-4\,\alpha\,(1-5\,\alpha+10\,\alpha^2-10\,\alpha^3+4\,\alpha^4)\,(\mathrm{F26}^{00}_{0000010}-\mathrm{F26}^{00}_{1000000}) \\
&+4\,\alpha\,(-1+3\,\alpha-4\,\alpha^2+2\,\alpha^3)\,(-2\,\alpha+2\,\alpha^2+\tau\,)\,\mathrm{F26}^{00}_{1100000} \\
&-8\,(-1+\alpha)^2\,\alpha^2\,(1-2\,\alpha+2\,\alpha^2)\,\mathrm{F26}^{00}_{2000000}
\end{aligned}
\tag{B.86}
$$

$$
\begin{aligned}
\mathcal{F}_{12}^{(27)}(T) = &-16\,\alpha\,(1-3\,\alpha+2\,\alpha^2)\,(-\alpha+\alpha^2+\tau)\,\mathrm{F27}^{00}_{0100000} \\
&+16\,(-1+\alpha)^2\,\alpha^2\,(-1+2\,\alpha)\,\mathrm{F27}^{00}_{1000000} \\
&+16\,(-1+\alpha)\,\alpha\,(-1+2\,\alpha)\,\mathrm{F27}^{10}_{0100000}
\end{aligned}
\tag{B.87}
$$

$$
\begin{aligned}
\mathcal{F}_{12}^{(28)}(T) = &-4\,\alpha\,(1-10\,\alpha+27\,\alpha^2-27\,\alpha^3+10\,\alpha^4)\,\tau\,\mathrm{F28}^{00}_{0010000} \\
&-4\,\alpha\,(4\,\alpha^4+\alpha^2\,(6-4\,\tau)+2\,\tau-\alpha\,(2+\tau)+2\,\alpha^3\,(-4+3\,\tau))\,\mathrm{F28}^{00}_{0100000} \\
&+4\,\alpha^2\,(12\,\alpha^5\,(-1+\tau)+6\,(1-2\,\tau)\,\tau+\alpha^2\,(28-5\,\tau-59\,\tau^2)+\alpha^4\,(40-44\,\tau \\
&-6\,\tau^2)+\alpha^3\,(-50+46\,\tau+32\,\tau^2)+\alpha\,(-6-15\,\tau+44\,\tau^2))\,\mathrm{F28}^{00}_{0110000} \\
&+4\,(-1+\alpha)\,\alpha\,(4\,\alpha^3-\tau+2\,\alpha\,(1+\tau)-\alpha^2\,(4+\tau))\,\mathrm{F28}^{00}_{1000000} \\
&-4\,(-1+\alpha)^2\,\alpha\,(12\,\alpha^4\,(-1+\tau)-3\,\tau^2+3\,\alpha\,\tau\,(3+\tau)+\alpha^3\,(16-3\,\tau+\tau^2) \\
&-\alpha^2\,(6+16\,\tau+\tau^2))\,\mathrm{F28}^{00}_{1010000}-8\,(-1+\alpha)^2\,\alpha^2\,(-2+5\,\alpha)\,\mathrm{F28}^{01}_{0010000} \\
&-8\,(-1+\alpha)^3\,\alpha\,\mathrm{F28}^{01}_{1000000} \\
&-8\,(-1+\alpha)^2\,\alpha\,(-15\,\alpha^2-2\,\tau+\alpha\,(5+\tau)+\alpha^3\,(11+\tau))\,\mathrm{F28}^{01}_{1010000} \\
&-16\,(-1+\alpha)^3\,\alpha^2\,\mathrm{F28}^{02}_{1010000}+8\,(-1+\alpha)^3\,\alpha\,(-2+5\,\alpha)\,\mathrm{F28}^{10}_{0010000} \\
&+8\,\alpha\,(1+\alpha-6\,\alpha^2+6\,\alpha^3)\,\mathrm{F28}^{10}_{0100000}+8\,\alpha^2\,(-3+\alpha\,(9-44\,\tau)+12\,\tau \\
&+6\,\alpha^4\,(1+\tau)-\alpha^3\,(7+32\,\tau)+\alpha^2\,(-5+59\,\tau))\,\mathrm{F28}^{10}_{0110000} \\
&+16\,(-1+\alpha)\,\alpha^2\,(3-8\,\alpha+6\,\alpha^2)\,\mathrm{F28}^{20}_{0110000}
\end{aligned}
\tag{B.88}
$$

B.3 Pentagon

The colour factor for the pentagon diagrams are $\mathcal{C}_{13} = N_c/2$ and the functions L_i are chosen as

$$
\begin{array}{ll}
(i=1) & \frac{c_\Gamma}{\epsilon^2}(-t_a)^{-\epsilon} \\
(i=2) & \frac{c_\Gamma}{\epsilon^2}(-t_b)^{-\epsilon} \\
(i=3) & \frac{c_\Gamma}{\epsilon^2}(-t)^{-\epsilon} \\
(i=4) & \frac{c_\Gamma}{\epsilon^2}(Q^2)^{-\epsilon} \\
(i=5) & \mathrm{Ld}_0^{op}(t_a, t_b, t, -Q^2) \\
(i=6) & \frac{2c_\Gamma}{\epsilon}\log\frac{1-\alpha}{\alpha} \\
(i=7) & \text{coefficient of } \frac{t_a\, t_b}{t(Q^2\, t + t_a\, t_b)}\left(\frac{H_T}{st_a} + \frac{\bar{H}_T}{t_b}\right) \\
(i=8) & \text{coefficient of } \frac{H_T}{stt_a} \\
(i=9) & \text{coefficient of } \frac{\bar{H}_T}{stt_b}
\end{array}
\tag{B.89}
$$

The choice for the first coefficients ($i = 1,\ldots,5$) is rather obvious, these are the terms in the amplitude (cf. (2.54) and (2.55)) that did not depend on s. It is important to note that we have considered the sum of the two pentagon diagrams, i.e. the results in this section are for the sum $\Phi_{13} + \bar{\Phi}_{13}$. Therefore the coefficients ($i = 1,\ldots,5$) already include a factor two.

The ($i = 6$) term stems from the pole contribution of the pentagon (2.56). The terms ($i = 6,\ldots,9$) are, aside any logarithmic function, the different $\boldsymbol{k}$ dependent terms in (2.57). The different logarithmic funtions lead to a replacement of the integrands, exactly as in the case of the box diagrams 2.2.2+3.

Longitudinal

$$
\begin{aligned}
\mathcal{F}_{13}^{(1)}(L) = &-\frac{1}{\tau}\, 16\, (-1+\alpha)^2\, \alpha^2\, (\mathrm{F1}^{00}_{0100000} - \mathrm{F1}^{00}_{1000000}) \\
&- \frac{32}{\tau}\, (-1+\alpha)^3\, \alpha^3\, (\mathrm{F1}^{00}_{1100000} - \mathrm{F1}^{00}_{2000000}) + 16\, (-1+\alpha)^3\, \alpha^2\, \mathrm{G1}^{00}_{0000010} \\
&- 8(-1+\alpha)^2\, \alpha(-\alpha + 2\,\alpha^2 + \tau)\mathrm{G1}^{00}_{0001000} + 16\, (-1+\alpha)^2\, \alpha^2\, (1+\alpha)\, \mathrm{G1}^{00}_{0100000} \\
&+ 16\, (-1+\alpha)^4\, \alpha^2\, \mathrm{G1}^{00}_{0100010} + 8\, (-1+\alpha)^3\, \alpha^2\, (-1+2\,\alpha)\, \tau\, \mathrm{G1}^{00}_{0101000} \\
&- 8\, (-1+\alpha)^2\, \alpha^2\, (-3+2\,\alpha)\, \mathrm{G1}^{00}_{1000000} - 16\, (-1+\alpha)^2\, \alpha\, \mathrm{G1}^{01}_{0001000} \\
&+ \frac{32}{\tau}\, (-1+\alpha)^2\, \alpha^2\, (\mathrm{G1}^{01}_{1000000} - \mathrm{G1}^{10}_{0100000})
\end{aligned}
\tag{B.90}
$$

$$\begin{aligned}\mathcal{F}_{13}^{(2)}(L) &= \frac{16}{\tau}\,(-1+\alpha)^2\,\alpha^2\,(\mathrm{F2}^{00}_{0100000}-\mathrm{F2}^{00}_{1000000})\\
&+\frac{32}{\tau}\,(-1+\alpha)^3\,\alpha^3\,(\mathrm{F2}^{00}_{0200000}-\mathrm{F2}^{00}_{1100000})-16\,(-1+\alpha)^2\,\alpha^3\,\mathrm{G2}^{00}_{0000001}\\
&+8\,(-1+\alpha)\,\alpha^2\,(1-3\,\alpha+2\,\alpha^2+\tau)\,\mathrm{G2}^{00}_{0000100}\\
&+8\,(-1+\alpha)^2\,\alpha^2\,(1+2\,\alpha)\,\mathrm{G2}^{00}_{0100000}-16\,(-2+\alpha)\,(-1+\alpha)^2\,\alpha^2\,\mathrm{G2}^{00}_{1000000}\\
&+16\,(-1+\alpha)^2\,\alpha^4\,\mathrm{G2}^{00}_{1000001}+8\,(-1+\alpha)^2\,\alpha^3\,(-1+2\,\alpha)\,\tau\,\mathrm{G2}^{00}_{1000100}\\
&-16\,(-1+\alpha)\,\alpha^2\,\mathrm{G2}^{10}_{0000100}+\frac{32}{\tau}\,(-1+\alpha)^2\,\alpha^2\,(\mathrm{G2}^{01}_{1000000}-\mathrm{G2}^{10}_{0100000})\end{aligned}\tag{B.91}$$

$$\begin{aligned}\mathcal{F}_{13}^{(3)}(L) &= -8\,(-1+\alpha)\,\alpha^2\,(1-3\,\alpha+2\,\alpha^2+\tau)\,\mathrm{G3}^{00}_{0000100}\\
&+8\,(-1+\alpha)^2\,\alpha\,(-\alpha+2\,\alpha^2+\tau)\,\mathrm{G3}^{00}_{0001000}\\
&-8\,(-1+\alpha)^2\,\alpha^2\,(1+2\,\alpha)\,\mathrm{G3}^{00}_{0100000}-8\,(-1+\alpha)^3\,\alpha^2\,(-1+2\,\alpha)\,\tau\,\mathrm{G3}^{00}_{0101000}\\
&+8(-1+\alpha)^2\,\alpha^2\,(-3+2\,\alpha)\,\mathrm{G3}^{00}_{1000000}-8(-1+\alpha)^2\,\alpha^3\,(-1+2\,\alpha)\,\tau\mathrm{G3}^{00}_{1000100}\\
&+16\,(-1+\alpha)^2\,\alpha\,\mathrm{G3}^{01}_{0001000}+16\,(-1+\alpha)\,\alpha^2\,\mathrm{G3}^{10}_{0000100}\\
&-\frac{32}{\tau}\,(-1+\alpha)^2\,\alpha^2\,(\mathrm{G3}^{01}_{1000000}-\mathrm{G3}^{10}_{0100000})\end{aligned}\tag{B.92}$$

$$\begin{aligned}\mathcal{F}_{13}^{(4)}(L) &= 16\,(-1+\alpha)^2\,\alpha^3\,(\mathrm{G4}^{00}_{0000001}-\mathrm{G4}^{00}_{0100000})\\
&-16\,(-1+\alpha)^4\,\alpha^2\,\mathrm{G4}^{00}_{0100010}+16\,(-1+\alpha)^3\,\alpha^3\,\mathrm{G4}^{00}_{0200000}\\
&-16\,(-1+\alpha)^3\,\alpha^2\,(\mathrm{G4}^{00}_{0000010}-\mathrm{G4}^{00}_{1000000})-16\,(-1+\alpha)^2\,\alpha^4\,\mathrm{G4}^{00}_{1000001}\\
&-32\,(-1+\alpha)^3\,\alpha^3\,\mathrm{G4}^{00}_{1100000}+16\,(-1+\alpha)^3\,\alpha^3\,\mathrm{G4}^{00}_{2000000}\end{aligned}\tag{B.93}$$

$$\begin{aligned}\mathcal{F}_{13}^{(5)}(L) &= 8\,(-1+\alpha)\,\alpha^2\,(-2+\alpha\,(2+\tau))\,\mathrm{G5}^{00}_{0100000}\\
&+8\,(-1+\alpha)^2\,\alpha^3\,(2+4\,\alpha^2-\tau^2+\alpha\,(-6+\tau+\tau^2))\,\mathrm{G5}^{00}_{0110000}\\
&+8\,(-1+\alpha)^2\,\alpha\,(-\tau+\alpha\,(2+\tau))\,\mathrm{G5}^{00}_{1000000}\\
&-8\,(-1+\alpha)^3\,\alpha^2\,(4\,\alpha^2+\tau-\alpha\,(2+\tau+\tau^2))\,\mathrm{G5}^{00}_{1010000}\\
&+\frac{16}{\tau}\,(-1+\alpha)^2\,\alpha\,(-\tau+\alpha\,(2+\tau))\,\mathrm{G5}^{01}_{1000000}\\
&+16\,(-1+\alpha)^3\,\alpha^2\,(-1+\alpha+\tau+\alpha\,\tau)\,\mathrm{G5}^{01}_{1010000}+32\,(-1+\alpha)^3\,\alpha^2\,\mathrm{G5}^{02}_{1010000}\\
&-\frac{16}{\tau}\,(-1+\alpha)\,\alpha^2\,(-2+\alpha\,(2+\tau))\,\mathrm{G5}^{10}_{0100000}\\
&-16\,(-1+\alpha)^2\,\alpha^3\,(\alpha-2\,\tau+\alpha\,\tau)\,\mathrm{G5}^{10}_{0110000}-32\,(-1+\alpha)^2\,\alpha^3\,\mathrm{G5}^{20}_{0110000}\end{aligned}\tag{B.94}$$

$$\begin{aligned}\mathcal{F}_{13}^{(6)}(L) &= \frac{8}{\tau}\,(-1+\alpha)^2\,\alpha^2\,(\mathrm{F6}^{00}_{0100000}-\mathrm{F6}^{00}_{1000000})\\
&+\frac{8}{\tau}\,(-1+\alpha)^3\,\alpha^3\,(\mathrm{F6}^{00}_{0200000}-\mathrm{F6}^{00}_{2000000})\end{aligned}\tag{B.95}$$

$$\begin{aligned}
\mathcal{F}_{13}^{(7)}(L) &= -8\,(-1+\alpha)^2\,\alpha^2\,(\mathrm{G7}^{00}_{0100000} - \mathrm{G7}^{00}_{1000000}) \\
&+ \frac{16}{\tau}\,(-1+\alpha)^2\,\alpha^2\,\mathrm{G7}^{01}_{1000000} + \frac{16}{\tau}\,(-1+\alpha)^2\,\alpha^2\,\mathrm{G7}^{10}_{0100000} \\
&+ \frac{8}{\tau}\,(-1+\alpha)\,\alpha\,\mathrm{S7}^{0100000}_{000001100} - \frac{8}{\tau}\,(-1+\alpha)\,\alpha\,\mathrm{S7}^{1000000}_{000001100}
\end{aligned} \tag{B.96}$$

$$\begin{aligned}
\mathcal{F}_{13}^{(8)}(L) &= \frac{4}{\tau}\,(-1+\alpha)^2\,\alpha^2\,(\mathrm{F8}^{00}_{0100000} - \mathrm{F8}^{00}_{1000000}) \\
&+ \frac{8}{\tau}\,(-1+\alpha)^3\,\alpha^3\,(\mathrm{F8}^{00}_{1100000} - \mathrm{F8}^{00}_{2000000})
\end{aligned} \tag{B.97}$$

$$\begin{aligned}
\mathcal{F}_{13}^{(9)}(L) &= \frac{4}{\tau}\,(-1+\alpha)^2\,\alpha^2\,(\mathrm{F9}^{00}_{0100000} - \mathrm{F9}^{00}_{1000000}) \\
&+ \frac{8}{\tau}\,(-1+\alpha)^3\,\alpha^3\,(\mathrm{F9}^{00}_{0200000} - \mathrm{F9}^{00}_{1100000})
\end{aligned} \tag{B.98}$$

Transverse

$$\begin{aligned}
\mathcal{F}_{13}^{(1)}(T) &= \frac{1}{\tau} - 16\,(-1+\alpha)^2\,\alpha^2\,(\mathrm{F1}^{00}_{0100000} - \mathrm{F1}^{00}_{1000000}) \\
&- \frac{32}{\tau}\,(-1+\alpha)^3\,\alpha^3\,(\mathrm{F1}^{00}_{1100000} - \mathrm{F1}^{00}_{2000000}) + 16\,(-1+\alpha)^3\,\alpha^2\,\mathrm{G1}^{00}_{0000010} \\
&- 8(-1+\alpha)^2\,\alpha\,(-\alpha+2\alpha^2+\tau)\mathrm{G1}^{00}_{0001000} + 16\,(-1+\alpha)^2\,\alpha^2\,(1+\alpha)\mathrm{G1}^{00}_{0100000} \\
&+ 16\,(-1+\alpha)^4\,\alpha^2\,\mathrm{G1}^{00}_{0100010} + 8\,(-1+\alpha)^3\,\alpha^2\,(-1+2\,\alpha)\,\tau\,\mathrm{G1}^{00}_{0101000} \\
&- 8\,(-1+\alpha)^2\,\alpha^2\,(-3+2\,\alpha)\,\mathrm{G1}^{00}_{1000000} - 16\,(-1+\alpha)^2\,\alpha\,\mathrm{G1}^{01}_{0001000} \\
&+ \frac{32}{\tau}\,(-1+\alpha)^2\,\alpha^2\,(\mathrm{G1}^{01}_{1000000} - \mathrm{G1}^{10}_{0100000})
\end{aligned} \tag{B.99}$$

$$\begin{aligned}
\mathcal{F}_{13}^{(2)}(T) &= \frac{16}{\tau}\,(-1+\alpha)^2\,\alpha^2\,(\mathrm{F2}^{00}_{0100000} - \mathrm{F2}^{00}_{1000000}) \\
&+ \frac{32}{\tau}\,(-1+\alpha)^3\,\alpha^3\,(\mathrm{F2}^{00}_{0200000} - \mathrm{F2}^{00}_{1100000}) - 16\,(-1+\alpha)^2\,\alpha^3\,\mathrm{G2}^{00}_{0000001} \\
&+ 8\,(-1+\alpha)\,\alpha^2\,(1-3\,\alpha+2\,\alpha^2+\tau)\,\mathrm{G2}^{00}_{0000100} \\
&+ 8\,(-1+\alpha)^2\,\alpha^2\,(1+2\,\alpha)\,\mathrm{G2}^{00}_{0100000} - 16\,(-2+\alpha)\,(-1+\alpha)^2\,\alpha^2\,\mathrm{G2}^{00}_{1000000} \\
&+ 16\,(-1+\alpha)^2\,\alpha^4\,\mathrm{G2}^{00}_{1000001} + 8\,(-1+\alpha)^2\,\alpha^3\,(-1+2\,\alpha)\,\tau\,\mathrm{G2}^{00}_{1000100} \\
&- 16\,(-1+\alpha)\,\alpha^2\,\mathrm{G2}^{10}_{0000100} + \frac{32}{\tau}\,(-1+\alpha)^2\,\alpha^2\,(\mathrm{G2}^{01}_{1000000} - \mathrm{G2}^{10}_{0100000})
\end{aligned} \tag{B.100}$$

$$\begin{aligned}
\mathcal{F}_{13}^{(3)}(T) &= -8\,(-1+\alpha)\,\alpha^2\,(1-3\,\alpha+2\,\alpha^2+\tau)\,\mathrm{G3}^{00}_{0000100} \\
&+ 8(-1+\alpha)^2\alpha(-\alpha+2\,\alpha^2+\tau)\mathrm{G3}^{00}_{0001000} - 8\,(-1+\alpha)^2\,\alpha^2(1+2\,\alpha)\mathrm{G3}^{00}_{0100000} \\
&- 8(-1+\alpha)^3\,\alpha^2\,(-1+2\,\alpha)\tau\,\mathrm{G3}^{00}_{0101000} + 8\,(-1+\alpha)^2\,\alpha^2\,(-3+2\,\alpha)\mathrm{G3}^{00}_{1000000} \\
&- 8\,(-1+\alpha)^2\,\alpha^3\,(-1+2\,\alpha)\,\tau\,\mathrm{G3}^{00}_{1000100} + 16\,(-1+\alpha)^2\,\alpha\,\mathrm{G3}^{01}_{0001000} \\
&+ 16\,(-1+\alpha)\,\alpha^2\,\mathrm{G3}^{10}_{0000100} - \frac{32}{\tau}\,(-1+\alpha)^2\,\alpha^2\,(\mathrm{G3}^{01}_{1000000} - \mathrm{G3}^{10}_{0100000})
\end{aligned} \tag{B.101}$$

$$\begin{aligned}\mathcal{F}_{13}^{(4)}(T) &= 16\,(-1+\alpha)^2\,\alpha^3\,(\mathrm{G4}^{00}_{0000001} - \mathrm{G4}^{00}_{0100000}) \\ &- 16\,(-1+\alpha)^4\,\alpha^2\,\mathrm{G4}^{00}_{0100010} + 16\,(-1+\alpha)^3\,\alpha^3\,\mathrm{G4}^{00}_{0200000} \\ &- 16\,(-1+\alpha)^3\,\alpha^2\,(\mathrm{G4}^{00}_{0000010} - \mathrm{G4}^{00}_{1000000}) - 16\,(-1+\alpha)^2\,\alpha^4\,\mathrm{G4}^{00}_{1000001} \\ &- 32\,(-1+\alpha)^3\,\alpha^3\,\mathrm{G4}^{00}_{1100000} + 16\,(-1+\alpha)^3\,\alpha^3\,\mathrm{G4}^{00}_{2000000}\end{aligned} \tag{B.102}$$

$$\begin{aligned}\mathcal{F}_{13}^{(5)}(T) &= 8\,(-1+\alpha)\,\alpha^2\,(-2+\alpha\,(2+\tau))\,\mathrm{G5}^{00}_{0100000} \\ &+ 8\,(-1+\alpha)^2\,\alpha^3\,(2+4\,\alpha^2-\tau^2+\alpha\,(-6+\tau+\tau^2))\,\mathrm{G5}^{00}_{0110000} \\ &+ 8\,(-1+\alpha)^2\,\alpha\,(-\tau+\alpha\,(2+\tau))\,\mathrm{G5}^{00}_{1000000} \\ &- 8\,(-1+\alpha)^3\,\alpha^2\,(4\,\alpha^2+\tau-\alpha\,(2+\tau+\tau^2))\,\mathrm{G5}^{00}_{1010000} \\ &+ \frac{16}{\tau}\,(-1+\alpha)^2\,\alpha\,(-\tau+\alpha\,(2+\tau))\,\mathrm{G5}^{01}_{1000000} \\ &+ 16\,(-1+\alpha)^3\,\alpha^2\,(-1+\alpha+\tau+\alpha\,\tau)\,\mathrm{G5}^{01}_{1010000} + 32\,(-1+\alpha)^3\,\alpha^2\,\mathrm{G5}^{02}_{1010000} \\ &- \frac{16}{\tau}\,(-1+\alpha)\,\alpha^2\,(-2+\alpha\,(2+\tau))\,\mathrm{G5}^{10}_{0100000} \\ &- 16\,(-1+\alpha)^2\,\alpha^3\,(\alpha-2\,\tau+\alpha\,\tau)\,\mathrm{G5}^{10}_{0110000} - 32\,(-1+\alpha)^2\,\alpha^3\,\mathrm{G5}^{20}_{0110000}\end{aligned} \tag{B.103}$$

$$\begin{aligned}\mathcal{F}_{13}^{(6)}(T) &= \frac{8}{\tau}\,(-1+\alpha)^2\,\alpha^2\,(\mathrm{F6}^{00}_{0100000} - \mathrm{F6}^{00}_{1000000}) \\ &+ \frac{8}{\tau}\,(-1+\alpha)^3\,\alpha^3\,(\mathrm{F6}^{00}_{0200000} - \mathrm{F6}^{00}_{2000000})\end{aligned} \tag{B.104}$$

$$\begin{aligned}\mathcal{F}_{13}^{(7)}(T) &= -8\,(-1+\alpha)^2\,\alpha^2\,(\mathrm{G7}^{00}_{0100000} - \mathrm{G7}^{00}_{1000000}) \\ &+ \frac{16}{\tau}\,(-1+\alpha)^2\,\alpha^2\,\mathrm{G7}^{01}_{1000000} + \frac{16}{\tau}\,(-1+\alpha)^2\,\alpha^2\,\mathrm{G7}^{10}_{0100000} \\ &+ \frac{8}{\tau}\,(-1+\alpha)\,\alpha\,\mathrm{S7}^{0100000}_{000001100} - \frac{8}{\tau}\,(-1+\alpha)\,\alpha\,\mathrm{S7}^{1000000}_{000001100}\end{aligned} \tag{B.105}$$

$$\begin{aligned}\mathcal{F}_{13}^{(8)}(T) &= \frac{4}{\tau}\,(-1+\alpha)^2\,\alpha^2\,(\mathrm{F8}^{00}_{0100000} - \mathrm{F8}^{00}_{1000000}) \\ &+ \frac{8}{\tau}\,(-1+\alpha)^3\,\alpha^3\,(\mathrm{F8}^{00}_{1100000} - \mathrm{F8}^{00}_{2000000})\end{aligned} \tag{B.106}$$

$$\begin{aligned}\mathcal{F}_{13}^{(9)}(T) &= \frac{4}{\tau}\,(-1+\alpha)^2\,\alpha^2\,(\mathrm{F9}^{00}_{0100000} - \mathrm{F9}^{00}_{1000000}) \\ &+ \frac{8}{\tau}\,(-1+\alpha)^3\,\alpha^3\,(\mathrm{F9}^{00}_{0200000} - \mathrm{F9}^{00}_{1100000})\end{aligned} \tag{B.107}$$

B.4 Opposite box

The contribution from the opposite box diagram 2.2.14 is one of the most complicated ones. We have made use of the fact, that the diagram is symmetric with respect to the interchange of quark and antiquark and in this way already reduced the number of terms roughly by a factor of two. The special functions L_i under the integrand are defined according to the following list:

$$
\begin{array}{ll}
(i=1) & \mathrm{Ld}_0^{op}(t_a,t_b,-Q^2,t) \\
(i=2) & \log(-t) \\
(i=3) & \log(-t_a) \\
(i=4) & \log(-t_b) \\
(i=5) & \log(Q^2) \\
(i=6) & 1 \\
(i=7) & \dfrac{c_\Gamma}{\epsilon} \\
(i=8) & \dfrac{c_\Gamma}{\epsilon^2}(-t)^{-\epsilon} \\
(i=9) & \dfrac{c_\Gamma}{\epsilon^2}(-t_a)^{-\epsilon} \\
(i=10) & \dfrac{c_\Gamma}{\epsilon^2}(-t_b)^{-\epsilon} \\
(i=11) & \dfrac{c_\Gamma}{\epsilon^2}(Q^2)^{-\epsilon}\ .
\end{array}
\tag{B.108}
$$

The colour factor is given by $\mathcal{C}_{14} = N_c/2$ for this diagram. The final answer is obtained after adding the transformed piece to the given result. In this way, the pieces that are zero ($i=4$ and $i=10$) contribute in the end.

Longitudinal

$$
\begin{aligned}
\mathcal{F}_{14}^{(1)}(L) = &-8\,\alpha^2\,(1-3\,\alpha+2\,\alpha^2)^2\,\tau\,\mathrm{G1}^{00}_{0010000} + 8\,(1-2\,\alpha)^2 \\
&\times(-1+\alpha)^3\,\alpha^3\,\tau\,(-1+3\,\tau)\,\mathrm{G1}^{00}_{0020000} - 16\,(-1+\alpha)^2\,\alpha^4\,\tau\,\mathrm{G1}^{00}_{0100000} \\
&- 16\,(-1+\alpha)^2\,\alpha^4\,\tau\,(-2+\alpha\,(4-5\,\tau)+2\,\alpha^2\,(-1+\tau)+4\,\tau)\,\mathrm{G1}^{00}_{0110000} \\
&- 16\,(-1+\alpha)^3\,\alpha^4\,\tau\,(\alpha^3\,(-1+\tau)^2+2\,(1-2\,\tau)\,\tau+2\,\alpha\,\tau\,(-2+3\,\tau) \\
&+ \alpha^2\,(-1+5\,\tau-4\,\tau^2))\,\mathrm{G1}^{00}_{0120000} - 32\,(-1+\alpha)^2\,\alpha^3\,(-1+2\,\alpha)\,\mathrm{G1}^{01}_{0010000} \\
&+ 32\,(-1+\alpha)^3\,\alpha^3\,(-1+2\,\alpha)\,(-\tau+\alpha\,(-1+6\,\tau))\,\mathrm{G1}^{01}_{0020000} \\
&- 32\,(-1+\alpha)^4\,\alpha^2\,\mathrm{G1}^{01}_{1000000} - 32\,(-1+\alpha)^4\,\alpha^2\,(2\,\alpha^2\,(-1+\tau) \\
&+ \tau+3\,\alpha\,\tau)\,\mathrm{G1}^{01}_{1010000} - 32\,(-1+\alpha)^4\,\alpha^3\,(\alpha^3\,(-1+\tau)^2+3\,\alpha^2\,(-1+\tau)\,\tau \\
&+ \tau\,(-1+2\,\tau)+\alpha\,\tau\,(1+2\,\tau)\ )\,\mathrm{G1}^{01}_{1020000} \\
&+ 64\,(-1+\alpha)^3\,\alpha^4\,(-1+3\,\alpha)\,\mathrm{G1}^{02}_{0020000} - 128\,(-1+\alpha)^4\,\alpha^3\,\mathrm{G1}^{02}_{1010000} \\
&- 64\,(-1+\alpha)^4\,\alpha^3\,(2\,\alpha^2\,(-1+\tau)+\tau+2\,\alpha\,\tau)\,\mathrm{G1}^{02}_{1020000} \\
&- 128\,(-1+\alpha)^4\,\alpha^4\,\mathrm{G1}^{03}_{1020000} - 32\,(-1+\alpha)^3\,\alpha^3\,(1-6\,\alpha+6\,\alpha^2)\,\mathrm{G1}^{11}_{0020000}
\end{aligned}
\tag{B.109}
$$

$$
\begin{aligned}
\mathcal{F}_{14}^{(2)}(L) = &-\frac{1}{\tau}\,(-1+\alpha)^2\,\alpha^2\,(2\,(5-3\,\tau)\,\tau+8\,\alpha^3\,(-3+2\,\tau) \\
&+ 2\,\alpha^2\,(22-22\,\tau+\tau^2)+\alpha\,(-20+11\,\tau+10\,\tau^2))\,\mathrm{F2}^{00}_{0010100}
\end{aligned}
$$

$$+\,4\,(-1+\alpha)^3\,\alpha^3\,(4\,\alpha^2-2\,(-1+\tau)\,\tau+\alpha\,(-4+3\,\tau))\,\mathrm{F2}^{00}_{0010200}$$
$$-\,\frac{2}{\tau}\,(-1+\alpha)\,\alpha^2\,(4\,\alpha^2+2\,(1+\tau)-\alpha\,(6+\tau))\,(\mathrm{F2}^{00}_{0000100}-\mathrm{F2}^{00}_{0100000})$$
$$-\,2\,(-1+\alpha)^3\,\alpha^2\,(-2+4\,\alpha+\tau)\,\mathrm{F2}^{00}_{0101000}$$
$$+\,\frac{1}{\tau}\,(-1+\alpha)\,\alpha^2\,(8\,\alpha^4\,(-3+4\,\tau)+\tau\,(-11+10\,\tau)+\alpha\,(20-6\,\tau-28\,\tau^2)$$
$$+\,2\,\alpha^3\,(34-50\,\tau+\tau^2)+\alpha^2\,(-64+85\,\tau+12\,\tau^2))\,\mathrm{F2}^{00}_{0110000}$$
$$-\,(-1+\alpha)^3\,\alpha^3\,(-4+7\,\tau+8\,\alpha^2\,(-1+2\,\tau)-2\,\alpha\,(-6+12\,\tau+\tau^2))\,\mathrm{F2}^{00}_{0111000}$$
$$-\,4\,(-1+\alpha)^4\,\alpha^4\,\tau\,(-4+4\,\alpha+\tau)\,\mathrm{F2}^{00}_{0112000}$$
$$+\,\frac{2}{\tau}\,(-1+\alpha)^2\,\alpha\,(24\,\alpha^3-3\,\tau+\alpha\,(7+2\,\tau)+2\,\alpha^2\,(-18+7\,\tau)\,)\,\mathrm{F2}^{01}_{0011000}$$
$$-\,8\,(-1+\alpha)^3\,\alpha^2\,(4\,\alpha^2+\tau+\alpha\,(-5+2\,\tau))\,\mathrm{F2}^{01}_{0012000}$$
$$+\,\frac{4}{\tau}\,(-1+\alpha)^2\,\alpha\,(\mathrm{F2}^{01}_{0001000}-\mathrm{F2}^{01}_{1000000})-\frac{2}{\tau}\,(-1+\alpha)^2\,\alpha\,(24\,\alpha^3-7\,\tau$$
$$+\,2\,\alpha^2\,(-18+7\,\tau)+\alpha\,(7+8\,\tau))\,\mathrm{F2}^{01}_{1010000}-16\,(-1+\alpha)^3\,\alpha^2\,\mathrm{F2}^{02}_{0012000}$$
$$+\,\frac{4}{\tau}\,(-1+\alpha)^2\,\alpha\,(-3+8\,\alpha)\,(\mathrm{F2}^{02}_{0011000}-\mathrm{F2}^{02}_{1010000})$$
$$+\,\frac{1}{2}\,(-1+\alpha)\,\alpha\,(-2-4\,\alpha\,(-1+\tau)+4\,\alpha^2\,(-1+\tau)+\tau)\,\mathrm{G2}^{00}_{0000000}$$
$$+\,(-1+\alpha)\,\alpha^2\,\tau\,(-1+\alpha+5\,\tau-12\,\alpha\,\tau+8\,\alpha^2\,\tau)\,\mathrm{G2}^{00}_{0000100}$$
$$-\,2\,(-1+\alpha)^3\,\alpha^3\,\tau^3\,\mathrm{G2}^{00}_{0000200}+\frac{1}{2}\,(-1+\alpha)\,\alpha\,(-4\,\alpha^3\,(-1+\tau)^2+2\,\alpha^4$$
$$\times\,(-1+\tau)^2-3\,\tau^2-3\,\alpha^2\,(-1+\tau+4\,\tau^2)+\alpha\,(-1-\tau+14\,\tau^2))\,\mathrm{G2}^{00}_{0010000}$$
$$+\,(-1+\alpha)^2\,\alpha^2\,\tau\,(10+8\,\tau-9\,\tau^2+\alpha^2\,(47+\tau-10\,\tau^2)$$
$$+\,4\,\alpha^3\,(-4-3\,\tau+2\,\tau^2)+\alpha\,(-42-2\,\tau+18\,\tau^2))\,\mathrm{G2}^{00}_{0010100}$$
$$-\,2\,(-1+\alpha)^3\,\alpha^3\,\tau^2\,(2\,(-1+\tau^2)+\alpha^2\,(-2-\tau+\tau^2)$$
$$-\,\alpha\,(-5+3\,\tau+\tau^2\,))\,\mathrm{G2}^{00}_{0010200}-(-1+\alpha)\,\alpha^2\,\tau\,(-11+4\,\alpha^3\,(-4+\tau)$$
$$-\,40\,\alpha\,(-1+\tau)+10\,\tau+4\,\alpha^4\,(4+\tau)+\alpha^2\,(-29+20\,\tau))\,\mathrm{G2}^{00}_{0110000}$$
$$-\,(-1+\alpha)^3\,\alpha^3\,\tau^2\,(1+4\,\alpha^2\,(5+\tau)+2\,\alpha\,(-7+2\,\tau))\,\mathrm{G2}^{00}_{0111000}$$
$$-\,2\,(-1+\alpha)^4\,\alpha^4\,(-1+2\,\alpha)\,\tau^3\,\mathrm{G2}^{00}_{0112000}+2\,\alpha\,(1-2\,\alpha+2\,\alpha^2)\,\mathrm{G2}^{01}_{0000000}$$
$$-\,2\,(-1+\alpha)^2\,(\tau+8\,\alpha^2\,\tau-\alpha\,(1+4\,\tau))\,\mathrm{G2}^{01}_{0001000}$$
$$-\,8\,(-1+\alpha)^3\,\alpha^2\,\tau^2\,\mathrm{G2}^{01}_{0002000}$$
$$+\,2\,(-1+\alpha)^2\,\alpha^2\,(2+2\,\alpha\,(-1+\tau)-\tau)\,\mathrm{G2}^{01}_{0010000}$$
$$-\,2\,(-1+\alpha)^2\,\alpha\,(5\,\alpha\,\tau\,(-1+3\,\tau)-\tau\,(1+5\,\tau)+\alpha^2\,(7-10\,\tau-12\,\tau^2)$$
$$+\,4\,\alpha^3\,(-3+5\,\tau+4\,\tau^2))\,\mathrm{G2}^{01}_{0011000}-4\,(-1+\alpha)^3\,\alpha^2\,\tau\,(\alpha$$
$$-\,\alpha\,\tau^2+\tau\,(-2+3\,\tau)+\alpha^2\,(-2+2\,\tau+3\,\tau^2))\,\mathrm{G2}^{01}_{0012000}$$
$$-\,2\,(-1+\alpha)^2\,\alpha\,(3\,\tau+4\,\alpha^3\,(3+\tau)-6\,\alpha^2\,(1+8\,\tau)$$
$$+\,\alpha\,(-1+26\,\tau))\,\mathrm{G2}^{01}_{1010000}-8\,(-1+\alpha)^3\,\alpha\,\tau\,\mathrm{G2}^{02}_{0002000}$$
$$-\,4\,(-1+\alpha)^2\,\alpha\,(-1+\tau+4\,\alpha^2\,(3+2\,\tau)-\alpha\,(7+4\,\tau))\,\mathrm{G2}^{02}_{0011000}$$

$$
\begin{aligned}
&- 8\,(-1+\alpha)^3\,\alpha\,\tau\,(-\alpha+\tau+\alpha^2\,(1+3\,\tau))\,\mathrm{G2}^{02}_{0012000}\\
&+ 4\,(-1+\alpha)^2\,\alpha\,(-1-6\,\alpha+12\,\alpha^2)\,\mathrm{G2}^{02}_{1010000}\\
&- 16\,(-1+\alpha)^3\,\alpha^2\,\tau\,\mathrm{G2}^{03}_{0012000}\\
&+ 2\,\alpha\,(-1+3\,\alpha-4\,\alpha^2+2\,\alpha^3)\,\mathrm{G2}^{11}_{0010000}\\
&- (-1+\alpha)^2\,(-\mathrm{S2}^{0010000}_{000001100}+\mathrm{S2}^{0300000}_{001101100})
\end{aligned}
\tag{B.110}
$$

$$
\begin{aligned}
\mathcal{F}^{(3)}_{14}(L) =\;& 2\,(-1+\alpha)^3\,\alpha^2\,(-3+8\,\alpha^2\,(-2+\tau)-6\,\tau+\alpha\,(19+8\,\tau))\,\mathrm{F3}^{00}_{0010010}\\
&+ 32\,(-1+\alpha)^5\,\alpha^2\,(1+\alpha)\,\tau\,\mathrm{F3}^{00}_{0010020} - \frac{1}{\tau}\,(-1+\alpha)^2\,\alpha^2\,(16\,\alpha^3\,(-1+\tau)\\
&+ (7-6\,\tau)\,\tau-2\,\alpha^2\,(-10+5\,\tau+\tau^2)+\alpha\,(-4-19\,\tau+10\,\tau^2))\,\mathrm{F3}^{00}_{0011000}\\
&- 4\,(-1+\alpha)^3\,\alpha^3\,(4\,\alpha^2+(5-2\,\tau)\,\tau-\alpha\,(4+3\,\tau))\,\mathrm{F3}^{00}_{0012000}\\
&+ 2\,(-1+\alpha)^3\,\alpha^2\,(-2+4\,\alpha+\tau)\,\mathrm{F3}^{00}_{0101000} + (-1+\alpha)^2\,\alpha^2\,(-7+16\,\alpha^3\\
&- 10\,\tau-2\,\alpha^2\,(26+5\,\tau)+\alpha\,(43+8\,\tau))\,\mathrm{F3}^{00}_{0110000}\\
&- 2\,(-1+\alpha)^4\,\alpha^2\,(3\,(1+\tau)+8\,\alpha^2\,(2+\tau)-\alpha\,(19+16\,\tau))\,\mathrm{F3}^{00}_{0110010}\\
&+ 32\,(-1+\alpha)^6\,\alpha^3\,\tau\,\mathrm{F3}^{00}_{0110020}\\
&+ (-1+\alpha)^3\,\alpha^3\,(-4+7\,\tau+16\,\alpha^2\,\tau-2\,\alpha\,(-2+11\,\tau+\tau^2))\,\mathrm{F3}^{00}_{0111000}\\
&+ 4\,(-1+\alpha)^4\,\alpha^4\,\tau\,(-4+4\,\alpha+\tau)\,\mathrm{F3}^{00}_{0112000}\\
&- \frac{2}{\tau}\,(-1+\alpha)^2\,\alpha\,(4\,\alpha^2+\alpha\,(-2+\tau)+\tau)\,(\mathrm{F3}^{00}_{0001000}-\mathrm{F3}^{00}_{1000000})\\
&+ 2\,(-1+\alpha)^2\,\alpha^2\,(\mathrm{F3}^{00}_{0100000}-\mathrm{F3}^{00}_{1000000}) - \frac{2}{\tau}\,(-1+\alpha)^2\,\alpha\,(8\,\alpha^4\,(-1+\tau)^2\\
&+ \alpha\,(-4+\tau)\,\tau+2\,\tau^2+\alpha^2\,(2+9\,\tau-13\,\tau^2)-2\,\alpha^3(5-7\,\tau+2\,\tau^2))\,\mathrm{F3}^{00}_{1010000}\\
&+ 4\,(-1+\alpha)^3\,\alpha^2\,(-3+8\,\alpha)\,\mathrm{F3}^{01}_{0010010} + 64\,(-1+\alpha)^5\,\alpha^2\,\mathrm{F3}^{01}_{0010020}\\
&- \frac{2}{\tau}\,(-1+\alpha)^2\,\alpha\,(7\,\alpha+16\,\alpha^3-3\,\tau+2\,\alpha^2\,(-13+5\,\tau))\,\mathrm{F3}^{01}_{0011000}\\
&+ 8\,(-1+\alpha)^3\,\alpha^2\,(4\,\alpha^2+\tau+\alpha\,(-5+2\,\tau))\,\mathrm{F3}^{01}_{0012000}\\
&- \frac{4}{\tau}\,(-1+\alpha)^2\,\alpha\,(\mathrm{F3}^{01}_{0001000}-\mathrm{F3}^{01}_{1000000}) - \frac{2}{\tau}\,(-1+\alpha)^2\,\alpha\,(\alpha^2\,(26-30\,\tau)\\
&+ 16\,\alpha^3\,(-1+\tau)+7\,\tau-\alpha\,(7+5\,\tau))\,\mathrm{F3}^{01}_{1010000} + 16\,(-1+\alpha)^3\,\alpha^2\,\mathrm{F3}^{02}_{0012000}\\
&- \frac{12}{\tau}\,(-1+\alpha)^2\,\alpha\,(-1+2\,\alpha)\,(\mathrm{F3}^{02}_{0011000}-\mathrm{F3}^{02}_{1010000})\\
&+ 2\,(-1+\alpha)^2\,\alpha^2\,(5+2\,\alpha)\,\mathrm{F3}^{10}_{0110000}\\
&- (-1+\alpha)^2\,(1+\alpha+2\,\alpha^2\,(-1+\tau)+\tau-2\,\alpha\,\tau)\,\mathrm{G3}^{00}_{0000000}\\
&- \frac{1}{1+\tau}\,(-1+\alpha)^2\,(2+3\,\tau-\tau^3+12\,\alpha^4\,(1+\tau)-2\,\alpha^3\,(11+13\,\tau+2\,\tau^2)\\
&- \alpha^2\,(-9+3\,\tau+22\,\tau^2+8\,\tau^3)+\alpha\,(-1+15\,\tau+32\,\tau^2+16\,\tau^3))\;\;\mathrm{G3}^{00}_{0000010}\\
&+ (-1+\alpha)^3\,(1-\alpha+\tau)^2\,(1+(-1+2\,\alpha)\,\tau\;)\,\mathrm{G3}^{00}_{0000020}\\
&+ \frac{2}{1+\tau}\,(-1+\alpha)^2\,\alpha^2\,\tau^2\,(5+6\,\tau)\,\mathrm{G3}^{00}_{0001000}\\
&- (-1+\alpha)\,(1-\tau-2\,\tau^2+\alpha^2\,(9-37\,\tau-41\,\tau^2)+\alpha^4\,(32+9\,\tau-11\,\tau^2)
\end{aligned}
$$

$$+ \alpha^5 (-11 - 2\tau + \tau^2) + \alpha(-1 + 18\tau + 21\tau^2)$$
$$+ \alpha^3 (-30 + 13\tau + 27\tau^2)) \, \mathrm{G3}^{00}_{0010000}$$
$$- \frac{1}{1+\tau} (-1+\alpha)^2 ((1+\tau)^3 (-2+3\tau) + 12\alpha^6 (-1+\tau^2)$$
$$+ \alpha^5 (42 + 32\tau - 14\tau^2 - 4\tau^3) - \alpha^4 (53 + 36\tau + 9\tau^2 + 38\tau^3 + 8\tau^4)$$
$$+ \alpha^2 (-9 + 43\tau + 142\tau^2 + 99\tau^3 + 9\tau^4) + \alpha^3 (29 - 33\tau - 86\tau^2 - 4\tau^3$$
$$+ 16\tau^4) - \alpha(-5 + 3\tau + 48\tau^2 + 59\tau^3 + 19\tau^4)) \, \mathrm{G3}^{00}_{0010010}$$
$$+ (-1+\alpha)^4 (2\alpha^4 (-3+\tau)\tau - (-1+\tau)(1+\tau)^3$$
$$+ \alpha^3 (-1 + 8\tau + 9\tau^2 - 4\tau^3) + \alpha(-3 - 8\tau + 2\tau^2 + 8\tau^3 + \tau^4)$$
$$+ \alpha^2 (3 + 4\tau - 13\tau^2 + 2\tau^4)) \, \mathrm{G3}^{00}_{0010020}$$
$$- \frac{1}{1+\tau} (-1+\alpha)^2 \alpha^2 \tau (-1 - 5\tau + 2\tau^2 + 6\tau^3 + 4\alpha^3 (4 + 5\tau + \tau^2)$$
$$- 2\alpha^2 \tau (7 + 11\tau + 6\tau^2) + \alpha(-5 + 17\tau + 14\tau^2 - 4\tau^3)) \, \mathrm{G3}^{00}_{0011000}$$
$$- 2(-1+\alpha)^3 \alpha^3 \tau^2 (-1 + \alpha + 2\alpha^2 + 4\tau - 4\alpha\tau - 2\tau^2) \, \mathrm{G3}^{00}_{0012000}$$
$$+ 4(-1+\alpha)^2 \alpha^2 (-1 + 3\alpha)\tau \, \mathrm{G3}^{00}_{0100000}$$
$$+ (-1+\alpha)^2 \alpha^2 (4 + 15\tau - 6\tau^2 + 4\alpha^3 (-1 + 3\tau + 4\tau^2)$$
$$- 2\alpha^2 (-6 + 5\tau + 10\tau^2) + \alpha(-12 - 17\tau + 44\tau^2)) \, \mathrm{G3}^{00}_{0110000}$$
$$- 2(-1+\alpha)^4 \alpha^2 (-2 + 2\alpha^2 (-1+\tau) - 7\tau - 3\tau^2$$
$$+ \alpha(4 + 5\tau - 4\tau^2)) \, \mathrm{G3}^{00}_{0110010}$$
$$- 4(-1+\alpha)^6 \alpha^2 (-1 + \alpha - \tau)\tau \, \mathrm{G3}^{00}_{0110020}$$
$$+ (-1+\alpha)^3 \alpha^3 \tau^2 (1 + 4\alpha^2 (5+\tau) + 2\alpha(-7 + 2\tau)) \, \mathrm{G3}^{00}_{0111000}$$
$$+ 2(-1+\alpha)^4 \alpha^4 (-1 + 2\alpha)\tau^3 \, \mathrm{G3}^{00}_{0112000}$$
$$- 2(-1+\alpha)^2 \alpha (-1 - 6\alpha + 12\alpha^2)\tau (\alpha(-1+\tau) + \tau) \, \mathrm{G3}^{00}_{1010000}$$
$$- 2(-1+\alpha)^2 \alpha \, \mathrm{G3}^{01}_{0000000}$$
$$+ \frac{2}{1+\tau} (-1+\alpha)^2 (-2 - 3\tau - \tau^2 + 12\alpha^3 (1+\tau) + 2\alpha^2 (-5 - \tau + 4\tau^2)$$
$$- \alpha(1 + 13\tau + 16\tau^2)) \, \mathrm{G3}^{01}_{0000010}$$
$$- 4(-1+\alpha)^3 (-1 + \alpha - 3\alpha\tau + 2\alpha^2\tau + \tau^2 - 2\alpha\tau^2) \, \mathrm{G3}^{01}_{0000020}$$
$$+ \frac{4}{1+\tau} (-1+\alpha)^2 \alpha\tau (5 + 7\tau) \, \mathrm{G3}^{01}_{0001000}$$
$$+ 2(-1+\alpha)\alpha (1 - \alpha^2 (-2+\tau) + \tau + 2\alpha(1+\tau) + \alpha^3 (-5 + 3\tau)) \, \mathrm{G3}^{01}_{0010000}$$
$$+ \frac{2}{1+\tau} (-1+\alpha)^2 (-((1+\tau)^2 (-3 + 5\tau)) + 12\alpha^5 (-2 - \tau + \tau^2)$$
$$+ \alpha^3 (-34 + 19\tau + 55\tau^2 - 8\tau^3) + 2\alpha^4 (24 + 23\tau + 3\tau^2 + 4\tau^3)$$
$$- \alpha^2 (-23 + 70\tau + 140\tau^2 + 37\tau^3)$$
$$+ \alpha(-16 + 16\tau + 71\tau^2 + 39\tau^3)) \, \mathrm{G3}^{01}_{0010010}$$
$$- 2(-1+\alpha)^4 (3(-1+\tau)(1+\tau)^2 + 2\alpha^3 (4 - 5\tau + 2\tau^2)$$
$$+ \alpha(14 + 4\tau - 18\tau^2 - 4\tau^3)$$

$$
\begin{aligned}
&+ \alpha^2 (-19 + 9\tau + 6\tau^2 - 4\tau^3)) \,\mathrm{G3}^{01}_{0010020} \\
&+ \frac{2}{1+\tau} (-1+\alpha)^2 \alpha (-(\tau (2 + 5\tau + 3\tau^2)) + 4\alpha^3 (-3 + 4\tau + 7\tau^2) \\
&+ \alpha (1 + 9\tau - 4\tau^2 - 22\tau^3) + 2\alpha^2 (3 - 12\tau + \tau^2 + 21\tau^3)) \,\mathrm{G3}^{01}_{0011000} \\
&+ 4 (-1+\alpha)^3 \alpha^2 \tau (\tau (-2 + 3\tau) + \alpha^2 (-2 + 4\tau) \\
&+ \alpha (1 - 2\tau + 2\tau^2)) \,\mathrm{G3}^{01}_{0012000} \\
&- 2 (-1+\alpha)^2 \alpha (-1 - 6\alpha + 12\alpha^2) (\alpha (-1+\tau) + 3\tau) \,\mathrm{G3}^{01}_{1010000} \\
&+ 4 (-1+\alpha)^3 (1 + (-1 + 2\alpha)\tau\ ) \,\mathrm{G3}^{02}_{0000020} \\
&- \frac{8}{1+\tau} (-1+\alpha)^2 \tau (\mathrm{G3}^{02}_{0000010} - \mathrm{G3}^{02}_{0001000}) \\
&+ \frac{4}{1+\tau} (-1+\alpha)^2 (12\alpha^4 (1+\tau) - \tau (1+\tau) + 2\alpha^3 (-5 - \tau + 4\tau^2) \\
&+ \alpha (-1 + 9\tau + 18\tau^2) - \alpha^2 (1 + 21\tau + 28\tau^2)) \,\mathrm{G3}^{02}_{0010010} \\
&+ 4 (-1+\alpha)^4 (3 - 3\tau^2 + 2\alpha^2 (2 - 3\tau + \tau^2) \\
&+ \alpha (-7 + 10\tau + 5\tau^2)) \,\mathrm{G3}^{02}_{0010020} \\
&+ \frac{4}{1+\tau} (-1+\alpha)^2 (12\alpha^3 (1+\tau) + \tau (1+\tau) + 2\alpha^2 (-3 + 6\tau + 13\tau^2) \\
&- \alpha (2 + 13\tau + 19\tau^2)) \,\mathrm{G3}^{02}_{0011000} \\
&+ 8 (-1+\alpha)^3 \alpha \tau (2\alpha^2 + \tau + \alpha (-2 + 3\tau)) \,\mathrm{G3}^{02}_{0012000} \\
&- 4 (-1+\alpha)^2 \alpha (-1 - 6\alpha + 12\alpha^2) \,\mathrm{G3}^{02}_{1010000} \\
&+ 8 (-1+\alpha)^4 (1 + (-1 + 2\alpha)\tau\ ) \,\mathrm{G3}^{03}_{0010020} \\
&- \frac{8}{1+\tau} (-1+\alpha)^2 (1 + (-1 + 2\alpha)\tau\ ) (\mathrm{G3}^{03}_{0010010} - \mathrm{G3}^{03}_{0011000}) \\
&+ 16 (-1+\alpha)^3 \alpha \tau \,\mathrm{G3}^{03}_{0012000} - 2 (-1+\alpha)^3 \,\mathrm{G3}^{10}_{0000000} \\
&- 2 (-1+\alpha)^2 \alpha (2 - 5\alpha (-1+\tau) + 5\tau + \alpha^2 (-7 + 5\tau)) \,\mathrm{G3}^{10}_{0010000} \\
&- 8 (-1+\alpha)^2 \alpha^2 (-1 + 3\alpha) \,\mathrm{G3}^{10}_{0100000} \\
&- 2 (-1+\alpha)^2 \alpha^2 (4 + \alpha^2 (20 - 36\tau) + 12\alpha^3 (-1+\tau) - 11\tau \\
&+ 4\alpha (-3 + 14\tau)) \,\mathrm{G3}^{10}_{0110000} - 4 (-1+\alpha)^3 \alpha \,\mathrm{G3}^{11}_{0010000} \\
&- 16 (-1+\alpha)^3 \alpha^2 (-1 + 3\alpha) \,\mathrm{G3}^{20}_{0110000} - \mathrm{S3}^{0010000}_{000001100} \\
&+ 2\alpha (\mathrm{S3}^{0010000}_{000001100} - \mathrm{S3}^{0300000}_{001001110}) - \alpha^2 (\mathrm{S3}^{0010000}_{000001100} - \mathrm{S3}^{0300000}_{001001110}) \\
&+ \mathrm{S3}^{0300000}_{001001110} - 5\alpha (\mathrm{S3}^{0200000}_{001001100} - \mathrm{S3}^{2000000}_{001001100}) \\
&+ 5\alpha^2 (\mathrm{S3}^{0200000}_{001001100} - \mathrm{S3}^{2000000}_{001001100})
\end{aligned} \tag{B.111}
$$

$$
\mathcal{F}^{(4)}_{14}(L) = 0 \tag{B.112}
$$

$$
\begin{aligned}
\mathcal{F}^{(5)}_{14}(L) = &\ 2 (-1+\alpha)^2 \alpha^3 (\alpha (13 - 40\tau) + 16\alpha^2 (-1+\tau) + 10\tau) \,\mathrm{F5}^{00}_{0010001} \\
&- 32 (-2+\alpha) (-1+\alpha)^2 \alpha^5 \tau \,\mathrm{F5}^{00}_{0010002} - 2 (-1+\alpha)^2 \alpha^2 (-3 + \alpha^2 (13 - 40\tau) \\
&+ 16\alpha^3 (-1+\tau) + 2\alpha (3 + 5\tau)) \,\mathrm{F5}^{00}_{0110000}
\end{aligned}
$$

$$
\begin{aligned}
&+ 2\,(-1+\alpha)^4\,\alpha^2\,(3 - 19\,\alpha + 16\,\alpha^2 + 3\,\tau - 8\,\alpha\,\tau)\,\mathrm{F5}^{00}_{0110010} \\
&- 32\,(-1+\alpha)^6\,\alpha^3\,\tau\,\mathrm{F5}^{00}_{0110020} - 64\,(-1+\alpha)^5\,\alpha^2\,\mathrm{F5}^{01}_{0010020} \\
&- 4\,(-1+\alpha)^3\,\alpha^2\,(-11 + 16\,\alpha)\,(\mathrm{F5}^{01}_{0010010} - \mathrm{F5}^{01}_{1010000}) \\
&+ 2\,\alpha^2\,(2 - 3\,\alpha + \alpha^2)\,(\alpha + \tau)\,\mathrm{G5}^{00}_{0000001} \\
&+ (-1+\alpha)\,\alpha\,(1 + \tau - \alpha\,(1 + 4\,\tau) + \alpha^2\,(1 + 4\,\tau))\,\mathrm{G5}^{00}_{0010000} \\
&- 2\,(-1+\alpha)\,\alpha^3\,(\alpha\,(19 - 34\,\tau)\,\tau + 24\,\tau^2 + \alpha^3\,(-1 + 3\,\tau) + \alpha^2\,\tau\,(-18 + 11\,\tau)) \\
&\quad \times \mathrm{G5}^{00}_{0010001} + 4\,(-1+\alpha)\,\alpha^5\,\tau\,(\alpha^2 - 4\,\tau + \alpha\,(-3 + 2\,\tau))\,\mathrm{G5}^{00}_{0010002} \\
&- 2\,(-1+\alpha)^2\,\alpha^2\,(2 + 7\,\tau - 8\,\tau^2 + \alpha^3\,(-2 + 4\,\tau) - \alpha^2\,(-6 + \tau + 12\,\tau^2) \\
&+ 2\,\alpha\,(-3 - 5\,\tau + 17\,\tau^2))\,\mathrm{G5}^{00}_{0110000} \\
&+ 2\,(-1+\alpha)^4\,\alpha^2\,(-2 + 2\,\alpha^2\,(-1 + \tau) - 7\,\tau - 3\,\tau^2 \\
&+ \alpha\,(4 + 5\,\tau - 4\,\tau^2))\,\mathrm{G5}^{00}_{0110010} + 4\,(-1+\alpha)^6\,\alpha^2\,(-1 + \alpha - \tau)\,\tau\,\mathrm{G5}^{00}_{0110020} \\
&+ 4\,(-1+\alpha)^2\,\alpha\,(1+\alpha)\,\mathrm{G5}^{01}_{0000010} \;\; + 4\,\alpha^2\,(1 - 3\,\alpha + 2\,\alpha^2)\,\mathrm{G5}^{01}_{0010000} \\
&- 4\,(-1+\alpha)^3\,\alpha\,(4 + \tau + 4\,\alpha\,(1 + 4\,\tau) + \alpha^2\,(-8 + 5\,\tau))\,\mathrm{G5}^{01}_{0010010} \\
&- 8\,(-1+\alpha)^5\,\alpha\,(2 + \alpha\,(-2 + \tau) + 3\,\tau)\,\mathrm{G5}^{01}_{0010020} \\
&+ 4\,(-1+\alpha)^2\,\alpha^2\,(-15\,\tau + 17\,\alpha\,\tau + \alpha^2\,(-2 + 6\,\tau))\,\mathrm{G5}^{01}_{1010000} \\
&- 40\,(-1+\alpha)^3\,\alpha^2\,\mathrm{G5}^{02}_{0010010} - 16\,(-1+\alpha)^5\,\alpha\,\mathrm{G5}^{02}_{0010020} \\
&+ 16\,(-1+\alpha)^2\,\alpha^2\,(-2 + 3\,\alpha)\,\mathrm{G5}^{02}_{1010000}
\end{aligned}
\tag{B.113}
$$

$$
\begin{aligned}
\mathcal{F}^{(6)}_{14}(L) = &+\frac{4}{\tau}\,(-1+\alpha)^4\,\alpha\,(1 + \tau + \alpha\,(-1 + \tau^2))\,\mathrm{F6}^{00}_{0000110} \\
&+ 36\,(-1+\alpha)^2\,\alpha^3\,(\mathrm{F6}^{00}_{0000001} - \mathrm{F6}^{00}_{0100000}) \\
&- \frac{2}{\tau}\,(-1+\alpha)^2\,\alpha\,(6\,\alpha^2 + 2\,(-1 + \tau) - \alpha\,(4 + \tau))\,(\mathrm{F6}^{00}_{0000100} - \mathrm{F6}^{00}_{0100000}) \\
&- \frac{4}{\tau}\,(-1+\alpha)^4\,\alpha\,(1 + \tau + \alpha\,(-1 + 8\,\tau))\,\mathrm{F6}^{00}_{0100010} \\
&- 2\,(-1+\alpha)^2\,\alpha^3\,(-8 + \tau + 2\,\alpha\,(4 + \tau))\,\mathrm{F6}^{00}_{0101000} \\
&+ \frac{4}{\tau}\,(-1+\alpha)\,\alpha^2\,(\mathrm{F6}^{01}_{0001000} - \mathrm{F6}^{01}_{1000000})
\end{aligned}
\tag{B.114}
$$

$$
\begin{aligned}
\mathcal{F}^{(7)}_{14}(L) = &\,16\,(-1+\alpha)^2\,\alpha^3\,(\mathrm{F7}^{00}_{0000001} - \mathrm{F7}^{00}_{0100000}) \\
&- \frac{2}{\tau}\,(-1+\alpha)^2\,\alpha\,(4\,\alpha^2 + 2\,\tau - \alpha\,(4 + \tau))\,(\mathrm{F7}^{00}_{0000100} - \mathrm{F7}^{00}_{0100000}) \\
&- 16\,(-1+\alpha)^4\,\alpha^2\,\mathrm{F7}^{00}_{0100010} - 2\,(-1+\alpha)^2\,\alpha^3\,(-4 + 4\,\alpha + \tau)\,\mathrm{F7}^{00}_{0101000} \\
&+ \frac{4}{\tau}\,(-1+\alpha)\,\alpha^2\,(\mathrm{F7}^{01}_{0001000} - \mathrm{F7}^{01}_{1000000})
\end{aligned}
\tag{B.115}
$$

$$
\begin{aligned}
\mathcal{F}^{(8)}_{14}(L) = &\,(-3 + 7\,\alpha - 7\,\alpha^2)\,\tau\,\mathrm{G8}^{00}_{0000000} \\
&+ 2\,(-1+\alpha)\,\alpha^2\,\tau\,(1 + 8\,\alpha^2 + \alpha\,(-9 + \tau) + \tau\,)\,\mathrm{G8}^{00}_{0000100}
\end{aligned}
$$

$$
\begin{aligned}
&- 2\,(-1+\alpha)^2\,\alpha^2\,\tau\,(4\,\alpha^2 - 2\,(-1+\tau)\,\tau + \alpha\,(-4+3\,\tau))\,\mathrm{G8}^{00}_{0000200}\\
&+ 2\,\alpha\,(-2\,\alpha^2 - 11\,\alpha^3 + 8\,\alpha^4 + \alpha\,(5-2\,\tau) - \tau)\,\tau\,\mathrm{G8}^{00}_{0100000}\\
&+ 2\,(-1+\alpha)^2\,\alpha^2\,\tau\,(3\,\tau + 4\,\alpha^2\,(1+2\,\tau) - 2\,\alpha\,(2+5\,\tau))\,\mathrm{G8}^{00}_{0101000}\\
&+ 2\,(-1+\alpha)^3\,\alpha^3\,\tau^2\,(-4+4\,\alpha+\tau)\,\mathrm{G8}^{00}_{0102000}\\
&+ 4\,(-1+\alpha)\,\alpha\,(4\,\alpha^2 + 2\,\alpha\,(-2+\tau) - 3\,\tau)\,\mathrm{G8}^{01}_{0001000}\\
&+ 4\,(-1+\alpha)^2\,\alpha\,\tau\,(4\,\alpha^2 + \tau + \alpha\,(-5+2\,\tau))\,\mathrm{G8}^{01}_{0002000}\\
&+ 8\,(-1+\alpha)\,(-4\,\alpha^2 + 4\,\alpha^3 + 3\,\tau - 2\,\alpha\,\tau)\,\mathrm{G8}^{01}_{1000000}\\
&+ 8\,(-1+\alpha)^2\,\alpha\,\tau\,\mathrm{G8}^{02}_{0002000} + 8\,(3-5\,\alpha+2\,\alpha^2)\,(\mathrm{G8}^{02}_{0001000} - \mathrm{G8}^{02}_{1000000})\\
&- 2\,(3-4\,\alpha+\alpha^2)\,(-\mathrm{S8}^{0100000}_{000001100} + \mathrm{S8}^{0200000}_{000101100})\\
&+ 2\,(3-5\,\alpha+2\,\alpha^2)\,(-\mathrm{S8}^{0100000}_{000001100} + \mathrm{S8}^{0200000}_{100001100})
\end{aligned}
\tag{B.116}
$$

$$
\begin{aligned}
\mathcal{F}^{(9)}_{14}(L) =& -2\,(-1+\alpha)^2\,\alpha\,\mathrm{G9}^{00}_{0000000}\\
&+ 2\,(-1+\alpha)\,\alpha\,(\alpha^2 + 8\,\alpha^3\,\tau + (1+\tau)^2 - 2\,\alpha\,(1+5\,\tau))\,\mathrm{G9}^{00}_{0000010}\\
&+ 16\,(-1+\alpha)^4\,\alpha\,(1+\alpha)\,\tau\,\mathrm{G9}^{00}_{0000020}\\
&+ 2\,(-1+\alpha)\,\alpha\,(7\,\alpha - 15\,\alpha^2 + 8\,\alpha^3 - 2\,\tau)\,\tau\,\mathrm{G9}^{00}_{0001000}\\
&+ 2\,(-1+\alpha)^2\,\alpha^2\,\tau\,(4\,\alpha^2 + (5-2\,\tau)\,\tau - \alpha\,(4+3\,\tau))\,\mathrm{G9}^{00}_{0002000}\\
&- 2\,(-1+\alpha)^2\,\alpha^2\,(5+8\,\alpha)\,\tau\,\mathrm{G9}^{00}_{0100000}\\
&+ 16\,(-1+\alpha)^3\,\alpha^2\,\tau\,\mathrm{G9}^{00}_{0100010} + 16\,(-1+\alpha)^5\,\alpha^2\,\tau\,\mathrm{G9}^{00}_{0100020}\\
&- 2\,(-1+\alpha)^2\,\alpha^2\,\tau\,(3\,\tau + 4\,\alpha^2\,(1+2\,\tau) - 2\,\alpha\,(2+5\,\tau))\,\mathrm{G9}^{00}_{0101000}\\
&- 2\,(-1+\alpha)^3\,\alpha^3\,\tau^2\,(-4+4\,\alpha+\tau)\,\mathrm{G9}^{00}_{0102000}\\
&- 16\,(-1+\alpha)^2\,\alpha^2\,(1+\alpha)\,\tau\,\mathrm{G9}^{00}_{1000000}\\
&+ 8\,(-1+\alpha)\,\alpha\,(1-5\,\alpha+4\,\alpha^2+\tau)\,\mathrm{G9}^{01}_{0000010} + 32\,(-1+\alpha)^4\,\alpha\,\mathrm{G9}^{01}_{0000020}\\
&- 4\,(-1+\alpha)\,\alpha\,(-4\,\alpha + 4\,\alpha^2 + 3\,\tau)\,\mathrm{G9}^{01}_{0001000}\\
&- 4\,(-1+\alpha)^2\,\alpha\,\tau\,(4\,\alpha^2 + \tau + \alpha\,(-5+2\,\tau))\,\mathrm{G9}^{01}_{0002000}\\
&+ 8\,(-1+\alpha)\,\alpha\,(\mathrm{G9}^{02}_{0000010} - \mathrm{G9}^{02}_{0001000}) - 8\,(-1+\alpha)^2\,\alpha\,\tau\,\mathrm{G9}^{02}_{0002000}\\
&- 32\,(-1+\alpha)^2\,\alpha^2\,(\mathrm{G9}^{01}_{1000000} - \mathrm{G9}^{10}_{0100000})\\
&+ 8\,(-1+\alpha)\,\alpha\,(\mathrm{S9}^{0100000}_{000001100} - \mathrm{S9}^{1000000}_{000001100})\\
&- 2\,(-1+\alpha)\,\alpha\,(\mathrm{S9}^{0200000}_{000001110} - \mathrm{S9}^{1000000}_{000001100})
\end{aligned}
\tag{B.117}
$$

$$
\mathcal{F}^{(10)}_{14}(L) = 0 \tag{B.118}
$$

$$
\begin{aligned}
\mathcal{F}^{(11)}_{14}(L) =& -16\,\alpha^4\,(2-3\,\alpha+\alpha^2)\,\tau\,\mathrm{G11}^{00}_{0000002}\\
&+ 16\,(-2+\alpha)\,(-1+\alpha)^2\,\alpha^2\,\tau\,(\mathrm{G11}^{00}_{0000001} - \mathrm{G11}^{00}_{0100000})\\
&- 16\,(-1+\alpha)^3\,\alpha^2\,\tau\,\mathrm{G11}^{00}_{0100010} - 16\,(-1+\alpha)^5\,\alpha^2\,\tau\,\mathrm{G11}^{00}_{0100020}\\
&- 32\,(-1+\alpha)^4\,\alpha\,\mathrm{G11}^{01}_{0000020} - 32\,(-1+\alpha)^2\,\alpha^2\,(\mathrm{G11}^{01}_{0000010} - \mathrm{G11}^{01}_{1000000})
\end{aligned}
\tag{B.119}
$$

Transverse

$$
\begin{aligned}
\mathcal{F}_{14}^{(1)}(T) &= 4\,(1-2\,\alpha+2\,\alpha^2)\,\tau\,\mathrm{G1}^{00}_{0000000} \\
&- 4\,(-1+\alpha)\,\alpha\,(\alpha^3\,(4-16\,\tau)+\tau\,(1+3\,\tau)+2\,\alpha^4\,(-1+4\,\tau) \\
&+ \alpha\,(1-6\,\tau-4\,\tau^2)+\alpha^2\,(-3+14\,\tau+4\,\tau^2))\,\mathrm{G1}^{00}_{0010000} \\
&+ 2\,(-1+\alpha)^2\,\alpha^2\,(6\,\alpha^2\,(1-4\,\tau)^2+\alpha\,(-2+20\,\tau-48\,\tau^2)+\tau\,(-2+9\,\tau \\
&+ 4\,\tau^2)-8\,\alpha^3\,(1-7\,\tau+12\,\tau^2)+4\,\alpha^4\,(1-7\,\tau+12\,\tau^2))\,\mathrm{G1}^{00}_{0020000} \\
&- 8\,\alpha^3\,(-1+3\,\alpha-4\,\alpha^2+2\,\alpha^3)\,(-1+\alpha+\tau)\,\mathrm{G1}^{00}_{0100000} \\
&- 4\,(-1+\alpha)^2\,\alpha^3\,(-2+8\,\alpha^4\,(-1+\tau)+11\,\tau-9\,\tau^2+4\,\alpha^3\,(5-9\,\tau+2\,\tau^2) \\
&- 4\,\alpha^2\,(5-13\,\tau+5\,\tau^2)+\alpha\,(10-37\,\tau+20\,\tau^2))\,\mathrm{G1}^{00}_{0110000} \\
&- 4\,(-1+\alpha)^2\,\alpha^3\,(4\,\alpha^6\,(-1+\tau)^2-2\,\tau\,(1-5\,\tau+6\,\tau^2) \\
&+ \alpha^2\,(10-52\,\tau+92\,\tau^2-53\,\tau^3)+4\,\alpha^5\,(-4+11\,\tau-8\,\tau^2+\tau^3) \\
&- 2\,\alpha^4\,(-13+44\,\tau-43\,\tau^2+10\,\tau^3)+\alpha\,(-2+17\,\tau-47\,\tau^2+40\,\tau^3) \\
&+ \alpha^3\,(-22+89\,\tau-113\,\tau^2+42\,\tau^3))\,\mathrm{G1}^{00}_{0120000} \\
&- 8\,(-1+\alpha)\,\alpha\,(-12\,\alpha^3+8\,\alpha^4+4\,\tau+2\,\alpha^2\,(4+3\,\tau)-\alpha\,(2+7\,\tau))\,\mathrm{G1}^{01}_{0010000} \\
&+ 8\,(-1+\alpha)^2\,\alpha^2\,(2\,\tau\,(1+3\,\tau)-20\,\alpha^3\,(-1+4\,\tau)+12\,\alpha^4\,(-1+4\,\tau) \\
&+ \alpha\,(4-23\,\tau-6\,\tau^2)+2\,\alpha^2\,(-7+33\,\tau+2\,\tau^2))\,\mathrm{G1}^{01}_{0020000} \\
&- 16\,(-1+\alpha)^3\,\alpha\,(1-2\,\alpha+2\,\alpha^2)\,\mathrm{G1}^{01}_{1000000}-8\,(-1+\alpha)^3\,\alpha^2\,(2 \\
&+ 8\,\alpha^3\,(-2+\tau)+5\,\tau-4\,\alpha\,(3+\tau)+4\,\alpha^2\,(5+\tau))\,\mathrm{G1}^{01}_{1010000} \\
&- 8\,(-1+\alpha)^3\,\alpha^2\,(-\tau^2+\alpha\,\tau\,(7+2\,\tau)-2\,\alpha^3\,(-7-6\,\tau+\tau^2)+4\,\alpha^5\,(3-4\,\tau \\
&+ \tau^2)+4\,\alpha^4\,(-5+\tau+2\,\tau^2)+\alpha^2\,(-4-20\,\tau+9\,\tau^2))\,\mathrm{G1}^{01}_{1020000} \\
&+ 16\,(-1+\alpha)^2\,\alpha^2\,(-16\,\alpha^3+12\,\alpha^4+2\,\tau+2\,\alpha^2\,(5+\tau) \\
&- \alpha\,(2+3\,\tau))\,\mathrm{G1}^{02}_{0020000}-64\,(-1+\alpha)^3\,\alpha^2\,(1-2\,\alpha+2\,\alpha^2)\,\mathrm{G1}^{02}_{1010000} \\
&- 16\,(-1+\alpha)^3\,\alpha^3\,(2-10\,\alpha+16\,\alpha^2+3\,\tau+4\,\alpha^3\,(-3+2\,\tau))\,\mathrm{G1}^{02}_{1020000} \\
&- 64\,(-1+\alpha)^3\,\alpha^3\,(1-2\,\alpha+2\,\alpha^2)\,\mathrm{G1}^{03}_{1020000}-8\,(-1+\alpha)^2\,\alpha^2\,(2-48\,\alpha^3 \\
&+ 24\,\alpha^4+3\,\tau-4\,\alpha\,(4+\tau)+4\,\alpha^2\,(10+\tau))\,\mathrm{G1}^{11}_{0020000}
\end{aligned} \tag{B.120}
$$

$$
\begin{aligned}
\mathcal{F}_{14}^{(2)}(T) &= -\frac{1}{\tau}\,(-1+\alpha)\,\alpha^2\,(-10+3\,\tau+12\,\tau^2+8\,\alpha^4\,(-3+2\,\tau) \\
&+ 2\,\alpha^3\,(34-30\,\tau+\tau^2)+2\,\alpha^2\,(-38+23\,\tau+11\,\tau^2\ ) \\
&- 3\,\alpha\,(-14+3\,\tau+14\,\tau^2)\ )\,\mathrm{F2}^{00}_{0010100} \\
&+ 4\,(-1+\alpha)^2\,\alpha^3\,(-2+4\,\alpha^3+\tau+\alpha^2\,(-8+3\,\tau)-2\,\alpha\,(-3+\tau^2))\,\mathrm{F2}^{00}_{0010200} \\
&- \frac{1}{\tau}\,\alpha\,(1-2\,\alpha+2\,\alpha^2)\,(2+4\,\alpha^2+3\,\tau-\alpha\,(6+\tau))\,(\mathrm{F2}^{00}_{0000100}-\mathrm{F2}^{00}_{0100000}) \\
&- \alpha\,(-1+3\,\alpha-4\,\alpha^2+2\,\alpha^3)\,(2+4\,\alpha^2+\alpha\,(-6+\tau))\,\mathrm{F2}^{00}_{0101000} \\
&+ \frac{1}{\tau}\,\alpha^2\,(10-9\,\tau-14\,\tau^2+8\,\alpha^5\,(-3+4\,\tau)+\alpha^2\,(118-125\,\tau-78\,\tau^2) \\
&+ 2\,\alpha^4\,(46-66\,\tau+\tau^2)+4\,\alpha\,(-13+11\,\tau+16\,\tau^2)
\end{aligned}
$$

$$
\begin{aligned}
&+ \alpha^3\,(-144 + 190\,\tau + 24\,\tau^2))\,\mathrm{F2}^{00}_{0110000} \\
&- (-1+\alpha)^2\,\alpha^2\,(-2 + \alpha\,(10 - 7\,\tau) + 8\,\alpha^4\,(-1 + 2\,\tau) + 10\,\alpha^2\,(-2 + 3\,\tau) \\
&- 2\,\alpha^3\,(-10 + 20\,\tau + \tau^2))\,\mathrm{F2}^{00}_{0111000} - 4\,(-1+\alpha)^3\,\alpha^3\,(-2 + 6\,\alpha + 4\,\alpha^3 \\
&+ \alpha^2\,(-8 + \tau))\,\tau\,\mathrm{F2}^{00}_{0112000} + \frac{2}{\tau}\,(-1+\alpha)^2\,(24\,\alpha^4 + 2\,\tau \\
&+ 2\,\alpha^3\,(-18 + 7\,\tau) + 2\,\alpha^2\,(12 + 7\,\tau) - \alpha\,(3 + 20\,\tau))\,\mathrm{F2}^{01}_{0011000} \\
&- 8\,(-1+\alpha)^3\,\alpha\,(4\,\alpha^3 - 2\,\tau + \alpha\,(3 + \tau) + \alpha^2\,(-5 + 2\,\tau))\,\mathrm{F2}^{01}_{0012000} \\
&+ \frac{2}{\tau}\,(-1 + 3\,\alpha - 4\,\alpha^2 + 2\,\alpha^3)\,(\mathrm{F2}^{01}_{0001000} - \mathrm{F2}^{01}_{1000000}) - \frac{2}{\tau}\,(-1+\alpha)^2\,(24\,\alpha^4 \\
&+ 3\,\tau + 2\,\alpha^3\,(-18 + 7\,\tau) + 2\,\alpha^2\,(12 + 7\,\tau) - \alpha\,(3 + 22\,\tau))\,\mathrm{F2}^{01}_{1010000} \\
&- 16\,(-1+\alpha)^4\,\alpha\,\mathrm{F2}^{02}_{0012000} \\
&+ \frac{4}{\tau}\,(-1+\alpha)^2\,(1 - 8\,\alpha + 8\,\alpha^2)\,(\mathrm{F2}^{02}_{0011000} - \mathrm{F2}^{02}_{1010000}) \\
&+ 8\,(-1+\alpha)^2\,\alpha^3\,(-1 + \tau)\,\tau\,\mathrm{G2}^{00}_{0000100} - 2\,(-1+\alpha)^3\,\alpha^3\,(-1+\tau)^2\,\tau\,\mathrm{G2}^{00}_{0000200} \\
&+ 2\,(-1+\alpha)\,\alpha\,\tau\,(-5\,\tau - 2\,\alpha\,(1 + \tau) + 2\,\alpha^2\,(1 + \tau))\,\mathrm{G2}^{00}_{0010000} \\
&+ 2\,(-1+\alpha)^2\,\alpha^2\,\tau\,(6 - 9\,\tau + 10\,\tau^2 - 3\,\alpha^2\,(-7 + \tau^2) + 2\,\alpha^3\,(-2 - 5\,\tau + 2\,\tau^2) \\
&+ \alpha\,(-23 - \tau + 3\,\tau^2))\,\mathrm{G2}^{00}_{0010100} - 2\,(-1+\alpha)^3\,\alpha^3\,\tau\,(4\,(-1+\tau)\,\tau^2 \\
&+ \alpha^2\,(-1 + \tau - 3\,\tau^2 + \tau^3) - \alpha\,(-1 - 2\,\tau + \tau^2 + \tau^3))\,\mathrm{G2}^{00}_{0010200} \\
&- 2\,(-1+\alpha)^2\,\alpha^2\tau\,(6 - 6\,\tau + 4\,\alpha^2\,\tau + 2\,\alpha^3\,(4 + \tau) + \alpha(-14 + 17\,\tau))\,\mathrm{G2}^{00}_{0110000} \\
&- 2\,(-1+\alpha)^2\,\alpha^3\,\tau^2\,(-7 - 17\,\alpha^2 + 2\,\alpha^3\,(5 + \tau) + \alpha\,(14 + \tau))\,\mathrm{G2}^{00}_{0111000} \\
&- 2\,(-1+\alpha)^4\,\alpha^4\,(-1 + 2\,\alpha)\,\tau^3\,\mathrm{G2}^{00}_{0112000} - 16\,(-1+\alpha)^3\,\alpha\,\tau\,\mathrm{G2}^{01}_{0001000} \\
&- 8\,(-1+\alpha)^3\,\alpha^2\,(-1 + \tau)\,\tau\,\mathrm{G2}^{01}_{0002000} + 4\,\alpha^2\,(1 - 3\,\alpha + 2\,\alpha^2)\,\tau\,\mathrm{G2}^{01}_{0010000} \\
&- 4\,(-1+\alpha)^2\,\alpha\,(-13\,\tau^2 + \alpha\,\tau\,(-7 + 8\,\tau) + \alpha^2\,(3 + 8\,\tau - 10\,\tau^2) \\
&+ 2\,\alpha^3\,(-3 + 3\,\tau + 4\,\tau^2))\,\mathrm{G2}^{01}_{0011000} - 4\,(-1+\alpha)^3\,\alpha^2\,\tau\,(\tau\,(-6 + 7\,\tau) \\
&- \alpha\,(2 - 4\,\tau + \tau^2\,) + \alpha^2\,(1 - 2\,\tau + 3\,\tau^2))\;\;\mathrm{G2}^{01}_{0012000} \\
&- 4\,(-1+\alpha)^2\,\alpha^2\,(13\,\tau + 2\,\alpha^2\,(3 + \tau) - 3\,\alpha\,(1 + 8\,\tau))\,\mathrm{G2}^{01}_{1010000} \\
&- 8(-1+\alpha)^3\,\alpha\,\tau\,\mathrm{G2}^{02}_{0002000} - 8(-1+\alpha)^2\,\alpha^2\,(-3 - 4\,\tau + \alpha\,(6 + 4\,\tau))\mathrm{G2}^{02}_{0011000} \\
&- 8\,(-1+\alpha)^3\,\alpha\,\tau\,(\alpha + 3\,\tau + \alpha^2\,(-1 + 3\,\tau))\,\mathrm{G2}^{02}_{0012000} \\
&+ 24\,(-1+\alpha)^2\,\alpha^2\,(-1 + 2\,\alpha)\,\mathrm{G2}^{02}_{1010000} - 16\,(-1+\alpha)^3\,\alpha^2\,\tau\,\mathrm{G2}^{03}_{0012000}
\end{aligned} \tag{B.121}
$$

$$
\begin{aligned}
\mathcal{F}^{(3)}_{14}(T) &= 2\,(-1+\alpha)^3\,\alpha\,(8\,\alpha^3\,(-2 + \tau) + 6\,\tau + \alpha^2\,(19 + 8\,\tau) \\
&- \alpha\,(7 + 12\,\tau))\,\mathrm{F3}^{00}_{0010010} + 8\,(-1+\alpha)^4\,\alpha^2\,(-1 + 4\,\alpha^2)\,\tau\,\mathrm{F3}^{00}_{0010020} \\
&- \frac{1}{\tau}\,(-1+\alpha)^2\,\alpha\,(16\,\alpha^4\,(-1 + \tau) - 2\,\tau\,(2 + 3\,\tau) + \alpha\,(2 + 25\,\tau - 4\,\tau^2) \\
&- 2\,\alpha^3\,(-10 + 5\,\tau + \tau^2) + 2\,\alpha^2\,(-6 - 13\,\tau + 12\,\tau^2)\;)\,\mathrm{F3}^{00}_{0011000} \\
&- 4\,(-1+\alpha)^3\,\alpha^2\,(4\,\alpha^3 + 2\,(-2 + \tau)\,\tau - \alpha^2\,(4 + 3\,\tau) \\
&+ \alpha\,(2 + 6\,\tau - 2\,\tau^2))\,\mathrm{F3}^{00}_{0012000}
\end{aligned}
$$

$$
\begin{aligned}
&+\alpha\,(-1+3\,\alpha-4\,\alpha^2+2\,\alpha^3)\,(2+4\,\alpha^2+\alpha\,(-6+\tau))\,\mathrm{F3}^{00}_{0101000}\\
&+(-1+\alpha)\,\alpha^2\,(11+16\,\alpha^4+2\,\tau+18\,\alpha^2\,(5+\tau)-2\,\alpha^3\,(34+5\,\tau)\\
&-\alpha\,(49+20\,\tau))\,\mathrm{F3}^{00}_{0110000}\\
&-2\,(-1+\alpha)^3\,\alpha^2\,(-7-7\,\tau-2\,\tau^2+8\,\alpha^3\,(2+\tau)-\alpha^2\,(35+24\,\tau)\\
&+\alpha\,(26+27\,\tau+4\,\tau^2))\,\mathrm{F3}^{00}_{0110010}\\
&+8\,(-1+\alpha)^4\,\alpha^2\,(-1+2\,\alpha)\,\tau\,(1-3\,\alpha+2\,\alpha^2+\tau)\,\mathrm{F3}^{00}_{0110020}\\
&+(-1+\alpha)^2\,\alpha^2\,(-2+\alpha\,(6-7\,\tau)+16\,\alpha^4\,\tau+2\,\alpha^2\,(-4+15\,\tau)\\
&-2\,\alpha^3\,(-2+19\,\tau+\tau^2))\,\mathrm{F3}^{00}_{0111000}\\
&+4\,(-1+\alpha)^3\,\alpha^3\,(-2+6\,\alpha+4\,\alpha^3+\alpha^2\,(-8+\tau))\,\tau\,\mathrm{F3}^{00}_{0112000}\\
&+\frac{1}{\tau}\,(1-3\,\alpha+4\,\alpha^2-2\,\alpha^3)\,(4\,\alpha^2+\alpha\,(-2+\tau)+2\,\tau)\,(\mathrm{F3}^{00}_{0001000}-\mathrm{F3}^{00}_{1000000})\\
&+\alpha\,(-1+3\,\alpha-4\,\alpha^2+2\,\alpha^3)\,(\mathrm{F3}^{00}_{0100000}-\mathrm{F3}^{00}_{1000000})\\
&-\frac{2}{\tau}\,(-1+\alpha)^2\,(8\,\alpha^5\,(-1+\tau)^2-\tau^2+\alpha\,\tau\,(2+5\,\tau)+\alpha^3\,(6+6\,\tau-14\,\tau^2)\\
&-2\,\alpha^4\,(5-7\,\tau+2\,\tau^2)+\alpha^2\,(-1-11\,\tau+4\,\tau^2))\,\mathrm{F3}^{00}_{1010000}\\
&+4\,(-1+\alpha)^3\,\alpha\,(1-3\,\alpha+8\,\alpha^2)\,\mathrm{F3}^{01}_{0010010}\\
&+16\,(1-2\,\alpha)^2\,(-1+\alpha)^4\,\alpha\,\mathrm{F3}^{01}_{0010020}\\
&-\frac{2}{\tau}\,(-1+\alpha)^2\,(16\,\alpha^4+2\,\tau+6\,\alpha^2\,(3+2\,\tau)+2\,\alpha^3\,(-13+5\,\tau)\\
&-\alpha\,(3+16\,\tau))\,\mathrm{F3}^{01}_{0011000}\\
&+8\,(-1+\alpha)^3\,\alpha\,(4\,\alpha^3-2\,\tau+\alpha\,(3+\tau)+\alpha^2\,(-5+2\,\tau))\,\mathrm{F3}^{01}_{0012000}\\
&+\frac{1}{\tau}\,(2-6\,\alpha+8\,\alpha^2-4\,\alpha^3)\,(\mathrm{F3}^{01}_{0001000}-\mathrm{F3}^{01}_{1000000})\\
&-\frac{2}{\tau}\,(-1+\alpha)^2\,(\alpha^3\,(26-30\,\tau)+16\,\alpha^4\,(-1+\tau)-3\,\tau-2\,\alpha^2\,(9+2\,\tau)\\
&+\alpha\,(3+17\,\tau))\,\mathrm{F3}^{01}_{1010000}+16\,(-1+\alpha)^4\,\alpha\,\mathrm{F3}^{02}_{0012000}\\
&-\frac{4}{\tau}\,(-1+\alpha)^2\,(1-6\,\alpha+6\,\alpha^2)\,(\mathrm{F3}^{02}_{0011000}-\mathrm{F3}^{02}_{1010000})\\
&+2\,\alpha^2\,(-1-\alpha+2\,\alpha^3)\,\mathrm{F3}^{10}_{0110000}-12\,\alpha\,(1-3\,\alpha+2\,\alpha^2)\,\tau\,\mathrm{G3}^{00}_{0000000}\\
&+2\,(-1+\alpha)^2\,\alpha\,(-1+6\,\alpha^3\,(-1+\tau)+\tau+\alpha\,(-1+5\,\tau-4\,\tau^2)\\
&+\alpha^2\,(5-9\,\tau+4\,\tau^2))\,\mathrm{G3}^{00}_{0001000}+2\,(-1+\alpha)^3\,\alpha^3\,(-1+\tau)^2\,\tau\,\mathrm{G3}^{00}_{0002000}\\
&-2\,(-1+\alpha)\,(2\,\tau+6\,\alpha^5\,\tau+\alpha\,(1+3\,\tau-16\,\tau^2)+\alpha^3\,(4+28\,\tau-16\,\tau^2)\\
&+3\,\alpha^4\,(-1-9\,\tau+4\,\tau^2)+2\,\alpha^2\,(-1-6\,\tau+13\,\tau^2))\,\mathrm{G3}^{00}_{0010000}\\
&-2\,(-1+\alpha)^2\,(2\,\alpha\,(2-3\,\tau)\,\tau-2\,\tau\,(2+\tau)+\alpha^5\,(-2+4\,\tau)\\
&+\alpha^4\,(6+7\,\tau-12\,\tau^2)+\alpha^2\,(2+10\,\tau+3\,\tau^2)\\
&-\alpha^3\,(6+21\,\tau+4\,\tau^2))\,\mathrm{G3}^{00}_{0010010}\\
&-2\,(-1+\alpha)^4\,\tau\,(6\,\alpha+2\,\alpha^4-4\,\alpha^3\,\tau-2\,(1+\tau)-\alpha^2\,(6+\tau))\,\mathrm{G3}^{00}_{0010020}\\
&+2\,(-1+\alpha)^2\,\alpha^2\,(-1+6\,\alpha^4\,(-1+\tau)^2+2\,\tau+19\,\tau^2-14\,\tau^3\\
&+\alpha\,\tau\,(7-31\,\tau+9\,\tau^2)-3\,\alpha^2\,(-2+7\,\tau-12\,\tau^2+3\,\tau^3)
\end{aligned}
$$

$$
\begin{aligned}
&+\alpha^3\,(-11+18\,\tau-21\,\tau^2+4\,\tau^3))\,\mathrm{G3}^{00}_{0011000}\\
&+2\,(-1+\alpha)^3\,\alpha^3\,\tau\,(\tau\,(3-8\,\tau+4\,\tau^2)-\alpha\,(-1+4\,\tau-7\,\tau^2+\tau^3)\\
&+\alpha^2\,(-1+\tau-3\,\tau^2+\tau^3))\,\mathrm{G3}^{00}_{0012000}\\
&+4\,(-1+\alpha)^2\,\alpha^2\,(-1+3\,\alpha)\,(-1+\alpha+\tau)\,\mathrm{G3}^{00}_{0100000}\\
&+2\,(-1+\alpha)^2\,\alpha^2\,(2+6\,\alpha^4\,(-1+\tau)+6\,\tau+\tau^2+\alpha^2\,(-4+13\,\tau-10\,\tau^2)\\
&+2\,\alpha^3\,(6-7\,\tau+4\,\tau^2)+\alpha\,(-4-11\,\tau+27\,\tau^2))\,\mathrm{G3}^{00}_{0110000}\\
&-2\,(-1+\alpha)^2\,\alpha^2\,(-2+2\,\alpha^4\,(-1+\tau)-6\,\tau-4\,\tau^2-\tau^3+\alpha^3\,(8+\tau-4\,\tau^2)\\
&+2\,\alpha^2\,(-6-7\,\tau+\tau^2)+\alpha\,(8+17\,\tau+6\,\tau^2-2\,\tau^3))\,\mathrm{G3}^{00}_{0110010}\\
&-2\,(-1+\alpha)^4\,\alpha^2\,\tau\,(-2+2\,\alpha^3-\tau-\tau^2+3\,\alpha\,(2+\tau)-2\,\alpha^2\,(3+\tau))\,\mathrm{G3}^{00}_{0110020}\\
&+2\,(-1+\alpha)^2\,\alpha^3\,\tau^2\,(-7-17\,\alpha^2+2\,\alpha^3\,(5+\tau)+\alpha\,(14+\tau))\,\mathrm{G3}^{00}_{0111000}\\
&+2\,(-1+\alpha)^4\,\alpha^4\,(-1+2\,\alpha)\,\tau^3\,\mathrm{G3}^{00}_{0112000}\\
&-12\,(-1+\alpha)^2\,\alpha^2\,(-1+2\,\alpha)\,\tau\,(\alpha\,(-1+\tau)+\tau)\,\mathrm{G3}^{00}_{1010000}\\
&+4\,(-1+\alpha)^2\,(1+\alpha+6\,\alpha^3-4\,\alpha\,\tau+\alpha^2\,(-5+4\,\tau))\,\mathrm{G3}^{01}_{0001000}\\
&+8\,(-1+\alpha)^3\,\alpha^2\,(-1+\tau)\,\tau\,\mathrm{G3}^{01}_{0002000}\\
&+4\,(-1+\alpha)\,\alpha^2\,(\alpha\,(3-9\,\tau)+3\,\tau+\alpha^2\,(-3+2\,\tau))\,\mathrm{G3}^{01}_{0010000}\\
&+4\,(-1+\alpha)^2\,(2+3\,\tau-12\,\alpha^2\,\tau+2\,\alpha^4\,(-5+3\,\tau)+\alpha\,(-6+5\,\tau)\\
&+\alpha^3\,(14+13\,\tau))\,\mathrm{G3}^{01}_{0010010}\\
&+4\,(-1+\alpha)^4\,(1+2\,\alpha^3\,(-2+\tau)+3\,\tau+4\,\alpha^2\,(2+\tau)-\alpha\,(5+4\,\tau))\,\mathrm{G3}^{01}_{0010020}\\
&+4\,(-1+\alpha)^2\,\alpha\,(2+12\,\alpha^4\,(-1+\tau)-2\,\tau-13\,\tau^2+\alpha\,\tau\,(-7+8\,\tau)\\
&+\alpha^2\,(-9+20\,\tau-10\,\tau^2)+8\,\alpha^3\,(2-2\,\tau+\tau^2))\,\mathrm{G3}^{01}_{0011000}+4\,(-1+\alpha)^3\,\alpha^2\\
&\quad\times\,\tau\,(\tau\,(-6+7\,\tau)-\alpha\,(2-4\,\tau+\tau^2\,)+\alpha^2\,(1-2\,\tau+3\,\tau^2))\;\;\mathrm{G3}^{01}_{0012000}\\
&-12\,(-1+\alpha)^2\,\alpha^2\,(-1+2\,\alpha)\,(\alpha\,(-1+\tau)+3\,\tau)\,\mathrm{G3}^{01}_{1010000}\\
&+8\,(-1+\alpha)^3\,\alpha\,\tau\,\mathrm{G3}^{02}_{0002000}+8\,(-1+\alpha)^2\,(1+\alpha-5\,\alpha^2+6\,\alpha^3)\,\mathrm{G3}^{02}_{0010010}\\
&+8\,(-1+\alpha)^4\,(1-2\,\alpha+2\,\alpha^2)\,\mathrm{G3}^{02}_{0010020}\\
&+8\,(-1+\alpha)^2\,(-1+6\,\alpha^4+\alpha^2\,(3-4\,\tau)+\alpha^3\,(-5+4\,\tau))\,\mathrm{G3}^{02}_{0011000}\\
&+8\,(-1+\alpha)^3\,\alpha\,\tau\,(\alpha+3\,\tau+\alpha^2\,(-1+3\,\tau))\,\mathrm{G3}^{02}_{0012000}\\
&-24\,(-1+\alpha)^2\,\alpha^2\,(-1+2\,\alpha)\,\mathrm{G3}^{02}_{1010000}+16\,(-1+\alpha)^3\,\alpha^2\,\tau\,\mathrm{G3}^{03}_{0012000}\\
&-4\,(-1+\alpha)^2\,\alpha\,(-3\,\tau+3\,\alpha\,(1+\tau)+\alpha^2\,(-3+2\,\tau))\,\mathrm{G3}^{10}_{0010000}\\
&-8\,(-1+\alpha)^2\,\alpha^2\,(-1+3\,\alpha)\,\mathrm{G3}^{10}_{0100000}-8\,(-1+\alpha)^2\,\alpha^2\,(1+3\,\alpha^3\,(-2+\tau)\\
&-9\,\alpha^2\,(-1+\tau)-2\,\tau+2\,\alpha\,(-2+7\,\tau))\,\mathrm{G3}^{10}_{0110000}\\
&-16\,(-1+\alpha)^3\,\alpha^2\,(-1+3\,\alpha)\,\mathrm{G3}^{20}_{0110000}
\end{aligned}
\tag{B.122}
$$

$$
\mathcal{F}^{(4)}_{14}(T)=0 \tag{B.123}
$$

$$
\mathcal{F}^{(5)}_{14}(T)=2\,(-1+\alpha)\,\alpha^3\,(4+\alpha^2\,(29-56\,\tau)+16\,\alpha^3\,(-1+\tau)-16\,\tau
$$

$$
\begin{aligned}
&+\alpha\,(-17+50\,\tau))\,\mathrm{F5}^{00}_{0010001}-8\,(-1+\alpha)^2\,\alpha^4\,(3-8\,\alpha+4\,\alpha^2)\,\tau\,\mathrm{F5}^{00}_{0010002}\\
&-2\,(-1+\alpha)\,\alpha^2\,(1+\alpha+\alpha^3\,(29-56\,\tau)+16\,\alpha^4\,(-1+\tau)-16\,\alpha\,\tau\\
&+5\,\alpha^2\,(-3+10\,\tau))\;\;\mathrm{F5}^{00}_{0110000}\\
&+2\,(-1+\alpha)^3\,\alpha^2\,(-7+16\,\alpha^3-5\,\tau-\alpha^2\,(35+8\,\tau)+\alpha\,(26+17\,\tau))\,\mathrm{F5}^{00}_{0110010}\\
&-8\,(-1+\alpha)^4\,\alpha^2\,(-1+2\,\alpha)\,\tau\,(1-3\,\alpha+2\,\alpha^2+\tau)\,\mathrm{F5}^{00}_{0110020}\\
&-16\,(1-2\,\alpha)^2\,(-1+\alpha)^4\,\alpha\,\mathrm{F5}^{01}_{0010020}\\
&-4\,(-1+\alpha)^3\,\alpha\,(3-11\,\alpha+16\,\alpha^2)\,(\mathrm{F5}^{01}_{0010010}-\mathrm{F5}^{01}_{1010000})\\
&+2\,\alpha^2\,(-1-\alpha+\alpha^2)\,(-1+2\,\alpha+\tau)\,\mathrm{G5}^{00}_{0000001}+(1-\tau-3\,\alpha\,(1+\tau)\\
&+8\,\alpha^3\,(1+3\,\tau)-4\,\alpha^4\,(1+3\,\tau)-\alpha^2\,(1+9\,\tau))\,\mathrm{G5}^{00}_{0010000}\\
&-2\,\alpha^2\,(2\,\alpha^5\,\tau+\alpha\,(11-62\,\tau)\,\tau+21\,\tau^2+\alpha^3\,(-3+41\,\tau-49\,\tau^2)\\
&+\alpha^4\,(1-19\,\tau+11\,\tau^2)+\alpha^2\,(1-33\,\tau+80\,\tau^2))\,\mathrm{G5}^{00}_{0010001}\\
&+2\,\alpha^4\,\tau\,(2\,\alpha^4+\alpha^2\,(6-13\,\tau)+4\,\alpha^3\,(-2+\tau)-7\,\tau\\
&+2\,\alpha\,(-1+7\,\tau))\,\mathrm{G5}^{00}_{0010002}-2\,(-1+\alpha)^2\,\alpha^2\,(2+6\,\tau-5\,\tau^2\\
&+\alpha^3\,(-2+4\,\tau)+3\,\alpha\,(-2-3\,\tau+12\,\tau^2)-\alpha^2\,(-6+\tau+12\,\tau^2))\,\mathrm{G5}^{00}_{0110000}\\
&+2\,(-1+\alpha)^2\,\alpha^2\,(-2+2\,\alpha^4\,(-1+\tau)-6\,\tau-4\,\tau^2-\tau^3+\alpha^3\,(8+\tau-4\,\tau^2)\\
&+2\,\alpha^2\,(-6-7\,\tau+\tau^2)+\alpha\,(8+17\,\tau+6\,\tau^2-2\,\tau^3))\,\mathrm{G5}^{00}_{0110010}\\
&+2\,(-1+\alpha)^4\,\alpha^2\,\tau\,(-2+2\,\alpha^3-\tau-\tau^2+3\,\alpha\,(2+\tau)\\
&-2\,\alpha^2\,(3+\tau))\,\mathrm{G5}^{00}_{0110020}+4\,(-1+\alpha)^2\,(-1-\alpha+\alpha^2)\,\mathrm{G5}^{01}_{0000010}\\
&-4\,(-1+\alpha)^2\,(\alpha^2\,(4-8\,\tau)+\tau+\alpha\,(-3+4\,\tau)+\alpha^4\,(-7+5\,\tau)\\
&+\alpha^3\,(6+13\,\tau))\,\mathrm{G5}^{01}_{0010010}\\
&-4\,(-1+\alpha)^4\,(1+2\,\alpha^3\,(-2+\tau)+3\,\tau+4\,\alpha^2\,(2+\tau)-\alpha\,(5+4\,\tau))\,\mathrm{G5}^{01}_{0010020}\\
&+4\,(-1+\alpha)^2\,\alpha^2\,(-16\,\tau+17\,\alpha\,\tau+\alpha^2\,(-2+6\,\tau))\,\mathrm{G5}^{01}_{1010000}\\
&-8\,(-1+\alpha)^2\,\alpha\,(1-3\,\alpha+5\,\alpha^2)\,\mathrm{G5}^{02}_{0010010}\\
&-8(-1+\alpha)^4(1-2\alpha+2\alpha^2)\,\mathrm{G5}^{02}_{0010020}+16\,(-1+\alpha)^2\alpha^2\,(-2+3\alpha)\mathrm{G5}^{02}_{1010000}
\end{aligned}
\tag{B.124}
$$

$$
\begin{aligned}
\mathcal{F}^{(6)}_{14}(T)=&+\frac{4}{\tau}\,(-1+\alpha)^4\,\alpha\,(1+\tau+\alpha\,(-1+\tau^2))\,\mathrm{F6}^{00}_{0000110}\\
&+2\,\alpha^2\,(-5+23\,\alpha-36\,\alpha^2+18\,\alpha^3)\,(\mathrm{F6}^{00}_{0000001}-\mathrm{F6}^{00}_{0100000})\\
&-\frac{2}{\tau}\,(-1+\alpha)\,\alpha\,(6\,\alpha^3+2\,(-1+\tau)+3\,\alpha\,(2+\tau)-\alpha^2\,(10+\tau))\\
&\quad\times(\mathrm{F6}^{00}_{0000100}-\mathrm{F6}^{00}_{0100000})-\frac{2}{\tau}\,(-1+\alpha)^2\,\alpha\,(2+\alpha^2\,(6-30\,\tau)-3\,\tau-3\,\tau^2\\
&+\alpha^3\,(-2+16\,\tau)+\alpha\,(-6+17\,\tau+8\,\tau^2))\,\mathrm{F6}^{00}_{0100010}\\
&-2\,(-1+\alpha)\,\alpha^2\,(-4+2\,\alpha^3\,(4+\tau)+\alpha\,(12+\tau)-\alpha^2\,(16+\tau))\,\mathrm{F6}^{00}_{0101000}\\
&+\frac{4}{\tau}\,\alpha\,(2-3\,\alpha+\alpha^2)\,(\mathrm{F6}^{01}_{0001000}-\mathrm{F6}^{01}_{1000000})
\end{aligned}
\tag{B.125}
$$

$$
\mathcal{F}^{(7)}_{14}(T)=4\,(1-2\,\alpha)^2\,(-1+\alpha)\,\alpha^2\,(\mathrm{F7}^{00}_{0000001}-\mathrm{F7}^{00}_{0100000})
$$

$$
\begin{aligned}
&- \frac{2}{\tau}\,(-1+\alpha)\,\alpha\,(-2+4\,\alpha^3-\tau-\alpha^2\,(8+\tau)+\alpha\,(6+4\,\tau)) \\
&\times\;(\mathrm{F7}^{00}_{0000100}-\mathrm{F7}^{00}_{0100000})-4\,(-1+\alpha)^2\,\alpha\,(-1+2\,\alpha)\,(1-3\,\alpha+2\,\alpha^2+\tau) \\
&\times\;\mathrm{F7}^{00}_{0100010}-2\,(-1+\alpha)\,\alpha^2\,(-2+6\,\alpha+4\,\alpha^3+\alpha^2\,(-8+\tau))\,\mathrm{F7}^{00}_{0101000} \\
&+\frac{4}{\tau}\,(-1+\alpha)^2\,\alpha\,(\mathrm{F7}^{01}_{0001000}-\mathrm{F7}^{01}_{1000000})
\end{aligned}
\tag{B.126}
$$

$$
\begin{aligned}
\mathcal{F}^{(8)}_{14}(T) =\;& \frac{1}{(-1+\alpha)\,\alpha}\,(-1+8\,\alpha-19\,\alpha^2+22\,\alpha^3-11\,\alpha^4)\,\tau\,\mathrm{G8}^{00}_{0000000}+2\,\alpha\,\tau\,(\\
&-1+8\,\alpha^4+\alpha^3\,(-17+\tau)+3\,\tau+\alpha^2\,(11+2\,\tau)-\alpha\,(1+8\,\tau))\,\mathrm{G8}^{00}_{0000100} \\
&-2\,(-1+\alpha)\,\alpha^2\,\tau\,(-2+4\,\alpha^3+\tau+\alpha^2\,(-8+3\,\tau)-2\,\alpha\,(-3+\tau^2))\,\mathrm{G8}^{00}_{0000200} \\
&+\frac{2}{-1+\alpha}\,\alpha\,(4+10\,\alpha^3-19\,\alpha^4+8\,\alpha^5+\alpha^2\,(9-2\,\tau) \\
&+2\,\alpha\,(-6+\tau)-\tau)\,\tau\,\mathrm{G8}^{00}_{0100000}+2\,(-1+\alpha)\,\alpha^2\,\tau\,(-2-4\,\tau \\
&+4\,\alpha^3\,(1+2\,\tau)+3\,\alpha\,(2+5\,\tau)-2\,\alpha^2\,(4+9\,\tau))\,\mathrm{G8}^{00}_{0101000} \\
&+2\,(-1+\alpha)^2\,\alpha^2\,(-2+6\,\alpha+4\,\alpha^3+\alpha^2\,(-8+\tau))\,\tau^2\,\mathrm{G8}^{00}_{0102000} \\
&+4\,(-1+\alpha)\,(4\,\alpha^3-\alpha\,(-2+\tau)+2\,\alpha^2\,(-2+\tau)+\tau)\,\mathrm{G8}^{01}_{0001000} \\
&+4\,(-1+\alpha)^2\,\tau\,(4\,\alpha^3-2\,\tau+\alpha\,(3+\tau)+\alpha^2\,(-5+2\,\tau))\,\mathrm{G8}^{01}_{0002000} \\
&+\frac{8}{\alpha}\,(-1+3\,\alpha-4\,\alpha^2+2\,\alpha^3)\,(2\,\alpha^2-\tau)\,\mathrm{G8}^{01}_{1000000}+8\,(-1+\alpha)^3\,\tau\,\mathrm{G8}^{02}_{0002000} \\
&+8\,(3-\tfrac{1}{\alpha}-4\,\alpha+2\,\alpha^2)\,(\mathrm{G8}^{02}_{0001000}-\mathrm{G8}^{02}_{1000000}) \\
&+(-4+\tfrac{2}{\alpha}+4\,\alpha-2\,\alpha^2)\,(-\mathrm{S8}^{0100000}_{000001100}+\mathrm{S8}^{0200000}_{000101100}) \\
&+(6-\tfrac{2}{\alpha}-8\,\alpha+4\,\alpha^2)\,(-\mathrm{S8}^{0100000}_{000001100}+\mathrm{S8}^{0200000}_{100001100})
\end{aligned}
\tag{B.127}
$$

$$
\begin{aligned}
\mathcal{F}^{(9)}_{14}(T) =\;& 2\,(1-\alpha^3+\tau-\alpha\,(3+2\,\tau)+\alpha^2\,(3+4\,\tau))\,\mathrm{G9}^{00}_{0000000} \\
&+2\,(-1+\alpha)\,(\alpha^3+8\,\alpha^4\,\tau-(1+\tau)^2-\alpha^2\,(3+8\,\tau) \\
&+\alpha\,(3+8\,\tau+\tau^2\;))\,\mathrm{G9}^{00}_{0000010}+4\,(-1+\alpha)^3\,\alpha\,(-1+4\,\alpha^2)\,\tau\,\mathrm{G9}^{00}_{0000020} \\
&+2\,(-1+\alpha)\,\tau\,(-15\,\alpha^3+8\,\alpha^4+2\,\alpha\,(-1+\tau)-2\,\tau+4\,\alpha^2\,(2+\tau))\,\mathrm{G9}^{00}_{0001000} \\
&+2\,(-1+\alpha)^2\,\alpha\,\tau\,(4\,\alpha^3+2\,(-2+\tau)\,\tau-\alpha^2\,(4+3\,\tau)+\alpha\,(2+6\,\tau \\
&-2\,\tau^2))\,\mathrm{G9}^{00}_{0002000}+2\,\alpha\,(4-10\,\alpha+3\,\alpha^2+11\,\alpha^3-8\,\alpha^4\;)\,\tau\,\mathrm{G9}^{00}_{0100000} \\
&+4\,(-1+\alpha)\,\alpha\,\tau\,(-1-8\,\alpha^2+4\,\alpha^3+\alpha\,(5+\tau))\,\mathrm{G9}^{00}_{0100010} \\
&+4\,(-1+\alpha)^3\,\alpha\,(-1+2\,\alpha)\,\tau\,(1-3\,\alpha+2\,\alpha^2+\tau)\,\mathrm{G9}^{00}_{0100020} \\
&-2\,(-1+\alpha)\,\alpha^2\,\tau\,(-2-4\,\tau+4\,\alpha^3\,(1+2\,\tau)+3\,\alpha\,(2+5\,\tau)-2\,\alpha^2\,(4+9\,\tau)) \\
&\times\;\mathrm{G9}^{00}_{0101000}-2\,(-1+\alpha)^2\,\alpha^2\,(-2+6\,\alpha+4\,\alpha^3+\alpha^2\,(-8+\tau))\,\tau^2\,\mathrm{G9}^{00}_{0102000} \\
&+8\,\alpha\,(1-2\,\alpha+\alpha^2+2\,\alpha^3-2\,\alpha^4)\,\tau\,\mathrm{G9}^{00}_{1000000} \\
&+8\,(-1+\alpha)\,(-1-5\,\alpha^2+4\,\alpha^3-\tau+\alpha\,(3+\tau)\;)\,\mathrm{G9}^{01}_{0000010} \\
&+8\,(1-2\,\alpha)^2\,(-1+\alpha)^3\,\mathrm{G9}^{01}_{0000020} \\
&-4\,(-1+\alpha)\,(-4\,\alpha^2+4\,\alpha^3-\tau+\alpha\,(2+\tau))\,\mathrm{G9}^{01}_{0001000}
\end{aligned}
$$

$$
\begin{aligned}
&- 4\,(-1+\alpha)^2\,\tau\,(4\,\alpha^3 - 2\,\tau + \alpha\,(3+\tau) + \alpha^2\,(-5+2\,\tau))\,\mathrm{G9}^{01}_{0002000}\\
&+ 8\,(-1+\alpha)^2\,(\mathrm{G9}^{02}_{0000010} - \mathrm{G9}^{02}_{0001000}) - 8\,(-1+\alpha)^3\,\tau\,\mathrm{G9}^{02}_{0002000}\\
&- 16\,\alpha\,(-1+3\,\alpha-4\,\alpha^2+2\,\alpha^3)\,(\mathrm{G9}^{01}_{1000000} - \mathrm{G9}^{10}_{0100000})\\
&+ 2\,(3-6\,\alpha+4\,\alpha^2)\,(\mathrm{S9}^{0100000}_{000001100} - \mathrm{S9}^{1000000}_{000001100})\\
&- 2\,(-1+\alpha)^2\,(\mathrm{S9}^{0200000}_{000001110} - \mathrm{S9}^{1000000}_{000001100})
\end{aligned}
\tag{B.128}
$$

$$
\mathcal{F}^{(10)}_{14}(T) = 0 \tag{B.129}
$$

$$
\begin{aligned}
\mathcal{F}^{(11)}_{14}(T) &= 4\,\alpha\,(3-12\,\alpha+21\,\alpha^2-16\,\alpha^3+4\,\alpha^4)\,\tau\,\mathrm{G11}^{00}_{0000001}\\
&+ 4\,\alpha^3\,(3-11\,\alpha+12\,\alpha^2-4\,\alpha^3)\,\tau\,\mathrm{G11}^{00}_{0000002}\\
&- 4\,\alpha\,(4-15\,\alpha+23\,\alpha^2-16\,\alpha^3+4\,\alpha^4)\,\tau\,\mathrm{G11}^{00}_{0100000}\\
&- 4\,(-1+\alpha)\,\alpha\,\tau\,(-1-8\,\alpha^2+4\,\alpha^3+\alpha\,(5+\tau))\,\mathrm{G11}^{00}_{0100010}\\
&- 4\,(-1+\alpha)^3\,\alpha\,(-1+2\,\alpha)\,\tau\,(1-3\,\alpha+2\,\alpha^2+\tau)\,\mathrm{G11}^{00}_{0100020}\\
&- 8\,(1-2\,\alpha)^2\,(-1+\alpha)\,\alpha\,\mathrm{G11}^{01}_{0000010} - 8\,(1-2\,\alpha)^2\,(-1+\alpha)^3\,\mathrm{G11}^{01}_{0000020}\\
&+ 16\,\alpha\,(-1+3\,\alpha-4\,\alpha^2+2\,\alpha^3)\,\mathrm{G11}^{01}_{1000000}
\end{aligned}
\tag{B.130}
$$

Bibliography

[1] R. K. Ellis, W. J. Stirling, B. R. Webber, *QCD and collider Physics*, Cambridge 1996.

[2] Y. L. Dokshitzer, Sov. Phys. JETP **46** (1977) 641 [Zh. Eksp. Teor. Fiz. **73** (1977) 1216]; V. N. Gribov and L. N. Lipatov, Yad. Fiz. **15** (1972) 781 [Sov. J. Nucl. Phys. **15** (1972) 438]; G. Altarelli and G. Parisi, Nucl. Phys. B **126** (1977) 298.

[3] J. R. Forshaw and D. A. Ross, *Quantum chromodynamics and the pomeron*, Cambridge 1997 (Cambridge lecture notes in physics. 9).

[4] A. Donnachie and P. V. Landshoff, Phys. Lett. B **296** (1992) 227 [hep-ph/9209205].

[5] E. A. Kuraev, L. N. Lipatov and V. S. Fadin, Sov. Phys. JETP **45** (1977) 199 [Zh. Eksp. Teor. Fiz. **72** (1977) 377]; I. I. Balitsky and L. N. Lipatov, Sov. J. Nucl. Phys. **28** (1978) 822 [Yad. Fiz. **28** (1978) 1597].

[6] J. Bartels and H. Lotter, Phys. Lett. B **309** (1993) 400.

[7] J. Bartels, H. Lotter and M. Vogt, Phys. Lett. B **373** (1996) 215 [hep-ph/9511399].

[8] C. Ewerz, *Unitarity corrections in high energy QCD*, PhD Thesis, Universität Hamburg 1998, DESY-THESIS-1998-025.

[9] J. Bartels and C. Ewerz, JHEP **9909** (1999) 026 [hep-ph/9908454].

[10] J. Bartels and H. Kowalski, Eur. Phys. J. C **19** (2001) 693 [hep-ph/0010345].

[11] A. H. Mueller, Nucl. Phys. Proc. Suppl. **18C** (1991) 125.

[12] J. Bartels, A. de Roeck and M. Loewe, Z. Phys. C **54** (1992) 635.

[13] J. Kwiecinski, A. D. Martin and P. J. Sutton, Phys. Rev. D **46** (1992) 921.

[14] A. H. Mueller and H. Navelet, Nucl. Phys. B **282** (1987) 727.

[15] J. Bartels, A. De Roeck and H. Lotter, Phys. Lett. B **389** (1996) 742 [hep-ph/9608401].

[16] S. J. Brodsky, F. Hautmann and D. E. Soper, Phys. Rev. D **56** (1997) 6957 [hep-ph/9706427]; Phys. Rev. Lett. **78** (1997) 803 [Erratum-ibid. **79** (1997) 3544] [hep-ph/9610260].

[17] J. Bartels, A. De Roeck, C. Ewerz and H. Lotter, in *ECFA/DESY Study on Physics and Detectors for a Linear Collider*, ed. R. Settles, DESY 97-123E, hep-ph/9710500.

[18] J. Bartels, C. Ewerz and R. Staritzbichler, Phys. Lett. B **492** (2000) 56 [hep-ph/0004029].

[19] L3 Collaboration, M. Acciarri *et. al.* , Phys. Lett. B **453** (1999) 333 [CERN-EP/98-205]; OPAL Collaboration, M. Przybycien, A. De Roeck, R. Nisius, OPAL Physics Note PN456 (2000);

[20] L3 $\gamma\gamma$ working group, `http://l3www.cern.ch/analysis/ggpage/epsfig99/lepc2.eps.gz`.

[21] L. N. Lipatov and V. S. Fadin, JETP Lett. **49** (1989) 352 [Yad. Fiz. **50** (1989) 1141].

[22] V. S. Fadin and L. N. Lipatov, Phys. Lett. B **429** (1998) 127 [hep-ph/9802290].

[23] M. Ciafaloni and G. Camici, Phys. Lett. B **430** (1998) 349 [hep-ph/9803389].

[24] C. R. Schmidt, Phys. Rev. D **60** (1999) 074003 [hep-ph/9901397]; J. R. Forshaw, D. A. Ross and A. Sabio Vera, Phys. Lett. B **455** (1999) 273 [hep-ph/9903390].

[25] M. Ciafaloni, D. Colferai and G. P. Salam, Phys. Rev. D **60** (1999) 114036 [hep-ph/9905566].

[26] G. P. Salam, Acta Phys. Polon. B **30** (1999) 3679 [hep-ph/9910492].

[27] K. Golec-Biernat and M. Wüsthoff, Phys. Rev. D **59** (1999) 014017 [hep-ph/9807513].

[28] A. H. Mueller, Nucl. Phys. B **335** (1990) 115.

[29] N. N. Nikolaev and B. G. Zakharov, Z. Phys. C **49** (1991) 607.

[30] N. Nikolaev and B. G. Zakharov, Z. Phys. C **53** (1992) 331.

[31] D. Yu. Ivanov, M. Wüsthoff, Eur. Phys. J. **C8** (1999) 107.

[32] S. Gieseke and C. F. Qiao, Phys. Rev. D **61** (2000) 074028 [hep-ph/9910531].

[33] A. Ballestrero and E. Maina, Phys. Lett. B **350** (1995) 225 [hep-ph/9403244].

[34] K. Golec-Biernat and M. Wüsthoff, Phys. Rev. D **60** (1999) 114023 [hep-ph/9903358].

[35] V. S. Fadin, M. I. Kotsky and R. Fiore, Phys. Lett. B **359** (1995) 181; V. S. Fadin, JETP Lett. **61** (1995) 346 [Pisma Zh. Eksp. Teor. Fiz. **61** (1995) 342]; M. I. Kotsky and V. S. Fadin, Phys. Atom. Nucl. **59** (1996) 1035; V. S. Fadin, R. Fiore and M. I. Kotsky, Phys. Lett. B **387** (1996) 593 [hep-ph/9605357].

[36] V. S. Fadin and L. N. Lipatov, Nucl. Phys. B **406** (1993) 259; V. Fadin, R. Fiore and A. Quartarolo, Phys. Rev. D **50** (1994) 5893 [hep-th/9405127]; V. S. Fadin, R. Fiore and M. I. Kotsky, Phys. Lett. B **389** (1996) 737 [hep-ph/9608229].

[37] V. S. Fadin and L. N. Lipatov, Nucl. Phys. B **477** (1996) 767 [hep-ph/9602287]; V. S. Fadin M. I. Kotsky and L. N. Lipatov, Phys. Lett. B **415** (1997) 97.

[38] G. Camici and M. Ciafaloni, Phys. Lett. B **386** (1996) 341 [hep-ph/9606427]; G. Camici and M. Ciafaloni, Nucl. Phys. B **496** (1997) 305 [hep-ph/9701303]; V. S. Fadin, R. Fiore, A. Flachi and M. I. Kotsky, Phys. Lett. B **422** (1998) 287 [hep-ph/9711427].

[39] S. J. Brodsky, V. S. Fadin, V. T. Kim, L. N. Lipatov and G. B. Pivovarov, JETP Lett. **70** (1999) 155 [hep-ph/9901229].

[40] V. S. Fadin and R. Fiore, Phys. Lett. B **440** (1998) 359 [hep-ph/9807472].

[41] V. S. Fadin, *BFKL news*, Talk given at LISHEP 98, Rio de Janeiro, Brazil, 16-20 Feb 1998 [hep-ph/9807528].

[42] V. Fadin, R. Fiore and A. Quartarolo, Phys. Rev. D **50** (1994) 2265 [hep-ph/9310252].

[43] J. Bartels, Nucl. Phys. B **175** (1980) 365.

[44] R. Mertig, M. Böhm and A. Denner, Comput. Phys. Commun. **64** (1991) 345.

[45] Z. Bern, L. Dixon and D. A. Kosower, Nucl. Phys. B **412** (1994) 751 [hep-ph/9306240]; Phys. Lett. B **302** (1993) 299 [Erratum-ibid. B **318** (1993) 649] [hep-ph/9212308].

[46] J. M. Campbell, E. W. Glover and D. J. Miller, Nucl. Phys. B **498** (1997) 397 [hep-ph/9612413].

[47] V. S. Fadin and A. D. Martin, Phys. Rev. D **60** (1999) 114008 [hep-ph/9904505].

[48] J. Bartels, S. Gieseke and C. F. Qiao, Phys. Rev. D **63** (2001) 056014 [hep-ph/0009102].

[49] D. Colferai, *Small-x processes in perturbative quantum chromodynamics*, PhD Thesis, University of Florence 1999, hep-ph/0008309.

[50] V. S. Fadin, R. Fiore, M. I. Kotsky and A. Papa, Phys. Rev. D **61** (2000) 094005 [hep-ph/9908264].

[51] V. S. Fadin, R. Fiore, M. I. Kotsky and A. Papa, Phys. Rev. D **61** (2000) 094006 [hep-ph/9908265].

Acknowledgments

First of all, I would like to thank Prof. J. Bartels for his permanent interest in my work and for his support during the years. In countless discussions I have benefitted from his criticism and his encouragement.

I am very grateful to Cong-Feng Qiao and to Albrecht Kyrieleis for very pleasant and fruitful collaborations.

I wish to thank Prof. J.C. Collins and Prof. L.N. Lipatov for very helpful discussions during their visits in Hamburg.

I wish to thank the members of the II. Institut für Theoretische Physik and the DESY Theory group for creating a very pleasant and stimulating working atmosphere. In particular, I wish to thank all the members of the small x group: Claas Bontus, Dimitri Colferai, Carlo Ewerz, Krzysztof Golec-Biernat, Hamid Kharraziha, Anatoly Kotikov, Krisztián Peters, René Staritzbichler and Gian-Paolo Vacca for all kinds of help and support on physics and non-physics issues.

This work was supported in part by the Graduiertenkolleg 'Theoretische Elementarteilchenphysik', the Graduiertenkolleg 'Zukünftige Entwicklungen der Teilchenphysik' and the EU TMR-network 'QCD and the deep structure of elementary particles', contract number FMRX-CT98-0194 (DG 12 - MIHT).

Last but not least, I wish to thank Claudia Koch for all her love and patience.